

INVESTIGATING THE ROLE OF GLYCOSAMINOGLYCANS IN THE  
DEVELOPMENT AND PRODUCTION OF BIRDSONG

by

Caitlin Paige Mencio

A dissertation submitted to the faculty of  
The University of Utah  
in partial fulfillment of the requirements for the degree of

Doctor of Philosophy

Interdepartmental Program in Neuroscience

The University of Utah

December 2014

Copyright © Caitlin Paige Mencio 2014

All Rights Reserved

# The University of Utah Graduate School

## STATEMENT OF DISSERTATION APPROVAL

The following faculty members served as the supervisory committee chair and members for the dissertation of \_\_\_\_\_ Caitlin Paige Mencio \_\_\_\_\_.

Dates at right indicate the members' approval of the dissertation.

\_\_\_\_\_ Kuberan Balagurunathan \_\_\_\_\_, Chair  
\_\_\_\_\_ 5/2/2014 \_\_\_\_\_  
Date Approved

\_\_\_\_\_ Joshua Bonkowsky \_\_\_\_\_, Member  
\_\_\_\_\_ 5/2/2014 \_\_\_\_\_  
Date Approved

\_\_\_\_\_ Franz Goller \_\_\_\_\_, Member  
\_\_\_\_\_ 5/2/2014 \_\_\_\_\_  
Date Approved

\_\_\_\_\_ Erik Jorgensen \_\_\_\_\_, Member  
\_\_\_\_\_ 5/2/2014 \_\_\_\_\_  
Date Approved

\_\_\_\_\_ Raymond Kesner \_\_\_\_\_, Member  
\_\_\_\_\_ 5/2/2014 \_\_\_\_\_  
Date Approved

The dissertation has also been approved by \_\_\_\_\_ Kristen Keefe \_\_\_\_\_

Chair of the Department/School/College of \_\_\_\_\_ Neuroscience \_\_\_\_\_

and by David B. Kieda, Dean of The Graduate School.

## ABSTRACT

Glycosaminoglycans are carbohydrate side chains of proteoglycans that have a myriad of biological functions. In the brain, these molecules are implicated in everything from development to plasticity to disease. Two of the main types of glycosaminoglycans (GAGs), heparan sulfate and chondroitin sulfate, have been implicated in both plasticity and learning; however, the exact role they play has remained unclear. One of the more interesting sensorimotor systems in the brain involves the learning and production of vocalizations. The goal of this work was to investigate the role GAGs play in two different aspects of this complex behavior, the neural control of vocal ontogeny and superfast muscle involvement in song production of zebra finch.

In order to fully understand the role GAGs play in complex biological behaviors, such as vocalizations, it is imperative that the proper tools be synthesized, characterized, and produced for the study of these carbohydrates. Enzymes, specifically sulfated polymers and oligosaccharides, and small molecules provide unique opportunities to examine the role of GAGs. The use of enzymes in the song-specific nucleus, HVC, allowed the validation of the functionality of these enzymes in the model system of interest. Changes in stereotyped song were observed showing that GAG modulation could lead to alteration of a learned behavior.

After this confirmation that GAGs were present and involved in song, small molecules called xylosides were used to examine the role of chondroitin sulfate

biosynthesis during vocal ontogeny. Infusion of xyloside into RA (robust nucleus of the arcopallium), a nucleus important for vocal ontogeny, led to a change in the development of song. This implies that regulated biosynthesis of chondroitin sulfate during the critical period for vocal ontogeny is important.

Lastly, the role of superfast syringeal muscles in song production was examined. Heparan sulfate degradation in these muscles alters the ability of the syrinx to modulate airflow. This change in muscle kinetics was correlated with significant, but temporary, differences in acoustic structure and frequency modulation while long-term differences showed aberrant syllable production.

## TABLE OF CONTENTS

ABSTRACT .....	iii
LIST OF FIGURES .....	vii
LIST OF TABLES .....	x
LIST OF ABBREVIATIONS.....	xi
ACKNOWLEDGEMENTS.....	xiv
CHAPTERS	
1 INTRODUCTION .....	1
1.1 Overview of glycosaminoglycans.....	1
1.2 Glycosaminoglycans in speech and song.....	15
1.3 Research objectives .....	22
1.4 References .....	33
2 THE PRODUCTION AND VALIDATION OF MOLECULAR TOOLS FOR THE STUDY OF GLYCOSAMINOGLYCANS IN VOCAL LEARNING AND PRODUCTION.....	42
2.1 Overview .....	42
2.2 Expression and purification of enzymes, polymers, oligosaccharides, and the characterization of xylosides .....	44
2.3 Degradation of HS in HVC leads to altered song in adult zebra finch.....	56
2.4 Discussion.....	60
2.5 References .....	74
3 MODULATION OF GLYCOSAMINOGLYCANS ALTERS VOCAL ONTOGENY IN ZEBRA FINCH.....	77
3.1 Introduction .....	77
3.2 Methods and materials.....	78
3.3 Results .....	82
3.4 Discussion .....	86
3.5 References.....	94

4	DEGRADATION OF HEPARAN SULFATE IN SYRINGEAL MUSCLE LEADS TO CHANGES IN CRYSTALLIZED ZEBRA FINCH SONG.....	98
4.1	Introduction .....	98
4.2	Methods and materials.....	100
4.3	Results .....	103
4.4	Discussion .....	106
4.5	References.....	118
5	CONCLUSIONS .....	121
5.1	Conclusions.....	121
5.2	References.....	125
APPENDICES		
	A: REVIEW ARTICLE ON GLYCOSAMINOGLYCANS IN THE NERVOUS SYSTEM.....	127
	B: USE OF ENZYMES AND POLYMERS IN COLLABORATIVE RESEARCH.....	153
	CURRICULUM VITA.....	172

## LIST OF FIGURES

FIGURE	PAGE
1.1 Examples of the different structures of a few proteoglycans.....	27
1.2 Disaccharide units for each type of GAG including all possible sites for modification by <i>O</i> -sulfotransferase.....	28
1.3 Illustration of GAG biosynthesis.....	29
1.4 The production of PAPS as a substrate for the modification of GAG chains.....	30
1.5 Timeline and neural circuitry for song learning in zebra finch.....	31
2.1 Specificity for enzymatic degradation by Heparin lyases.....	62
2.2 Purification and activity of glycosaminoglycan degradation enzymes.....	63
2.3 HPLC profile of preparative scale partial digestion of heparin to produce oligosaccharides.....	64
2.4 Mass spectrometry analysis of heparin oligosaccharides.....	65
2.5 Comparison of priming activity by scintillation count for Cu vs Ru-click xylosides.....	68
2.6 Comparison of overall sulfation density and disaccharide composition for Cu-click and Ru-click xylosides.....	69
2.7 Spectrogram and frequency analysis of a specific syllable in the motif of an adult zebra finch before and 24 h after treatment with heparitinase (A) or vehicle (B), respectively.....	71
2.8 Spectrogram analysis indicates a shift in timing between song syllables in enzyme treated birds as compared to controls.....	72



2.9 Production of a novel motif at one month post heparitinase injection in adult zebra finch.....	73
3.1 Spectrograms of multiple bouts from two birds treated with vehicle (A,B) and two birds treated with compound 1 (C, D) at 60-70 PHD and 110+ PHD. In the vehicle treated birds, song consists of variable syntax early in development but crystallizes into a stereotypic motif. In xyloside treated birds, song begins the same way, but treated birds lack stereotypy in adult song as well.....	91
3.2 Analysis of motifs between time-points using 110+ PHD song as template (A-C) and comparison of motifs within time-points (D-F) for both xyloside treated and vehicle treated birds.....	92
3.3 Confirmation of decoy and priming effect of xylosides in juvenile zebra finch.....	93
4.1 The schematic of a syrinx, the avian vocal organ that shows the six pairs of syringeal muscles.....	110
4.2 An overview of airsac pressure patten and sound (shown as oscillogram, spectrogram, and amplitude) for 2 birds (A,B) who received bilateral injections of heparitinase enzyme into the ventral syringeal muscles.....	111
4.3 Comparison of song amplitude (in dB) before and 24 h after heparitinase treatment.....	112
4.4 Examples from two different birds (A & B) that show the loss of high-frequency syllables at 24 h post enzyme injection, as seen by the sound trace and spectrograms (marked by red rectangles).....	113
4.5 Pressure at phonation onset is changed 24 h after enzyme treatment, with 22 of the 26 syllables examined showing at least a 5% increase in pressure (A). When comparing the change in pressure as a function of frequency, no obvious correlation is seen between frequency and changes in phonation onset pressure (B).....	114
4.6 Changes in frequency modulation are measured in 6 specific syllables from 4 different enzyme treated birds and significant changes are shown to be syllable dependent.....	115
4.7 Birds treated with enzyme show changes in motif syntax and accompanying pressure pattern (as seen in A & B) 7 d after injection of heparitinases into syringeal muscle. (A) and (B) show the inclusion of a single novel syllable, as indicated by the red boxes and (A) the atypical return to introductory notes after the new syllable. (C) shows the example of the repetition of syllables, indicated by the red box, that increased over time after injection.....	116

4.8 The percent modulation of airflow by syringeal muscle during stimulation of vehicle and enzyme treatment 24 h after injection as compared to that at 10 Hz. Enzyme treated muscle shows an inability to modulate airflow at lower frequencies of stimulation compared to vehicle treated controls.....117

## LIST OF TABLES

TABLE	PAGE
1.1 Proteoglycans and associated enzymes and factors found in the zebra finch brain and known associations to song.....	32
2.1 Table of specifically sulfated polymers synthesized for research purposes.....	66
2.2 Structures of the Cu- and Ru-click-xylosides that were screened.....	67
2.3 Size of primed GAG chains of dimeric Cu- and Ru-catalyzed click xylosides .....	70
3.1 Structures of xylosides used in the current study.....	90

## LIST OF ABBREVIATIONS

PG:	Proteoglycan
GAG:	Glycosaminoglycan
HS:	Heparan sulfate
CS:	Chondroitin Sulfate
DS:	Dermatan Sulfate
KS:	Keratan Sulfate
GPI:	Glycosylphosphatidylinositol
ECM:	Extracellular Matrix
GlcNAc:	<i>N</i> -acetyl glucosamine
GlcA:	Glucuronic acid
Ido A:	Iduronic acid
GalNAc:	<i>N</i> -acetyl galactosamine
Gal:	Galactose
CSPG:	Chondroitin Sulfate Proteoglycan
GALT-I:	Galactosyltransferase-I
GALT-II:	Galactosyltransferase-II
GLCAT-I:	Glucuronic acid transferase-I
EXT1:	Exostose-I
EXT2:	Exostose-II
NDST:	<i>N</i> -deacetyl- <i>N</i> -sulfotransferase
C5-Epi:	C5-epimerase
OST:	<i>O</i> -sulfotransferase
6OST:	6- <i>O</i> -sulfotransferase

3OST:	3- <i>O</i> -sulfotransferase
2OST:	2- <i>O</i> -sulfotransferase
PAPS:	3'-phosphoadenosine-5'-phosphosulfate
NS:	<i>N</i> -sulfated
NA:	<i>N</i> -Acetylated
SULF:	Sulfatase
CNS:	Central Nervous System
HSPG:	Heparan Sulfate Proteoglycan
NCAM:	Neural Cell Adhesion Molecule
FGF:	Fibroblast Growth Factor
TGF- $\beta$ :	Transforming growth factor- $\beta$
LTP:	Long Term Potentiation
BACE1:	Alzheimer's $\beta$ -secretase-1
APP:	Amyloid Precursor Protein
NMJ:	Neuromuscular Junction
ChABC:	Chondroitinase ABC
HGF:	Hepatocyte Growth Factor
TGF- $\beta$ R:	Transforming Growth Factor- $\beta$ Receptor
WT:	Wild type
AChR:	Acetylcholine Receptor
AChE:	Acetylcholinesterase
MPS:	Mucopolysaccharoidosis
HA:	Hyaluronic Acid
PHD:	Post Hatch Days
LMAN:	Lateral Magnocellular Nucleus of the Anterior Neostriatum
DLM:	Medial Nucleus of the dorsolateral thalamus
RA:	Robust Nucleus of the Arcopallium
nXIIts:	Hypoglossal Motorneuron Nucleus

BMP:	Bone Morphogenic Protein
PNN:	Perineuronal Net
Hep:	Heparitinase
ChABC:	Chondroitinase ABC
ChAC:	Chondroitinase AC
ChB:	Chondroitinase B
OD:	Optical Density
Dp:	Degree of polymerization
LC-MS:	Liquid Chromatography Mass Spectrometry
BSA:	Bovine Serum Albumin
Cu:	Copper
Ru:	Ruthenium
CHO:	Chinese Hampster Ovary
HPLC:	High Pressure Liquid Chromatography
PBS:	Phosphate Buffered Saline
FBS:	Fetal Bovine Serum
MWCO:	Molecular Weight Cut-Off
SHh:	Sonic Hedgehog
PHD:	Post Hatch Days
Hz:	Hertz
dB:	Decibel
SAP:	Sound Analysis Pro
PFA:	Paraformaldehyde
FM:	Frequency Modulation

## ACKNOWLEDGEMENTS

First and foremost, I would like to acknowledge my mentors Prof. Kuberan Balagurunathan and Dr. Franz Goller and express my gratitude for their support, guidance, and motivation throughout my graduate study. They were always encouraging and positive with their support and I cannot thank them enough for their assistance. I would also like to thank Prof. Reymond Kesner, Prof. Erik Jorgensen, and Prof. Joshua Bonkowsky for their service on my thesis committee and their helpful comments, constructive criticism, and encouragement.

My thankfulness also extends to my lab mates (current and former) in both Prof. Balagurunathan and Prof. Goller's labs who have supported me throughout this process. The insightful discussions, laughter, and support you gave me was vital to the completion of this work.

Last but not least, I would like to thank my family and friends for their never-ending support, encouragement, understanding, and love. My father instilled in me the curiosity and love of science that led me to graduate school and my mother gave me the stubborn streak that pushed me to the end. Without them, I would not be where I am or who I am today. I love you both very much.

Salt Lake City, May 2014 Caitlin Mencio

## CHAPTER 1

### INTRODUCTION

#### 1.1 Overview of glycosaminoglycans

##### 1.1.1 Structures of glycosaminoglycans

Proteoglycans (PGs) are macromolecules consisting of a core protein and multiple glycosaminoglycan (GAG) side chains. PGs can be further defined into families by their core protein sequence, the type of protein, and the number/type of GAG chains that extend from the core protein. There are four main types of PG: heparan sulfate (HS), chondroitin sulfate (CS), dermatan sulfate (DS), and keratan sulfate (KS). PGs are attached to cell membranes through either transmembrane domains (i.e., syndecan) or glycosylphosphatidylinositol (GPI) anchored (i.e., glypican). Alternatively, PGs can be secreted into the extracellular matrix (ECM) such as the PGs biglycan, decorin, aggrecan, and perlecan. Most PGs have two or more GAG side chains; however, some PGs can have hundreds.<sup>1,2</sup> Examples of the different structures of PG can be seen in Figure 1.1.

Extending from specific serine residues on the core protein, GAGs are linear polysaccharides with varying sulfation patterns. Each chain consists of repeating disaccharide units of hexosamine, either glucosamine or galactosamine, and hexuronic acid, either glucuronic or iduronic. This diversity allows the classification of GAG chains into four major types. HS chains have repeating disaccharide units of *N*-acetyl glucose-



amine (GlcNAc) and either glucuronic acid (GlcA) or iduronic acid (IdoA). CS chains have repeating units of GlcA and N-acetyl galactosamine (GalNAc). DS chains have repeating units of GalNAc and IdoA/GlcA and KS chains have repeating units of galactose (Gal) and GlcNAc. Chains of different type can be found on the same core protein. For example, aggrecan has both KS and CS, but it is considered a chondroitin sulfate proteoglycan (CSPG) because it has a larger number of CS chains than KS chains. The disaccharide units of each type of GAG chain are shown in Figure 1.2. It is the repeating units that provide the heterogeneity of the GAG chains themselves. Within each major type, the disaccharide units can vary in glycosidic linkage, type of sugar, and number of the sulfate groups. This provides additional heterogeneity and gives GAGs a unique, nontemplated assembly that allows for multiple functions of a single GAG chain. The two of the major types of GAG that dominate glycobiology research are HS and CS. It is these molecules that are the focus of this work.

### 1.1.2 Biosynthesis of glycosaminoglycans

Biosynthesis of GAGs is a nontemplated process that requires the use of many different enzymes, sugar activators, and transporters. It has been shown that the expression of these enzymes and transporters is tightly controlled developmentally and occurs in a tissue-specific manner. Temporal and spatial control creates a diverse set of fine structures and can result in PGs in two separate tissues with the same core protein but different GAG chain structure<sup>3-6</sup>.

Figure 1.3 depicts HS and CS biosynthesis. Biosynthesis begins with the xylosylation step. During this step, Xylosyltransferase transfers a xylose (Xyl) residue

from a UDP-xylose to a specific serine residue present within the core protein. This begins the formation of the linkage region found in GAGs. After the addition of the xylose, two galactosyltransferases (GALT-I, GALT-II) add two Gal residues followed by the addition of GlcA by glucuron transferase-I (GLCAT-I) to complete assembly of the linkage region. This linkage region can be further modified through phosphorylation and/or sulfation of Xyl or Gal residues<sup>3</sup>. The addition of a 1,4 linked GlcNAc as a fifth residue dictates the formation of HS, whereas the addition of a 1,4 linked GalNAc at the fifth residue directs the synthesis of CS. The mechanism that regulates the addition of the fifth residue is largely unknown.

HS/CS chain biosynthesis consists of two main steps: extension and modification. For HS, following the addition of the GlcNAc after the linkage region, exostosins, EXT1 and EXT2, add repeating disaccharide units of GlcA and GlcNAc to extend the chain. While extension occurs, other enzymes follow behind the exostosins and modify the GAG chain<sup>3</sup>. This is believed to take place in the Golgi apparatus in specialized compartments which house specific enzyme complexes called GAGOSOMES.

The gateway modification appears to be the *N*-deacetylation and *N*-sulfation of GlcNAc residues by the *N*-deacetyl-*N*-sulfotransferase (NDST) enzyme. *N*-sulfation is required or preferred for subsequent modifications. Immediately after *N*-sulfation, C5-epimerase (C5-Epi) can convert GlcA to IdoA. A variety of *O*-sulfotransferase (OST) enzymes can add sulfate groups to specific locations on the disaccharide unit. Sulfate groups can be added to C6 (6-OST) and C3 (3-OST) of glucosamine residues and C2 (2-OST) of IdoA predominantly and GlcA rarely<sup>3-6</sup>. These modifications are the result of the transfer of a sulfate group from 3'-Phosphoadenosine-5'-phosphosulfate (PAPS) to the HS

chain by the OST enzymes. PAPS is formed in animals by a single enzyme that has both a sulfurylase and kinase activity. However, in plants and fungi, PAPS synthesis is carried out by two separate enzymes. Figure 1.4 shows the cycle of PAPS production and use, requiring separate and fused enzymes<sup>7</sup>. Previous studies indicate that the concentration of PAPS partially controls the level of GAG sulfation<sup>7</sup>.

The OST enzymes are developmentally regulated as well as tightly controlled in a spatio-temporal manner. The OST biosynthetic enzymes have multiple isoforms. For example, four NDST, one C5-epimerase, one 2-OST, seven 3-OST, and three 6-OST isoforms have been found in humans and other organisms. Specificity of enzyme isoforms in regard to sulfation and polymer size have been studied *in vitro*<sup>8,9</sup>. Though it is unclear if this specificity is maintained inside the cell or if specificity is cell type dependent, controlled expression of enzymes leads to the creation of three domains in HS: highly sulfated domains (NS domains), nonsulfated domains (NA domains), and partially sulfated domains (NA/NS domains). These domains increase the complex architecture of the GAG chain. It is believed that the presence of GAGOSOMES, containing specific composition and location of HS biosynthetic enzymes, gives rise to these different domains as well as the influence of additional enzymes outside the cell such as sulfatase (SULF) which can remove 6-*O*-sulfate<sup>10</sup>. The diversity of structure provided by modifications in HS results in a wide array of biological function<sup>1,6</sup>. Understanding the structure-function relationship of HS and other molecules remains one of the most intriguing questions in the field of glycobiology.

CS chains are synthesized in a similar fashion. After formation of the linkage region, a GalNAc is added as the fifth residue. Chondroitin synthase enzymes then extend

the chain through the addition of repeating disaccharide units of GlcA and GalNAc. Modification of the chain by sulfation can occur at the C4 or C6 of the GalNAc residue as extension occurs. This sulfation is performed by the CS-specific sulfotransferases: chondroitin-4-sulfotransferase and chondroitin-6-sulfotransferase. Other than DS, one other CS has IdoA. Sulfation allows the classification of CS into specific classes: CS-A, CS-C, CS-D, and CS-E. DS chains were commonly referred to as CS-B, but are now primarily labeled as DS. The major difference in DS/CS-E versus other CS classes is the prevalent epimerization of GlcA to IdoA in the disaccharide units and the presence of a sulfate group at the C2 position of the IdoA<sup>11</sup>.

The modifications are believed to occur in specific compartments within the Golgi apparatus containing the specific enzymes complexes called GAGOSOMES<sup>9</sup>. There is also a large degree of heterogeneity and structural diversity in CS. The structure-function relationship of CS and binding ligands, as well as how the different classes can influence distinct biological functions, are the subject of much current research<sup>12,13</sup>.

### 1.1.3 Glycosaminoglycans in learning and memory

A variety of proteoglycans has been found to exist in both the developing and mature central nervous system (CNS). GAGs in the CNS are found to be primarily HS or CS and constitute part of the ECM or are located at the cell surface. These GAGs have many different functions in the CNS and multiple forms of the same core protein exist within the tissue. For example, there are four known mammalian syndecans, which are structurally similar but have distinct cellular distributions<sup>14,15</sup>.

HS plays a role in many neuronal processes and in neuronal development. During

development, HS is known to be involved in axon guidance, synaptogenesis, synaptic plasticity, patterning, and cell proliferation. Another major role is the interaction of HS and external ligands not only in the developing but also in the mature CNS<sup>14</sup>. These external ligands include growth factors, matrix ligands, and cell surface and cell adhesion molecules. Interactions of HSPGs with growth factors active in the CNS include: neural cell adhesion molecule (NCAM), fibroblast growth factor (FGF), Wnt, transforming growth factor- $\beta$  (TGF- $\beta$ ), and heparin-binding growth factors<sup>10,16-22</sup>. Interaction of HS with many of these external ligands is essential for the formation of many different neural structures and networks<sup>13,23,24</sup>.

CS is shown to affect axon growth, cell plasticity, and cell migration in the CNS. CS binds ligands such as NCAM, tenascin-C, and tenascin-R. The core protein from phosphacan, a CSPG, has been found to bind FGF-2. However, the primary function of CSPGs in neural development is to serve as barrier molecules to regulate growth and neuronal plasticity. CS can act as a repulsive cue during neuronal cell migration, axon growth, or elongation and after CNS lesion. Neurocan and phosphacan are present in large quantities during neuronal development, with neurocan being synthesized by neurons and phosphacan being made by astrocytes<sup>25</sup>. After development, brevican, the most predominant form of CS, is produced by astrocytes and serves as a component of the perineuronal network. The presence of these CSPGs is one of the main barriers to axon re-growth following injury. Digestion of these GAG chains with a CS degrading enzyme, chondroitinase ABC, results in enhanced axon elongation<sup>26-28</sup>.

Recent studies have begun to show a link between GAGs and the neurological processes involved in learning and memory. The interaction of GAGs with growth factors

as well as their involvement in synaptic plasticity and axon growth makes them viable candidates for affecting learning and memory. The most commonly studied form of learning and memory is the hippocampus-dependent spatial learning. One measure for this is hippocampal synaptic plasticity, which can be studied as changes in long-term potentiation (LTP). LTP also serves as a measure for activity-dependent plasticity in the hippocampus. Spatial learning and memory are often, but not always, correlated with LTP in the hippocampus<sup>29</sup>.

HS can act as a modulator of synaptic plasticity in the hippocampus. Synaptic modification can regulate the plasticity of learning and memory in the brain. This can be seen in syndecan deficient mice. Syndecan-3 deficient mice show enhanced LTP in the CA1 region of the hippocampus. This occurs because syndecan-3 in wildtype (WT) mice responds to a ligand that is a heparin-binding growth-association molecule. This molecule inhibits LTP in the CA1 region of the hippocampus<sup>29</sup>. Syndecan-2 plays a role in dendritic spine development in hippocampal neurons. Spine formation and changes in spine morphology are known to occur in LTP, sensory deprivation, some forms of mental retardation, and autism<sup>30-33</sup>. Maturation of dendritic spines in the hippocampus is important for learning and memory. Syndecan-2 is localized to dendritic spines and appears during the time frame for development and maturation of the spines. When syndecan-2 expression is induced in hippocampal dendrites in young neurons, there are morphological changes in the protrusions that would be dendritic spines. These changes were similar to those found in mature neurons<sup>34</sup>. Changes in sulfation patterns of HS can also lead to alterations in synaptic plasticity in the hippocampus. Mice deficient in SULF1 or SULF2 have aberrant neurite outgrowth in hippocampal and cerebellar neurons. These sulfatases are responsible

for removing specific 6-*O*-sulfate groups from HS. The removal of these sulfates modulates signaling pathways involved in development and homeostasis. A loss of the SULF1 enzyme results in a reduced hippocampal spine density and impaired LTP in the CA1 of the hippocampus<sup>35</sup>.

CS can also affect synaptic plasticity in the hippocampus. Removal of CS from the hippocampus can result in altered synaptic plasticity as seen by changes in LTP. When hippocampal slices were pretreated with chondroitinase ABC to remove all CS, subsequent treatment with chondroitinase ABC did not affect single pulse excitatory synaptic transmission or short-term plasticity. However, LTP in CA1 of the hippocampus was reduced. The loss of the tenascin-R ligand results in increased single pulse transmission and reduced short-term plasticity. LTP is reduced in a manner similar to enzyme treated slices<sup>36</sup>. Neurocan deficient mice show no change in early phase LTP but show impairment in late-phase LTP<sup>37</sup> and mice deficient in brevican, which is found in the adult brain, show a lack of LTP<sup>38</sup>. The differences in effects of neurocan, which is prevalent earlier in development, and brevican, which is more prevalent in the adult nervous system, show that the different CSPGs are involved in the different stages of LTP<sup>39</sup>.

While these changes in hippocampal synaptic plasticity lay the ground work for the argument for the involvement of GAGs in learning and memory, simple changes in LTP are not sufficient as evidence for changes in learning. In order to better examine the relationship between GAGs and learning, it is necessary to examine behavioral changes that may result from alterations in GAGs in the CNS. A number of learning and memory task assays, such as operant chambers, radial arm mazes, water mazes, and delayed match to sample, have been used to examine the relationship between GAGs and learning and

memory. Both HS and CS can affect learning and memory as seen by altered behavior.

Alteration of LTP in the hippocampus due to HS can also affect the behavioral response of the animals. In syndecan-3 deficient mice, deficits in hippocampus-dependent forms of learning and memory were observed. Syndecan-3 deficient mice were impaired in the water maze test and showed reduced context-dependent freezing in response to fear conditioning<sup>29</sup>. More evidence for the role of HSPGs in learning and memory is found by the deficits that are seen in mice that are deficient in SULF1 and SULF2. These SULF-deficient mice showed deficits in neuromotor test performance and learning performance. SULF2-deficient mice show a reduction in grip strength and a deficiency in the water maze task as seen by slower escape latency. SULF1-deficient mice showed a reduction in nocturnal exploration and slower rate of acquisition during the water maze task<sup>35</sup>.

HS can also be linked to enhanced learning in rats. The injection of heparin, a complex polysaccharide closely related to heparan sulfate, into the ventral pallidum after learning had occurred facilitated both the short-term and long-term retention of a conditioned avoidance response task. These effects followed an inverted u-shaped curve and were only present if heparin was administered immediately after the task. A delay of the injection by 5 h no longer produced the effect. The mechanism behind this improved performance is still unknown but could be related to growth factor signaling or the influence of extra-synaptic communication through heparin-binding molecules<sup>40</sup>.

The effects of CS on behavioral aspects of learning and memory have been examined in mutants. While some mutants show alterations in LTP, some have no apparent effects on learning and memory. Brevican-null mice, who lack LTP, show no obvious deficits in learning and memory in a behavioral task<sup>38</sup>. Additionally, learning can be



facilitated by CS. Biglycan and CS-C, injected into the ventral pallidum, facilitate learning. Injections of biglycan immediately after training influenced the performance and facilitated inhibitory avoidance learning, while delayed injections after training did not affect performance, suggesting that the CSPG most likely influences memory storage rather than retrieval. Biglycan also shows facilitation of habituation of exploratory learning. Injections of CS C also improved habituation learning<sup>41</sup>. CS is also known to be involved in fear learning. CS makes up a large portion of the perineuronal nets (PNNs) around the amygdala and are thought to protect fear memory formation. Destruction of the PNN using chondroitinase ABC makes subsequently acquired fear memories susceptible to forgetting, and subjects showed no spontaneous recovery<sup>42</sup>. These examples show that the effect of CS on learning and memory is CS class and learning/memory task dependent.

Evidence for the involvement of GAGs in learning and memory is slowly accumulating. This evidence provides a strong foundation for future research that focuses on GAGs in various aspects of learning and memory and for the exploration of the mechanisms that are responsible for these changes at both the synaptic and behavioral level. Along with being involved in normal learning and memory, as well as synaptic plasticity, GAG chains and their sulfation moieties play important roles in abnormal states, including Alzheimer's disease, glioma, and the mental deficiencies seen in lysosomal storage disorders.

Alzheimer's disease patients show signs of cognitive deficits such as memory loss, inability to learn, and confusion. Currently, there is no positive diagnostic test for Alzheimer's and the diagnosis can only be confirmed upon autopsy. Alzheimer's disease is caused by the accumulation of neuritic plaques and neurofibrillary tangles in the cortex.

One of the major components of the plaques is amyloid protein and co-localized with these deposits is highly sulfated heparan sulfate<sup>43</sup>. Previous studies have shown that the heparan sulfate that co-localizes with these deposits is more highly sulfated than heparan sulfate found in other areas of the cortex. It has also been shown that the source of this highly sulfated HS is the nearby neuronal population and that HS is important for regulation of the  $\beta$ -secretase (BACE1). HS and heparin bind to BACE1 and inhibit cleavage of amyloid precursor protein (APP)<sup>44</sup>. Other GAG chains are found within these plaques, including CS and DS, and may contribute to plaque formation and overall progression of the disease. HS, CS, and KS can all interact with  $\beta$ -amyloid peptides and enhance the shift of A $\beta$ 42 peptides to the  $\beta$ -sheet confirmation. GAGs have also been shown to be involved with aggregation and precipitation of the fibrils. This aggregation leads to a loss of solubility and increases neurotoxicity. Low molecular weight (LMW) heparin can compete with endogenous HS and inhibit the formation of fibrils<sup>45,46</sup>. The sulfate moiety present on the heparan sulfate is important for the formation and progression of these neuritic plaques. Nonsulfated GAGs have no effect on fibril formation and aggregation<sup>46</sup>.

Sulfated GAGs have also been implicated in Alzheimer's-like changes seen in Tau protein. Incubation of this protein with heparin results in the formation of Alzheimer's-like filaments and promotes the phosphorylation of Tau. This phosphorylation prevents the binding of the Tau protein to stabilized microtubules and results in the rapid disassembly of microtubules assembled from Tau and tubulin. The effects seen from a variety of GAGs are proportional to the amount of sulfation present on the chain<sup>47</sup>.

Proteoglycans are also involved in a variety of mechanisms for the survival and metastasis of glioma. A glioma is a tumor in the central nervous system that arises from

the glia. For this cancer to be invasive, it must deal with the unique environment of the brain, which is fundamentally different from the rest of the body. For example, the neural ECM is naturally resistant to cell and neurite motility. A major component of this inhibitory practice is the presence of CS. Previous studies show that the CSPG brevican is upregulated in gliomas and appears to play a role in cellular dispersion of the glioma. Brevican must be cleaved by metalloproteases in order to promote cell motility with the cleaved N-terminal being sufficient to promote dispersion<sup>48</sup>. HS is also upregulated in some gliomas. HS found in gliomas have been shown to interact with growth factors that promote glioma growth and invasion. Specifically, several of these HS chains promote the activity of FGF-2 signaling and its mitogenic properties<sup>49</sup>. However, the GAG chains also play an important role in glioma progression.

Not only the presence of GAG but the sulfation as well can alter the behavior of glioma cells. Studies have examined how sulfation density affects glioma proliferation and invasion. Reduction of sulfation using sodium chlorate treatment on GAGs produced by glioma cells resulted in lower levels of cell proliferation<sup>50</sup>. Intracerebral inoculation of glioma cells pretreated with sodium chlorate also led to a decrease in instances of glioma in treated animals and reduced tumor size. This resulted in longer survival of treated animals<sup>51</sup>. Changes are also seen in specific sulfation patterns present on HS. Enhanced FGF-2 activity is correlated with higher sulfation levels in the HS present in gliomas with a higher amount of 2-*O* and 6-*O*-sulfations<sup>49</sup>.

Alterations of normal GAG levels and sulfation are also seen in a variety of other neurological disorders, including epilepsy, Parkinson's, and schizophrenia. In epilepsy, increases in CS and HA are seen in the hippocampus of mesial temporal lobe of patients<sup>52</sup>.

HS has been indicated to be associated with Parkinson's disease lesions through interaction with fibril formation similar to that found in Alzheimer's disease<sup>53</sup>. Increases of CS were found in the glia in the amygdala and entorhinal cortex but reductions were seen in the extracellular space in these nuclei<sup>54</sup>. While GAGs are altered in these disease states, the full extent of their involvement in the initiation and progression of these disorders remains unclear. Research into the role of GAG and whether changes in GAG are a symptom, cause, or effect of the disease requires further study. For a full review of GAGs in nervous system injury and disease, see Appendix A.

#### 1.1.4 Glycosaminoglycans at the neuromuscular interface

GAGs are also present in skeletal muscle and at the neuromuscular junction (NMJ). As in the CNS, GAG composition in muscle is regulated during development. CS is tightly regulated and controlled during development. The mouse myogenic cell line C2C12 shows that PG expression is modulated during myogenesis. Changes in sulfation and expression affect *in vitro* myogenesis in myoblasts as well as isolated myofibers. These PGs are also responsible for binding growth factors, which affect skeletal regeneration and repair, such as FGF, hepatocyte growth factor (HGF), and TGF- $\beta$ <sup>55</sup>.

Beyond development, GAGs are involved in skeletal muscle maintenance, function, and recovery after injury. After injury to the skeletal muscle, perlecan, glypican, syndecan-3, and syndecan-4 are upregulated with transient expression seen 5 to 7 d after injury. Syndecan-3, specifically, is detected earliest. The presence of syndecan-3 in myoblast plasma membrane is essential for proper fiber formation in myoblast transplant studies, as disruptions of syndecan-3 expression result in a lack of differentiation in

myoblasts. The lack of myoblast differentiation inhibits muscle repair. This aspect of muscle repair is likely a HS-specific effect as decorin, a CS/DS PG, remains unchanged during this same timeframe<sup>56</sup>. However, CS is not without its importance. Decorin and biglycan can be involved in skeletal muscle regeneration and differentiation, specifically in the binding of TGF- $\beta$ . TGF- $\beta$  can inhibit myoblast differentiation after injury. Both of these CS/DS PGs modulate TGF- $\beta$  availability for transduction receptor binding and this modulation of bioavailability of TGF- $\beta$  is believed to help prevent TGF- $\beta$  inhibition of myoblast differentiation. Without decorin, myoblasts show an increased binding of TGF- $\beta$  to receptors TGF- $\beta$ RI and TGF- $\beta$ RII as compared to WT<sup>57</sup>.

GAGs are also involved in the signaling that occurs between neurons and muscle at the NMJ. GAGs are associated with acetylcholine receptor (AChR) organization and acetylcholinesterase (AChE) tethering. The most prominent PG found at the NMJ is agrin. Agrin is a HSPG that can be found expressed in both neurons, developing myotubules, Schwann cells, and is present in the basal lamina throughout the embryo<sup>58</sup>. Named for its ability to induce aggregation of a variety of other proteins in the membrane, matrix, and ECM, an alternatively spliced form of this HSPG is synthesized by motor neurons and is more active than that expressed elsewhere. This alternatively spliced agrin is released from the motor neuron into the synapse and is believed to assist in the synthesis of the postsynaptic apparatus necessary for muscle innervation by becoming stably associated with the basal lamina and aggregating the necessary proteins, such as AChRs, to develop and maintain the NMJ<sup>58,59</sup>. Deficiencies in agrin lead to defective synaptogenesis and AChR clustering at the NMJ in mice<sup>60</sup>.

In addition to the clustering of AChR, GAGs are involved with AChE at the NMJ.

In the vertebrate NMJ, there is a concentration of collagen-tailed AChE. This form of AChE consists of three tetramers covalently attached to a collagen-like tail and is preferentially expressed where the motor neuron innervates the muscle. Heparin has been shown to solubilize the asymmetric AChE<sup>61</sup> and HS is likely to be involved with tethering of AChE at the NMJ. Mice deficient in perlecan, a HSPG found in the ECM, exhibit a lack of this form of AChE in the NMJ. This indicates that perlecan likely serves as an acceptor for collagen-tailed AChE and is largely responsible for the localization of collagen-tailed AChE. Perlecan is in turn bound to dystroglycan. It is this complex that anchors AChE to the NMJ<sup>62,63</sup>.

Our knowledge of the effects of HS and CS in skeletal muscle and the NMJ is still incomplete. Knocking out the protein portion of the PG has provided information about the overall effect of PGs at the NMJ. However, this finding does not specify if the effect is due to the protein or the GAG chain. Many of these studies focus on muscle formation and innervation during development or muscle recovery after injury<sup>55-63</sup> but do not address the role GAGs play in the function of healthy adult muscle or how changes in the presence of GAG or GAG fine-structure can alter the mechanical or electrical properties of muscle, and the results these changes may have in biologically relevant situations such as locomotion or vocalization.

## 1.2 Glycosaminoglycans in speech and song

### 1.2.1 Implication of glycosaminoglycans in speech disorders

Deafness and resulting communication disorders affect people of all ages around the world. Some causes of deafness can be treated with a cochlear implant. However,

development of language is best facilitated if these implants are done between the ages of 2 and 6 in children and are coupled with intensive speech therapy. This age limitation reflects a critical period for language learning<sup>64,65</sup>. After closure of this critical window, the success rate of language acquisition for children with cochlear implants decreases. Effective treatment of speech disorders in adults and young children is critically linked to neural plasticity and recovery of injury to the vocal fold, but little is known about which underlying biochemical functions influence these processes for both the learning of speech in children and continued production in adolescents and adults.

GAGs have been implicated in many different diseases both somatic and neurological. The most obvious circumstance of GAG-induced disease is that of the lysosomal storage disorders. These disorders, called Mucopolysaccharidoses (MPS), are caused by deficiencies in the enzymes that break down GAG chains. These diseases are classified based on the deficient enzyme and often divided further into various syndromes based on clinical presentation. For example, MPS type I is caused by a lack of  $\alpha$ -iduronidase and is further divided into three groups: Hurler syndrome, Hurler-Scheie syndrome, and Scheie syndrome. The symptoms of these range from severe to mild, respectively. Within these disorders, a variety of developmental and behavioral issues arise. Communication disorders can be seen in these patients. Children with severe forms of MPS type I have been found to have minimal language skills. This deficit is largely attributed to a combination of physical malformations, hearing loss, and developmental delays<sup>66</sup>. This provides the most direct evidence of the importance of GAG biosynthesis for proper development of complex sensorimotor integrated behaviors like speech, and alterations in GAG populations leading to long-term deficits or alterations in normal

behaviors, like speech.

Language delays and communication deficits are often seen in the autism spectrum disorders as well. The BTBR T+tf/J mouse has recently emerged as a model for autism. BTBR mice show several autism-like characteristics that strengthen their use as a model including: poor social learning, lower level of vocalizations, an unusual repertoire of ultrasonic vocalizations during pup separation, and repetitive grooming behaviors. These mice show a reduction in fractone-associated heparan sulfate in the subventricular zone (SVZ), suggesting that the presence of HS in the subventricular zone (SVZ) in the lateral ventricles is important for normal neuroanatomy as well as behavior<sup>67</sup>. This example is not the only case that implicates HS in autism-like sociocommunicative deficits. Conditional inactivation of the *Ext1* in postnatal neurons causes impaired ultrasonic vocalizations in mice as well as other autism-like symptoms. Examining the electrophysiology after inactivation shows that HS is required for normal function of glutamatergic synapses<sup>68</sup>. These studies implicate GAGs in neural control of vocalizations. Through changes of enzymes important for GAG biosynthesis or a reduction in SVZ HS, vocalizations are altered.

### 1.2.2 Glycosaminoglycans in the vocal organ

GAGs are not only important to the neural aspect of vocalizations but also required for proper formation and utilization of the vocal organ. The vocal folds consist of connective tissue stretched across the larynx and are capable of self-sustained oscillation, which generates sound, including speech. The vocal folds are attached to both cartilages and muscles and their core contains muscle fibers. The majority of the vocal folds consists



of ECM, which gives it its elastic properties and enables rapid movement without physical damage. High-frequency vibratory behavior affects ECM composition. Exposure of fibroblasts that were cultured in hydrogels to high-frequency vibrations resulted in altered mRNA expression. Specifically, hyaluronic acid (HA) synthase 2, decorin, fibromodulin, and matrix metalloproteinase-1 were temporally up regulated. The controlled regulation of these molecules, which are most commonly found in the ECM, provides evidence that ECM development and maintenance responds in part to exposure to vibrational stimuli which are common in speech or other vocalizations<sup>69</sup>.

The presence and location of ECM proteins such as PGs are expressed in an age-dependent manner<sup>70,71</sup>. In conjunction with the skeletal muscle controlling the vocal organ, arrangement of the ECM in the vocal folds has been shown to play a role in determining the biomechanics of voice production<sup>72,73</sup>.

The role of GAGs and ECM in vocal folds can also be seen after injury. It is estimated that voice dysfunction occurs in 3% to 9% of the population at any time. The etiology for these dysfunctions is relatively unknown but injury is believed to be responsible in most cases. These injuries can affect the expression and maintenance of ECM components, including GAGs, which may play a role in voice dysfunction<sup>74</sup>.

To study the role of GAGs in vocal learning and production, the use of a good model system is required. Songbirds are one of the few other species in which development of species-specific acoustic behavior involves vocal learning. Songbirds learn songs in a similar manner to how humans acquire speech. Using songbirds as a model system allows for the study of not only the production of vocalizations but vocal ontogeny as well.

### 1.2.3 Zebra finch as a model for speech

Sound production requires complex integration of sensory information and motor output filtered and controlled through brain nuclei. The zebra finch model system is ideal as it displays a well-researched timeline and developmental progression. In oscine songbird species, as in humans, vocal learning requires time and rehearsal. In these cases, male juvenile songbirds acquire an auditory template of conspecific song from an adult. This auditory template acquisition phase is often the first step in vocal development and is followed by a period of rehearsal. Both the acquisition and sensorimotor phase are usually limited by critical periods for vocal ontogeny<sup>75</sup>. Again, this mirrors human speech development as humans also have a critical period for speech development as evidenced by cases of extreme neglect in children<sup>76,77</sup> and some cases of deafness<sup>78,79</sup>.

One of the most commonly studied songbirds for vocal learning is the zebra finch (*Taeniopygia guttata*). In zebra finch, only the males exhibit song learning and production. The timeline for the development of song and the neural circuitry for song learning and production has been extensively characterized in this species. Zebra finches are age-limited or sensitive period learners, and males therefore sing an invariant song after reaching adulthood (approx. at age 90 d post hatch, PHD). This age-limited plasticity is in contrast to open-ended learners, such as the canary or starling, which can develop new songs seasonally even after the first year of life<sup>80</sup>. The model used in this thesis is the zebra finch model of song.

Male zebra finches acquire their song in the first 80 PHD using song from one or more adult males to which they are exposed<sup>81,82</sup>. This timeframe has been broken into two critical periods. The first is a critical period for acquisition of the auditory template. This

sensitive period is between 25 and 50 PHD. Males begin to generate song-like vocal behavior at 28-35 PHD and these songs have poor syllable structure and syntax. This song is then rehearsed by the juvenile until around 90 PHD. During this time, the song becomes more stereotyped and begins to closely resemble the tutor song or songs, which leads to crystallization, or the formation of stable adult song. Crystallization marks the end of the second critical period, the sensorimotor period<sup>81-84</sup>. See Figure 1.5 for the timeline of zebra finch learning.

The neurological circuits involved in song learning and production in zebra finch also have been well characterized. The neural control system for song production and learning consists of many discrete brain nuclei. Two distinct circuits exist for production and song plasticity: the anterior or learning pathway and the posterior or production pathway. A simplified schematic of these pathways can be found in Figure 1.5. The learning pathways consists of connections between anterior forebrain nuclei and follows a hierarchical pathway. This pathway begins with HVC (proper name), then Area X, the medial nucleus of the dorsolateral thalamus (DLM), and the lateral magnocellular nucleus of the anterior neostriatum (LMAN). From LMAN, the information flows to the production pathway, which involves the posterior forebrain nuclei, including the robust nucleus of the arcopallium (RA) and the hypoglossal motor nucleus (nXIIts). nXIIts then innervates the muscles of the trachea and syrinx, the bird's vocal organ. HVC is also connected to RA and is considered to be a part of both the learning and production pathways<sup>85-87</sup>.

Lesions in the learning pathway, with few exceptions, show little effect on stereotyped adult song, indicating that this pathway's primary importance occurs during

development. Evidence from several different experimental approaches, including electrophysiological recordings, molecular manipulations, and lesions studies, suggests that the anterior forebrain learning pathway is not involved in the production of stereotyped song in adult zebra finch<sup>88,89</sup>.

#### 1.2.4 Glycosaminoglycans in zebra finch song system

The well-characterized and specialized neural circuitry for song production makes it particularly well suited for investigating the role of GAGs in the acquisition and production of this complex behavior. As with humans, PGs and sulfated GAGs are found in the vocal organ and song system of the zebra finch. The sound-generating labia in the syrinx of the zebra finch, as well as other songbird species, contains collagen, elastin, HA, and GAGs. The presence, distribution, and expression of these molecules may be responsible for differences in the fine acoustic structure of song<sup>91,92</sup>. Neurologically, PGs are involved at every level of vocal ontogeny and production through the presence, modification, and interaction with other factors. Table 1.1 provides an overview of known PGs, modifying enzymes, and associated factors found in song-specific nuclei and known situations for expression.

Both HSPGs and CSPGs are expressed in song-specific nuclei<sup>93-97</sup>. Several OST enzymes required for GAG biosynthesis are developmentally regulated. Others such as 6-OST, sulfatase-2, and chondroitin sulfate glucuronyltransferase appear to be specifically regulated during vocal learning<sup>93-97</sup>. It is likely that the two major types of GAGs, HS and CS, play a major role in song learning and production. The better studied of the two GAG types in song development and production is CS. HS is present and the enzymes that

modify it appear to be developmentally regulated. CS occurs in the form of perineuronal nets (PNNs) in most major song specific nuclei, including LMAN, Area X, HVC, and RA, and their expression can be sexually dimorphic. Whereas PNNs in the nuclei of the anterior forebrain pathway were indistinguishable between the sexes, nuclei in the posterior pathway in females showed little to no PNN as compared to males<sup>103</sup>. PNNs are often used as markers for the end of critical periods, and their presence in these nuclei has been linked to song development. The level of CS staining in both HVC and RA was correlate with song maturity, with the greatest CS staining seen in RA at the mature song stage. This was true, even if the vocal period was shifted and a lack of CS staining was seen in isolate birds, or birds raised without auditory input. This study served as the first actual characterization of the developmental control of GAGs in any song nucleus, noting that total production was modulated by vocal development as evidenced by the lack of CS in isolates<sup>104</sup>.

### 1.3 Research Objectives

GAGs serve roles in both the development and production of vocalizations. Studies have linked PGs and GAGs to both the neural and muscular control of vocal learning and production. The existing data infer importance of GAG after injury or correlation of GAG presence with learning during development. Further research is needed to gain a more refined understanding of the role of CS and HS in a complex biological system such as vocal ontogeny and production. Our focus is the role of GAGs in vocal ontogeny and production at both the neural and muscular level. We will be using the zebra finch song system as our model of behavior. However, studying GAGs serves as a challenge. The methods commonly used for GAG manipulation are limited and do not allow for complete

comprehension of their role in biological systems. Our primary goal is to generate GAG based biochemical tools to obtain novel insights on vocal development. Our major questions are: What are the tools available for the manipulation of GAGs and can we expand that toolbox? Will the current tools be effective for *in vivo* studies of vocal production in zebra finch? How important is the biosynthesis of GAGs during vocal ontogeny? Finally, how do alterations of GAG profiles in syringeal muscles affect stereotyped vocalizations?

To answer these fundamental questions, one needs to create and test an array of GAG based biochemical tools. After creating and validating the molecular tools, two approaches are implemented for further investigation. The first approach involves the utilization of xylosides, synthetic small molecules that can initiate the formation of single CS chains and also serve to inhibit the endogenous GAG production<sup>105</sup>, to examine the role of CS in the RA during vocal development in the zebra finch. The second approach involves the utilization of enzymatic degradation to examine how removal of HS from the syringeal muscle can change the stereotyped vocalizations in adult zebra finches.

### 1.3.1 Chapter 2

**The production and validation of molecular tools is required for the study of glycosaminoglycans in vocal learning and production.**

GAGs have been shown to play important roles in neural development and muscular maintenance and function. In studying these roles, researchers have been limited by tools and techniques to examine structure-function relationships, required sulfation for binding, and differentiation between the effects of core protein and GAG modulation. In

order to adequately explore these areas of research, it is necessary to create, understand and expand the toolbox for glycol-specific manipulations. For use in the current and future studies, we needed to create and characterize small molecules, enzymes, polymers, and specifically sulfated oligosaccharides to provide a wider range of understanding about specific roles. To validate that our molecular approach does alter song in our chosen model system, the effect of enzymatic degradation of HS in HVC on adult stereotyped song production was also investigated.

### 1.3.2 Chapter 3

#### **Modulation of CS biosynthesis in RA through direct infusion of small molecule xylosides leads to a change in vocal ontogeny in juvenile zebra finches.**

CS has been shown to serve as the marker for the end of critical periods in sensory and sensorimotor learning. In the zebra finch, deposits of CS, in the form of PNNs, appear in song-specific nuclei during vocal ontogeny. The formation of these PNNs appears to be dependent upon vocal learning as isolates or birds raised with no auditory feedback do not exhibit normal PNN development. The song-specific nucleus RA shows increased CS at the end of the sensorimotor phase of song learning with a complete PNN seen when the bird reaches the age of mature song<sup>104</sup>. Using a direct infusion of xyloside into RA early in vocal ontogeny, we were able to examine how modulating CS biosynthesis during the critical period for sensorimotor learning has lasting effects on song development.

### 1.3.3 Chapter 4

#### **Degradation of HS in syringeal muscle alters sound amplitude, pressure, and acoustic structure of stereotyped vocalizations in adult zebra finches.**

Complex vocalizations require integration of both neural and muscular control. HS has been shown to be vital to the development and maintenance of skeletal muscle and should therefore also play a role in the muscles that control the syrinx. However, there have been no studies to elucidate how the temporary removal of HS alters muscle function, such as the superfast muscle of the syrinx, and consequently affects song features. Therefore, by employing the use of heparan sulfate lyases, we were able to study how a loss of HS in the syrinx alters muscle function, song, and somatosensory systems, revealing a complex role of GAG in muscular control of song production. The results from this study provide some of the first evidence for the importance of GAGs in both vocal ontogeny and production.

### 1.3.4 Summary

Song is a complex behavior that requires complex sensorimotor integration during development and our results show that altering GAG biosynthesis early in this critical period can alter the developmental trajectory permanently. Additionally, the role of HS in syringeal muscle function indicates that acute changes to muscle activity can have both short- and long-term effects on vocal production and provides a unique tool for examining the sensitivity of the proprioceptive feedback loop for song. Both of these results open new doors for continued study of GAGs in vocal ontogeny and production with the goal of providing new avenues for treatment, therapies, and understanding for those who suffer



from communication disorders. However, to fully understand these results, it is necessary to expand and refine the tools and methods available for exploring the role of GAGs in any biological system.

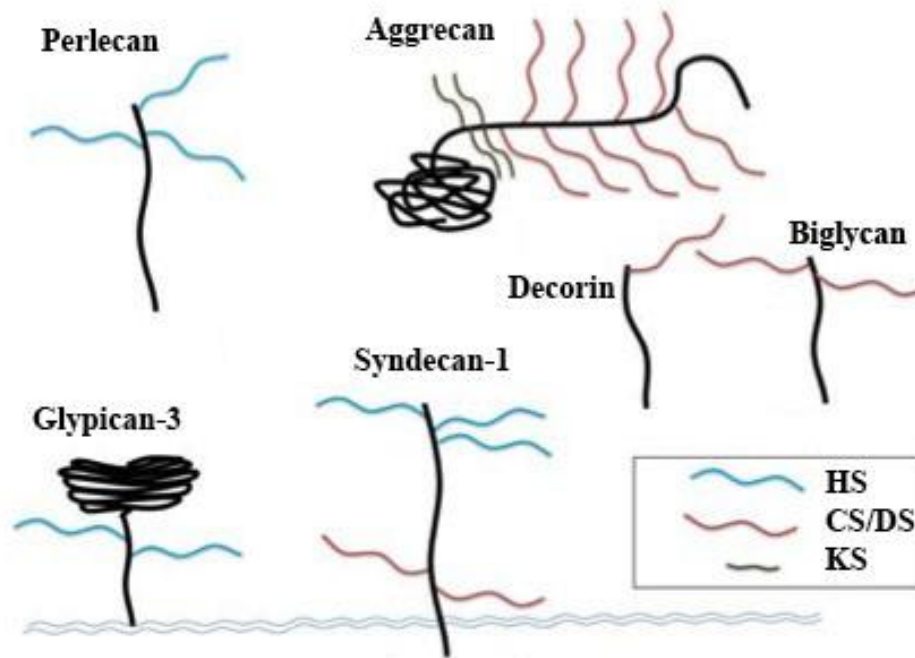


**Figure 1.1** Examples of the different structures of a few proteoglycans.<sup>2</sup> GPI-linked PGs at the cell surface such as Glypicans, transmembrane proteins including syndecans, PGs with globular domains such as aggrecan, and secreted PGs such as perlecan, decorin, and biglycan which contain few or many GAG chains.

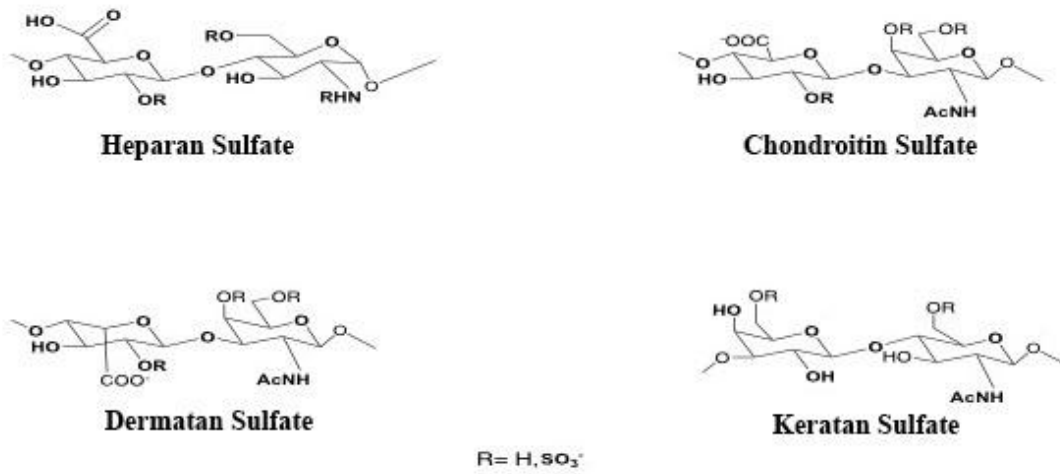


**Figure 1.2:** Disaccharide units for each type of GAG including all possible sites for modification by *O*-sulfotransferase.

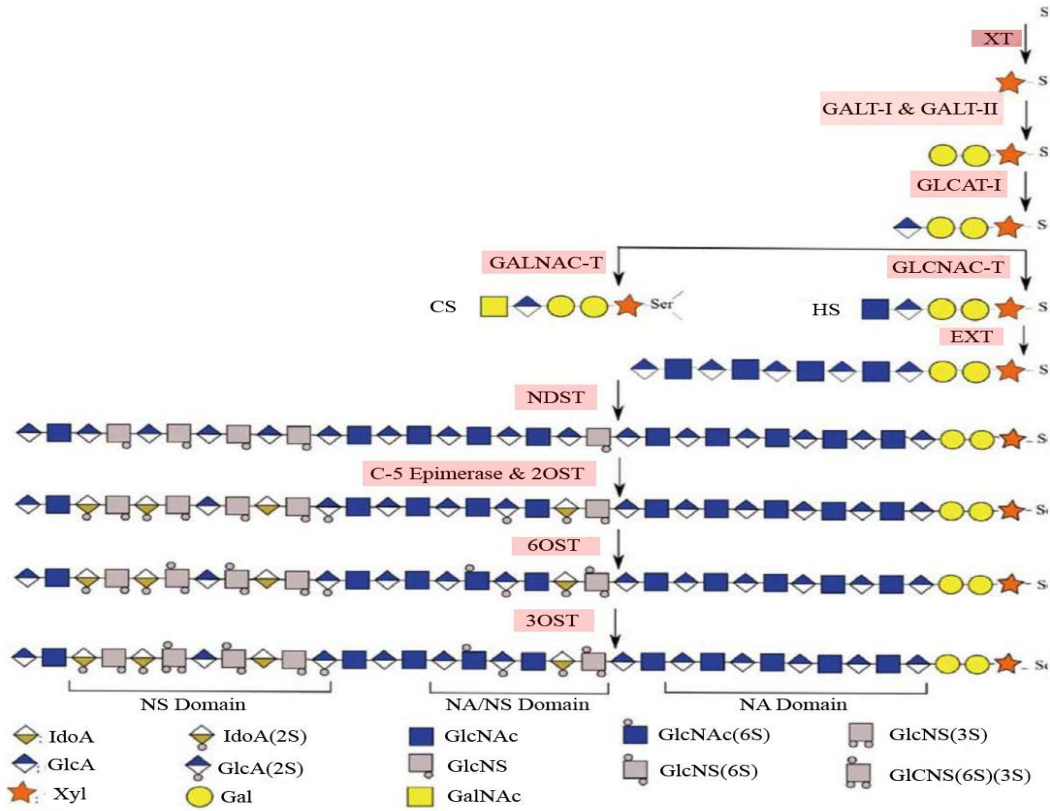


**Figure 1.3:** Illustration of GAG biosynthesis; for a detailed description see text; adapted from<sup>3</sup>

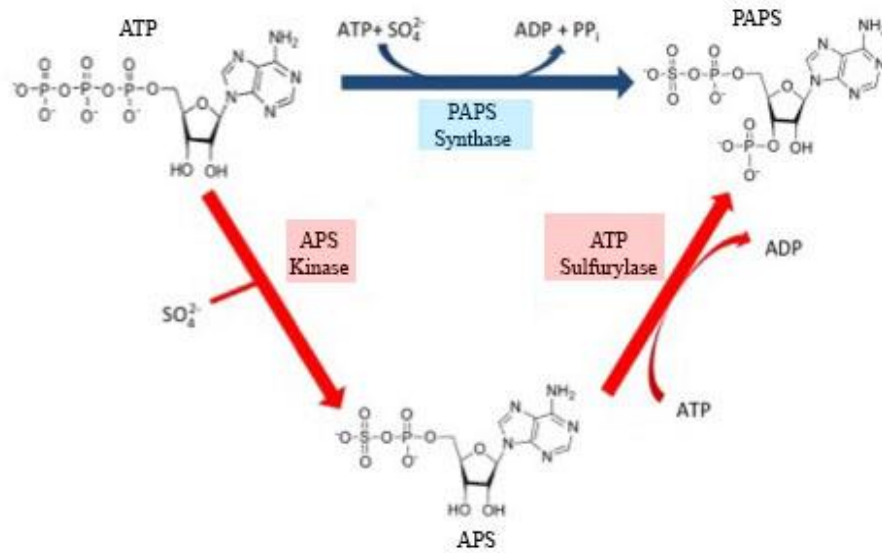


**Figure 1.4:** The production of PAPS as a substrate for the modification of GAG chains. Two pathways, one in plants, fungi and some animals (red arrows), require two separate enzymes while a bifunctional enzyme found in humans and other animals (blue arrow) directly converts ATP into PAPS.

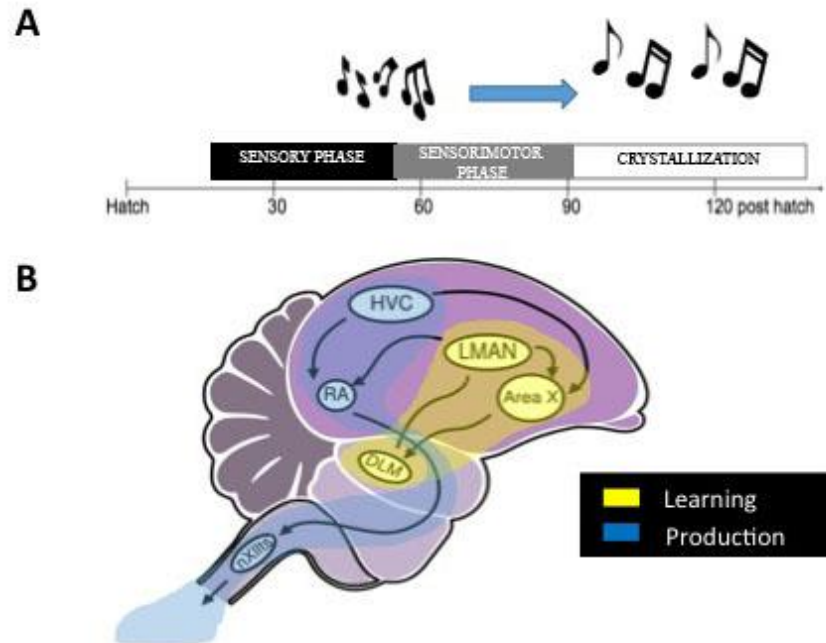


**Figure 1.5** Timeline and neural circuitry for song learning in zebra finch. (A) Timeline for learning in the zebra finch. (B) A simplified cartoon of the song system in the avian brain. The yellow pathway is the learning pathway. The blue pathway signifies the motor or vocal production pathway.

**Table 1.1** Proteoglycans and associated enzymes and factors found in the zebra finch brain and known associations to song

Category	Type found in zebra finch brain
Heparan Sulfate Proteoglycans	Syndecan-2,4, similar to 3; Glypican-similar to 1,3,4,5,6 <sup>93-97</sup>
Chondroitin Sulfate Proteoglycans	CSPG2 (versican); CSPG6; similar to CSPG5; similar to CSPG3 <sup>93-97</sup>
Heparan Sulfate Modifying Enzymes	6-OST (silent and singing males); 6-OST1 (post-hatch development); sulfatase-2 (learning conditions) <sup>95,96</sup>
Chondroitin Sulfate Modifying Enzymes	Chondroitin sulfate glucuronyltransferase (found in forebrain nuclei during vocal learning) <sup>95,96</sup>
Heparan Sulfate Proteoglycan Associated Factors Found in Song Nuclei	Insulin-like Growth Factor <sup>98,99</sup> ; wnt <sup>99,100</sup> ; bone morphogenic protein (BMPs) <sup>99,100</sup>
Chondroitin Sulfate Proteoglycan Associated Factors Found in Song Nuclei	TGF- $\beta$ <sup>100,101</sup> ; Tenascin-R <sup>100-102</sup>

#### 1.4 References

1. Varki, A.; Cummings, R.; Esko, J.; Freeze, H.; Hart, G.; Marth, J. *Essentials of glycobiology*, 2<sup>nd</sup> Ed; Cold Spring Harbor Laboratory Press, 1999.
2. Perrimon, N.; Bernfield, M. Specificities of heparan sulphate proteoglycans in developmental processes, *Nature*, **2000**, *404*, 725-728.
3. Esko, J. D.; Lindahl, U. Molecular diversity of heparan sulfate, *J Clin Invest*, **2001**, *108*, 169-173.
4. Raman, K.; Kuberan, B. Chemical tumor biology of heparan sulfate proteoglycans, *Cur. Chem. Biol.*, **2009**, *4*, 20-31.
5. Bernfield, M.; Gotte, M.; Park, P. W.; Reizes, O.; Fitzgerald, M. L.; Lincecum, J.; Zako, M. Functions of cell surface heparan sulfate proteoglycans, *Annu Rev Biochem*, **1999**, *68*, 729-777.
6. Gandhi, N. S.; Mancera, R. L. The structure of glycosaminoglycans and their interactions with proteins, *Chem Biol Drug Des*, **2008**, *72*, 455-482.
7. Rosenthal, E.; Leustek, T. A multifunctional *Urechis caupo* protein, PAPS synthetase, has both ATP sulfurylase and APS kinase activities, *Gene*, **1995**, *165*, 243-248.
8. Nguyen, T.; Arungundram, S.; Tran, V.; Raman, K.; Al-Mafraji, K.; Venot, A.; Boons, G.; Kubern, B. A synthetic heparan sulfate oligosaccharide library reveals the novel enzymatic action of D-glucosaminyl 3-O-sulfotransferase-3a, *Mol Biosyst*, **2012**, *8*, 6009-614.
9. Liu, J.; Shworak, N.W.; Sinay, P.; Schwartz, J.J.; Zhang, L.; Fritze, L.M.S.; Rosenberg, R.D. *J Biol Chem*, **1999**, *274*, 5165-5192.
10. Esko, J.D.; Selleck, S.B. Order out of chaos: assembly of ligand binding sites in heparan sulfate 1, *Annu Rev biochem*, **2002**, *71*, 435-471.
11. Silbert, J.E.; Sugumaran, G. Biosynthesis of chondroitin/dermatan sulfate, *IUBMB Life*, **2002**, *54*, 177-186.
12. Telser, A.; Robinson, H.C.; Dorfman, A. The biosynthesis of chondroitin-sulfate protein complex, *PNAS*, **1965**, *54*, 912-919.
13. Grumet, M.; Flaccus, A.; Margolis, R.U. Functional characterization of chondroitin sulfate proteoglycans of brain: interactions with neurons and neural cell adhesion molecules, *J Chem Biol*, **1993**, *120*, 815-824.
14. Perrimon, N.; Bernfield, M. Cellular functions of proteoglycans-an overview, *Sem Cell Dev Biol*, **2001**, *12*, 65-67.



15. Bernfield, M.; Kokenyesi, R.; Kato, M.; Hinkes, M.T.; Spring, J.; Gallo, R.L.; Lose, E.J. Biology of the syndecans: a family of transmembrane heparan sulfate proteoglycans, *Annu Rev Cell Biol*, **1992**, *8*, 365-393.
16. Cole, G.J.; Loewy, A.; Glaser, L. Neuronal cell-cell adhesion depends on interactions of N-CAM with heparin-like molecules, *Nature*, **1986**, *320*, 445-447.
17. Kallapur, S.G.; Akeson, R.A. The neural cell adhesion molecule (NCAM) heparin binding domain binds to cell surface heparan sulfate proteoglycans, *J Neurosci Res*, **2004**, *33*, 538-548.
18. Nurcombe, V.; Ford, M.D.; Wildschut, J.A.; Bartlett, P.F. Developmental regulation of neural responses to FGF-1 and FGF-2 by heparan sulfate proteoglycan, *Science*, **1993**, *260*, 103-106.
19. Yayon, A.; Klagsbrun, M.; Esko, J.D.; Leder, P.; Ornitz, D.M. Cell surface, heparin-like molecules are required for binding of basic fibroblast growth factor to its high affinity receptor, *Cell*, **1991**, *64*, 841-848.
20. Inatani, M.; Irie, F.; Plump, A.S.; Tessier-Lavigne, M.; Yamaguchi, Y. Mammalian brain morphogenesis and midline axon guidance require heparan sulfate, *Science*, **2003**, *302*, 1044-1046.
21. Lin, X. Functions of heparan sulfate proteoglycans in cell signaling during development, *Development*, **2004**, *131*, 6009-6021.
22. Turnova, S.; Woods, A.; Couchman, J.R. Heparan sulfate proteoglycans on the cell surface: versatile coordinators of cellular functions, *Int J Biochem Cell B*, **2000**, *32*, 269-288.
23. Inatani, M.; Yamaguchi, Y. Gene expression of EXT1 and EXT2 during mouse brain development, *Dev Brain Res*, **2003**, *141*, 129-136.
24. Hienola, A.; Turnova, S.; Kuleskiy, E.; Rauvala, H. N-syndecan deficiency impairs neural migration in brain, *J Cell Biol*, **2006**, *174*, 569-80.
25. Laabs, T.; Carulli, D.; Geller, H.M.; Fawcett, J.W. Chondroitin sulfate proteoglycans in neural development, *Curr Opin Neurobiol*, **2005**, *15*, 116-120.
26. Zou, J.; Hernandez, Y.J.; Muir, D. Chondroitin sulfate proteoglycan with neurite-inhibiting activity is up-regulated following peripheral nerve injury, *Dev Neurobiol*, **1998**, *34*, 41-54.
27. Moon, L.D.F.; Asher, R.A.; Rhodes, K.E.; Fawcett, J.W. Regeneration of CNS axons back to their target following treatment of adult rat brain with chondroitinase ABC, *Nature Neurosci*, **2001**, *4*, 465-466.

28. Jones, L.L.; Sajed, D.; Tuszynski, M.H. Axonal regeneration through regions of chondroitin sulfate proteoglycan deposition after spinal cord injury: a balance of permissiveness and inhibition, *J Neurosci*, **2003**, *23*, 9276-9288.
29. Kaksonen, M.; Pavlov, I.; Volkar, V.; Lauri, S.E.; Hienola, A.; Riekk, R.; Lasko, M.; Taira, T.; Rauvala, H. Syndecan-3-deficient mice exhibit enhanced LTP and impaired hippocampus-dependent memory, *Mol Cell Neurosci*, **2002**, *21*, 158-172.
30. Fifkova, E. A possible mechanism of morphometric changes in dendritic spines induced by stimulation, *Cell Mol Neurobiol*, **1985**, *5*, 47-63.
31. Lund, J.S.; Holbach, S.M.; Chung, W. Postnatal development of thalamic recipient neurons in the monkey striate cortex: Influence of afferent driving on spine acquisition and dendritic growth of layer 4c spiny stellate neurons, *J Comp Neurol*, **2004**, *309*, 129-140.
32. Rudelli, R.D.; Brown, W.T.; Wisniewski, K.; Jenkins, E.C.; Laure-Kamionowska, M.; Connell, F.; Wisniewski, M. Adult fragile X syndrome, *Acta Neuropathol*, **1985**, *3-4*, 269-295.
33. Hinton, V.J.; Brown, W.T.; Wisniewski, K.; Rudelli, R.D. Analysis of neocortex in three males with the fragile X syndrome, *Am J Med Gen*, 1991, *41*, 289-294.
34. Ethell, I.M.; Yamaguchi, Y. Cell surface heparan sulfate proteoglycan syndecan-2 induces the maturation of dendritic spines in rat hippocampal neurons, *J Cell Biol*, **1999**, *144*, 575-586.
35. Kalus, I.; Salmen, B.; Viebahn, C.; von Figura, K.; Schmitz, D.; D'Hooge, R.; Dierks, T. Differential involvement of the extracellular 6-O-endosulfatases Sulf1 and Sulf2 in brain development and neuronal behavioral plasticity, *J Cell Mol Med*, **2008**, *13*, 4505-4521.
36. Bukalo, O.; Schachner, M.; Dityatev, A. Modification of extracellular matrix by enzymatic removal of chondroitin sulfate and by lack of tenascin-R differentially affects several forms of synaptic plasticity in the hippocampus, *Neuroscience*, **2001**, *104*, 359-369.
37. Zhou, X.; Brakebusch, C.; Matthies, H.; Oohashi, T.; Hirsch, E.; Moser, M.; Krug, M.; Seidenbecher, C. I.; Boeckers, T.M.; Rauch, U.; Buettner, R.; Gundelfinger, E.; Fässler, R. Neurocan is dispensable for brain development, *Mol Cell Biol*, **2001**, *21*, 5970-5978.
38. Brakebusch, C.; Seidenbecher, C.I.; Asztely, F.; Rauch, U.; Matthies, H.; Meyer, H.; Krug, M.; Bockers, T.M.; Zhou, X.H.; Kretuz, M.R. Brevican-deficient mice display impaired hippocampal CA1 long-term potentiation but show no obvious deficits in learning and memory, *Mol Cell Biol*, **2002**, *22*, 7417-7427.

39. Galtrey, C.M.; Fawcett, J.W. The role of chondroitin sulfate proteoglycans in regeneration and plasticity in the central nervous system, *Brain Res Rev*, **2007**, *54*, 1-18.
40. De Souza Silva, M.A.; Jezek, K.; Weth, K.; Müller, H.W.; Huston, J.P.; Brandao, M.L.; Hasenöhrl, R.U. Facilitation of learning and modulation of frontal cortex acetylcholine by ventral pallidal injection of heparin glycosaminoglycan, *Neuroscience*, **2002**, *113*, 529-535.
41. Huston, J.P.; Weth, K.; De Souza Silva, A.; Junghans, U.; Müller, H.W.; Hasenöhrl, R.U. Facilitation of learning and long-term ventral pallidal-cortical cholinergic activation by proteoglycan biglycan and chondroitin sulfate C, *Neuroscience*, **2000**, *100*, 355-361.
42. Gogolla, N.; Caroni, P.; Lüthi, A.; Herry, C. Perineuronal nets protect fear memories from erasure, *Science*, **2009**, *325*, 1258-1261.
43. Snow, A.D.; Mar, H.; Nochlin, D.; Sekiguchi, R.T.; Kimata, K.; Koike, Y.; Wight, T.N. Early accumulation of heparan sulfate in neurons and in the beta-amyloid protein-containing lesions of Alzheimer's disease and Down's syndrome, *Am J Pathol*, **1990**, *137*, 1253-1270.
44. Schwörer, R.; Zubkova, O.V.; Turnbull, J.E.; Tyler, P.C. Synthesis of a targeted library of heparan sulfate hexa- to dodecasaccharides as inhibitors of  $\beta$ -secretase: potential therapeutics for Alzheimer's disease, *Chem Eur J*, **2013**, *19*, 6817-6823.
45. McLaurin, J.; Franklin, T.; Zhang, X.; Deng, J.; Fraser, P.E. Interactions of Alzheimer amyloid- $\beta$  peptides with glycosaminoglycans, *Eur J Biochem*, **1999**, *266*, 1101-1110.
46. Agria, T.; Miyatake, T.; Yu, R.K. Role of proteoglycans and glycosaminoglycans in the pathogenesis of Alzheimer's disease and related disorders: Amyloidogenesis and therapeutic strategies- A review, *J Neurosci Res*, **2010**, *88*, 2303-2315.
47. Hasegawa, M.; Crowther, R.A.; Jakes, R.; Goedert, M. Alzheimer-like changes in microtubule-associated protein Tau induced by sulfated glycosaminoglycans. Inhibition of microtubule binding, stimulation of phosphorylation, and filament assembly depend on the degree of sulfation, *J Biol Chem*, **1997**, *272*, 33118-33124.
48. Hu, B.; Kong, L.L.; Matthews, R.T.; Viapiano, M.S. The proteoglycan brevican binds to fibronectin after proteolytic cleavage and promotes glioma cell motility, *J Biol Chem*, **2008**, *283*, 24848-24859.
49. Su, G.; Meyer, K.; Nandini, C.D.; Qiao, D.; Salamat, S.; Friedl, A. Glypican-1 is frequently overexpressed in human gliomas and enhances FGF-2 signaling in glioma cells, *Am J Pathol*, **2006**, *168*, 2014-2026.
50. Mendes De Aguiar, C.B.N.; Garcez, R.C.; Alvarez-Silva, M.; Trentin, A.G. Undersulfation of proteoglycans and proteins and proteins alter C6 glioma cells

- proliferation, adhesion and extracellular matrix organization, *Int J Dev Neurosci*, **2002**, *20*, 563-570.
51. Lobao-Soares, B.; Alvarez-Silva, M.; Mendes De Aguiar, C.B.N.; Nicolau, M.; Trentin, A.G. Undersulfation of glycosaminoglycans induced by sodium chlorate treatment affects the progression of C6 rat glioma, in vivo, *Brain Res*, **2007**, *1131*, 29-36.
52. Perosa, S.R.; Porcionatto, M.A.; Cukiert, A.; Martins, J.R.M.; Passeroti, C.C.; Amando, D.; Matas, S.L.A.; Nader, H.B.; Cavalheiro, E.A.; Leite, J.P.; Naffah-Mazzacoratti, M.G. Glycoaminoglycan levels and proteoglycans expression are altered in the hippocampus of patients with mesial temporal lobe epilepsy, *Brain Res Bull*, **2002**, *58*, 509-516.
53. Liu, I.H.; Uversky, V.N.; Munishkina, L.A.; Fink, A.L.; Halfter, W.; Cole, G.J. Agrin binds  $\alpha$ -synuclein and modulates  $\alpha$ -synuclein fibrillation, *Glycobiology*, **2005**, *15*, 1320-1331.
54. Pantazopoulos, H.; Woo, T.W.; Lim, M.P.; Lange, N.; Berretta, S. Extracellular matrix-glia abnormalities in the amygdala and entorhinal cortex of subjects with schizophrenia, *Arch Gen Psychiat*, **2010**, *67*, 155-166.
55. Brandan, E.; Cabello-Verrugio, C.; Vial, C. Novel regulatory mechanisms for the proteoglycans decorin and biglycan during muscle formation and muscular dystrophy, *Matrix Biol*, **2008**, *27*, 700-708.
56. Casar, J.C.; Cabello-Verrugio, C.; Olguin, H.; Aldunate, R.; Inestrosa, N.C.; Brandan, E. Heparan sulfate proteoglycans are increased during skeletal muscle regeneration: requirement of syndecan-3 for successful fiber formation, *J Cell Sci*, **2003**, *117*, 73-84.
57. Drouguett, R.; Cabello-Verrugio, C.; Riquelme, C.; Brandan, E. Extracellular proteoglycans modify TGF- $\beta$  bio-availability attenuating its signaling during skeletal muscle differentiation, *Matrix Biol*, **2006**, *25*, 332-341.
58. Burgess, R.W.; Nguyen, Q.T.; Son, Y.; Lichtman, J.W.; Sanes, J.R. Alternatively spliced isoforms of nerve- and muscle-derived agrin: their roles at the neuromuscular junction, *Neuron*, **1999**, *23*, 33-44.
59. Anderson, M.; Klier, F.; Tanguay, K. Acetylcholine receptor aggregation parallels the deposition of a basal lamina proteoglycan during development of the neuromuscular junction, *J Cell Biol*, **1984**, *99*, 1769-1784.
60. Guatam, M.; Noakes, P.G.; Moscoso, L.; Rupp, F.; Scheller, R.H.; Merlie, J.P.; Sanes, J.R. Defective neuromuscular synaptogenesis in agrin-deficient mutant mice, *Cell*, **1996**, *85*, 525-535.
61. Torres, J.C.; Inestrosa, N.C. Heparin solubilizes asymmetric acetylcholinesterase

from rat neuromuscular junction, *FEBS Lett*, **1983**, *154*, 265-268.

62. Arikawa-Hirasawa, E.; Rossi, S.G.; Rotundo, R.L.; Yamada, Y. Absence of acetylcholinesterase at the neuromuscular junctions of perlecan-null mice, *Nature Neurosci*, **2002**, *5*, 119-123.

63. Peng, H.B.; Xie, H.; Rossi, S.G.; Rotundo, R.L. Acetylcholinesterase clustering at the neuromuscular junction involves perlecan and dystroglycan, *J Cell Biol*, **1999**, *145*, 911-921.

64. Marcotte, A.C. Speech lateralization in deaf populations: evidence for a developmental critical period, *Brain Lang*, **1990**, *39*, 134-152.

65. Dunn, C.C.; Walker, E.A.; Oleson, J.; Kenworthy, M.; Van Voorst, T.; Tomblin, J.B.; Ji, H.; Kirk, K.I.; McMurray, B.; Hanson, M.; Gantz, B.J. Longitudinal speech perception and language performance in pediatric cochlear implant users: the effect of age at implantation, *Ear Hearing*, **2014**, *35*, 148-160.

66. Muenzer, J.; Wraith, J.; Clarke, L. Mucopolysaccharidosis I: management and treatment guidelines, *Pediatrics*, **2009**, *123*, 19-29

67. Meyza, K.; Blanchard, D.; Pearson, B.; Pobbe, R.; Blanchard, R. Fractone-associated N-sulfated heparan sulfate shows reduced quantity in BTBR T+tf/J mice: a strong model of autism, *Behav Brain Res*, **2012**, *228*, 247-253.

68. Irie, F.; Badie-Mahdavi, H.; Yamaguchi, Y. Autism-like socio-communicative deficits and stereotypies in mice lacking heparan sulfate, *PNAS*, **2012**, *109*, 5052-5056.

69. Kutty, J.; Webb, K. Vibration stimulates vocal mucosa-like matrix expressions by hydrogel-encapsulated fibroblasts, *J Tissue Eng Regen Med*, **2010**, *4*, 62-72.

70. Buhler, R.; Sennes, L.; Mauad, T.; Melo, E.; Silva, L.; Saldiva, P. Collagen fiber and versican distribution within the lamina propria of fetal vocal folds, *Laryngoscope*, **2008**, *118*, 371-374.

71. Hahn, M.S.; Kobler, J.B.; Zeitels, S.M.; Langer, R. Midmembranous vocal fold lamina propria proteoglycans across selected species, *Ann Otol Rhinol Laryngol*, **2005**, *114*, 451-462.

72. Gray, S.D.; Titze, I.R.; Chan, R.; Hammond, T.H. Vocal fold proteoglycans and their influence on biomechanics, *Laryngoscope*, **2009**, *109*, 845-854.

73. Chan, R.W.; Gray, S.D.; Titze, I.R. The importance of hyaluronic acid in vocal fold biomechanics, *Otolaryng Head Neck*, **2001**, *124*, 607-614.

74. Branski, R.; Verdolini, K.; Sandulache, V.; Rosen, C.; Hebda, P. Vocal fold wound healing: a review for clinicians, *J Voice*, **2005**, *20*, 432-442.

75. Bolhuis, J.J.; Gahr, M. Neural mechanisms of birdsong memory, *Nat Rev Neurosci*, **2006**, *7*, 347-357.
76. Curtiss, S.; Fromkin, V.; Krashen, S.; Rigler, D.; Rigler, M. The linguistic development of Genie, *Language*, **1974**, *50*, 528-550.
77. Davis, K. Extreme social isolation of a child, *Am J Sociol*, **1940**, *45*, 554-565.
78. Ling, D. Speech development in hearing-impaired children, *J Commun Disord*, **1978**, *11*, 119-124.
79. Svirsky, M.A.; Teoh, S.W.; Neuburger, H. Development of language and speech perception in congenitally, profoundly deaf children as a function of age at cochlear implantation, *Audiol Neurotol*, **2004**, *9*, 224-233.
80. Brenowitz, E.A.; Margoliash, D.; Nordeen, K.W. An introduction to birdsong and the avian song system, *J Neurobiol*, **1997**, 495-5
81. Immelmann, K. Song development in the zebra finch and other estrildid finches, *Bird Vocal*, **1969**, , 61-74.
82. Böhner, J. Song learning in the zebra finch (*Taeniopygia guttata*) selectivity in the choice of a tutor and accuracy of song copies, *Anim Behav*, **1983**, *31*, 231-237
83. Derégnaucourt, S.; Poirier, C.; Van der Kant, A.; Van der Linden, A.; Gahr, M. Comparisons of different methods to train a young zebra finch (*Taeniopygia guttata*) to learn a song, *J Physiol Paris*, **2013**, *107*, 210-218.
84. Kriengwatana, B.; Wada, H.; Schmidt, K.L.; Taves, M.D.; Soma, K.K.; MacDougall-Shackleton, S.A. Effects of nutritional stress during different developmental periods on song and the hypothalamic-pituitary-adrenal axis in zebra finches, *Horm Behav*, **2014**, *65*, 285-293.
85. Nottebohm, F.; Stokes, T.M.; Leonard, C.M. Central control of song in the canary, *Serinus canaries*, *J Comp Neurol*, **1976**, *165*, 457-486.
86. Amador, A.; Perl, Y.S.; Mindlin, G.B.; Margoliash, D. Elemental gesture dynamics are encoded by song premotor cortical neurons, *Nature*, **2013**, *495*, 59-64.
87. Korsia, S.; Bottjer, S.W. Chronic testosterone treatment impairs vocal learning in male zebra finches during a restricted period of development, *J Neurosci*, **1991**, *11*, 2362-2371.
88. Sharff, C.; Nottebohm, F. Lesions in area X affect song in juvenile but not adult male zebra finches, *Soc Neurosci Abst*, **1989**, *15*, 618.
89. Schraff, C.; Nottebohm, F. A comparative study of the behavioral deficits following

lesions of various parts of the zebra finch song system: implication for vocal learning, *J Neurosci*, **1991**, *11*, 2896-2913.

90. Nordeen, K.W.; Nordeen, E.J. Long-term maintenance of song in adult zebra finches is not affected by lesions of a forebrain nucleus involved in song learning, *Behav Neural Biol*, **1993**, *59*, 79-81.

91. Riede, T.; Goller, F. Functional morphology of the sound-generating labia in the syrinx of two songbird species, *J Anat*, **2010**, *216*, 23-36.

92. Riede, T.; Goller, F. Morphological basis for the evolution of acoustic diversity in oscine songbirds, *Proc R Soc B*, **2014**, *281*, 1-7.

93. Kanehisa, M.; Goto, S.; Furumichi, M.; Tanabe, M.; Hirakawa, M. KEGG for representation and analysis of molecular networks involving diseases and drugs. *Nucleic Acids Res.*, **2010**, *38*, D355-D360

94. Kanehisa, M.; Goto, S.; Hattori, M.; Aoki-Kinoshita, K.F.; Itoh, M.; Kawashima, S.; Katayama, T.; Araki, M.; Hirakawa, M. From genomics to chemical genomics: new developments in KEGG. *Nucleic Acids Res.*, **2006**, *34*, D354-357

95. Kanehisa, M.; Goto, S. KEGG: Kyoto Encyclopedia of Genes and Genomes. *Nucleic Acids Res*, **2000**, *28*, 27-30

96. Hashimoto, K.; Goto, S.; Kawano, S.; Aoki-Kinoshita, K.F.; Ueda, N.; Hamajima, M.; Kawasaki, T.; Kanehisa, M. KEGG as a glycome informatics resource. *Glycobiology*, **2006**, *16*, 63R-70R

97. Jarvis, E.D; Smith, V.A; Wada, K.; Rivas, M.V.; McElroy, M.; Smulders, T.V.; Carninci, P; Hayashizaki, Y; Dietrich, F; Wu, X; McConnell, P; Yu, J; Wang, P.P; Hartemink, A.J.; Lin, S A framework for integrating the songbird brain. *J Comp Physiol A*, **2002**, *188*, 961-980.

98. Holzenberger, M.; Jarvis, E.; Chong, C.; Grossman, M.; Nottebohm, F.; Scharff, C. Selective Expression of insulin-like growth factor II in the songbird brain. *J Neurosci*, **1997**, *17*, 6974-6987

99. Bernfield, M.; Gotte, M.; Park, P.; Reizes, O.; Fitzgerald, M.; Lincecum, J.; Zako, M. Functions of cell surface heparan sulfate proteoglycans. *Annu Rev Biochem*, **1999**, *68*, 729-777.

100. Lovell, P.; Clayton, D.; Replogle, K.; Mello, C. Birdsong "Transcriptomics": Neurochemical Specializations of the Oscine Song System. *PLoS ONE*, **2008**

101. Rauch, U.; Feng, K.; Zhou, X. Neurocan: a brain chondroitin sulfate. *Cell Mol Life Sci*, **2001**, *58*, 1842-1856.

102. Burkhardt-Holm, P.; Kafitz, K.; Guttinger, H.; Schachner, M. Testosterone elevates expression of Tenascin-R and oligomannosidic carbohydrates in developing male zebra finches. *J Neurosci Res*, **1996**, *46*, 385-392.
103. Meyer, C.; Boroda, E.; Nick, T. Sexually dimorphic perineuronal net expression in songbird, *Basal Ganglia*, **2013**
104. Balmer, T.; Carels, V.; Frisch, J.; Nick, T. Modulation of perineuronal nets and parvalbumin with developmental song learning, *J Neurosci*, **2009**, *29*, 12878-12885.
105. Schwartz, N.B. Regulation of chondroitin sulfate synthesis. Effect of beta-xylosides on synthesis of chondroitin sulfate proteoglycan, chondroitin sulfate chains, and core protein, *J Biol Chem*, **1977**, *252*, 6316-6321.



## CHAPTER 2

### THE PRODUCTION AND VALIDATION OF MOLECULAR TOOLS FOR THE STUDY OF GLYCOSAMINOGLYCANS IN VOCAL LEARNING AND PRODUCTION

#### 2.1 Overview

Glycosaminoglycans (GAGs) have been shown to be involved with a wide array of biological functions, including: axon guidance<sup>1-4</sup>, growth factor binding<sup>5-7</sup>, receptor aggregation<sup>8</sup>, and coagulation<sup>9,10</sup>. While it is understood that GAGs play a role, the structural requirements of GAGs for interaction remain unclear. One of the few known carbohydrate structural sequences for protein interaction is the specifically sulfated pentasaccharide that binds anti-thrombin III<sup>9,10</sup>. Forays have been made into examining specific GAG fine structure for the binding of FGFs<sup>11,12</sup>; however, clear definition of structure-function relationships remains elusive.

This lack of knowledge is due to the restricted set of widely available molecular tools with which to study how the structure or biosynthesis of GAGs affects biological outcomes. The most commonly used manipulation involves the use of GAG lyases<sup>13-15</sup>. While these enzymes are effective for showing the importance of GAG in a system, enzymatic degradation does not show if there is a specific sulfation pattern that is required, nor does it alter biosynthetic production of the GAG. Additionally, enzymes degrade

GAG that is already present and are subject to biological constraints such as temperature and degradation or inactivation over time<sup>16,17</sup>. As a result, there exists a need for the expansion of the molecular toolbox to improve the current understanding of the role of GAGs in biological systems.

In an attempt to fill this void, the production and characterization of more specific enzymes, specifically sulfated polymers and oligosaccharides, and the expansion of a library of small molecules, called xylosides, is ongoing. Both HS and CS consist of heterogeneous mixtures that can be selectively cleaved by specific enzymes. This would allow for the study of partial loss of GAG as opposed to complete degradation. Additionally, to truly understand structure-function relationships and the minimum requirement for interaction, it is necessary to create and maintain a fully characterized library of oligosaccharides and polymers. Finally, monomeric xylosides have been used for several decades both *in vitro* and *in vivo*. However, recently, the importance of valence has become apparent<sup>12</sup>. This has led to a need to expand the library of di-, tri-, and tetrameric xylosides. The focus of this chapter is the production and characterization of enzymes, specifically sulfated polymers and oligosaccharides, and xylosides. To validate that the molecular manipulations will function in the zebra finch model system, enzymatic degradation in a song specific nucleus was employed. In this preliminary study, it was seen that degradation can lead to a changes in stereotyped adult song.

## 2.2 Expression and purification of enzymes, polymers, oligosaccharides, and the characterization of xylosides

### 2.2.1 Production and purification of GAG degrading enzymes

Enzymes are one of the most commonly used methods for the study of the role of GAGs *in vitro* and *in vivo*. There are several enzymes that degrade GAG chains. Hep I,II, and III digest HS and heparin. ChAC, ChB, and ChABC digest CS and DS. Each of these enzymes preferentially digests chains based on a characteristic of the GAG chain. Figure 2.1 shows the activity of each enzyme. Hep I digests unsulfated regions while Hep III digests highly sulfated regions. Hep II digests both sulfated and unsulfated regions<sup>16</sup>. Similarly, ChAC digests chondroitin A and chondroitin C. ChB digests dermatan sulfate while ChABC digests chondroitin A, C, and dermatan sulfate<sup>17</sup>. Cloning and producing these enzymes allows us to digest specific targets within our area of interest both in the brain and in the muscle.

2.2.1.1 Production and purification of heparan and chondroitin lyase enzymes in E. coli. ChB was cloned into a pET<sub>19</sub> vector and transformed into BL21 *E. coli*. Heparitinase I, II, and III were cloned previously into the same vector and strain of bacteria. All heparan lyase enzymes and ChB were produced and purified as described below. A 10 ml culture of LB broth with 50-100 µg/ml ampicillin was inoculated with bacteria from the BL21 stock and grown overnight at 37°C, shaking at 200 rpm. The next day, the 10 ml culture was added to 1 L of LB broth containing 50-100 µg/ml ampicillin and was allowed to incubate at 37°C, shaking at 200 rpm until it reached an optical density (O.D.) of 0.6. The culture was then treated with 200 µl of 1M IPTG and incubated at 25°C, shaking at 150 rpm overnight. The culture is then spun at 4000 rpm for 30 min or until bacteria formed

a pellet. The supernatant was removed.

The pellet was then re-suspended in lysis buffer (100 mM Tris; 25% w/v sucrose; 1mg/ml lysozyme; 10  $\mu$ l DNase; 2mM PMSF) and incubated at 4°C for 30 min. Next Triton-X was added to a final concentration of 0.1% and the mixture was incubated at 4°C for 30 min, while being rotated. The mixture was sonicated for 30 s at a pulse rate of 1 s pulse with 2 s intervals. This was repeated thrice. The sonicated mixture was spun at 15000 rpm for 30 min at 4°C. The supernatant was then filtered through a 0.45 micron filter. The filtrate was purified for 6-His tag labeled protein using a Nickel (Ni) column. The column has a bed volume of 3 ml/ 1 of culture. The column was washed with 4 column volumes of water and equilibrated with 4 column volumes of wash buffer (100 mM Tris, pH 7.5; 0.5M NaCl; 5% v/v glycerol; 20 mM Imidazole; 5 mM 2-thioethanol). The filtrate was loaded onto the column thrice, washed with 30 column volumes of wash buffer, and then eluted using a linear gradient of elution buffer (100 mM Tris, pH 7.5; 0.5M NaCl; 5% v/v glycerol; 500 mM Imidazole; 5 mM 2-thioethanol) concentrated and buffer-exchanged into protein buffer (10 mM PIPES; 5% glycerol) using a 10 kDa MWCO Amicon column.

2.2.1.2 Confirmation of enzyme and activity. After purification, all enzyme batches were tested for protein concentration, the presence of desired enzyme, and rate of enzyme activity. The presence of enzymes was confirmed by western blot (Figure 2.2A). To assess protein concentration, a BCA was run on each sample. Concentrated sample was tested undiluted and at various dilutions to ensure that our concentrations did not fall at the extreme ends of the standards. All samples and standards were run in triplicate. Concentration was calculated using the standard curve created with known concentrations

of bovine serum albumin (BSA).

An activity assay was conducted to examine the enzymatic activity present in the sample (Figure 2.2B). All heparitinase and chondroitinase enzyme activity can be measured by increasing absorbance at 232 nm. This is due to the formation of a carbon-carbon double bond when the enzyme cleaves between sugar residues. Using overall rate of increase, each enzyme batch can be normalized so aliquots have approximately equal activity. Each enzyme was run with the polymer that provided the most efficient cleavage. Hep I was tested with heparosan, HepII with *N*-sulfated heparosan, Hep III with Heparin, CsAC with chondroitin A or C, CsB with dermatan sulfate, and CsABC with a mixture of chondroitin A, C, and dermatan sulfate. A negative control, a polymer that the enzyme did not digest, was also run to exclude the possibility that increase in 232 nm was seen due to factors not related to GAG polymer cleavage. Active enzyme was aliquoted into 10  $\mu$ l aliquots and stored at -80°C until needed.

### 2.2.2 Production, purification, and characterization of modified polymers and oligosaccharides

While degradation allows us another avenue of study, it is still an incomplete method. In order to truly understand structure function-relationships, it is necessary to control several aspects of the GAG chains, including the size and sulfation pattern. This work often begins *in vitro* and requires the production of HS polymers that are specifically sulfated. Additionally, these polymers can be broken down into oligosaccharides through controlled degradation. The production of these oligosaccharides from the starting polymers provides a method for the study of the minimum requirement for interaction.

These oligosaccharides can also be modified to produce specific sulfation patterns that may be useful.

2.2.2.1 Preparation of oligosaccharides. Commercial heparin was purchased and partially digested through the addition of Hep III enzyme. A 15 ml, 100 mg reaction was set up and digested through the addition of Hep III enzyme to the reaction and immediately spun at 4000 rpm for 45 min in a 20 kDa MWCO Amicon column. The flow-through was collected and lyophilized. This process was repeated for several hundred milligrams. The lyophilized sample was rehydrated in 10 ml of ddH<sub>2</sub>O. The oligosaccharide mixture was separated on a preparative CarboPac column (22 x 250 mm) by HPLC. The oligosaccharides were eluted with a gradient of 2 M NaCl (pH 3.5) for 90 min at a flow rate of 10 ml/min and monitored by absorbance at 232 nm.

Each peak represented an oligosaccharide of different degree of polymerization (Dp) and sulfate density. Fractions were collected at a rate of 5ml/30s. Those containing each size and sulfate-defined oligosaccharide were pooled together and desalted using a G-25 column (1.5 cm x 50 cm). The size and sulfation of each desalted oligosaccharide was confirmed by mass spectrometry (LC-MS).

Heparosan and *N*-sulfated heparosan oligosaccharides were prepared in the lab and partially digested by Hep I following the previously listed procedure with the exception of using a linear gradient of 1 M NaCl (pH 3.5).

2.2.2.2 Enzymatic modifications of HS polymer or oligosaccharide. 1mg of polymer (heparosan, *N*-sulfated heparosan, *N*- and *O*-sulfated heparosan, heparin) or desired oligosaccharide was incubated with 40 µl of desired OST enzyme (~1 mg/ml) and 800 µg of PAPS in a total volume of 1 ml. The reactions were performed at 37°C for 24 h

in MES buffer (25 mM MES, pH 7.0, 0.02 % Triton X-100, 2.5 mM MgCl<sub>2</sub>, 2.5 mM MnCl<sub>2</sub>, 1.25 mM CaCl<sub>2</sub>, 0.75 mg/ml BSA). The reaction mixtures were purified through a DEAE-sepharose column (0.25 ml) that had been pre-equilibrated with wash buffer (20 mM NaOAc, 0.1 M NaCl, pH 6.0). After washing with 30 column volumes of wash buffer, the bound HS was eluted with 6 column volumes of elution buffer (20 mM NaOAc, 1 M NaCl, pH 6.0). The samples were desalted and concentrated with 3000 MWCO Amicon columns. Samples were then lyophilized, weighed, and reconstituted to a concentration of 1 mg/ml. 50 µg of polymer was digested with Hep I,II,III and modifications were analyzed by mass spectrometry or HPLC. 50 µg of oligosaccharide was analyzed by mass spectrometry without digestion.

2.2.2.3 Mass spectrometry analysis of oligosaccharides and polymers. The di- and oligosaccharides were analyzed using a capillary C18-HPLC column (0.3 x 30 mm) coupled to an electrospray ionization time-of-flight MS (Bruker Daltonics, USA). The oligosaccharides were eluted with a linear gradient of acetonitrile at a flow rate of 5 µl/min for 30 min. Dibutylammonium acetate (5 mM) was used as an ion-pairing agent. The MS was acquired in the negative ion mode at the following conditions: cone gas flow rate at 50 l/h, nozzle temperature at 130°C, drying gas (N<sub>2</sub>) flow rate at 450 l/h, spray tip potential at 2.3 kV, and nozzle potential at 35 V.

2.2.2.4 Confirmation of oligosaccharide production. Heparin oligos are confirmed after HPLC strong anion-exchange on a preparative scale (Figure 2.3). The first and largest peak in the HPLC trace contained fully, or tri-sulfated, disaccharides, indicating that heparitinase enzymes may prefer exolytic cleavage of polymer. In uniformly sulfated polymers such as heparosan or *N*-sulfated heparosan, this disaccharide (dp2) peak

remained the largest and all subsequent peaks correspond to higher oligosaccharides that differ by one disaccharide. If the first peak is a disaccharide, or dp2, then subsequent peaks are dp4, dp6, dp8, and so on. However, in heparin oligosaccharides, this is not always the case.

Heparin polymers have highly sulfated, nonsulfated, and moderately sulfated regions. This presents an opportunity for differentially sulfated oligosaccharides. The highest level of sulfation seen in heparin is three sulfates per disaccharide; however, two, one, or none is also possible. This gives us the possibility of four different disaccharides, seven different tetrasaccharides, ten different hexasaccharides, and so on. This makes complete separation more difficult. In the heparin digest, the first peak was pure trisulfated disaccharide. The second peak, when analyzed by mass spectrometry, shows that it contains less sulfated dp4 molecules. The third peak was where the fully sulfated dp4 is located. Therefore, it is important to characterize each peak separately to ensure that it is the correct size and sulfation density. Figure 2.4 shows the mass spectrometry analysis of several heparin oligosaccharides. The enzymatic synthesis of polymers allows for the preparation of specifically sulfated HS-like polymers. Table 2.1 shows all structures that have been chemoenzymatically synthesized. These molecules are available for experiments that are beyond the scope of this work.

### 2.2.3 Priming analysis of click-xylosides

Previous studies have found the addition of xylose residues attached to an aglycone, called xylosides, can induce the formation of GAG chains without the presence of a core protein<sup>18-20</sup>. Alteration of the aglycone attached to the xylose can alter the priming activity



of the molecule as well as the type, sulfation pattern, and molecular weight of the primed GAGs<sup>18-20</sup>. The most commonly studied xylosides have been the O-xylosides. O-xylosides are often unstable, so alternative types of xylosides are currently being explored<sup>18-20</sup>. Promising sets of new xylosides, called click xylosides, are formed by copper (Cu) (I)-catalyzed click reactions. Stable in culture and *in vivo*, recent studies have examined how these click xylosides induce GAG formation and how alteration of the aglycone can change the primed GAGs<sup>19,20</sup>. Libraries of these molecules have been synthesized and tested. Monomeric xylosides, or molecules containing a single xylose residue, represent the majority of xylosides that are screened. One of these molecules which has been shown to prime only CS at a high level will be used in Chapter 3. Should the small molecule approach for study of GAGs in a biological system show promise, it is important to have a variety of xylosides with different structures and priming capabilities. Xylosides that contain multiple xyloside residues, such as dimeric xylosides, may be more analogous to endogenous PGs. This may allow for a more accurate study for the separation of GAG and protein activities. Dimeric xylosides can be synthesized using click chemistry as well, but often show lower priming capabilities. The reduction in priming necessitates continued exploration of dimeric xylosides and how changes in structure may result in better activity. To examine this, we compared Cu-click dimeric xylosides and dimeric xylosides made using a ruthenium (Ru) catalyst.

2.2.3.1 Methods and materials. The chinese hamster ovary (CHO) cell line (pgsA-745) was obtained from American Type Culture Collection. All cell culture reagents were obtained from Invitrogen. The radiochemical, <sup>35</sup>S-Na<sub>2</sub>SO<sub>4</sub>, and the flow scintillation cocktail, Ultima-FloAP, were obtained from Perkin Elmer Life and Analytical

Sciences. The 6X pronase solution was prepared using *Streptomyces griseus* protease type XIV (1 mg/ml). The DEAE-sepharose gel was purchased from Amersham Biosciences. The high pressure liquid chromatography (HPLC) column involved for anion-exchange chromatography was the DEAE-3SW (7.5 mm x 7.5 mm, 10  $\mu$ m), for size-exclusion chromatography was the G3000SWXL (7.8 mm x 30 cm, 5  $\mu$ m), and for chondroitin sulfate disaccharide analysis was the TSKgel SAX (6 mm x 15 cm, 5  $\mu$ m). All columns were purchased from Tosoh Bioscience LLC. The HPLC column used for heparan sulfate disaccharide analysis was the CarboPac Analytical PA1 (4 mm x 25 cm, 10  $\mu$ m) column from Dionex. Amicon Ultra-0.5 ml centrifugal filters (3000 MWCO) were purchased from Millipore. Compounds were sent from Gifu University in Japan. Structures can be found in Table 2.2.

To determine the ability of xylosides to prime the synthesis of glycosaminoglycans in culture, experiments were performed *in vitro* using the CHO cell line pgsA-745. Cells ( $1 \times 10^5$  per well) were plated in appropriate medium in a 6-well plate. The cells were incubated in a humidified incubator at 37°C for 48 h to a confluency around 50%. After being washed with sterile phosphate buffered saline (PBS), appropriate medium containing 10% dialyzed fetal bovine serum (FBS) (989  $\mu$ l) was added to each well along with 1  $\mu$ l of 100 mM concentration of specific xyloside (final concentration of primer is 100  $\mu$ M), and 100  $\mu$ Ci  $^{35}\text{S-Na}_2\text{SO}_4$ . The plates were then placed in the incubator for 48 h before 6 x pronase solution was added, and the plates were incubated overnight at 37°C.

After incubation with pronase, the entire contents of each well were transferred to a microcentrifuge tube and spun at  $>12,000 \times g$  for 10 min. The supernatant was transferred to a clean tube and then loaded on to a DEAE-sepharose column (0.25 ml) that had been

pre-equilibrated with 10 column volumes of wash buffer (20 mM NaOAc buffer, pH 6.0, containing 0.1 M NaCl). Next the column was washed with 20 column volumes of wash buffer. Elution of the bound GAG chains from the column was accomplished using 6 column volumes of elution buffer (20 mM NaOAc buffer, pH 6.0, containing 1 M NaCl) and the amount of GAG chain primed was determined by quantifying <sup>35</sup>S-radioactivity incorporated into the eluted GAG chains. 50 µl of the elution was added to 5 ml of scintillation cocktail and measured for total radioactivity using a scintillation counter.

The extent of sulfation of primed GAG chains was determined by assessing migration time on an anion-exchange column using HPLC with inline flow scintillation analyzer. Each elution was desalted using a 3000 molecular weight cut off (MWCO) spin column at <12,000 x g centrifugation. The remaining 100 µl was diluted to 200 µl total. 150 µl was loaded onto a HPLC-DEAE column and eluted with a linear NaCl gradient of 0.2 M to 1 M.

Primed GAG chain length was determined by assessing their migration time on a size exclusion column using HPLC with inline flow scintillation analysis. Two G3000SWXL (7.8 mm x 30 cm, 5 µm) size exclusion columns were connected in tandem and the eluted GAG chains were loaded onto the columns. These chains were eluted over 60 min using a phosphate buffer containing 100 mM KH<sub>2</sub>PO<sub>4</sub> and 100 mM NaCl at pH 6.0. The size was calculated based on comparing the migration time of polystyrene sulfonate standards with the calculated migration time of primed GAGs (average of peak-width at half maximum).

Primed GAG chains were digested using heparitinase I, II, and III (Hep I, II, III) or chondroitinase ABC (ChABC) at 37°C overnight. Samples were then boiled to inactivate

enzyme and centrifuged at  $>12,000 \times g$  for 10 min. The supernatant was transferred into HPLC vials and samples that had been digested by Hep I, II, III were loaded onto the CarboPac PA1 column. Samples that were digested by ChABC were loaded onto the TSKgel SAX column. Both the Hep I, II, III and CsABC samples were eluted over a 1M NaCl gradient, pH 3.5, and compared to standards.

2.2.3.2 Results of priming analysis. Two sets of dimeric molecules were synthesized and then assessed in an *in vitro* model of GAG priming (Table 2.2). All molecules were tested for their priming ability using previously described techniques<sup>19,20</sup>. As determined by S<sup>35</sup> incorporation, both Cu- and Ru-click xylosides primed but there were distinct differences in priming between 1,4 and 1,5-xylosides (Figure 2.5). Dimeric xylosides synthesized using Ru-click chemistry showed higher priming activity when compared to their Cu counterparts.

After assessing the priming activity of the molecules, the primed GAGs were characterized. Examination of sulfate density showed all compounds primed highly sulfated GAG chains. Primed GAGs elute at similar times in weak-anion exchange HPLC (Figure 2.6A), regardless of method of synthesis and length of the carbon linker. After determining sulfation density, the size of the primed GAGs was assessed (Table 2.3). While the primed GAGs showed slight differences in size, these differences were not significant. Finally, the disaccharide compositions of the primed GAGs were analyzed (Figure 2.6B). All molecules produce primarily CS GAG chains. After digestion of these chains using ChABC, the disaccharide profiles show that the primary disaccharide produced is a mono-sulfated disaccharide. It is the same disaccharide for each molecule. In Cu-click xylosides, the length of the linker between xylose residues plays a role in priming as there appears to

be a negative correlation between the length of the linker and the priming activity of the molecule. However, this is not as clear in the Ru-click xylosides. The compound with the three and four carbon linker (**4a**, **4b**) show similar priming activity with a reduction in activity seen in the molecules containing the five carbon linker (**4c**).

The data show that Ru-click chemistry produces more potent dimeric xylosides and the length of the carbon chain linker may influence 1,4 Cu-mediated orientation of the xylosides more than the 1,5 orientation found in Ru-mediated xylosides. The obvious difference in priming activity shows that the triazole linkage is important for priming activity. Changing from a 1,4 to a 1,5 linkage may provide the molecule with a higher percentage of entry into the cell and Golgi. Further exploration of how alterations to the aglycone linking the xylose residues coupled with a 1,5 linkage would alter both priming activity and GAG structure are needed. While Cu-click chemistry has been the predominant method for the synthesis of click-xylosides, the increased priming activity of the dimeric Ru-click xylosides versus the dimeric Cu-click shows a need to explore other forms of click chemistry for more active xylosides.

2.2.3.3 Summary of xyloside priming analysis. The production, purification, and characterization of a variety of tools is necessary for the proper study of the role of GAGs in biological systems such as vocal ontogeny and production. This chapter serves to present several different methods for GAG manipulation and show how these molecular tools were produced. The use of enzymes in exploration of GAGs is the most common molecular manipulation<sup>13-15</sup>. The cloning, expressing, and purification of enzymes provides the initial step for examining the importance of GAGs in neural and muscular control of behaviors. The use of Hep I, II, III together or ChABC results in the

degradation of all HS or CS, respectively. Using a single heparitinase or ChAC or ChB would allow the selective degradation of specific structures for the study of the role of specific GAGs. Hep I, II, III enzymes were employed in this chapter as well as Chapter 4. Based on the results, further exploration can be conducted using a single or mix of two enzymes. Additionally, the use of chondroitinase enzymes can also be examined in future studies as well.

Enzymatic degradation, while the most common, may not provide structure-specific information for GAG interactions, especially in regards to the sulfation patterns of heparan sulfate. Studying sulfation patterns requires controlling GAG structure. For HS, controlling sulfation pattern can be done chemically, but is a long and arduous process<sup>21</sup>. Chemoenzymatic synthesis of HS is a less exacting, but more scalable, method for creating specifically sulfated polymers. By enzymatically modifying the HS backbone with OSTs allows for the production of polymers with a single, two, or three specific sulfations. These specifically modified HS polymers can then be used to examine structure-function relationships. Similarly, oligosaccharides produced from these polymers will allow the study of the minimum requirement for GAG function. Several of these molecules have been or are being used by collaborators in other areas of study such as cancer, coagulation, and the development of nano-sensors (see Appendix B for published material). Future use of these molecules in vocal research is currently being discussed.

Small molecules present another method for GAG manipulation. Xylosides are small molecules that can alter GAG biosynthesis *in vitro* and *in vivo*<sup>12,18-20</sup>. These molecules are constantly being synthesized and screened for priming activity and GAG type. A monomeric xyloside that has been characterized<sup>19</sup> and used *in vivo*<sup>12</sup> in a different model

system will be used in Chapter 3. This molecule primes at a high level and primes only CS. The specificity of this molecule allows the modulation of a single type of GAG that is known to be expressed during this period in development. As compared to enzymes, which only digest present GAGs, using xylosides allows us to modulate biosynthesis itself, not simply alter GAG chains present in the ECM and on the cell surface. The use of multimeric xylosides is a viable option for future research; however, continued screening for molecules that prime well, produce a single type of GAG (HS or CS), produce both HS and CS, or produce a specific sulfation is required to allow for a better understanding of exactly how GAGs function *in vivo*.

### 2.3 Degradation of HS in HVC leads to altered song in adult zebra finch

After creating a variety of tools for the study and characterization of GAGs, we wanted to verify that manipulation of GAGs in a song-related forebrain area would lead to a measurable behavioral change in the zebra finch. The most straightforward test was to use the most common method of GAG manipulation, enzymes, and target a song-specific nucleus known to contain a PG. The literature is limited in this area, consisting of a handful of papers that directly mention HS or CS. Two of these papers focus on the role of PNNs during vocal ontogeny and will be discussed in the next chapter. A proteomic overview of the telencephalic sensorimotor nucleus, HVC (used as proper name), points out that a HSPG is present and is presumably involved in neural connectivity, differentiation, and neuronal survival in the adult zebra finch<sup>23</sup>. Outside of these studies that directly mention PGs, there are many publications that express the importance of growth factors and other signaling molecules in song development and production<sup>24-27</sup>. Many of these molecules,

such as BMP<sup>28</sup>, FGF<sup>12</sup>, and SHh<sup>29</sup>, are regulated or interact with GAGs in other systems.

This direct and indirect evidence led us to examine whether degradation of HS in HVC causes changes to adult stereotyped song. The proteomic study states that HS is likely involved with integration of neurons into circuits and neuronal survival<sup>23</sup>. If that is the case, then disruption of the HS should lead to changes in song, which should be detectable as adult song is highly stereotyped. This provides a test of whether GAGs are important for neural control of song production in adult.

In summary, examining of the role of HS in HVC in controlling adult song production will provide the preliminary evidence to confirm our choice of model system and employ other techniques to examine GAG influence in song learning and production

### 2.3.1 Methods and materials

2.3.1.1 Subjects. All male zebra finches used in this study were bred in our aviaries. The surgical procedures used were in accordance with National Institutes of Health guidelines and the Animal Care and Use Committee at the University of Utah.

2.3.1.2 Procedure for injection of enzyme into HVC. Heparitinase enzymes were produced, purified, and characterized as described previously. Adult male zebra finches (120+ PHD) were housed individually in acoustic chambers and song was recorded for several days, or until at least 20 distinct motifs were recorded. Birds were then anesthetized with Ketamine/Xylazine (0.012-0.02 ml), restrained with a cloth jacket, and placed in a stereotaxic apparatus with the horizontal head axis 45° relative to the vertical axis of the instrument. A small area of the skull was removed and an opening was made bilaterally in the dura 1-1.4 mm lateral to Y0. Birds received an acute injection (5 µl, at a rate of 1



$\mu\text{l}/\text{min}$ ) bilaterally of Hep I, II, III enzyme mixture ( $n = 6$ ) or buffer ( $n = 6$ ) at 0.4 mm depth from the brain surface. The exposed tissue was covered with hydrophilic vinyl polysiloxane (Reprosil; Dentsply International Inc.) and the polymer was then fixed to the skull using dental cement (Dentsply International Inc). After surgery, each bird was returned to individual housing for recovery. After recovering from surgery, birds were recorded in their acoustic chambers.

2.3.1.3 Recording and analysis of song. The songs of birds from both enzyme treated and sham groups were recorded weekly after infusion. All songs were recorded digitally using an omni-directional microphone (Audiotechnica) and software from Avisoft (SASLab, Berlin, Germany). At least 20 song motifs from each bird were selected randomly from the recordings made each week and spectrographic representations were visually inspected for changes in song structure. Variability within the adult song was assessed as changes in syllable sequence and acoustic structure using Sound Analysis Pro ([www.soundanalysispro.com](http://www.soundanalysispro.com)), and Praat ([www.praat.org](http://www.praat.org)).

### 2.3.2 Analysis and interpretation of changes in song

Birds that received a sham infusion showed no change in song. Motifs and bouts remained stereotyped and syllable structure remained unchanged. Enzyme treated birds, however, showed a wide range of changes within a month after treatment. These changes ranged from changes in harmonic emphasis and changes in timing between syllables to the production of entirely novel syllables and motifs.

An example of changes in harmonic emphasis is shown in Figure 2.7. Typical adult zebra finches present a stereotyped pattern of harmonic emphasis, or emphasis of

specific frequencies within a syllable. This is maintained between bouts and motifs. After treatment, this emphasis began to shift. Interestingly, the energy in the lower frequencies was reduced while higher frequencies were emphasized.

In terms of timing, there was an obvious change in the timing between specific syllables in some of the treated individuals. Figure 2.8 shows an example of such a change. In this instance, the intersyllable interval between two syllables was shortened one month after treatment, whereas it was relatively invariant before treatment. Timing changes were observed in 3 out of 6 individuals, while sham infusion birds did not show such a change. Finally, novel syllables appeared in the motifs of 4 out of 6 birds at one month post-treatment. In many cases, it was a single syllable that appeared occasionally in motifs but in the rare case, an entirely new motif was constructed and added to the end of pre-existing stereotypic song (Figure 2.9). Although this analysis was a test of concept only, it became apparent that not only are GAGs involved in neural control of vocal production, but loss of these carbohydrates can alter song output in a myriad number of ways. This was further complicated by the fact that treated birds did not always display the same characteristic changes in song, or if similarities were observed, it was with a wide range of severity. This was no more apparent than in the formation of new syllables. Not all birds created novel syllables, some created a single syllable that was rarely seen in motifs, others a single syllable that appeared more frequently, or another that produced an entirely new motif that was frequently added to the end of the pre-existing stereotypic motif. This makes quantification and complete understanding of the data and the importance of HS in zebra finch song production difficult and further emphasizes the need for a more sophisticated tool for studying how GAGs affect neural function and control of sensorimotor systems

such as that of learned vocal behavior.

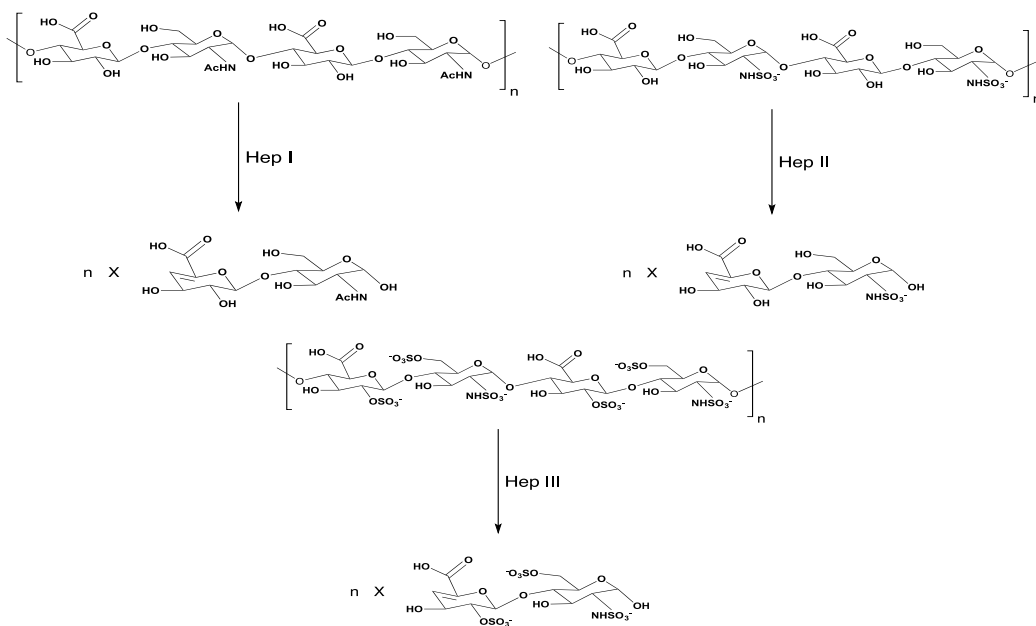
#### 2.4 Discussion

While GAGs have been implicated in almost every biological system, there is still only superficial knowledge of the exact functions of these complex carbohydrates in these systems. One of the major reasons for this is the dearth of tools that exist to study and really understand the structure and function of GAGs and the importance of specific structures to specific functions. GAGs are not easily sequenced, as they are formed in a nontemplated process with several steps of modification that can, but are not required, to occur. These differences in length and sulfation can lead to largely heterogeneous structures with numerous possible functions. In order to better understand how they function, specific tools for study are required.

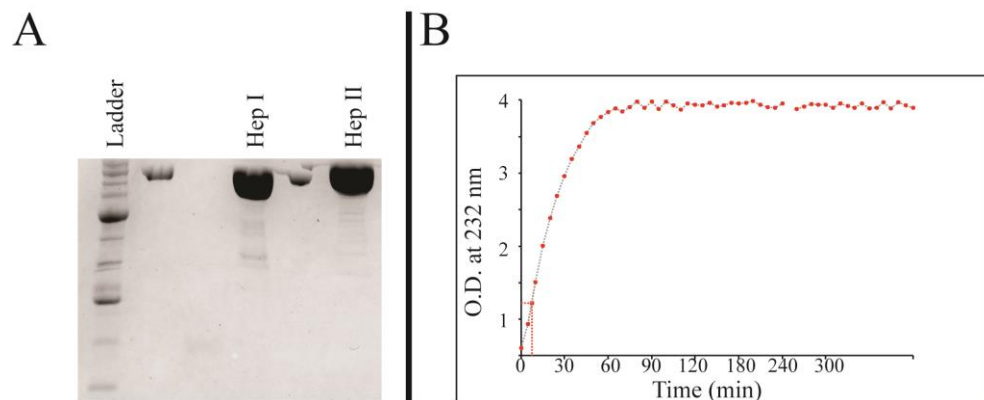
We set about to create this toolbox and show basic application *in vivo* of how degradation of one type of GAG can lead to a multitude of behavioral outcomes that are specific to individuals. Unlike a protein knockout, which may produce universally specific symptoms, removal of a specific type of GAG in the brain, such as HS, can lead to a variety of different outcomes. This shows that understanding the interaction between GAGs and proteins is vital for a complete understanding of how the brain connects, develops, and functions in both normal and diseased states. Using a variety of enzymatic and chemical methods, we were able to produce several reliable and novel molecules for studying GAGs. By producing, purifying, and screening enzymes, HS-like polymers, and oligosaccharides, and small molecules, we have been able to expand our capabilities to examine the function of GAGs in biological systems.

These tools, while shown to be active *in vitro* and in other systems, had yet to be tested in our desired model system. With the production of enzymes, we are able to look at overall degradation and how the loss of GAG may affect behavioral outcomes, as seen in changes in a stereotyped behavior such as crystallized song production in the zebra finch. The application of heparitinases *in vivo* led to a multitude of behavioral outcomes, specific to individuals, which shows that small changes can have profound but diverse effects.

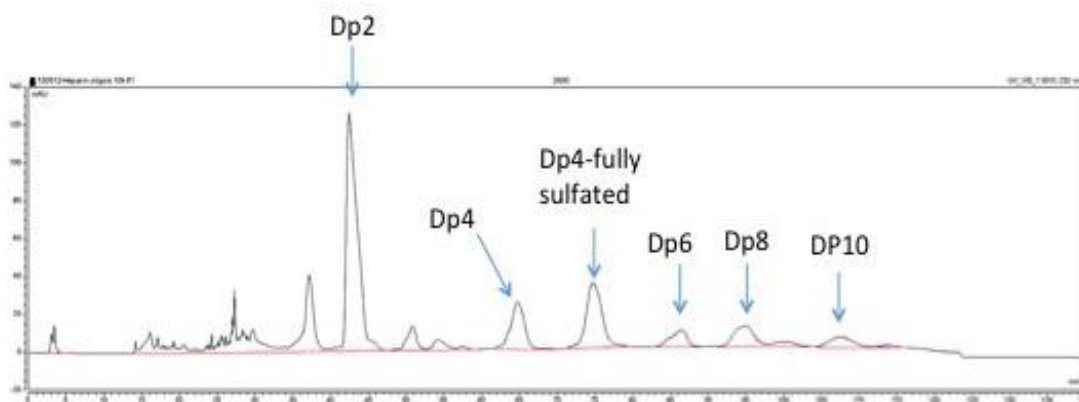
The diversity of these changes implicates GAGs and GAG-protein interaction factor into several aspects of neural development and plasticity. Small and transient changes in GAG profiles in the brain can result in a variety of changes to a stereotyped behavior. The variety of outcomes also emphasizes the importance of understanding exactly how GAGs function *in vivo* and how important sulfation pattern is to specific outcomes. The production and characterization of xylosides allows us to create molecules that can alter GAG biosynthesis and possibly serve as mimics for the naturally occurring proteoglycans. The creation of a library of specifically sulfated polymers and production of their oligosaccharides also presents a unique tool for understanding the optimum and minimum requirements for protein-GAG interaction. Each of these provides a different method of approaching the exploration of GAGs and their importance to vocal ontogeny and production.



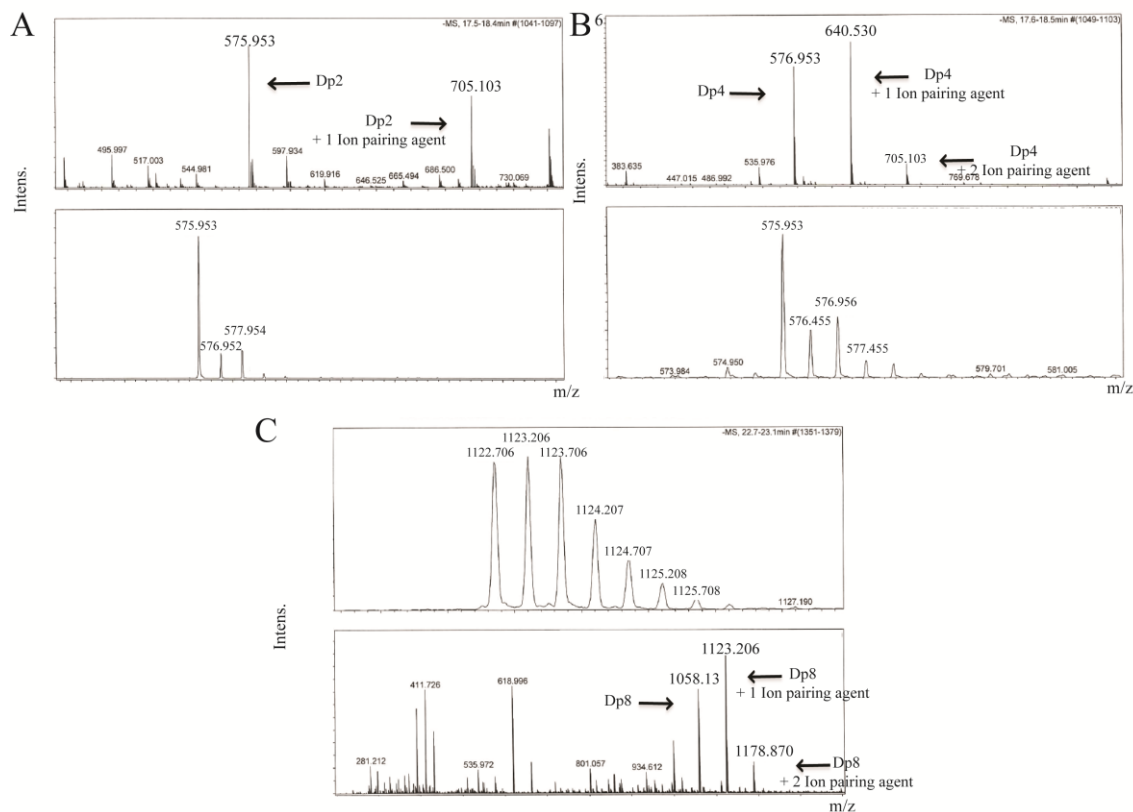
**Figure 2.1** Specificity for enzymatic degradation by Heparin lyases. Hep I digests primarily unsulfated HS polymer, Hep II digests sulfated and unsulfated HS, and Hep III is specific for highly sulfated polymer



**Figure 2.2** Purification and activity of glycosaminoglycan degradation enzymes. (A) A western blot that has been probed with anti-HIS tag antibody shows the presence of heparinase enzymes. (B) Activity of Hep III is observed with the increase in O.D. reading at 232 nm showing cleavage of heparin.



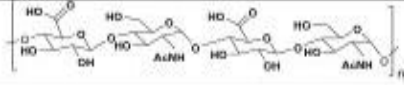
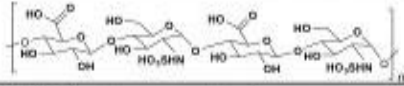
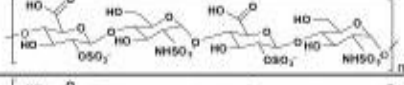
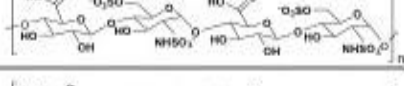
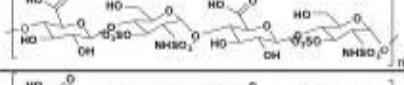
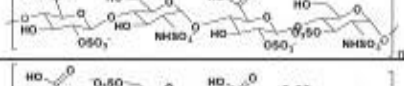

**Figure 2.3** HPLC profile of preparative scale partial digestion of heparin to produce oligosaccharides. Unlike uniformly labeled polymers, peaks must be characterized to ensure the correct size as neighboring peaks may be the same size and differ only by sulfation.



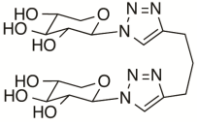
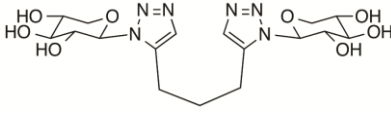
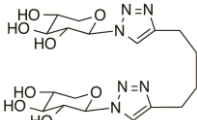
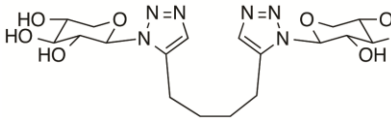
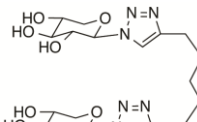
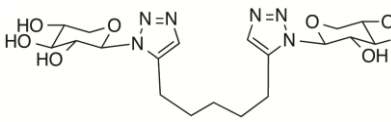
**Figure 2.4** Mass spectrometry analysis of heparin oligosaccharides. Strong anion exchange HPLC separates sulfated oligosaccharides based on their degree of polymerization (dp). Peaks correspond to different size or sulfated molecules. (A) Fully-sulfated disaccharide is present as seen in the peak at 575.993, z1. (B) Fully-sulfated tetrasaccharide can be seen at the same peak, 575.953, z2. (C) As the size of the oligosaccharide increases, often the mass at which you see the molecule increases as well. An 8-mer is often seen as a tetrasaccharide, z2.



**Table 2.1** Table of specifically sulfated polymers synthesized for research purposes

Polymer Name	Structure
Heparosan (K5)	
N-sulfated Heparosan (K5NS)	
NS2S	
NS6S	
NS3S	
NS2S3S	
NS6S3S	

**Table 2.2** Structures of the Cu- and Ru-click-xylosides that were screened

Compound Name	Structure	Compound Name	Structure
3a		4a	
3b		4b	
3c		4c	

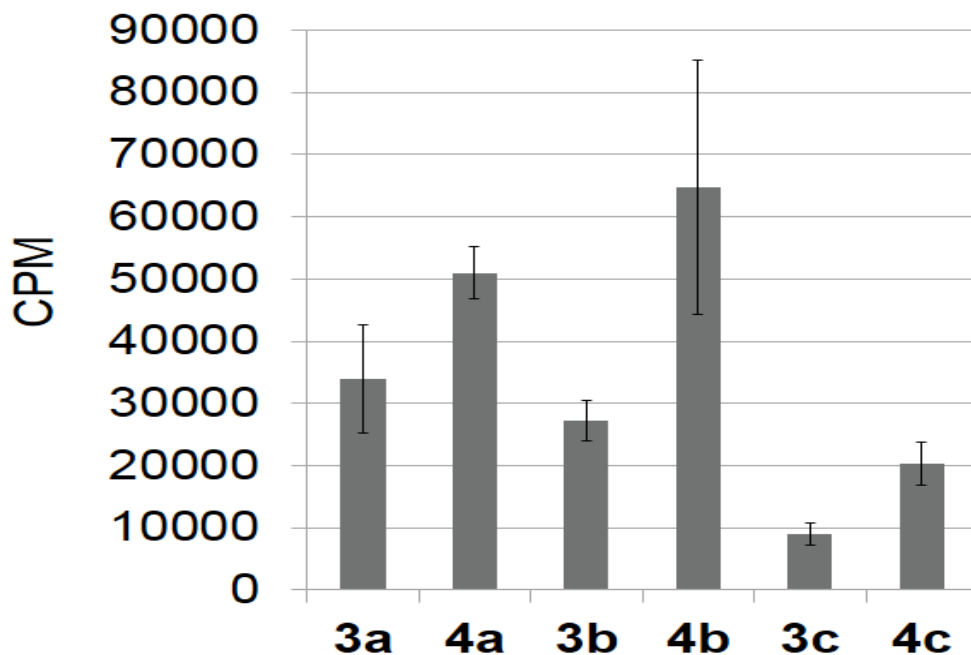


**Figure 2.5** Comparison of priming activity by scintillation count for Cu-click vs Ru-click xylosides. This shows the incorporation of radioactive sulfate in GAG chains primed by Cu-click dimeric xylosides (3a,3b,3c) and Ru-click dimeric xylosides (4a,4b,4c). Ru-click xylosides show higher priming in all compounds tested and do not show priming dependence on the length of carbon linking chain between xylose residues.

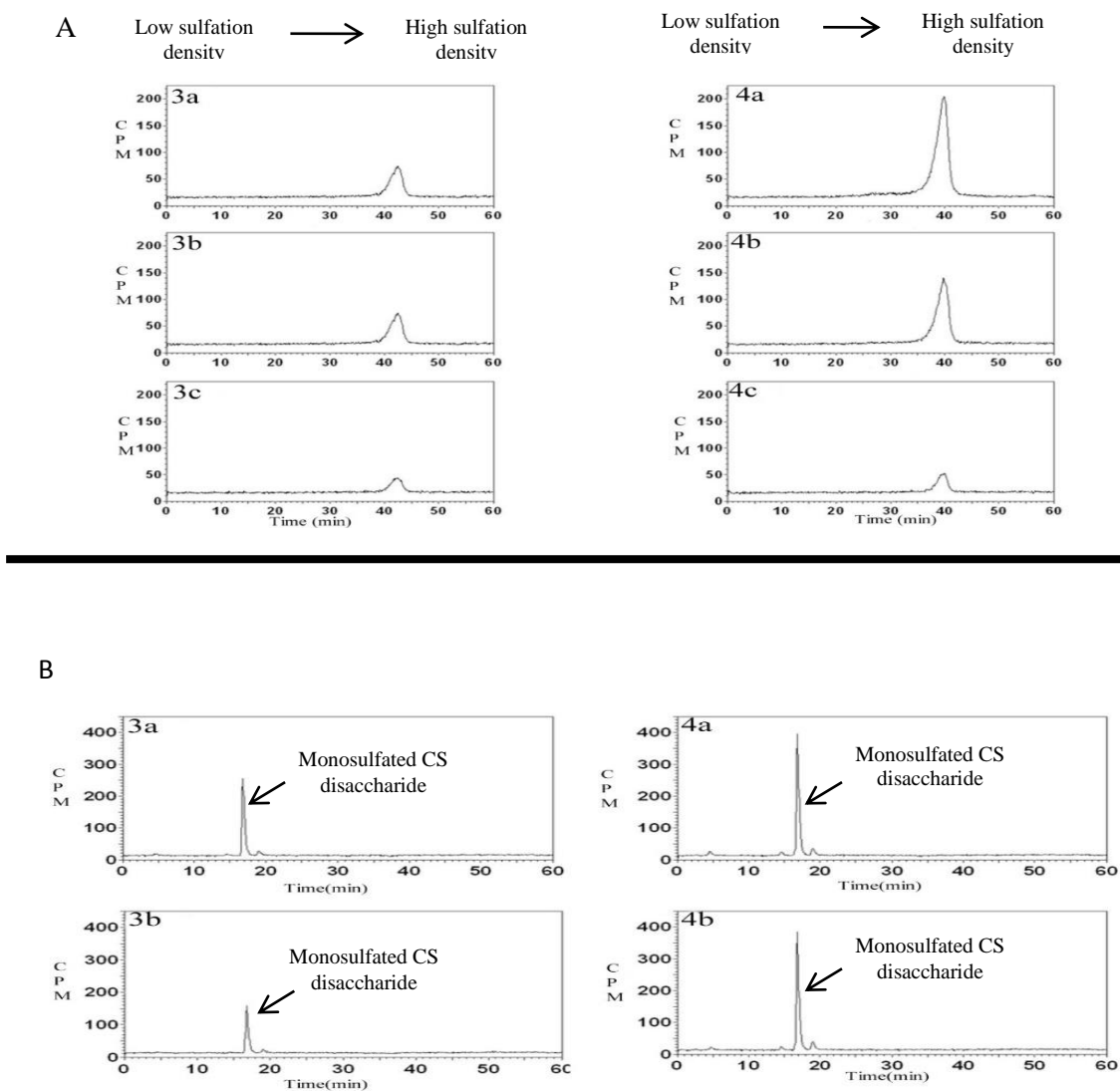


**Figure 2.6.** Comparison of overall sulfation density and disaccharide composition for Cu-click and Ru-click xylosides (A) weak-anion exchange HPLC profiles of GAG chains primed by Cu-xylosides (3a,3b,3c) versus Ru-xylosides (4a,4b,4c). This shows that sulfation density of the primed GAG chains is similar for all compounds. (B) Disaccharide composition of primed GAG chains as measured by strong-anion exchange HPLC. All compounds produce primarily monosulfated CS disaccharides.

**Table 2.3** Size of primed GAG chains of dimeric Cu- and Ru-catalyzed click xylosides

Xyloside	M.W. of Primed GAGs (kDa)
<b>3a</b>	42.3
<b>3b</b>	44.6
<b>3c</b>	43.1
<b>4a</b>	40.1
<b>4b</b>	41.7
<b>4c</b>	46.2

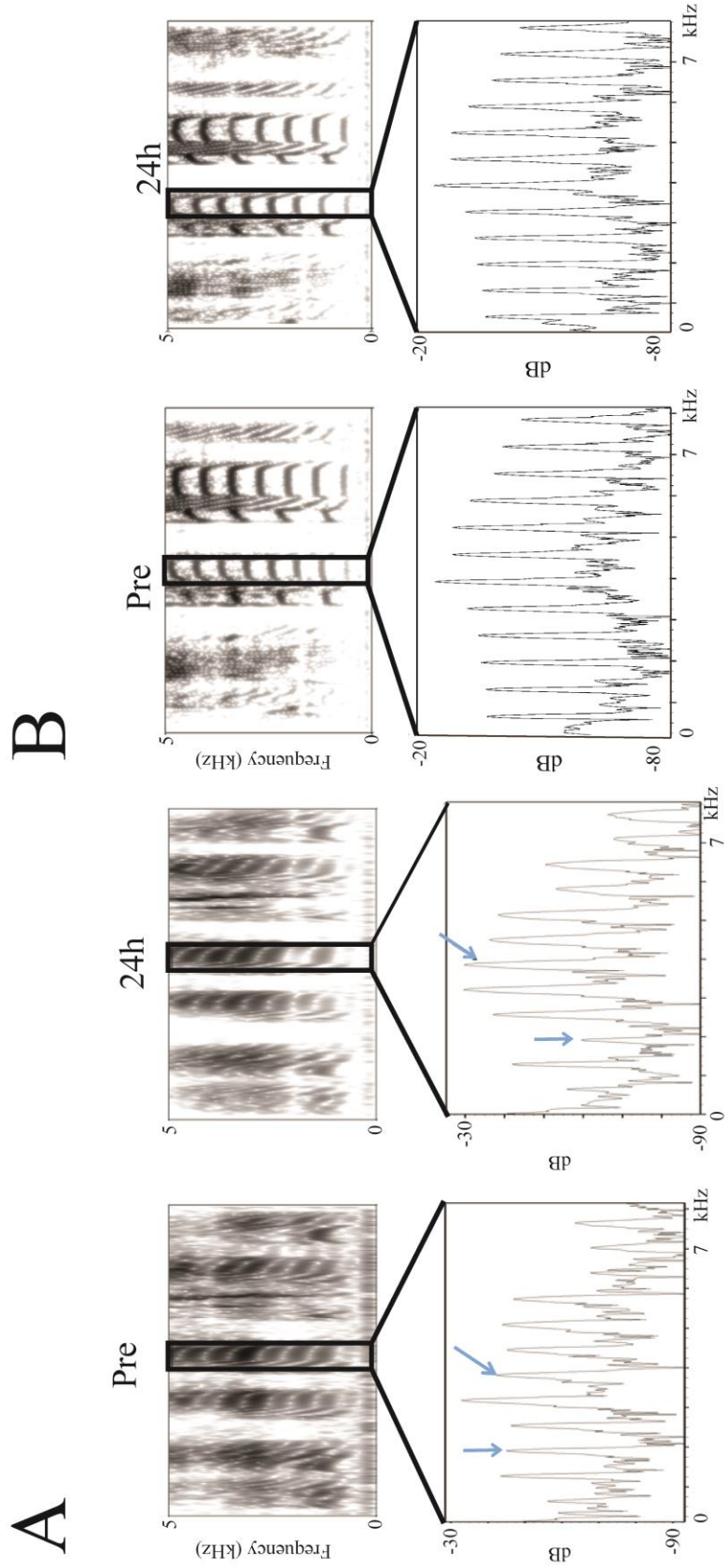


**Figure 2.7** Spectrogram and frequency analysis of a specific syllable in the motif of an adult zebra finch before and 24 h after treatment with heparitinase (A) or vehicle (B), respectively. A clear shift of harmonic emphasis can be seen in enzyme-treated birds. Arrows indicate two specific frequencies that are altered within the syllable.

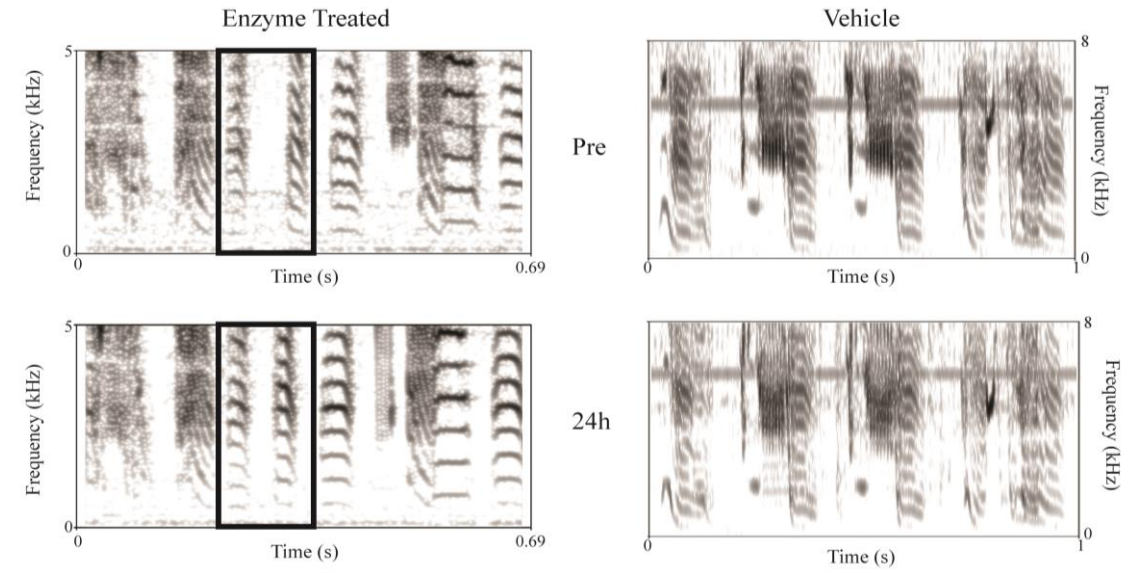


**Figure 2.8** . Spectrogram analysis indicates a shift in timing between song syllables in enzyme treated birds as compared to controls. This change can be seen one month after treatment. The black rectangle outlines the two syllables that show the shift.

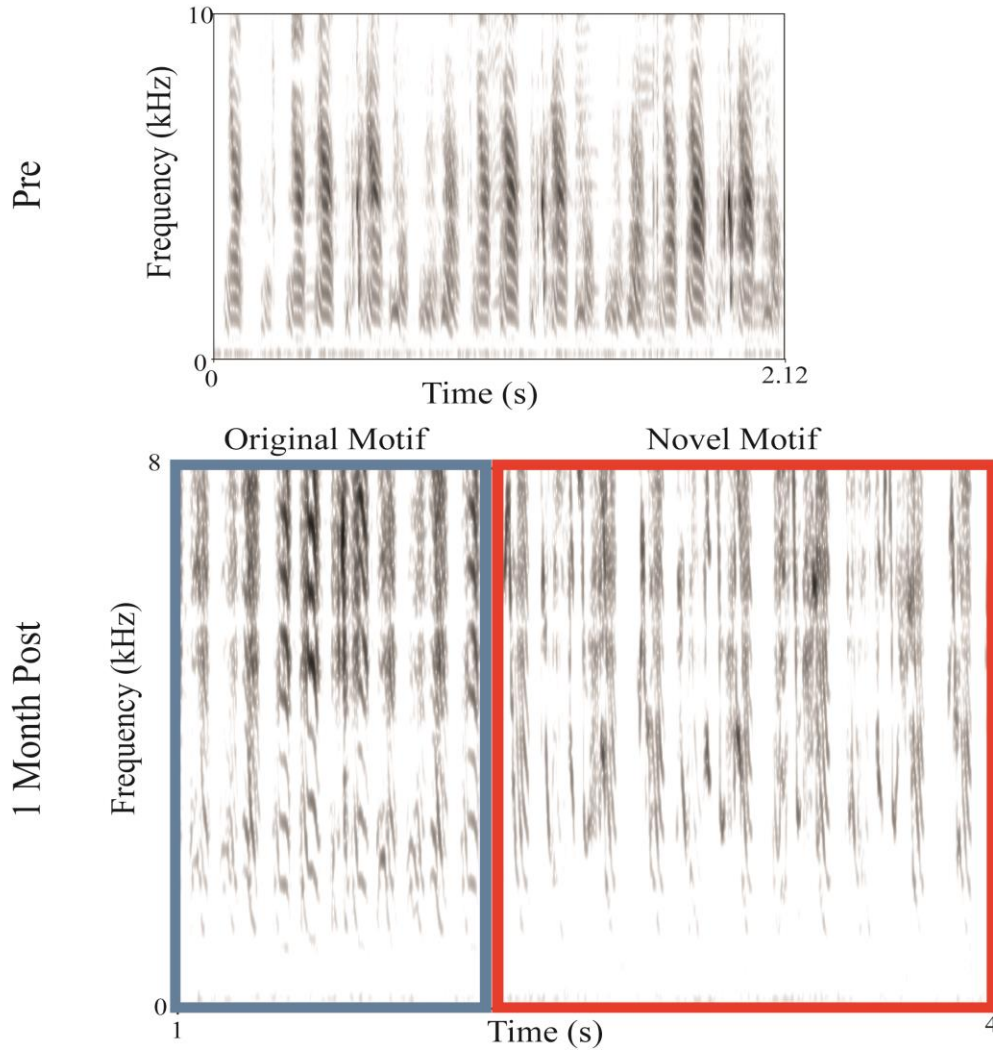


**Figure 2.9** Production of a novel motif at one month post heparitinase injection in adult zebra finch. The original motif, boxed in blue, is stereotyped and was present prior to enzymatic manipulation of HVC as seen by the pre-infusion song presented on the left. One month after treatment, the treated bird consistently produced a novel motif, outlined here in red. This indicates a significant change in song pattern and was not found in controls.



## 2.5 References

1. Kantor, D.B.; Chivatakarn, O.; Peer, K.L.; Oster, S.F.; Inatani, M.; Hansen, M.J.; Flanagan, J.G.; Yamaguchi, Y.; Sretavan, D.W.; Giger, R.J.; Kolodkin, A.L. Semaphorin 5A is a bifunctional axon guidance cue regulated by heparan and chondroitin sulfate proteoglycans, *Neuron*, **2004**, *44*, 961-975.
2. Becker, C.G.; Becker, T. Repellent guidance of regenerating optic axons by chondroitin sulfate glycosaminoglycans in zebrafish, *J Neurosci*, **2002**, *22*, 842-853.
3. Fernaud-Espinosa, I.; Nieto-Sampedro, M.; Bovolenta, P. Developmental distribution of glycosaminoglycans in embryonic rat brain: relationship to axonal tract formation, *Dev Neurobiol*, **1996**, *30*, 410-424.
4. Laabs, T.; Carulli, D.; Geller, H.M.; Fawcett, J.W. Chondroitin sulfate proteoglycans in neural development and regeneration, *Curr Opin Neurobiol*, **2005**, *15*, 116-120.
5. Esko, J.D.; Selleck, S.B. (2002) Order out of chaos: assembly of ligand binding sites in heparan sulfate 1, *Annu Rev Biochem*, **2002**, *71*, 435-471.
6. Grumet, M.; Flaccus, A.; Margolis, R.U. Functional characterization of chondroitin sulfate proteoglycans of brain: interactions with neurons and neural cell adhesion molecules, *J Chem Biol*, **1993**, *120*, 815-824.
7. Perrimon, N.; Bernfield, M. Cellular functions of proteoglycans-an overview, *Sem Cell Devl Biol*, **2001**, *12*, 65-67.
8. Anderson, M.; Klier, F.; Tanguay, K. Acetylcholine receptor aggregation parallels the deposition of a basal lamina proteoglycan during development of the neuromuscular junction, *J Cell Biol*, **1984**, *99*, 1769-1784.
9. Atha, D. H.; Stephens, A. W.; Rosenberg, R. D. Evaluation of critical groups required for the binding of heparin to antithrombin, *PNAS*, **1984**, *81*, 1030-1034.
10. Lindahl, U.; Backstrom, G.; Thunberg, L.; Leder, I. G. Evidence for a 3-O-sulfated D-glucosamine residue in the antithrombin-binding sequence of heparin, *PNAS*, **1980**, *77*, 6551-6555.
11. Nguyen, T.K.N.; Raman, K.; Tran, V.M.; Kuberan, B. Investigating the mechanism of the assembly of FGF1-binding heparan sulfate motifs, *FEBS Lett*, **2011**, *585*, 2698-2702.
12. Ngyuen, T.K.N.; Tran, V.M.; Sorna, V.; Eriksson, I.; Kojima, A.; Koketsu, M.; Loganathan, D.; Kjellén, L; Dorsky, R.I.; Chien, C.; Kuberan, B. Dimerized glycosaminoglycan chains increase FGF signaling during zebrafish development, *ACS Chem Biol*, **2013**, *8*, 939-948.

13. Nakajima, M.; Irimura, T.; Di Ferrante, D.; Di Ferrante, N.; Nicolson, G.L Heparan sulfate degradation: relation to tumor invasive and metastatic properties of mouse B16 melanoma sublines, *Science*, **1983**, *220*, 611-613.
14. Bradbury, E.J.; Moon, L.D.F.; Popat, R.J.; King, V.R.; Bennett, G.S.; Patel, P.N.; Fawcett, J.W.; McMahon, S.B. Chondroitinase ABC promotes functional recovery after spinal cord injury, *Nature*, **2002**, *416*, 636-640.
15. Garcia-Alias, G.; Barkhuysen, S.; Buckle, M.; Fawcett, J. Chondroitinase ABC treatment opens a window of opportunity for task-specific rehabilitation, *Nat Neurosci*, **2009**, *12*, 1145-1151.
16. Lohse, D.L.; Linhardt, R.J. Purification and characterization of heparin lyases from flavobacterium heparinum, *J Biol Chem*, **1992**, *267*, 24347-24355.
17. Yamagata, T.; Saito, H.; Habuchi, O.; Suzuki, S. Purification and properties of bacterial chondroitinases and chondrosulfatases, *J Biol Chem*, **1968**, *243*, 1523-1535.
18. Schwartz, N.B. Regulation of chondroitin sulfate synthesis. Effect of beta-xylosides on synthesis of chondroitin sulfate proteoglycan, chondroitin sulfate chains, and core protein, *J Biol Chem*, **1977**, *252*, 6316-6321.
19. Victor, X.V.; Nguyen, T.K.N.; Ethirajan, M.; Tran, V.M.; Nguyen, K.V.; Kuberan, B. Investigating the elusive mechanism of glycosaminoglycan biosynthesis, *J Biol Chem*, **2009**, *284*, 25842-25853.
20. Kuberan, B.; Ethirajan, M.; Victor, X.; Tran, V.M.; Nguyen, K.V.; Do, A. "Click"-xylosides initiate glycosaminoglycan biosynthesis in a mammalian cell line, *ChemBioChem*, **2008**, *9*, 198-200.
21. Lee, J.; Lu, X.; Kulkarni, S.S.; Wen, Y.; Hung, S. Synthesis of heparin oligosaccharides, *J Am Chem Soc*, **2004**, *126*, 476-477.
22. Balmer, T.; Carels, V.; Frisch, J.; Nick, T. Modulation of perineuronal nets and parvalbumin with developmental song learning, *J Neurosci*, **2009**, *29*, 12878-12885.
23. Lovell, P.; Clayton, D.; Replogle, K.; Mello, C. Birdsong "Transcriptomics": Neurochemical Specializations of the Oscine Song System. *PLoS ONE*, **2008**.
24. Miller, J.E.; Spiteri, E.; Condoro, M.C.; Dosumu-Johnson, R.T.; Geschwind, D.H.; White, S.A. Birdsong decreases protein levels of FoxP2, a molecule required for human speech, *J Neurophysiol*, **2008**, *100*, 2015-2025
25. Nordeen, E.J.; Voelkel, L.; Nordeen, K.W. Fibroblast growth factor-2 stimulates cell proliferation and decreases sexually dimorphic cell death in an avian song control nucleus, *J Neurobiol*, **1998**, *37*, 573-581.

26. Nordeen, K.W.; Nordeen, E.J. Anatomical and synaptic substrates for avian song learning, *J Neurobiol*, **1997**, *33*, 532-548.
27. Sakaguchi, H.; Saito, N. The acetylcholine and catecholamine contents in song control nuclei of zebra finch during song ontogeny, *Dev Brain Res*, **1989**, *47*, 313-317.
28. Gandhi, N.S.; Mancera, R.L. Prediction of heparin binding sites in bone morphogenetic proteins (BMPs), *Biochim Biophys Acta- Proteins & Proteomics*, **2012**, *1824*, 1374-1381.
- 29 Whalen, D.M.; Malinauskas, T.; Gilbert, R.J.C.; Siebold, C. Structural insights into proteoglycan-shaped hedgehog signaling, *PNAS*, **2013**, *110*, 16420-16425.

## CHAPTER 3

### MODULATION OF GLYCOSAMINOGLYCANS ALTERS

### VOCAL ONTOGENY IN ZEBRA FINCH

#### 3.1 Introduction

In the brain, PGs function to form PNNs<sup>1-4</sup>, bind morphogens and ligands to form gradients<sup>5,6</sup>, have strict developmental regulation<sup>7-9</sup>, and are involved in axon pathfinding<sup>10</sup>, neuron migration, and connection<sup>11-13</sup>. While the importance of the biosynthesis of GAGs in sensory system critical periods, such as vision, have been studied<sup>14-16</sup>, research has yet to consider their role in more complicated aspects of neural control such as systems and behaviors that require a large degree of sensory-motor integration. One such behavior is songbird vocal behavior.

In zebra finch, vocal ontogeny has been well documented. Both the timeline<sup>17-19</sup> and the neural circuitry for learning and producing song in zebra finch has been well characterized<sup>18,20-22</sup>. Song is developed by obtaining an auditory template, rehearsal and refinement of song, and finally crystallization of song into stereotyped motifs, which occurs around 90 PHD<sup>17-19</sup>. However, the importance of GAGs in this process and how changes in GAG biosynthesis affect overall vocal ontogeny is still unclear.

Vocal ontogeny requires integration of sensory (auditory) feedback with a motor (song output) system through central processing in specific nuclei in the forebrain<sup>23-25</sup>.

This provides a system uniquely designed to allow us to examine how altering GAG biosynthesis in the central control can affect sensorimotor integration. In this manner, it is possible to examine how GAG biosynthesis contributes to complex behavior and modulation of carbohydrate polymers can result in altering a distinct behavior. This study presents the first evidence that modulations in GAG biosynthesis in the central nervous system during development can have long lasting effects on complex learned behaviors that require sensorimotor integration, such as learned vocal behavior.

### 3.2 Methods and materials

#### 3.2.1 Animals

Juvenile male zebra finches were used in this study. The birds were bred in flight aviaries at the University of Utah. The surgical procedures used were in accordance with National Institutes of Health guidelines and the Animal Care and Use Committee at the University of Utah.

#### 3.2.2 Reagents

Immunohistochemistry was performed using Hoechst 33342 (Fisher Scientific). Western blots were conducted with monoclonal antibody CS56 (Sigma Aldrich). All secondary antibodies were purchased from Fisher Scientific. Xylosides were synthesized, purified, and analyzed in the Balagurunathan lab<sup>26</sup>.

### 3.2.3 Surgery and microinjection

Birds were anesthetized with (0.012-0.02 ml) of Ketamine/Xylazine, restrained with a cloth jacket, and placed in a stereotaxic apparatus with the horizontal head axis 45° relative to the vertical axis of the instrument. A small area of the skull was removed and an opening was made in the dura 2 mm lateral and 1.4 mm posterior to Y0 bilaterally as determined by a stereotaxic atlas in lab. A precut 1.5 mm 26G guide cannula (Plastics One, Roanoke, VA) was implanted and a 33G dummy cannula inserted to prevent blocking of the guide cannula. The cannulae were fixed at the skull with dental cement (Dentsply International Inc). After surgery, each bird was housed individually for recovery. After recovering from surgery, birds were moved to an acoustic chamber for song recording. Microinjections were given according to their experimental group every 48 h for a total of 5 injections beginning at 55-60 PHD in all birds. Injection sites were confirmed by histology after perfusion. Immediately before injection, the dummy cannula was replaced by a 33G internal cannula, which was connected via tubing to a syringe. Microinfusion was driven by a microinfusion pump (KD Scientific, New Hope, PA). Each injection was performed bilaterally to a total injection volume of 5 µl at a rate of 1µl/min. The bird was then returned to the acoustic recording chamber for continued song recording.

### 3.2.4 Song recordings and analysis

The songs of birds from both experimental and control groups (n= 6 experimental, 6 control) were recorded from the date of first microinjection to 110+ PHD. All songs were recorded digitally using an omni-directional microphone (Audiotechnica) and software from Avisoft (SASLab, Berlin, Germany). At least 25 song motifs from each bird

were selected randomly from the recordings made during the recording period. Spectrograms of these motifs were used to analyze the variability of adult song through analysis of the sequence of syllables and the syllable morphology using Sound Analysis Pro ([www.soundanalysispro.com](http://www.soundanalysispro.com)). All birds sang readily in the recording chambers. To quantify the degree of stereotypy in the song phrases of control and experimental birds, 30 motifs were examined from each of three timepoints: 60-70 PHD, 80-90 PHD, and 110+ PHD. Each motif was analyzed using Sound Analysis Pro (SAP)<sup>27</sup>. Motifs were compared for accuracy, % sequential, and % similarity.

### 3.2.5 Histology, western blot, and HPLC analysis

All animals were deeply anesthetized with an overdose of Ketamine/Xylazine and perfused through the heart with phosphate buffered saline (PBS), followed by 4% paraformaldehyde (PFA) in PBS, pH 7 after reaching 120 PHD, with the exception of birds used for western blot and HPLC purposes who were perfused 24 h after the final infusion. Brains were removed from the skull and post-fixed in 4% PFA, dehydrated through an alcohol gradient, imbedded using ImmunoBed (Polysciences, Inc.) and sectioned at 5  $\mu$ m in the sagittal plane. Slice sampling was done in a systematic-random manner. Confirmation of injection site was done using widefield fluorescence on a microscope (Olympus IX73).

Tissue was homogenized and proteoglycans extracted using a NP-40 buffer (Fisher Scientific) following recommended procedure. The extract was transferred to a clean tube and then loaded three times on to a DEAE-sepharose column (0.25 ml) that had been pre-equilibrated with 10 column volumes of wash buffer (20 mM NaOAc buffer, pH 6.0,

containing 0.1 M NaCl). The column was then washed with 20 column volumes of wash buffer. Elution of the bound proteoglycans from the column was accomplished using 6 column volumes of elution buffer (20 mM NaOAc buffer, pH 6.0, containing 1 M NaCl). The elution was then filter-desalted using a spin filtration unit MWCO 3000 (Amicon). After desalting, sample was used based on the xyloside treated. Samples from birds treated with compound **1** were diluted to 100  $\mu$ l and a BCA was run to assess protein content using Pierce BCA Protein Assay kit (Thermo Scientific). Based on the outcome of the BSA, equal amounts of protein from all samples were loaded and run on a polyacrylamide 4-15% gel (Biorad) at 200V for 40 min. The proteins were then transferred to a nitrocellulose membrane at 25V for 45 min. The membrane was then blocked in 1% evaporated milk (Carnation) in TBST buffer and probed with CS56 antibody (1:1000 dilution) overnight at 4°C, shaking. The secondary used was goat anti-mouse IgM-HRP (Fisher Scientific). The membrane was analyzed using the Chemi-doc system (Biorad).

Samples from tissue treated with compound **2** were incubated overnight with streptavidin-AF488 (Fisher Scientific) at room temperature. After incubation, half the mixture was digested with ChABC (Sigma Aldrich) overnight. Both the undigested and digested samples were assessed for a shift in their migration time as compared to only streptavidin-AF 488 on a size exclusion column using HPLC. Two G3000SWXL (7.8 mm x 30 cm, 5  $\mu$ m) size exclusion columns were connected in tandem and the eluted GAG chains were loaded onto the columns. These chains were eluted over 60 min using a phosphate buffer containing 100 mM  $\text{KH}_2\text{PO}_4$  and 100 mM NaCl at pH 6.0.



### 3.2.6 Statistical analysis and data presentation

All data was analyzed by SAP or 3 independent observers. Data are presented as mean  $\pm$  SD and were compared with an unpaired, or paired, Student's t-test (two-tailed) where appropriate. Significance was defined as  $p < 0.05$ . These were calculated using Kaleidograph.

### 3.3 Results

Compound 1 (Table 3.1) showed a high level of GAG priming in multiple cell types and has been shown to be nontoxic in cell culture. Due to these properties, this was the molecule used in this study. Song comparisons showed significant differences between song at all three time-points in control birds, using adult song as a template. Song at that age is expected to be highly stereotyped in both acoustic structure and order of syllables.

Figure 3.1 shows representations of song in spectrograms that show how frequency changes over time. Bouts from two different birds in each group are shown at 60 PHD and 110+ PHD. At 60 PHD, both groups lacked stereotypy in both sequence of syllables produced as well as in the syllable fine structure. At 110+ PHD, control birds showed highly stereotyped motifs strung together into bouts. This is normal song development and is expected in the zebra finch<sup>17-22</sup>. However, the bouts sung by treated birds lacked the syntactical stereotypy of the controls. Syllable fine structure becomes stereotypic in both groups. To compare these measures, multiple motifs were analyzed at each time-point for all subjects. First song within the groups was compared at each time-point to the song at 110+ PHD. The song at 110+ PHD should be the mature, crystallized song of the bird. This comparison would allow the mapping of the developmental trajectory as it approaches

crystallized song. Figure 3.2A-C shows a comparison of these measures. As expected, significant differences ( $p < 0.05$ ) were seen in the sequential and similarity scores as the bird developed. Accuracy scores, which accounted for syllable fine structure, did not show as dramatic an improvement, but there was an overall increase between the earliest and latest time-points.

In the treated groups (Figure 3.2A-C), the two areas that showed the most improvement in the control birds, similarity and sequential, showed no changes between any time points measured. Accuracy scores showed the same overall increase between the earliest and latest time-point. These data suggest that the infusion of xyloside had a marked effect on normal song development, specifically influencing the ordering of syllables into stereotypic patterns. To be sure that one group was not starting with more accurate song, data between treatment groups were compared. Figure 3.2A-C showed that both the control and treated groups began at similar scores for all three categories at the 60-70 PHD time point.

As time progressed it became clear that the control group was moving toward mature song while the treated birds' scores remained relatively plateaued. Again, the two measures that showed the largest disparity between the groups were similarity and sequential scores. These measures were significantly different ( $p > 0.005$ ) at the 80-90 PHD measurements and remained that way ( $p > 0.05$ ) at the latest recording dates. Accuracy scores were not significantly different and increased over time in almost a linear fashion. Next motifs within time-points were compared (Figure 3.2D-F). This allowed an assessment of how stable or stereotyped the motifs were within a measured time frame. These data were used to compare between groups and show when song development

among the two groups diverged.

In all three categories, both groups were relatively equal at 60-70 PHD. The motif at 60-70 PHD compared to others from the same time-frame would show the two groups began as equal, not only in comparison to the bird's adult song, but also when comparing the juvenile song to itself. Song at this time point was expected to be variable in acoustic structure and syllable sequence. Between groups at 80-90 PHD, it was shown that the motifs at 80-90 PHD were not that different; however, the trend showed the control groups beginning to rise in both sequential and similarity. Additionally, the standard deviation for the control groups was becoming smaller. Treated birds did not show this improvement. By 110+ PHD, there is a clear difference between the control and treated groups in similarity and sequential scores as well as their standard deviations. This indicated that while the control groups were improving over time toward their mature song, but when comparing between groups within time-points, the songs only showed clear differences at 110+ PHD.

With song development clearly altered by xyloside infusion, the question arose as to how the xyloside is changing GAG biosynthesis in the zebra finch brain and how these changes may be responsible for the behavioral changes measured. Xylosides have two major functions: priming and serving as a decoy.

To prime, xylosides enter the Golgi and the enzymatic machinery extends and modifies a carbohydrate chain on the xylose. The primed GAG chain is then sent out of the cell and into the ECM<sup>28-30</sup>. The expulsion of these chains into the ECM may allow them to function in a manner similar to endogenous PGs such as binding ligands and/or receptors, providing axonal guidance cues, or stabilizing synapses. Additionally, xylosides

are known to serve as “decoy” molecules for these enzymes<sup>28,29</sup>. In this instance, the function of priming occupies enzymes that would normally be functioning on endogenous proteins to make proteoglycans. This results in a loss of protein-bound GAGs, but not a loss of the core protein itself. This decrease in endogenous PGs may affect gradient formation of morphogens/ligands, axonal pathfinding, neurite outgrowth and support, as well as overall ECM structure.

First the possible decoy action of the xyloside was examined. Figure 3.3 showed that in the xyloside treated samples, there was a distinct lack of chondroitin sulfate as compared to vehicle treated samples as seen by western blot. The ladder shows that both transfer and antibody probing procedures were followed correctly. As the antibody used is against CS specifically, this is responsible for the larger band size. The lanes containing wash for each condition show that our purification was effective. In comparing the purified proteoglycans from both groups, xyloside treated birds show a reduction in CS as compared to vehicle treated controls. This indicated that the xyloside was serving as a decoy and prevented the synthesis of endogenous PGs. However, analysis of the GAG chains by mass spectrometry did not indicate a loss of overall GAG. This was an indication of priming. To examine priming, it was necessary to use a molecule that would allow us to capture only the GAGs that were attached to the xyloside. To accomplish this, a biotinylated click-xyloside, or a xylose with a biotin molecule as the aglycone (compound **2**) was used. Figure 3.4B shows that compound **2** primed GAG chains in the juvenile brain and these chains were primarily CS.

### 3.4 Discussion

The data presented in this study offer a new look at developing song and the role of GAGs in the nervous system. Tightly regulated GAG biosynthesis is critical for the developing nervous system,<sup>2,3,5-10</sup> and modulation of biosynthesis can lead to permanent changes in a learned behavior. The data show that induced modulation of CS, even relatively early in a critical period, can have lasting effects on neural development. Using song as an assay allows the examination of the role of CS in establishing a motor program for a complex behavior that requires sophisticated sensory-motor integration.

The time course of song development and ontogeny of vocal features following GAG modulation suggests a specific rather than global effect. The improved accuracy scores indicate that the acoustic structure becomes stereotyped as seen in both the control and treatment group. However, while acoustic structure shows less variation in the treated birds, this increase in scores does not include an improvement in stabilizing frequency trajectories of modulated syllables. The retained wavy nature of frequency trajectories is indicative of plastic song in the zebra finch<sup>31</sup> and is not seen in the control group after or near crystallization. Because syringeal muscles play an important role in frequency control<sup>32</sup> the failure to sing smooth frequency trajectories indicates an unstable neural control strategy.

In addition, the main difference between treatment and control birds is a lack of progress in developing stereotypy of song syllable sequence in the former, whereas a typical trajectory of increased stereotypy is seen in the control birds<sup>19,20-22</sup>. Control of syllable sequence is thought to arise from combined input from HVC and the cortico-thalamic anterior forebrain pathway into RA. Interestingly, disruption of acoustic

feedback causes a loss of stereotypy in adult zebra finches<sup>33-35</sup>, and this effect is mediated through anterior forebrain pathway<sup>36</sup>. The lack of stereotypy in song sequence after manipulation of the CS dynamics in RA thus suggests that changes in RA circuitry that are associated with perineuronal net formation account for the lack of stereotypy in song sequence.

The respective roles of HVC and RA have been inferred from single cell recordings in each nucleus during song production<sup>37</sup>. The model postulates a major role of HVC in controlling all major aspects of temporal structure, including syllable sequence<sup>37,38</sup>. RA was assigned a less significant role in the control of temporal aspects of song. This view seems consistent with effects on song from electrical stimulation of each nucleus. Electrical stimulation in HVC of singing birds caused abortion of song motifs, while stimulation of RA resulted in changes in the acoustic structure of individual syllables<sup>38</sup>. However, this model has been challenged by an alternative model that postulates a more distributed control of temporal aspects of song<sup>39</sup>. Our data do not directly address this question, but indirectly support the distributed control hypothesis. The fact that song syllable sequence ontogeny depends on the internal circuitry of RA is in apparent contradiction with the stimulation results. However, if one considers that electrical stimulation affects the downstream circuitry of the stimulated area, rather than the fine processing in the stimulated nucleus, then the results are not contradictory.

Our data also strongly suggest that the developmental trajectories of stereotyped acoustic structure and stereotypy in syllable sequence are not interdependent. Because the acoustic structure showed increased stereotypy over developmental time, while syllables retained less controlled frequency trajectories in the treated birds, it is likely that

these two aspects of vocal ontogeny are not tightly linked. The change in RA circuitry following CS manipulation must have prevented the generation of a smooth neural signal for frequency control in the hypoglossal nucleus, but allowed this frequency control mechanism to become stereotyped over the course of vocal ontogeny.

These results indicate that the role of CS in RA during song development is complex. We have shown that xylosides can have two distinct roles *in vivo*, serving as either a decoy which disrupts endogenous GAG biosynthesis<sup>28,29</sup> or as a primer on which GAG is formed and released into the ECM<sup>27</sup>. One possible mechanism of xyloside action is that it reduces endogenous GAGs. Reduction of CS may lead to changes in synapse formation and maturation<sup>40,41</sup>. These alterations may lead to continued plasticity through adulthood or deficits in neural wiring which may be necessary for vocal ontogeny. However, unlike juvenile zebra finches, treated birds did not incorporate new syllables into their songs after treatment, which argues against the idea that the treatment prolonged plasticity beyond the normal age for song crystallization.

The more likely mechanism is that the priming effect of xylosides may provide the nucleus with a premature PNN like structure, which may lead to the change in behavior. Infusion occurred between 55 and 65 PHD, but primed GAG and xyloside remain in the tissue and may still be priming for several days after infusion. These primed GAGs may function in a fashion similar to a PNN and support synapses and reduce plasticity. This reduction of plasticity could be manifested in a reduction in the normal pruning of synapses during development. Eventually, these primed GAGs would be cleared or disposed of, allowing normal development to continue. However, by this time, the developmental window for vocal ontogeny may be closing naturally as the

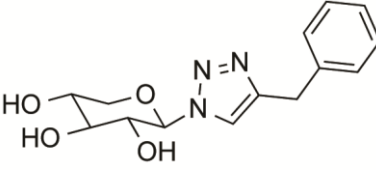
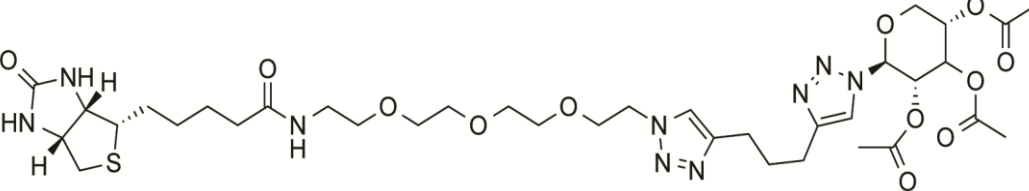
critical period comes to an end. This would explain the slight improvement seen between 70-80 PHD and 110+ PHD in sequential scores in the treatment groups. Improvement towards stereotypy is stopped by normal crystallization and adult song consists of somewhat immature syntax.

Finally, it is possible that both the decoy and priming aspects of xyloside treatment are required for the developmental deficit to occur. In this scenario, the loss of endogenous GAG chains through the decoy effect and the primed GAG chains present in the ECM network serve to amplify inhibition of neural plasticity in RA. This combined effect would make it difficult to complete normal developmental changes in the nucleus. After some time, the effect may wear off, which would explain the slight improvement in similarity and sequential scores. However, normal crystallization occurred before the bird could completely recover.

Understanding whether the results seen are due to a single mechanism or require both priming and decoy function will be vital to a better understanding of the role of GAGs and their biosynthesis in complex neural systems. Future studies will examine both the decoy and priming effects of xylosides and allow us to determine which is responsible for the changes in vocal ontogeny that were observed.



**Table 3.1** Structures of xylosides used in the current study

Compound	Structure of xyloside
<b>1</b>	
<b>2</b>	

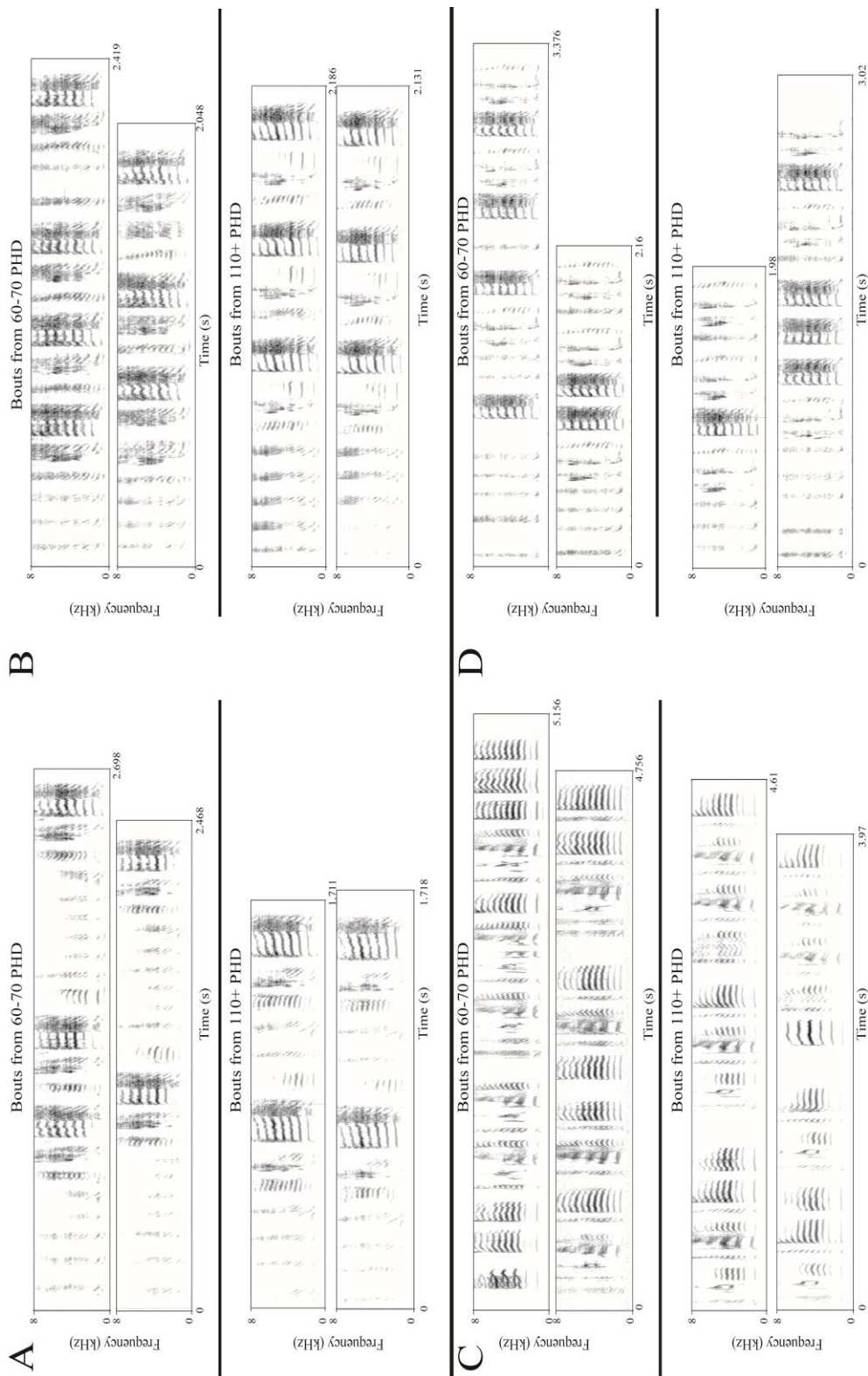


**Figure 3.1** Spectrograms of multiple bouts from two birds treated with vehicle (A,B) and two birds treated with compound 1 (C, D) at 60-70 PHD and 110+ PHD. In the vehicle treated birds, song consists of variable syntax early in development but crystallizes into a stereotypic motif. In xyloside treated birds, song begins the same way, but treated birds lack stereotypy in adult song as well.

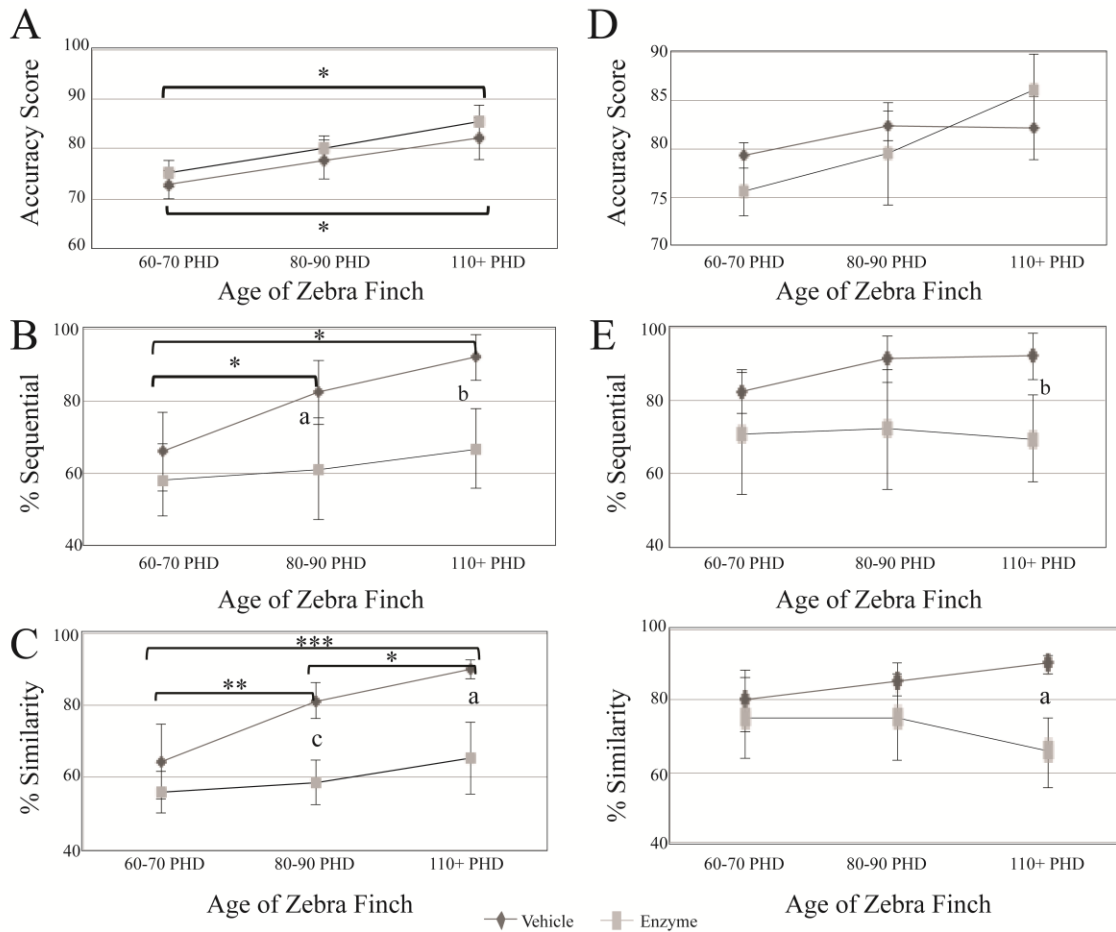


**Figure 3.2** Analysis of motifs between time-points using 110+ PHD song as template (A-C) and comparison of motifs within time-points (D-F) for both xyloside treated and vehicle treated birds. The three measures that were assessed in both instances were accuracy (A, D), the sequence of the motif (B,E) and the overall similarity (C,F) of the motifs. Significant differences are marked by \* or letters (a, b, c). \*,a indicates  $p < 0.05$ , \*\*,b indicates  $p < 0.005$ , and \*\*\*,c indicates  $p < 0.001$ . Letters were used to indicate significance between groups.

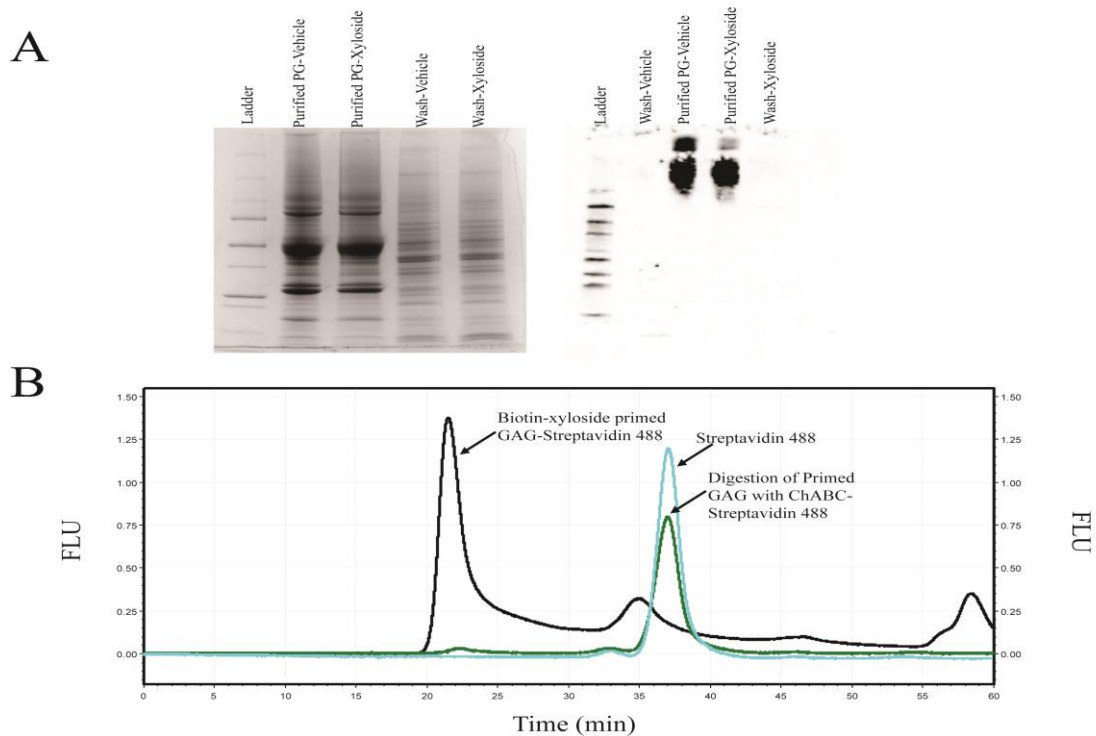


**Figure 3.3** Confirmation of decoy and priming effect of xylosides in juvenile zebra finch. (A) Coomassie and western blot using CS56, a CS antibody, of purified proteoglycans from treated (xyloside) and sham (vehicle) tissue from zebra finch brain after normal treatment schedule. Western blot analysis shows that CS bound to protein is reduced after xyloside treatment. As the antibody is against CS, the area stained is wider as compared to a protein. (B) Priming using a biotinylated xyloside shows primed GAGs by the shift in fluorescence, which is abolished after ChABC treatment. This indicates the priming of CS.

### 3.5 References

1. Pizzorusso, T.; Medini, P.; Berardi, N.; Chirzi, S.; Fawcett, J.W. Reactivation of ocular dominance plasticity in the adult visual cortex, *Science*, **2002**, *8*, 1248-1251.
2. Galtrey, C.M.; Fawcett, J.W. The role of chondroitin sulfate proteoglycans in regeneration and plasticity in the central nervous system, *Brain Res Rev*, **2007**, *54*, 1-18.
3. Balmer, T.; Carels, V.; Frisch, J.; Nick, T. Modulation of perineuronal nets and parvalbumin with developmental song learning, *J Neurosci*, **2009**, *29*, 12878-12885.
4. Meyer, C.; Boroda, E.; Nick, T. Sexually dimorphic perineuronal net expression in songbird, *Basal Ganglia*, **2014**, *3*, 229-237.
5. Umulis, D.; O'Conner, M.B.; Blair, S.S. The extracellular regulation of bone morphogenetic protein, *Development*, **2009**, *136*, 3715-3728.
6. Chen, Y.; Mohammadi, M.; Flanagan, J.G. Graded levels of FGF protein span the midbrain and can instruct graded induction and repression of neural mapping labels, *Neuron*, **2009**, *62*, 773-780.
7. Akita, K.; von Holst, A.; Furukawa, Y.; Mikami, T.; Sugahara, K.; Faissner, A. Expression of multiple chondroitin/dermatan sulfotransferases in neurogenic regions of embryonic and adult central nervous system implies that complex chondroitin sulfates have a role in neural stem cell maintenance, *Stem Cells*, **2008**, *26*, 798-809.
8. Lindahl, U.; Kusche-Gullberg, M.; Kjellén, L. Regulated diversity of heparan sulfate, *J Biol Chem*, **1998**, *273*, 24979-24982.
9. Domowicz, M.S.; Sanders, T.A.; Ragsdale, C.W.; Schwartz, N.B. Aggrecan is expressed by embryonic brain glia and regulates astrocyte development, *Dev Biol*, **2008**, *315*, 114-124.
10. Bixby, J.L.; Harris, W.A. Molecular mechanisms of axon growth and guidance, *Annu Rev Cell Biol*, **1991**, *7*, 117-159.
11. Bukalo, O.; Schachner, M.; Dityatev, A. Modification of extracellular matrix by enzymatic removal of chondroitin sulfate and by lack of tenascin-R differentially affects several forms of synaptic plasticity in the hippocampus, *J Neurosci*, **2001**, *104*, 359-369.
12. Landolt, R.M.; Vaughan, L.; Winterhalter, V.K.H.; Zimmermann, D.R. Versican is selectively expressed in embryonic tissue that acts as barriers to neural crest cell migration and axon outgrowth, *Development*, **1995**, *121*, 2303-2312.

13. Laabs, T.; Carulli, D.; Geller, H.M.; Fawcett, J.W. Chondroitin sulfate proteoglycans in neural development and regeneration, *Curr Opin Neurobiol*, **2005**, *15*, 116-120.
14. Berardi, N.; Pizzorusso, T.; Ratto, G.M.; Maffei, L. Mechanisms of plasticity in the visual cortex, *Trends Neurosci*, **2003**, *26*, 369-378.
15. Lander, C.; Kind, P.; Maleski, M.; Hockfield, S. A family of activity-dependent neuronal cell-surface chondroitin sulfate proteoglycans in cat visual cortex, *J Neurosci*, **1997**, *17*, 1928-1939.
16. Berardi, N.; Pizzorusso, T.; Maffei, L. Extracellular matrix and visual cortical plasticity: freeing the synapse, *Neuron*, **2004**, *44*, 905-908.
17. Marler, P.; Peters, S. Long-term storage of learned birdsongs prior to production, *Anim Behav*, **1982**, *30*, 472-482.
18. Bolhuis, J.J.; Gahr, M. Neural mechanisms of birdsong memory, *Nat Rev Neurosci*, **2006**, *7*, 347-357
19. Immelmann, K. Song development in the zebra finch and other estrildid finches, *Bird Vocalizations*, **1969**, *61*, 61-74.
20. Schraff, C.; Nottebohm, F. A comparative study of the behavioral deficits following lesions of various parts of the zebra finch song system: implication for vocal learning, *J Neurosci*, **1991**, *11*, 2896-2913.
21. Nottebohm, F.; Stokes, T.M.; Leonard, C.M. Central control of song in the canary, *Serinus canaries*, *J Comp Neurol*, **1976**, *165*, 457-486.
22. Akutagawa, E.; Konishi, M. Connections of thalamic modulatory centers to the vocal control system of the zebra finch, *PNAS*, **2005**, *102*, 14086-14091.
23. Doupe, A.; Konishi, M. Song-selective auditory circuits in the vocal control system of the zebra finch, *PNAS*, **1991**, *88*, 11339-11343.
24. McCasland, J.S.; Konishi, M. Interaction between auditory and motor activities in an avian song control nucleus, *PNAS*, **1981**, *78*, 7815-7819.
25. Shank, S.S.; Margoliash, D. Sleep and sensorimotor integration during early vocal learning in a songbird, *Nature*, **2009**, *458*, 73-77.
26. Victor, X.V.; Nguyen, T.K.N.; Ethirajan, M.; Tran, V.M.; Nguyen, K.V.; Kuberan, B. Investigating the elusive mechanism of glycosaminoglycan biosynthesis, *J Biol Chem*, **2009**, *284*, 25842-25853.

27. Tchernichovski, O.; Nottebohm, F.; Ho, C.E.; Pesaran, B.; Mitra, P.P. A procedure for an automated measurement of song similarity, *Anim Behav*, **1999**, *59*, 1167-1176.
28. Galligani, L.; Hopwood, J.; Schwartz, N.B.; Dorfman, A. Stimulation of free chondroitin sulfate chains by beta-D-xylosides in cultured cells, *J Biol Chem*, **1975**, *250*, 5400-5406.
29. Schwartz, N.B. Regulation of chondroitin sulfate synthesis. Effect of beta-xylosides on synthesis of chondroitin sulfate proteoglycan, chondroitin sulfate chains, and core protein, *J Biol Chem*, **1977**, *252*, 6316-6321.
30. Sobue, M.; Habuchi, H.; Ito, K.; Yonekura, H.; Oguri, K.; Sakurai, K.; Kamohara, S.; Ueno, Y.; Noyori, R.; Suzuki, S. beta-D-xylosides and their analogues as artificial initiators of glycosaminoglycan chain synthesis. Aglycone-related variation in the effectiveness in vitro and in ovo, *Biochem J*, **1987**, *241*, 591-601.
31. Charlesworth, J.D.; Tumer, E.C.; Warren, T.L.; Brainard, M.S. Learning the microstructure of successful behavior, *Nat Neurosci*, **2011**, *14*, 373-380.
32. Riede, T.; Fisher, J.H.; Goller, F. Sexual dimorphism of the zebra finch syrinx indicates adaptation for high fundamental frequencies in males, *Plos One*, **2010**, *5*, e11368.
33. Nordeen, K.W.; Nordeen, E.J. Auditory feedback is necessary for the maintenance of stereotyped song in adult zebra finches, *Behav Neural Biol*, **1992**, *57*, 58-66.
34. Leonard, A.; Konishi, M. Decrystallization of adult birdsong by perturbation of auditory feedback, *Nature*, **1999**, *399*, 466-470.
35. Brainard, M.S.; Doupe, A.J. Auditory feedback in learning and maintenance of vocal behavior, *Nat Neurosci*, **2000**, *1*, 31-40.
36. Vicario, D.S.; Yohay, K.H. Song-selective auditory input to a forebrain vocal control nucleus in zebra finch, *Dev Neurobiol*, **2004**, *24*, 488-505.
37. Hahnloser, R.H.R.; Kozhevnikov, A.A.; Fee, M.S. An ultra-sparse code underlies the generation of neural sequences in a songbird, *Nature*, **2002**, *419*, 65-70.
38. Vu, E.T.; Mazurek, M.E.; Kuo, Y.C. Identification of a forebrain motor programming network for the learned song of zebra finches, *J Neurosci*, **1994**, *14*, 6924-6934.
39. Margoliash, D. Functional organization of forebrain pathways for song production and perception, *Dev Neurobiol*, **1997**, *33*, 671-693.

40. Ashmore, R.C.; Wild, J.M.; Schmidt, M.F. Brainstem and forebrain contribute to generation of learned motor behavior, *J Neurosci*, **2005**, *25*, 8543-8554.
41. Faissner, A.; Pyka, M.; Geissler, M.; Sobik, T.; Frischknecht, R.; Gundelfinger, E.D.; Seidenbecher, C. Contributions of astrocytes to synapse formation and maturation-potential functions of the perisynaptic extracellular matrix, *Brain Res Rev*, **2010**, *63*, 26-38.
42. Snow, D.M.; Mullins, N.; Hynds, D.L. Nervous system-derived chondroitin sulfate proteoglycans regulate growth cone morphology and inhibit neurite outgrowth: a light, epifluorescence and electron microscopy study, *Microsc Res Tech*, **2001**, *54*, 273-286.



## CHAPTER 4

# DEGRADATION OF HEPARAN SULFATE IN SYRINGEAL MUSCLE LEADS TO CHANGES IN CRYSTALLIZED ZEBRA FINCH SONG

### 4.1 Introduction

Human speech and birdsong are complex behaviors that require central neural control in conjunction with precisely coordinated muscle output to control respiration, vocal parameters, and upper vocal tract movements<sup>1-4</sup>. Birdsong is produced by the avian vocal organ, the syrinx, through airflow that is generated by respiratory control. In birds, both expiration and inspiration are active processes and require concerted muscle activity<sup>5,6</sup>.

Located at the junction of the primary bronchi and the trachea, the syrinx consists of two ipsilaterally controlled sound generators. These sound generating tissue masses, the labia, are attached to modified cartilage rings and can act as airflow control valves as well as a sound source. The position of the labia in the bronchial lumen as well as their vibratory behavior is controlled by at least six pairs of muscles (Figure 4.1)<sup>6-8</sup>.

In the zebra finch, variation in spiking patterns in neurons is correlated with variation in temporal song characteristics<sup>9,10</sup>. This suggests temporal precision in the CNS is expressed at the behavioral level in song. This high precision in neural motor

commands can be translated into rapid movements of the vocal organ and thus into acoustic features. Syringeal muscles contain superfast contractile kinetics allowing for unique acoustic modulations. These kinetics allow for rapid modulation of syringeal airflow and sound amplitude<sup>12,13</sup>. In the zebra finch, the fiber type composition and speed of syringeal muscles are sexually dimorphic. Male muscles contain a higher percentage of superfast fibers (75-85% in males vs 50-60% in females<sup>14</sup>) and show faster contraction kinetics<sup>14</sup>. Emg recordings<sup>1,2,7,16</sup> and denervation studies<sup>15,17,18</sup> indicate that syringeal muscles play important roles in song production and control of acoustic parameters. For example, in canaries (*Serinus canaria*), active control of the syringeal valve is required for phonation<sup>19</sup>. Syringeal muscles are also critical for control of fundamental frequency. The frequency of song syllables drops drastically after denervation in all investigated oscine species<sup>15,17</sup>.

However, the specific contributions of muscles to acoustic features are still largely unknown and therefore, how the presence of superfast fibers affects acoustic characteristics of song, such as frequency and amplitude, remains unknown. While the sexual dimorphism in syringeal muscle morphology and kinetics<sup>15</sup> suggests that these muscles may have evolved for vocal control, there is not experimental data to substantiate this hypothesis. To address the question of muscle contribution to song characteristics, the use of heparitinase enzymes to alter the ECM of the syringeal muscle was employed.

Skeletal muscles are known to contain heparan sulfate. HS is primarily found at the NMJ and are involved with its formation during development, aggregation of AChR, and the tethering of AChE<sup>20-24</sup>. This study provides the first evidence that superfast muscle activity is involved in a wide array of song features such as amplitude, high-frequency syllables, and frequency modulation, that degradation of HS in these

superfast muscles alters their kinetic activity, and that altering this activity can lead to changes in nonsyringeal muscle-based components of song, including pressure and CNS song control.

## 4.2 Methods and materials

### 4.2.1 Animals

Adult male zebra finches were used in this study. Birds were bred in a flight aviary at the University of Utah. Birds were housed in the aviary until experimental testing. During testing, birds were housed in 32 x 23 x 30-cm wire cages and kept on a 13:11-h light:dark cycle.

### 4.2.2 Air sac pressure measurements and recordings

Males were removed from the aviary and placed into individual cages and isolated in acoustic recording chambers. Several bouts of control song were recorded after which an elastic belt was placed around the thorax with a leash connected to the belt using a Velcro tab. The leash was put through the top of the cage and connected to a counterbalanced tether arm to allow free movement around the cage. After the bird was accustomed to the tether, as indicated by singing, surgery was performed. Birds were deprived of food and water for 1 h prior to surgery and then anesthetized using isoflurane. A small hole was made in the abdominal wall to insert a flexible cannula into a thoracic air sac. The cannula was sutured to the rib cage and the insertion site sealed with tissue adhesive (VetBond) to prevent air leakage. The other end of the tube was connected to a pressure transducer (Fujikura FPM-02PG) mounted on the bird as a backpack connected to the Velcro tab on the belt. Birds were allowed to recover until several bouts of control song with

simultaneous air sac pressure were recorded. Song was recorded with an omni-directional microphone and amplified (Digital Preamp system II, Applied Research Technology). Air sac pressure was simultaneously recorded on a separate channel using amplified output (Hector Engineering) from the pressure transducer. Both channels were recorded with a Data Translation AD-board at 44.1 kHz sampling rate using Avisoft Recorder software. After sufficient control song was recorded, birds received injections of enzyme.

#### 4.2.3 Injection into syringeal muscles

Several groups of birds received bilateral injections of heparitinase enzymes or vehicle in the syrinx. Heparitinase enzymes were expressed and purified as previously described. Vehicle consists of the same buffer the enzymes are stored in to serve as a control. This includes birds for the examination of song alone (n=6), those for examining song and pressure patterns (n=5), and birds in which the effect of enzyme treatment on syringeal muscle function was studied (n=8; see below). All procedures were as follows, regardless of experimental group. Birds were deprived of food for 1 h prior to surgical procedure and then anesthetized using isoflurane. The thoracic cavity was opened and 10  $\mu$ l of a mixture of heparinase enzymes or vehicle were injected bilaterally into the ventral muscles of the syrinx. The membrane of the interclavicular air sac was sealed with tissue adhesive and the overlying skin was sutured closed. Birds were allowed to recover from anesthesia and then returned to their recording chambers. Song, and air sac pressure in the subset, was recorded as described previously. Birds designated for the investigation of the treatment on song features (song alone as well as song and air sac pressure) were recorded for up to fourteen days post injection. For birds the effect of the infusion on muscle kinetics was tested through measurement of the stimulation threshold and

assessment of air flow modulation at varying frequencies. Additionally, their song was recorded for up to 24 h post injection at which time the syringeal muscle kinetics were assessed.

#### 4.2.4 Recording of muscle kinetics

To assess how enzyme treatment affects muscle contraction kinetics, the effect of oscillatory *in situ* muscle contractions on airflow was monitored. To do so, a custom-built flow probe was inserted into the trachea. This flow sensor was constructed with a miniature thermistor (Thermometrics BB05JA202), which was connected to a feedback circuit (Hector Engineering) that heated the thermistor to approximately 60 °C via output current. This feedback circuit provides sensitive detection of airflow in the trachea, as the convective cooling of the flow induces adjustments in the heating current and thus provides a proportional voltage signal. Syringeal muscles were stimulated directly with a pair of silver wires (AM-Systems) inserted into the ventral tracheobronchial muscle. To detect the abductive activity of this muscle, the respiratory system of the bird was perfused through a cannula in the posterior thoracic air sac. This procedure turned off the bird's respiratory drive and allowed us to test modulation of a constant air stream by the muscle without interference from fluctuations in airflow associated with the natural breathing rhythm. Stimulation pulses were delivered in trains and between trains the muscle was allowed to recover for at least 2 min. Pulse frequency was first ramped up in discrete steps (10, 20, 25, 30, 40, 50 Hz) and then ramped down (50, 40, 30, 25, 20, 10 Hz). Airflow and pulse were recorded as separate channels using Avisoft Recorder software.

#### 4.2.5 Song and air sac pressure analyses

At least 15 motifs from each bird were selected randomly from the recordings. Within these selected motifs frequency modulation, fundamental frequency, sound onset pressure, and amplitude were analyzed using Praat software ([www.praat.org](http://www.praat.org))<sup>25</sup>. Frequency modulation was examined (n = 6) by calculating the change in frequency over time using the fundamental frequency from the highest point to the lowest point in a sweep. Amplitude was calculated by averaging intensity over the entire motif (at least 15 motifs analyzed for 4 birds in each treatment group). Pressure at the onset of phonation was measured by high-pass filtering the pressure pattern for each bird to reveal the syringeal oscillations and accurate measurement of the fundamental. The pressure level at the onset of vibration was measured. This was considered the start of phonation and a power spectra of this time showed the fundamental frequency (n = 4). Statistics were calculated using a paired or unpaired Student t-test where appropriate.

### 4.3 Results

After injection, a timeline for the effectiveness of the treatment was established. Birds were allowed to recover and song was recorded for up to two weeks post injection. Data analysis consists of primarily three time-points: prior to injection, 24 h post injection, and 7 d post injection. These time-points were chosen due to the fact that data analysis shows the greatest differences in song attributes at 24 h post injection with many of these resolving by 7 d post injection and others becoming more apparent at this time. Using this timeframe, song with pressure components were analyzed. Muscle activity was examined 24 h post injection.

Examples of pressure pattern, sound traces, spectrograms, and intensity (or

amplitude) over a motif can be seen for two enzyme treated birds in Figure 4.2. One of the most obvious changes at 24 h post injection was to the sound amplitude of song. Vehicle treatment resulted in a slight but significant decrease in sound amplitude (~2dB). Treatment with enzyme resulted in a consistent decrease in mean song amplitude of 4-6 dB at 24 h post injection relative to that before injection (Figure 4.3A). Seven days after the injection, sound amplitude had returned to pre-injection levels. In comparison to the overall effect on song amplitude, the amplitude of high frequency notes even further reduced (Figure 4.2, shown at the asterisk; Figure 4.4). These notes between 3.5-7 kHz were either significantly reduced by >5 dB or were not present at all. This effect was temporary as by 7 d post injection the notes had returned.

Loss of high frequency syllables could not be attributed to a change in airflow as inferred from the largely intact air sac pressure patterns (Figure 4.4). Pressure patterns in adult zebra finch song are as stereotyped as the syllables sung. Pressure is the result of the respiratory effort and syringeal resistance. Syringeal muscles through their gating activity can affect air sac pressure. Whereas the overall pressure amplitude remained unaffected by the injection, relative amplitude of pressure peaks did change after injection (e.g., Figure 4.4) Enzyme injection also altered the phonation onset pressure (Figure 4.5A). In all subjects, the phonation onset pressure for most syllables was increased post injection (average increase was 56.1%). This increase does not appear to be frequency dependent (Figure 4.5B)

With the exception of the high frequency syllables, no substantial change in fundamental frequency was observed after treatment. However, frequency modulation (FM) was affected by the treatment. FM-rate was found to decrease at 24 h post injection, but only in specific syllables (Figure 4.6). From the limited sample it appears that this

change was dependent upon the higher FM rate and not on the fundamental frequency.

Changes to amplitude and frequency features of song were not the only observed outcomes of enzyme treatment. Syntax of motifs within bouts began to show unusual patterns several days after treatment (Figure 4.7). These changes included the presence of syllables and associated pressure pulses that were not present in the motifs before injection of enzyme, an unusual number of introductory notes inserted between the motifs of a song bout, and even increasing repetition of syllables at the end of motifs. These changes occurred several days after enzyme injection and persisted beyond the 7 d post injection mark.

In examining changes to the actual muscle, neuromuscular transmission was first examined. Stimulation of the tracheosyringeal nerve produced muscle twitches, indicating that neural transmission to the muscle remained intact. Using direct stimulation of the muscles revealed a change in the stimulation threshold current with enzyme treatment. Whereas muscle contractions could be elicited with  $<0.5$  mA stimulation current in vehicle injected birds, in enzyme injected birds, the threshold was between 0.5-1 mA.

The frequency response of muscles was significantly lower after enzyme, as tested via muscle-mediated airflow modulation. Reduced ability to modulate airflow occurred at lower stimulation frequencies in enzyme treated birds compared to vehicle injected birds (Figure 4.8). Stimulation of enzymatically treated muscle no longer caused visible modulation at 30 Hz. This is a significant reduction compared to vehicle treated muscle (50 Hz).



#### 4.4 Discussion

Syringeal muscles play a role in controlling airflow and the tension of the vibrating labia<sup>1-9,11-18</sup>. They consist of a high percentage of superfast fibers with extremely fast contraction kinetics<sup>12,14</sup>. Eliminating contributions from muscles through denervation results in drastic changes to fundamental frequency and some temporal characteristics<sup>15-18</sup>. Aside from this demonstration that muscle activity is required for normal song production, it is completely unknown to what degree the kinetics of syringeal muscles affect acoustic features. These results provide the first data to answer this question.

Syringeal muscles are involved in several aspects of song production and, interestingly, play a role in maintenance of stereotyped song<sup>1-9,11-13,15-19</sup>. Treatment of these muscles with HS degrading enzyme caused a change in muscle kinetics, increasing the stimulation threshold and lowering the frequency at which tetanus is observed. The change in kinetics indicates that HS in the ECM of syringeal muscles plays a role in maintaining proper muscle response and affects the contractile properties of the muscle. Removal of HS leads to changes in the superfast characteristics of syringeal muscles, which allowed us to study the importance of muscle function for stereotyped song production.

Because syringeal muscles play a major role in the control of fundamental frequency<sup>15</sup>, changes in frequency after HS manipulation could be expected. However, after enzymatic treatment of syringeal muscles, a universal change in fundamental frequency did not occur. In many syllables, the fundamental frequency remained unchanged at 24 h post enzyme injection, which is in contrast to a global change after denervation<sup>15-18</sup>. The manipulation did affect high-frequency syllables, such as the more tonal notes or harmonic-stack syllables with fundamental frequency over 2 kHz. However,

the main effect was a reduction in sound amplitude or complete loss of high-frequency syllables and not a decrease in frequency. Furthermore, significant changes in frequency modulation also occurred for high-frequency components. This loss is not attributable to a reduction in driving pressure, which did not significantly change after infusion of enzyme. The reduction in sound amplitude of tonal syllables, rather than a lowering of the fundamental frequency, is surprising and must be caused by the altered kinetics of the syringeal muscle.

The loss of high-frequency syllables may indicate an important, more general function of syringeal muscles that has not been appreciated until now. The overall reduction in sound amplitude (4-6 dB) suggests that muscle activity controls sound amplitude in a general way. This change is not explained by a surgery effect, as control birds showed at most a 1-2 dB reduction. Although amplitude modulation is controlled by syringeal muscles that gate airflow<sup>1,2,4</sup>, the general influence on sound amplitude seen here implies a different mechanism. Perhaps, muscle activity positions the syrinx and the labia in a way that allows optimal transfer of aerodynamic energy into sound energy. The manipulation with enzyme may have disrupted this positioning movement.

This interpretation is further supported by the fact that phonation threshold pressure was affected by the manipulation. The pressure at which phonation began at the onset of syllables was increased by at least 10% in 76% of all syllables. This is likely caused by reduced ability for proper positioning of the labia in the airstream or an overall reduction in the configuration and tension of syringeal structures. This result is particularly interesting because phonation threshold pressure did not change between the *in situ* intact and denervated syrinx as well as the excised syrinx that were artificially phonated<sup>24</sup>. It therefore implies that syringeal muscles actively increase vocal efficiency and that this

mechanism is dependent on contraction kinetics or excitability of the muscles.

Reduction of amplitude and the loss of higher frequencies are reversible alterations to song that occur swiftly after enzymatic treatment and have a time-course of about a week after treatment before returning to normal levels. Other changes in the stereotyped adult song appear later and persist well beyond the one-week timeframe. In birds who received injections of heparitinase enzymes, novel syllables, or atypical repetition of syllables was seen as early as 2 d post injection and persisted beyond 7 d post injection. Similar changes to song in adult zebra finches were reported following either manipulations of brain nuclei<sup>27-29</sup> manipulations of acoustic feedback (deafening, noise distortion, syringeal denervation<sup>14-18,30-32</sup>) or muting<sup>33</sup>, but the time course is typically much slower. Enzyme injection to the syrinx resulted in changes to song which produced altered auditory feedback and must also have altered somatosensory and proprioceptive feedback. The more rapid time course for song changes after this manipulation suggests that a more subtle disruption of feedback information, auditory or somatosensory, produces a more rapid response in song output, perhaps through sensitive compensatory mechanisms. The fact that these changes persist beyond 7 d implies that once the feedback loop induced compensation occurs, the process is not easily reversed or halted. Novel patterns are then incorporated into and maintained in adult song, even after feedback presumably returns to the original state as acoustic changes are reversed around 7 d after infusion of enzyme.

This study provides a novel method for examining the specific roles of syringeal muscles in song production as well as the sensitivity and reactivity of the feedback loop that maintains adult zebra finch song. The kinetics of syringeal muscles can be altered by injection of heparitinase enzymes, which leads to reversible changes in amplitude, frequency modulations, and the production of high frequencies in stereotyped song.

These changes may lead to disruption of the normal feedback system used to maintain stereotyped adult song, which could result in new or repeating syllables. These long-term changes emphasize that temporary modulation may have dramatic effects on a stereotyped behavior and that the kinetics of the syringeal muscles are important for the production and maintenance of song. This study provides a starting point for a better understanding of the roles of syringeal muscles in producing specific song features and for examining how GAGs are involved with superfast muscle function. Additionally, it provides an interesting tool for examining the feedback system of adult zebra finch song and how changes in muscle may lead to changes in neural control.

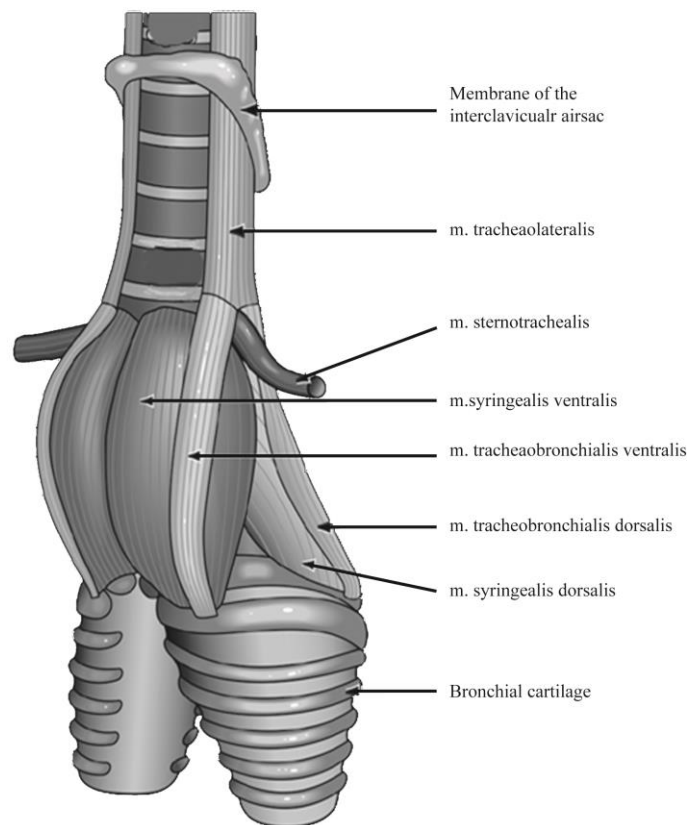


**Figure 4.1.** The schematic of a syrinx, the avian vocal organ that shows the six pairs of syringeal muscles. Adapted from<sup>11</sup>

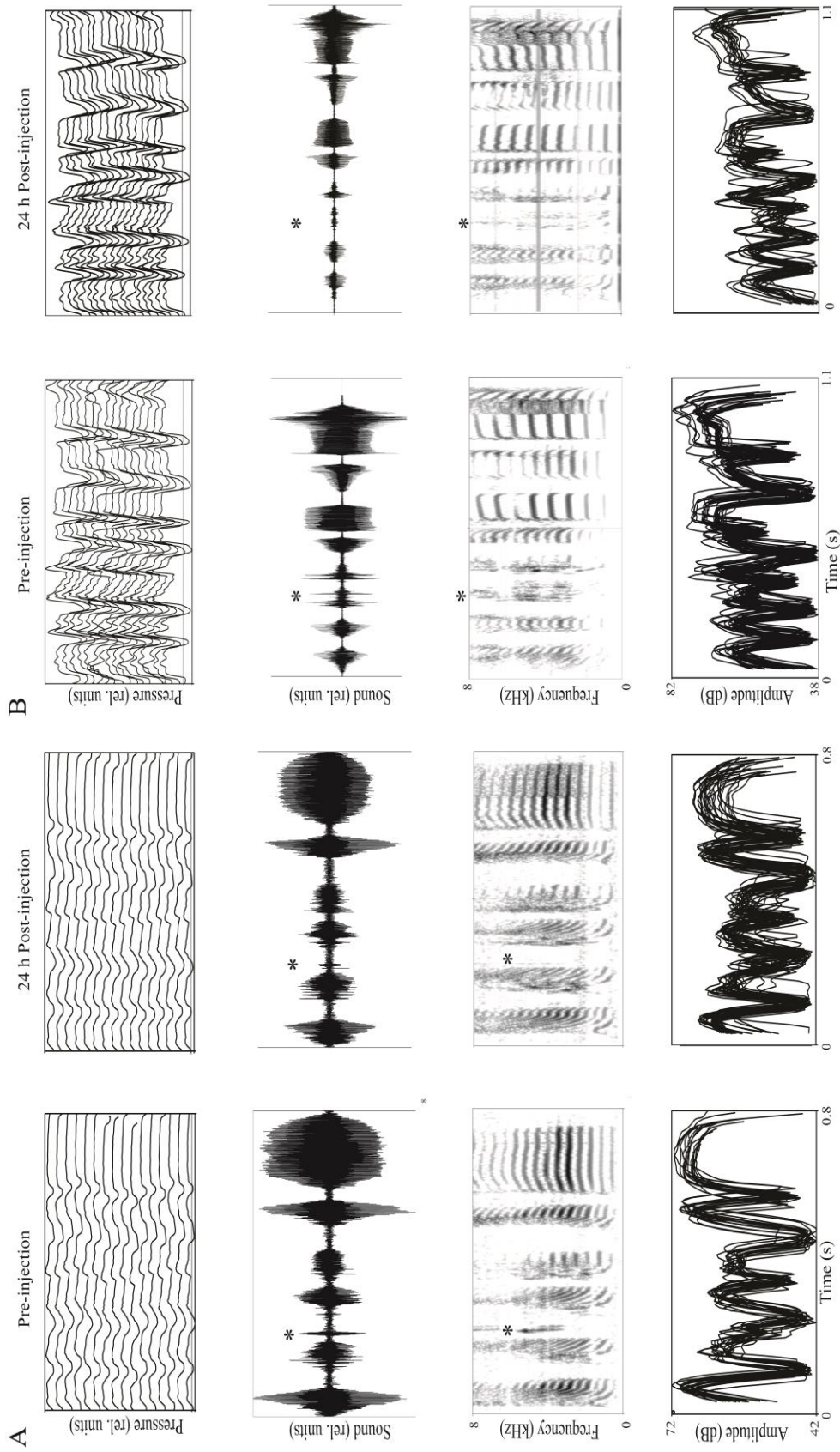
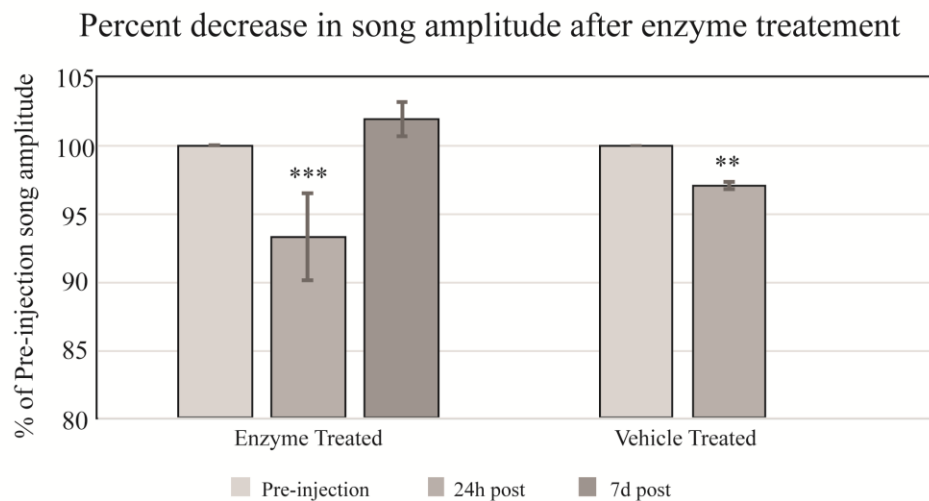


**Figure 4.2.** An overview of airsac pressure pattern and sound (shown as oscillogram, spectrogram, and amplitude) for 2 birds (A,B) who received bilateral injections of heparitinase enzyme into the ventral syringeal muscles. Pressure shows that pressure patterns during motifs remained stereotyped. Sound shows the loss or reduction of high-frequency syllables, denoted by the \*. In spectrograms, the \* demarks high frequency syllables. Consistently, reduced amplitude is visible at 24 h post injection.

A



B

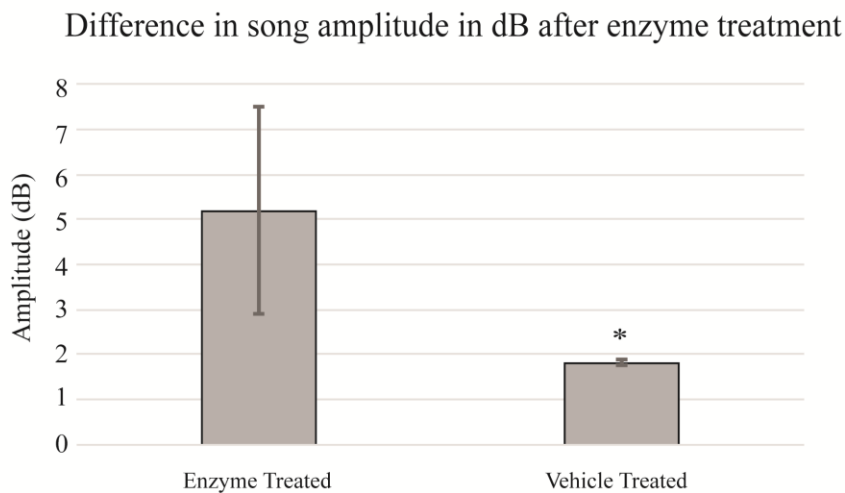


**Figure 4.3** Comparison of song amplitude (in dB) before and 24 h after heparitinase treatment. (A) Shows the % of pre-injection amplitude of song at 24 h and 7 d for enzyme treated and 24 h for vehicle treated birds. (B) The difference in dB of song amplitude 24 h after injection by vehicle or enzyme. (n=4 for each condition, \*p<0.05, \*\*p<0.005; \*\*\*p<0.001)

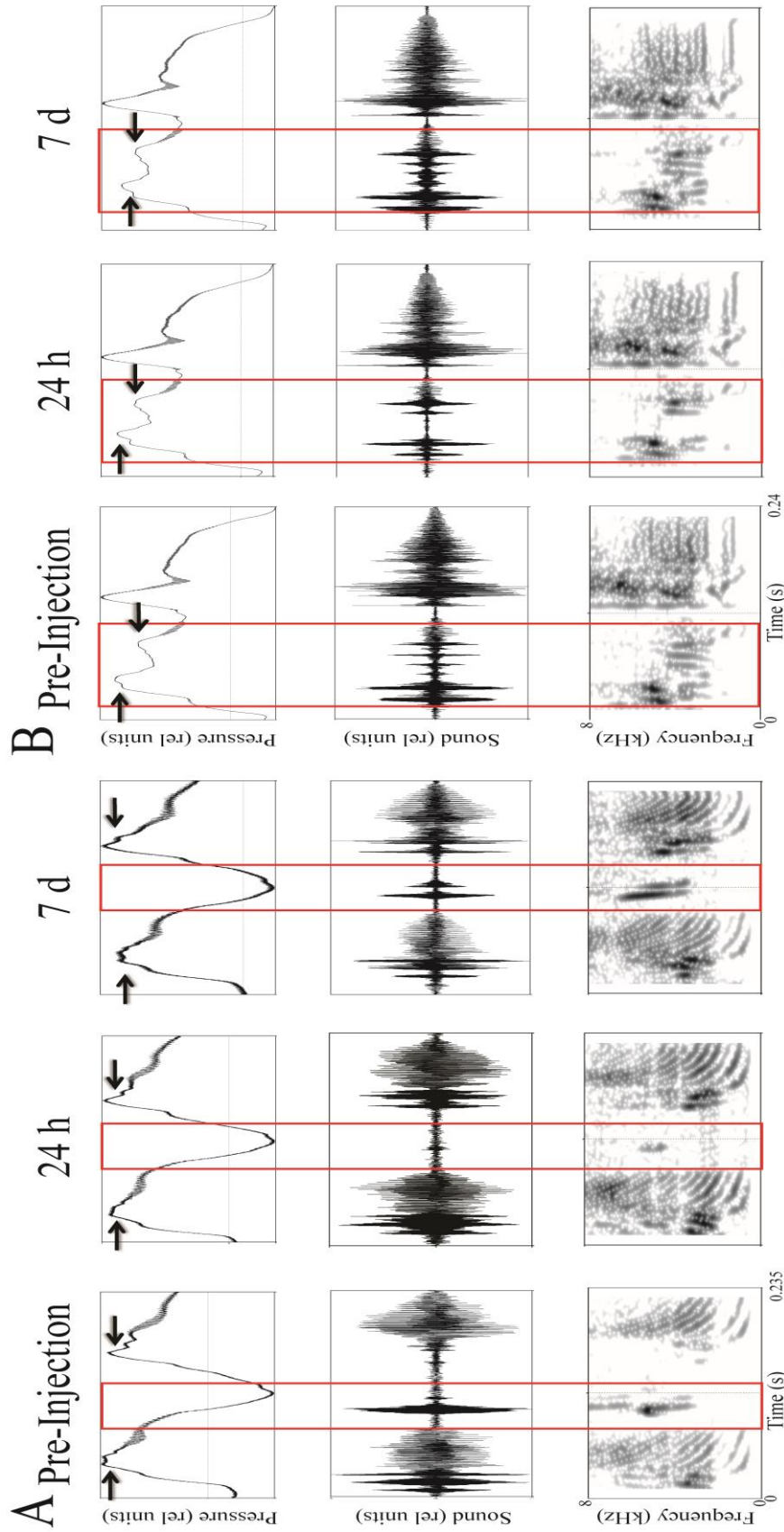
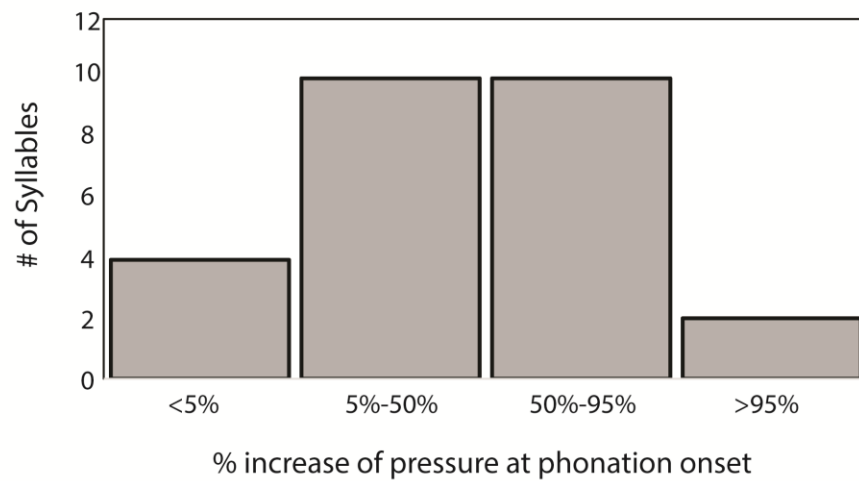


**Figure 4.4** Examples from two different birds (A & B) that show the loss of high-frequency syllables at 24 h post enzyme injection, as seen by the sound trace and spectrograms (marked by red rectangles). These syllables return by 7 d post injection, indicating this loss is temporary. Overall amplitude of the sound is reduced, but specific high-frequency syllables show the greatest reduction in amplitude. This occurs in both (A) inspiratory and (B) expiratory high-frequency syllables. This is not due to changes in pressure. While peaks within the pressure pattern can also be seen to shift (black arrows), this shift occurs independently of high-frequency syllable production.



A

% Change of phonation onset pressure 24 h after enzyme treatment



B

% Change of pressure at phonation onset as a function of frequency

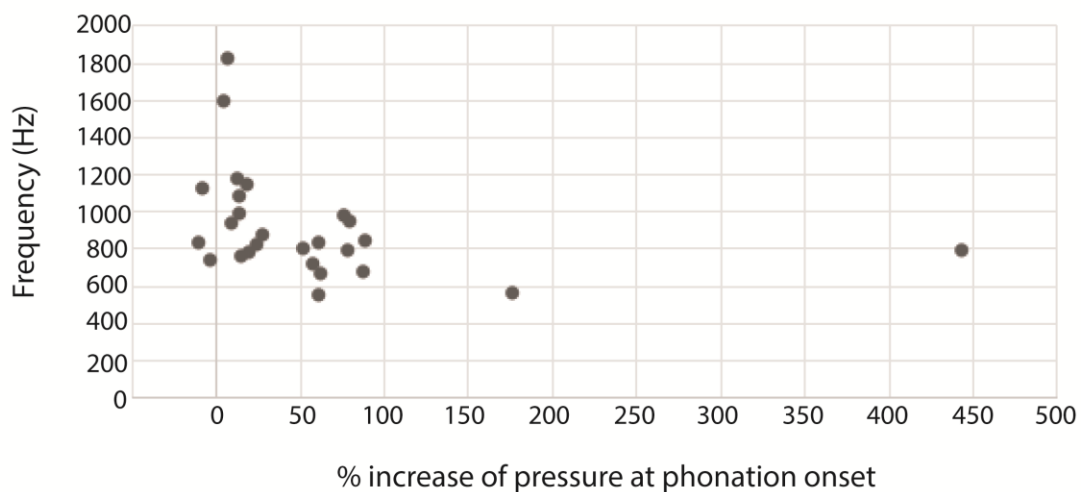


**Figure 4.5** Pressure at phonation onset is changed 24 h after enzyme treatment, with 22 of the 26 syllables examined showing at least a 5% increase in pressure (A). When comparing the change in pressure as a function of frequency, no obvious correlation is seen between frequency and changes in phonation onset pressure (B).

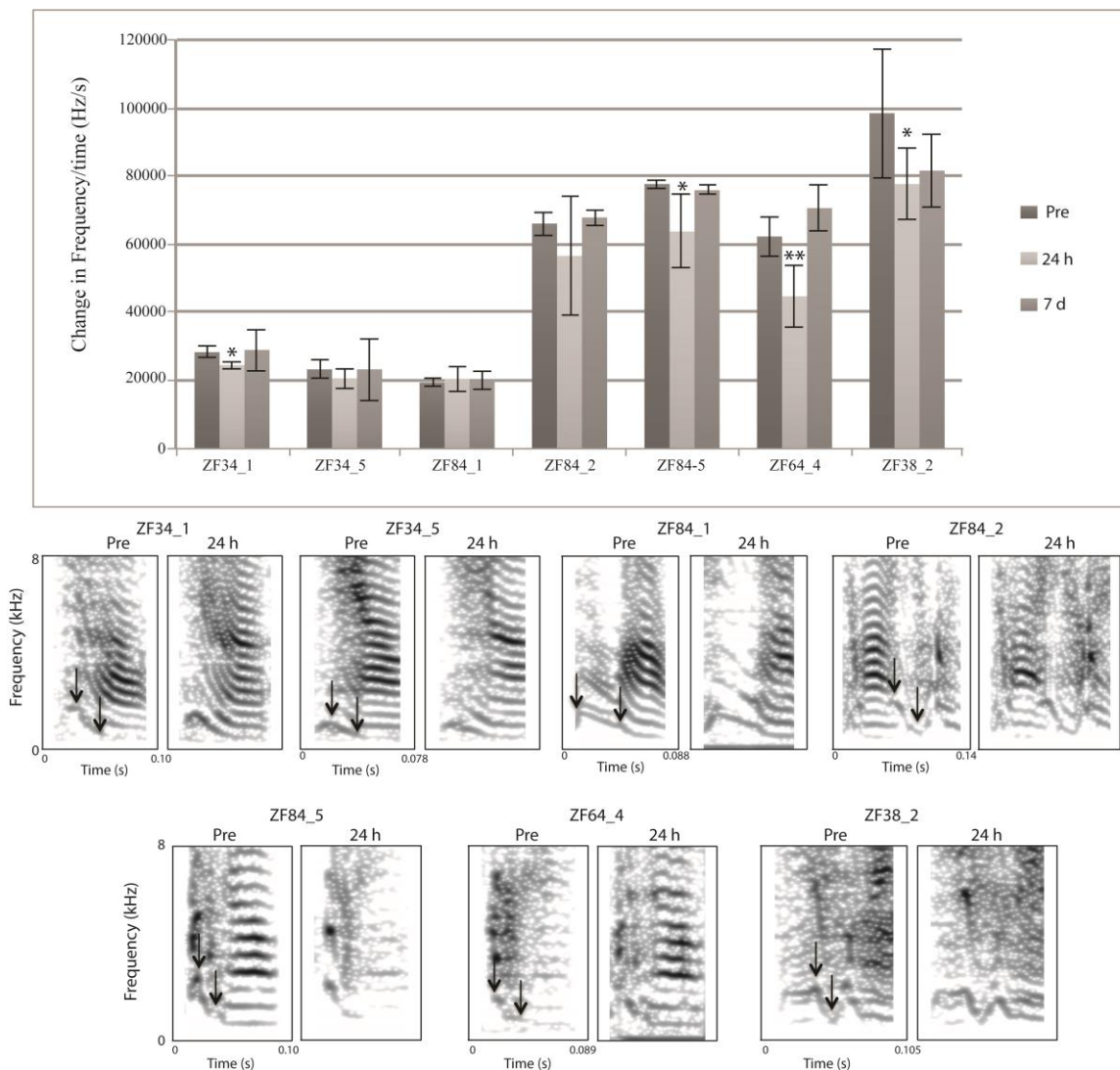


**Figure 4.6.** Changes in frequency modulation are measured in 6 specific syllables from 4 different enzyme treated birds and significant changes are shown to be syllable dependent. In several syllables, there is a significant change in FM (\* $p < 0.05$ ; \*\* $p < 0.005$ ), but others show no change. This may be due to the highest frequency in the sweep. If it is above a certain frequency, it may be lost in a similar fashion to the tonal syllables. The start and end of the measured sweep for FM are marked by the arrows in the presyllables.

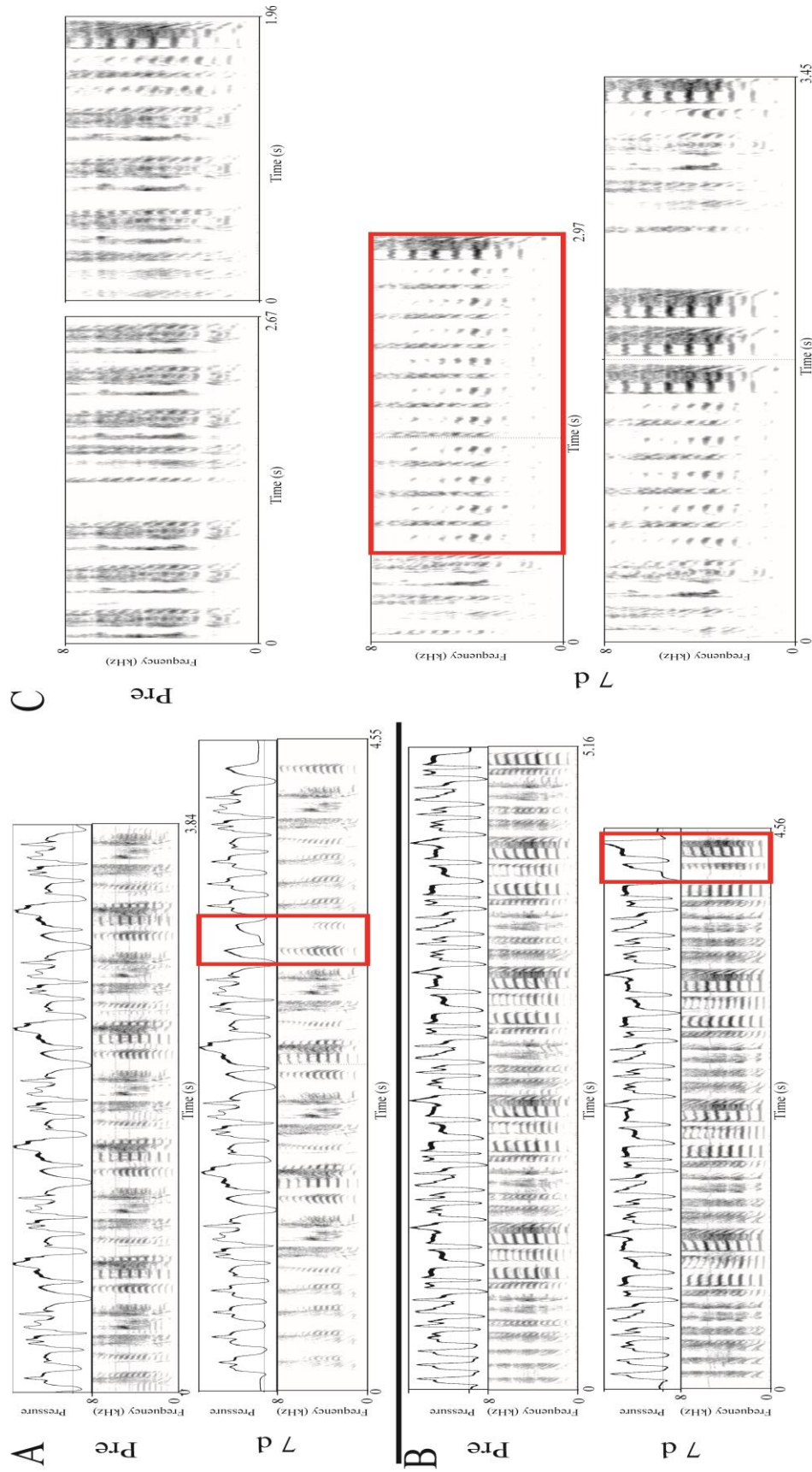


**Figure 4.7** Birds treated with enzyme show changes in motif syntax and accompanying pressure pattern (as seen in A & B) 7d after injection of heparitinases into syringeal muscle. (A) and (B) show the inclusion of a single novel syllable, as indicated by the red boxes and (A) the atypical return to introductory notes after the new syllable. (C) shows the example of the repetition of syllables, indicated by the red box, that increased over time after injection.

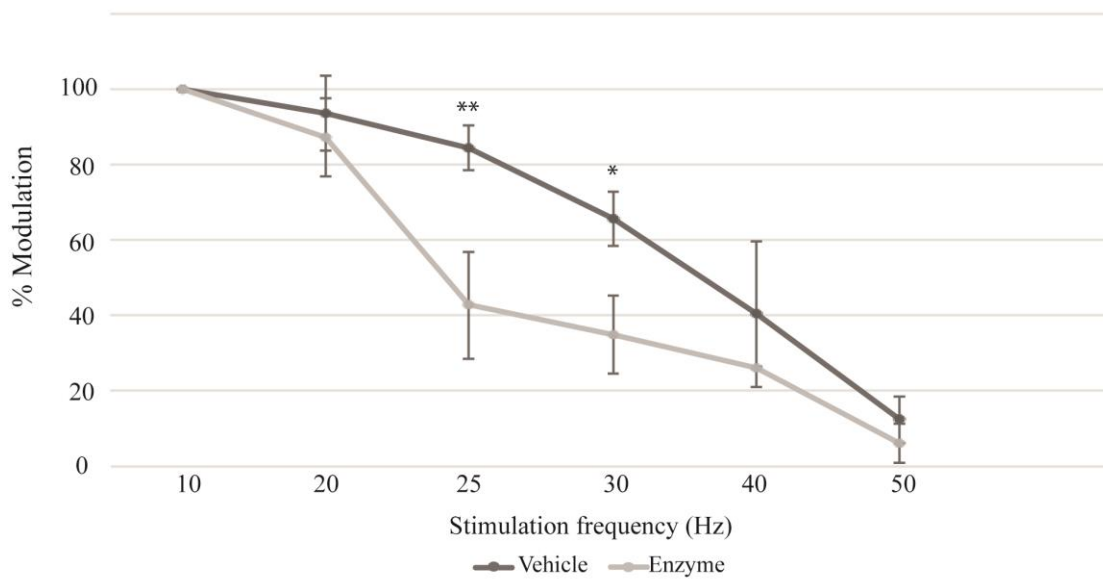


**Figure 4.8** The percent modulation of airflow by syringeal muscle during stimulation of vehicle and enzyme treatment 24 h after injection as compared to that at 10 Hz. Enzyme treated muscle shows an inability to modulate airflow at lower frequencies of stimulation compared to vehicle treated controls.

#### 4.5 References

1. Goller, F.; Cooper, B.G. Peripheral motor dynamics of song production in the zebra finch, *Ann N Y Acad Sci*, **2004**, *1016*, 130-152.
2. Vicario, D.S. Contributions of syringeal muscles to respiration and vocalization in the zebra finch, *Dev Neurobiol*, **1991**, *22*, 63-73.
3. Daly, M.; Goller, F. Tracheal length changes during zebra finch song and their possible role in upper vocal tract filtering, *J Neurobiol*, **2003**, *59*, 319-339.
4. Franz, M.; Goller, F. Respiratory units of motor production and song imitation in the zebra finch, *Dev Neurobiol*, **2002**, *51*, 129-141.
5. Fee, M.S.; Shraiman, B.; Pesaran, B.; Mitra, P.P. The role of nonlinear dynamics of the syrinx in the vocalizations of a songbird, *Nature*, **1998**, *395*, 67-71.
6. Suthers, R.; Goller, F.; Pytte, C The neuromuscular control of birdsong, *Phil Trans R Soc B*, **1999**, *354*, 927-939.
7. Suthers, R.A.; Margoliash, D. Motor control of birdsong, *Curr Opin Neurobiol*, **2002**, *12*, 684-690.
8. Suthers, R.A.; Zollilnger, S.A. Producing song: the vocal apparatus, *Ann N Y Acad Sci*, **2004**, *1016*, 109-129.
9. Chi, Z.; Margoliash, D. Temporal precision and temporal drift in brain and behavior of zebra finch song, *Neuron*, **2001**, *32*, 899-910.
10. Fee, M.S.; Kozhevnikov, A.A.; Hahnloser, R.H.R. Neural mechanisms of vocal sequence generation in the songbird, *Ann N Y Acad Sci*, **2004**, *1016*, 153-170.
11. Larson, O.N.; Goller, F. Direct observation of syringeal muscle function in songbirds and a parrot, *J Exp Biol*, **2001**, *205*, 25-35.
12. Elemans, C.P.H.; Mead, A.F.; Rome, L.C.; Goller F. Superfast vocal muscle control song production in songbirds, *Plos One*, **2008**, *3*, e2581.
13. Uchida, A.M.; Meyers, R.A.; Cooper, B.G.; Goller, F. Fibre architecture and song activation rates of syringeal muscles are not lateralized in the European starling, *J Exp Biol*, **2010**, *213*, 1069-1078.
14. Uchida, A.M.; Green, J.; Ahmad, S.; Goller, F.; Meyers, R.A.. Sexual dimorphism of syringeal muscles in songbirds, Abstract, *Society for Intergrative and comparative biology 2009 annual meeting*, **2009**

15. Riede, T.; Fisher, J.H.; Goller, F. Sexual dimorphism of the zebra finch syrinx indicates adaptation for high fundamental frequencies in males, *Plos One*, **2010**, *5*, e11368.
16. Goller, F.; Suthers, R.A. Role of syringeal muscles in gating airflow and production in singing brown thrashers, *J Neurophysiol*, **1996**, *75*, 867-876.
17. Okanoya, K.; Yoneda, T. Effect of tracheosyringeal nerve section on sexually dimorphic distance calls in benagalese finches (*Lonchura striata var. domestica*), *Zool Sci*, **1995**, *12*, 801-805.
18. Williams, H.; Crane, L.A.; Hale, T.K.; Esposito, M.A.; Nottebohm, F. Right-side dominance for song control in the zebra finch, *Dev Neurobiol*, **2004**, *23*, 1006-1020.
19. Nottebohm, F.; Stokes, T.M.; Leonard, K.M. Central control of song in the canary, *Serinus canaries*, *J Comp Neurol*, **2004**, *165*, 457-486.
20. Anderson, M.; Klier, F.; Tanguay, K. Acetylcholine receptor aggregation parallels the deposition of a basal lamina proteoglycan during development of the neuromuscular junction, *J Cell Biol*, **1984**, *99*, 1769-1784.
21. Burgess, R.W.; Nguyen, Q.T.; Son, Y.; Lichtman, J.W.; Sanes, J.R. Alternatively spliced isoforms of nerve- and muscle-derived agrin: their roles at the neuromuscular junction, *Neuron*, **1999**, *23*, 33-44.
22. Guatam, M.; Noakes, P.G.; Moscoso, L.; Rupp, F.; Scheller, R.H.; Merlie, J.P.; Sanes, J.R. Defective neuromuscular synaptogenesis in agrin-deficient mutant mice, *Cell*, **1996**, *85*, 525-535.
23. Torres, J.C.; Inestrosa, N.C. Heparin solubilizes asymmetric acetylcholinesterase from rat neuromuscular junction, *FEBS lett*, **1983**, *154*, 265-268.
24. Arikawa-Hirasawa, E.; Rossi, S.G.; Rotundo, R.L.; Yamada, Y. Absence of acetylcholinesterase at the neuromuscular junctions of perlecan-null mice, *Nat Neurosci*, **2002**, *5*, 119-123.
25. Boersma, P.; Weenick, D. Praat, a system for doing phonetics by computer, *Glott Int*, **2001**, *5*, 341-345.
26. Elemans, C.P.H.; Laje, R.; Mindlin, G.B.; Goller, F. Smooth operator: avoidance of subharmonic bifurcation through mechanical mechanisms simplifies song motor control in zebra finches, *J Neurosci*, **2010**, *30*, 13246-13253.
27. Foster, E.F.; Bottjer, S.W. Lesions of a telencephalic nucleus in male zebra finches: influences on vocal behavior in juveniles and adults, *Dev Neurobiol*, **2001**, *46*, 142-165.

28. Coleman, M.J.; Vu, E.T. Recovery of impaired songs following unilateral but not bilateral lesions of nucleus uvaeformis of adult zebra finches, *J Neurol*, **2005**, *63*, 70-89.
29. Kobayashi, K.; Uno, H.; Okanoya, K. Partial lesions in the anterior forebrain pathway affect song production in adult Bengalese finches, *Neuroreport*, **2001**, *12*, 353-358.
30. Nordeen, K.W.; Nordeen, E.J. Auditory feedback is necessary for the maintenance of stereotyped song in adult zebra finches, *Beh Neural Biol*, **1992**, *57*, 58-66.
31. Leonard, A.; Konishi, M. Decrystallization of adult birdsong by perturbation of auditory feedback, *Nature*, **1999**, *399*, 466-470.
32. Brainard, M.S.; Doupe, A.J. Auditory feedback in learning and maintenance of vocal behavior, *Nat Neurosci*, **2000**, *1*, 31-40.
33. Cooper, B.G.; Goller, F. Partial muting leads to age dependent modification of motor patterns underlying crystallized zebra finch song, *J Neurobiol*, **2004**, *61*, 317-332.

## CHAPTER 5

### CONCLUSIONS

#### 5.1 Conclusions

Song learning and production is a complex process that requires intricate coordination of multiple neuromuscular systems<sup>1-10</sup>. The zebra finch model system for vocal learning closely mirrors vocal learning in humans<sup>11-13</sup>. This dissertation examines the role of GAGs in both the neural and muscle control of vocalizations. GAGs are present and play critical roles in the brain<sup>14-18</sup> as well as in skeletal muscle<sup>19-21</sup>; however, the exact mechanism of GAG function is unclear in most cases. In order to expand our understanding of these carbohydrate molecules, it is necessary to first modify and create tools and methods for the study of GAGs. Chapter 2 shows the production, purification, and characterization of GAG degrading enzymes, sulfated polymers and oligosaccharides, and xylosides. Utilizing these tools will allow for a better understanding of GAGs in biological systems such as vocal learning; however, it is imperative to continue to improve and create methods to understand and manipulate GAGs and their biosynthetic pathways.

To prove the efficacy of the most commonly used of these tools, degradation of GAG by enzymes, heparitinase enzymes were infused into the posterior forebrain nucleus HVC, which is known to be involved in song production. Infusion of these enzymes into adult male zebra finches resulted in changes to both acoustic syllable structure, timing between syllables, and (in some cases) overall syntax. As adult zebra finch song is highly



stereotyped, any of these alterations is notable. These preliminary data showed that the GAG degradation enzymes can be used effectively in the zebra finch and that GAGs appear to have an important role in vocalizations.

The research presented in Chapters 3 and 4 shows two examples of how these biochemical tools can be used to examine roles of GAGs in vocal ontogeny and production in the zebra finch. Because the involvement of GAGs in vocal behavior is relatively unexplored, this research provides an interesting backdrop for exploration into speech learning and disorders. Many speech and communication disorders have no known cause and show no obvious anatomical defect. This leads to the possibility that perhaps it is small changes, or specific changes, during development that may lead to these disorders.

In Chapter 3, Xylosides were used to alter CS biosynthesis early in development, which led to distinct changes in vocal ontogeny. Treated birds showed little if any improvement in song syntax and similarity, effectively singing juvenile song at adult ages. This suggests that the biosynthesis of GAGs, specifically CS, is critical for proper vocal development in the zebra finch. CS is known to play a role in plasticity<sup>14-17</sup>, so manipulation through xyloside offers a unique method for understanding CS in plasticity. As xylosides can serve as both an inhibitor and a primer<sup>22-24</sup>, it is important for future studies to thoroughly examine if only one aspect is required for the changes in vocal ontogeny or if it is necessary for both inhibition and priming to occur. Additionally, the concept of GAG chain valency for biological action is becoming increasingly important. The xyloside employed in this work is monomeric, having only one xylose residue. As seen in Chapter 2, the production and analysis of multimeric xylosides is ongoing. Multimeric xylosides, or molecules with two or more xylose residues, can prime multiple GAG chains per molecule. Using these multimeric xylosides may result in primed

multimeric GAGs that can react in a fashion that mimics endogenous proteoglycans<sup>25</sup>. Future studies in the zebra finch can explore whether infusion of xylosides, monomeric or multimeric, into song specific nuclei, including but not limited to RA, may alter vocal ontogeny differently. Understanding the differences that may occur due to valency, modulation of biosynthesis, or altering the GAG profile in each song nucleus may provide a clearer picture for the timeline of neural changes that underlie critical periods of vocal ontogeny and how manipulation may be possible. This goal of understanding vocal critical periods would lend itself to a better understanding of vocal ontogeny in general and possible targets that may allow for delayed closure of the critical periods in both vocal and other systems. Delaying the critical period for vocal development in humans would provide more successful results for those who receive a cochlear-implant later in life.

Chapter 4 shows that HS degradation in syringeal muscles can impact muscle kinetics and alter stereotyped song in adult zebra finches. The data suggest that syringeal muscles play a role in several aspects of song, including: amplitude, production of high frequencies, frequency modulation, and pressure at phonation onset. Additionally, disrupting the muscle output may disrupt song feedback, through auditory or proprioceptive means, into the neural control system and result in rapid and long-lasting alterations to crystallized song. These data are the first to show the role of syringeal muscle kinetics in acoustic structure. The addition of novel, or repeating, syllables provides an interesting look into the song feedback system and an opportunity for further study. Novel, or repeating, syllables can appear as early as 48 h after infusion, suggesting a rapid response to the temporary acoustic effects. It would be interesting to explore the function of this feedback loop and if these alterations to stereotyped song are due to the change in auditory feedback (lower song amplitude, changes in frequency) or whether proprioceptive

mechanisms are involved. Since research into disruption of auditory feedback show that changes in song are mediated by the anterior forebrain pathway<sup>26-28</sup>, similar research could be used to explore if similar neural mediation is used after changes in syringeal muscle kinetics. While these studies show only the initial steps into understanding how GAGs are involved in complex sensorimotor behaviors such as song learning and production, they emphasize the importance of looking into nontemplated molecules as modulators of complex learned behavior.

## 5.2 References

1. Vu, E.T.; Mazurek, M.E.; Kuo, Y.C. Identification of a forebrain motor programming network for the learned song of zebra finches, *J Neurosci*, **1994**, *14*, 6924-6934.
2. Margoliash, D. Functional organization of forebrain pathways for song production and perception, *Dev Neurobiol*, **1997**, *33*, 671-693.
3. Charlesworth, J.D.; Tumer, E.C.; Warren, T.L.; Brainard, M.S. Learning the microstructure of successful behavior, *Nat Neurosci*, **2011**, *14*, 373-380.
4. Riede, T.; Fisher, J.H.; Goller, F. Sexual dimorphism of the zebra finch syrinx indicates adaptation for high fundamental frequencies in males, *Plos One*, **2010**, *5*, e11368.
5. Bolhuis, J.J.; Gahr, M. Neural mechanisms of birdsong memory, *Nat Rev Neurosci*, **2006**, *7*, 347-35715.
6. Immelmann, K. Song development in the zebra finch and other estrildid finches, *Bird Vocalizations*, **1969**, *61*, 61-74.
7. Schraff, C.; Nottebohm, F. A comparative study of the behavioral deficits following lesions of various parts of the zebra finch song system: implication for vocal learning, *J Neurosci*, **1991**, *11*, 2896-2913.
8. McCaseland, J.S.; Konishi, M. Interaction between auditory and motor activities in an avian song control nucleus, *PNAS*, **1981**, *78*, 7815-7819.
9. Williams, H.; Crane, L.A.; Hale, T.K.; Esposito, M.A.; Nottebohm, F. Right-side dominance for song control in the zebra finch, *Dev Neurobiol*, **2004**, *23*, 1006-1020.
10. Elemans, C.P.H.; Mead, A.F.; Rome, L.C.; Goller F. Superfast vocal muscle control song production in songbirds, *Plos One*, **2008**, *3*, e2581.
11. Doupe, A.J.; Kuhl, P.K. Birdsong and human speech: common themes and mechanisms, *J Neurosci*, **1999**, *22*, 567-631.
12. King, A.P.; West, M.J.; Goldstein, M.H. Non-vocal shaping of avian song development: parallels to human speech development, *Ethology*, **2005**, *111*, 101-117.
13. Goldstein, M.H.; King, A.P.; West, M.J. Social interaction shapes babbling: testing parallels between birdsong and speech, *PNAS*, **2003**, *100*, 8030-8035.
14. Galtrey, C.M.; Fawcett, J.W. The role of chondroitin sulfate proteoglycans in regeneration and plasticity in the central nervous system, *Brain Res Rev*, **2007**, *54*, 1-18.

15. Akita, K.; von Holst, A.; Furukawa, Y.; Mikami, T.; Sugahara, K.; Faissner, A. Expression of multiple chondroitin/dermatan sulfotransferases in neurogenic regions of embryonic and adult central nervous system implies that complex chondroitin sulfates have a role in neural stem cell maintenance, *Stem Cells*, **2008**, *26*, 798-809.
16. Domowicz, M.S.; Sanders, T.A.; Ragsdale, C.W.; Schwartz, N.B. Aggrecan is expressed by embryonic brain glia and regulates astrocyte development, *Dev Biol*, **2008**, *315*, 114-124.
17. Bixby, J.L.; Harris, W.A. Molecular mechanisms of axon growth and guidance, *Annu Rev Cell Biol*, **1991**, *7*, 117-159.
18. Landolt, R.M.; Vaughan, L.; Winterhalter, V.K.H.; Zimmermann, D.R. Versican is selectively expressed in embryonic tissue that acts as barriers to neural crest cell migration and axon outgrowth, *Development*, **1995**, *121*, 2303-2312.
19. Anderson, M.; Klier, F.; Tanguay, K. Acetylcholine receptor aggregation parallels the deposition of a basal lamina proteoglycan during development of the neuromuscular junction, *J Cell Biol*, **1984**, *99*, 1769-1784.
20. Guatam, M.; Noakes, P.G.; Moscoso, L.; Rupp, F.; Scheller, R.H.; Merlie, J.P.; Sanes, J.R. Defective neuromuscular synaptogenesis in agrin-deficient mutant mice, *Cell*, **1996**, *85*, 525-535.
21. Arikawa-Hirasawa, E.; Rossi, S.G.; Rotundo, R.L.; Yamada, Y. Absence of acetylcholinesterase at the neuromuscular junctions of perlecan-null mice, *Nat Neurosci*, **2002**, *5*, 119-123.
22. Victor, X.V.; Nguyen, T.K.N.; Ethirajan, M.; Tran, V.M.; Nguyen, K.V.; Kuberan, B. Investigating the elusive mechanism of glycosaminoglycan biosynthesis, *J Biol Chem*, **2009**, *284*, 25842-25853.
23. Galligani, L.; Hopwood, J.; Schwartz, N.B.; Dorfman, A. Stimulation of free chondroitin sulfate chains by beta-D-xylosides in cultured cells, *J Biol Chem*, **1975**, *250*, 5400-5406.
24. Schwartz, N.B. Regulation of chondroitin sulfate synthesis. Effect of beta-xylosides on synthesis of chondroitin sulfate proteoglycan, chondroitin sulfate chains, and core protein, *J Biol Chem*, **1977**, *252*, 6316-6321.
25. Ngyuen, T.K.N.; Tran, V.M.; Sorna, V.; Eriksson, I.; Kojima, A.; Koketsu, M.; Loganathan, D.; Kjellén, L.; Dorsky, R.I.; Chien, C.; Kuberan, B. Dimerized glycosaminoglycan chains increase FGF signaling during zebrafish development, *ACS Chem Biol*, **2013**, *8*, 939-948.

APPENDIX A

REVIEW ARTICLE ON GLYCOSAMINOGLYCANS

IN THE NERVOUS SYSTEM

## Review

Vimal P. Swarup, Caitlin P. Mencio, Vladimir Hlady and Balagurunathan Kuberan\*

## Sugar glues for broken neurons

**Abstract:** Proteoglycans (PGs) regulate diverse functions in the central nervous system (CNS) by interacting with a number of growth factors, matrix proteins, and cell surface molecules. Heparan sulfate (HS) and chondroitin sulfate (CS) are two major glycosaminoglycans present in the PGs of the CNS. The functionality of these PGs is to a large extent dictated by the fine sulfation patterns present on their glycosaminoglycan (GAG) chains. In the past 15 years, there has been a significant expansion in our knowledge on the role of HS and CS chains in various neurological processes, such as neuronal growth, regeneration, plasticity, and pathfinding. However, defining the relation between distinct sulfation patterns of the GAGs and their functionality has thus far been difficult. With the emergence of novel tools for the synthesis of defined GAG structures, and techniques for their characterization, we are now in a better position to explore the structure-function relation of GAGs in the context of their sulfation patterns. In this review, we discuss the importance of GAGs on CNS development, injury, and disorders with an emphasis on their sulfation patterns. Finally, we outline several GAG-based therapeutic strategies to exploit GAG chains for ameliorating various CNS disorders.

**Keywords:** chondroitin sulfate; glycosaminoglycans; heparan sulfate; nervous system disorders; proteoglycans; spinal cord injury; sulfotransferases.

\*Corresponding author: Balagurunathan Kuberan, Department of Medicinal Chemistry, University of Utah, Salt Lake City, 84112 UT, USA, e-mail: KUBY@pharm.utah.edu; Department of Bioengineering, University of Utah, Salt Lake City, 84112 UT, USA; and Interdepartmental Program in Neuroscience, University of Utah, Salt Lake City, 84112 UT, USA

Vimal P. Swarup and Vladimir Hlady: Department of Bioengineering, University of Utah, Salt Lake City, 84112 UT, USA

Vimal P. Swarup and Caitlin P. Mencio: Department of Medicinal Chemistry, University of Utah, Salt Lake City, 84112 UT, USA

Caitlin P. Mencio: Interdepartmental Program in Neuroscience, University of Utah, Salt Lake City, 84112 UT, USA

## List of abbreviations

3OST, 3-O-sulfotransferase; 6OST, 6-O-sulfotransferase; 6OST1, 6-O-sulfotransferase 1; AB, amyloid- $\beta$ ; AD, Alzheimer's disease; APP, amyloid precursor protein; BACE1,  $\beta$ -secretase-1; BDNF, brain-derived neurotrophic factor; ChABC, chondroitinase ABC; ChAC, chondroitinase AC; ChB, chondroitinase B; CNS, central nervous system; CS, chondroitin sulfate; CSPG, chondroitin sulfate proteoglycan; DRG, dorsal root ganglion; DS, dermatan sulfate; ECM, extracellular matrix; FGF, fibroblast growth factor; FGFR, fibroblast growth factor receptor; GAG, glycosaminoglycan; Gal, galactose; GalNAc, N-acetylgalactosamine; GDNF, glial cell-derived neurotrophic factor; GlcA, glucuronic acid; GlcNAc, N-acetylglucosamine; GPI, glycosyl phosphatidyl inositol; HA, hyaluronan; HB-EGF, heparin-binding epidermal growth factor; HBGAM, heparin-binding growth-associated molecule; Hep I, II, III, heparitinase I, II, and III; HS, heparan sulfate; HSPG, heparan sulfate proteoglycan; IdoA, iduronic acid; KS, keratan sulfate; MAPK, mitogen-activated protein kinase; NCAM, neural cell adhesion molecule; NDST, N-deacetylase/N-sulfotransferase; NGF, nerve growth factor; NgR, Nogo receptor; NPCs, neuronal progenitor cells; NT, neutrophin; NFT, neurofibrillary tangles; OST, O-sulfotransferase; PD, Parkinson's disease; PG, proteoglycan; PKC, protein kinase C; PNN, perineuronal net; PTN, pleiotrophin; RPTP $\beta$ , receptor type protein-tyrosine phosphatase beta; RPTP $\sigma$ , receptor type protein tyrosine phosphatase sigma; SCI, spinal cord injury; SE, status epilepticus; TGF- $\beta$ , transforming growth factor beta; Trk, tyrosine receptor kinase.

## Introduction

Glycosaminoglycans (GAGs) are a family of linear, sulfated polysaccharides that are associated with central nervous system (CNS) development, maintenance, and disorders. For example, the heparan sulfate (HS) chain, a member of the GAG family, regulates receptor-ligand interactions that control neurite outgrowth and pathfinding (1–3, and references therein). Similarly, the chondroitin sulfate

(CS) chain, another common GAG, is overexpressed at the scar site in spinal cord injuries (SCIs), and is a major roadblock to regeneration (4, 5). All GAGs but hyaluronan are found associated with a core protein that belongs to a special class of biomolecules called proteoglycans (PGs). HS and CS are the two most common and prominent GAG types found in the CNS. Although these chains have been reported to affect various functions in the CNS, a comprehensive understanding of their structure-function relation is still lacking. Sulfate groups present in these molecules impart negative charge at discrete positions defining not only the fine structure but also the interactions with various signaling factors. Sulfation of GAG chains is a non-template process that occurs in the Golgi apparatus and relatively little is understood about specific contributions of various 'sulfation patterns' on GAG functionality (6, 7, and references therein). However, with recent advancements in GAG synthesis and characterization, many critical functions of sugar moieties of HSPGs/CSPGs are being revealed. In this review, we focus on the role of HS and CS chains, in particular their sulfation patterns, in various CNS pathophysiological processes. Finally, we propose various GAG-based therapeutic approaches to combat different CNS disorders for which no cure exists at present.

## Molecular perspective of PGs

GAGs can be distinguished into four groups depending on their sugar building blocks and the nature of their glycosidic linkages: HS/heparin, CS/dermatan sulfate (DS/CS-B), keratan sulfate (KS), and hyaluronan (HA). HS is composed of alternating glucosamine (GlcN) and glucuronic acid (GlcA) or iduronic acid (IdoA); CS/DS is composed of alternating *N*-acetylgalactosamine (GalNAc) and GlcA or IdoA; KS is composed of alternating galactose (Gal) and *N*-acetylglucosamine (GlcNAc); HA is a non-sulfated GAG, composed of alternating GlcNAc and GlcA residues (Figure 1). Furthermore, unlike other GAG chains, HA is not covalently bound to any protein and exists exclusively in the extracellular matrix (ECM) (8).

The synthesis of HS and CS polysaccharide chains involves two main steps: (i) attachment of linkage tetrasaccharide (GlcA-Gal-Gal-Xyl) to the core proteins through the serine residue, and (ii) subsequent elongation and modification of the GAG chains. GAG chains undergo diverse modifications by the action of various enzymes in a tissue-specific manner. These modifications include epimerization, *N*-deacetylation/sulfation, and *O*-sulfation by various *O*-sulfotransferases (OSTs), which act by sulfating residues at specific positions (Table 1). The review

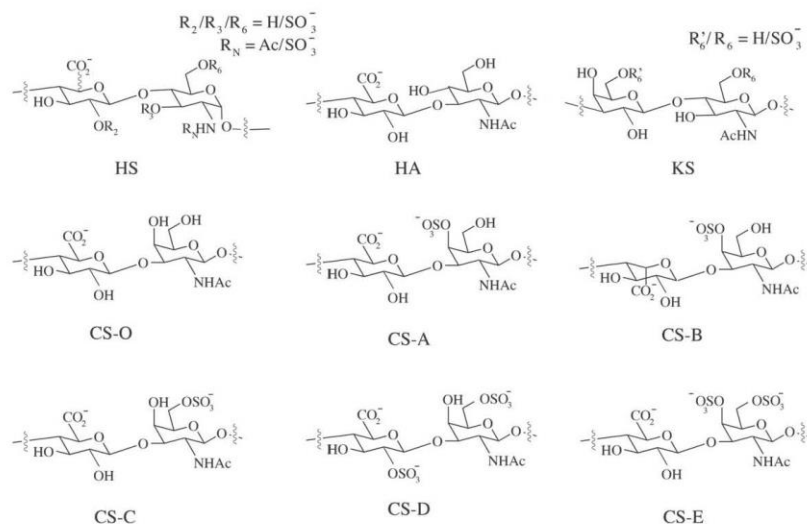


Figure 1 Schematic representation of disaccharide units found in HS, HA, KS, and CS.



**Table 1** Enzymes associated with HS and CS modifications and their implications in the CNS.

Enzymes	Role in GAG modification	Known implications	References
HS C-5 epimerase	Epimerization of GlcA to IdoA of HS	<i>Caenorhabditis elegans</i> lacking the enzyme showed axonal and cellular guidance defects	(2, 198)
HS NDST (1–4)	Converts GalNAc to GalNS	Initiated sulfation of HS; required for FGF-4 signaling; disruption can impair wingless, FGF, and hedgehog signaling in mice	(199)
HS 2-OST	2-O-sulfation of GlcA/IdoA		(198)
HS endosulfatase	Removes 6S, preference for NS256S	Expression regulated <i>Wnt</i> signaling positively and FGF signaling negatively	(200–202)
HS 3-OST	3-O-sulfation	Dramatic changes in its expression were seen in developing zebrafish; expression observed in various locations during mouse development	(139–141)
HS 6-OST	6-O-sulfation	Modified HS chains on syndecan-1; enhanced Slit signaling; dramatic changes in its expression were seen in developing zebrafish; expression reported during mouse development	(139, 142, 198, 203, 204)
CS/DS 2-OST	2-O-sulfation	Knockdown led to failure of neuronal polarization; upregulated in differentiated neuronal cells	(92, 205, 206)
CS 6-OST	6-O-sulfation	Ratio of 4S/6S varied during development and affected neuronal plasticity; upregulated after CNS injury; upregulated in neuronal stem cells	(81, 160, 205, 207)
CS 4-OST	4-O-sulfation	Upregulated in neuronal stem	(205)
<i>N</i> -acetylgalactosamine 4-sulfate-6-OST	6-O-sulfation	Knockdown led to failure of neuronal polarization in mice hippocampal neurons; downregulation reduced CSPG-mediated inhibition in E18 rat cortical neurons	(92, 161)
CS/DS C5-epimerase	Epimerization of GlcA to IdoA	Upregulated in astrocytes and neurons as compared with neuronal stem cells	(205, 208)
DS 4-OST1		Mutation associated with adducted thumb-clubfoot syndrome; deficiency resulted in impaired differentiation and proliferation of neural stem cells	(209, 210)

by Sugahara and Kitagawa (6 and references therein) provides a detailed description of HS and CS biosynthesis.

Two of the most abundant HSPGs in the CNS are syndecans and glypicans. Syndecans belong to transmembrane core protein family composed of four distinct members and carry both HS and CS chains (9, 10). Unlike syndecans, glypicans are attached to the cell membrane through a glycosyl phosphatidyl inositol (GPI) linkage, are composed of six distinct members, and carry the HS chain exclusively (11 and references therein). CS chains are primarily carried by large PGs such as hyalactans or lecticans, the most abundant PGs found in the ECM of the CNS (11). The lectican family consists of four members that have been cloned thus far: versican (also called PG-M) aggrecan, neurocan, and brevican (12–15). It has been suggested that the number of GAG chains per unit length in versican, neurocan, and brevican is fairly constant. However, the number, size, and composition of the GAG chains are not only influenced by the core protein but also by the tissue from which the lectican originates. For example, the number of KS-binding

domains of aggrecan varies among different species and tissues. Aggrecan DNA sequence shows the number of domains to be 13 in human, 4 in rat and mouse, and none in chicken (16). PGs other than syndecans, glypicans, and lecticans exist in the CNS; however, many of these are structurally unique. One example of such a PG is the receptor-type protein tyrosine phosphatase RPTP $\beta$ . Two of the three identified isoforms of RPTP $\beta$  have been found to carry CS chains (17). This article mainly focuses on GAGs, and detailed description of PGs can be found elsewhere (11, 18).

## Influence of HS and CS in the CNS

### (i) Neural development

HSPGs are expressed in actively mitotic areas of the brain. Glypican-1 transcripts have been reported in the ventricular zone, the area of neurogenesis, during CNS development

(19). Most neuronal precursor cells do not express glypican-2, -4, and -5, excluding glypican-4 (or K-glypican) expression in the ventricular zone of the cerebral cell wall (20) and glypican-5 expression in the ganglionic eminence (21). In *Drosophila*, mutations in the gene associated with glypican (*Dally* locus) results in alteration of the cell division pattern at the larval stage (22). Loss of Dally protein delays lamina precursor cells from entering into the final round of cell division. Furthermore, in humans, mutations in glypican-3 result in human X-linked Simpson-Golabi-Behmel syndrome (SGBS) (23). SGBS results in prenatal and postnatal overgrowth and has been associated with the high incidence of neuroblastoma. Syndecan-3 is the most prominent syndecan family member expressed in the adult mammalian CNS; its maximal expression in rats was found on postnatal day 7 and corresponded to glial cell differentiation, myelination, and formation of neuronal connections. The expression declined in adult neurons, where it was mainly found in axons (24).

CSPGs have also been found to influence CNS development by regulating cell division, neuronal stem cell proliferation, secondary neurosphere formation, and neurogenesis (25–27). For example, phosphacan, an RPTP $\beta$  variant, is upregulated in areas of active cell proliferation during embryonic development of rats (11, 28, 29). Neurosphere-forming cells in rat fetal telencephalons were found to express neurocan, phosphacan, and neuroglycan C. In addition, CS chains have been associated with neural stem cell proliferation through FGF-2 signaling (30).

## (ii) Neuronal migration

In addition to affecting various developmental processes, PGs (mainly CS) also affect the signaling properties of the ECM that control neuronal migration. In the CNS, neuronal migration is guided by a radial glial fiber system that acts as a scaffold for migrating neurons. In early cortical neurons, CSPGs such as protein tyrosine phosphatase RPTP $\beta$ /phosphacan are localized along radial glial fibers and on migrating neurons (31). RPTP $\beta$ /phosphacan binds to several adhesion molecules, including  $\beta$ 3/contactin, N-CAM, L1, TAG1, and tenascin (32). The most important factor that interacts with RPTP $\beta$  is pleiotrophin (PTN). PTN is a member of the HS-binding proteins that stimulates neurite outgrowth *in vitro* (33). The CS side chain and protein of RPTP $\beta$  form the binding site for pleiotrophin, and several GAGs have been reported to inhibit this binding (34). In the developing cortex, PTN is synthesized by radial glial cells and is deposited along their fibers (35). Antibodies against RPTP $\beta$  and treatment with exogenous

GAGs were reported to disturb PTN-induced migration of neurons (36). This evidence suggests that a PG-dependent ligand receptor mechanism must play a role in neuronal migration.

Studies also indicate that changes in CSPG expression are inversely correlated with migration pathways of neural crest (NC) cells. Immunohistochemical studies of chick embryos showed the restricted appearance of the CSPG versican into the CNS barrier tissues (37). In addition, surface-immobilized versican does not support the attachment of NC cells *in vitro* (38). Thus, the avoidance of versican-expressing regions by NC cells should have functional importance in their migration within the CNS. However, not all CSPGs are inhibitory. For example, highly sulfated CS motifs have been shown to enhance neuronal migration. Ishii and Maeda (39) used shRNA constructs to downregulate the production of highly sulfated CS chains, CS-D and CS-E types. The treatment of neuronal progenitor cells with such shRNA constructs in mouse embryos resulted in the accumulation of non-migrated neurons in the subventricular and intermediate zones of the cortex. This evidence further strengthens the argument that GAG type as well as their sulfation influences crucial processes in neuronal development.

## (iii) Neurite outgrowth

One of the most widely studied roles of GAGs is their effect on neurite outgrowth and axonal pathfinding. Both HS and CS chains are known to be involved in neurite outgrowth. The expression pattern of HSPGs, such as glypicans and syndecans, is tightly regulated in the developing nervous system and is closely associated with neurite outgrowth (40–42). The study by Wang and Denburg (43) showed that exogenous GAGs can alter axon growth *in situ*. The involvement of HS was confirmed by using HS-degrading enzymes that led to perturbation of axonal pathfinding. Another study on the developing *Xenopus* optic pathway showed that HS binding of exogenous FGF-2, but not FGF-1, disrupts target recognition (44).

*In vitro* studies have indicated that HSPGs support neurite outgrowth by sequestering growth-enhancing molecules such as laminin, NCAM, heparin-binding EGF (HB-EGF), and several other midkine (MK) family members (45, 46). In addition to their growth-promoting effects, glypican-1 has been reported to serve as a receptor for Slit proteins (47). Slit proteins function as chemorepellants and inhibit axonal growth upon binding to their roundabout (Robo) receptors (48). Syndecan-3 has been identified as a possible receptor for HB-GAM (49). Inhibitors

of Src family kinases affect HB-GAM-dependent neurite outgrowth of syndecan-3-transfected cells. Therefore, Kinnunen et al. (50) suggested that syndecan-3-mediated neurite growth is associated with the cortactin-Src kinase pathway. The role of HSPGs is dependent on the developmental stage of the CNS (18). Various HS-modifying enzymes (Table 1) regulate the spatiotemporal variations in the sulfations of HS chains. The affinity of HS-signaling complexes is highly dependent on the subtle structural changes of their sulfated motifs. Hence, the diversity in HS-ligand interactions forms the basis of their observed variations in their influence on neurons. An overview of the prominent HSPG-mediated ligand-receptor interactions of the CNS is shown in Figure 2. More information in

this regard can be found in the review by Lee and Chien (3) and the references cited therein.

Similar to the influence of HSPGs, the roles of CSPGs on axonal growth are multifaceted and have been studied more extensively. CSPGs are well known to inhibit axonal growth in several regions or developmental stages of the CNS (4, 51, 52, and references therein), and *in vivo* evidences have shown the inability of axons to penetrate a lectican-containing glial scar (5, 53, 54). However, tissues that express higher levels of CSPGs are not always inhibitory to neural proliferation. In fact, in several studies, CS has been shown to coincide with developing axonal pathways (55–57). Neurocan and phosphacan serve as good examples in highlighting

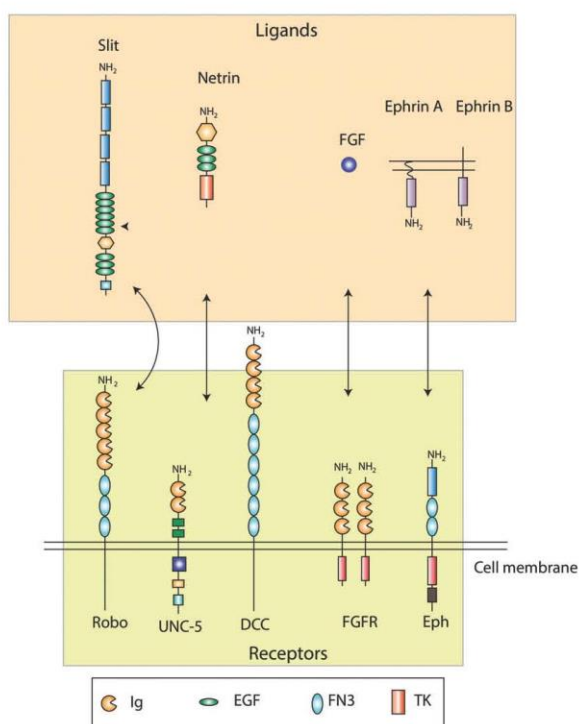


**Figure 2** Receptors of HSPGs.

Prominent interactions in the CNS that are mediated by HSPGs are shown. Robo receptors bind to Slit ligands, UNC-5 and DCC (deleted in colorectal cancer) receptors bind to Netrin, FGF binds to FGFR, and ephrin receptors (Eph) bind to ephrin ligands. Box contains the definition for conserved protein domains. Ig, immunoglobulin; EGF, epidermal growth factor; FN3, fibronectin type III domain; TK, tyrosine kinase domain. [The figure has been modified from the review by Lee et al. (3).]

the contrasting roles of CSPGs. While phosphacan was reported to promote neurite outgrowth in rat cortical neurons, neurocan inhibited the growth in embryonic chick neurons (34, 58). Evidence suggests that the stimulatory/inhibitory functions of CSPGs depend on their spatiotemporal expression and interactions that are defined by their sulfation patterns.

The interactions of CS chains with various signaling molecules lead to the promotion of neurite growth. RPTP $\beta$  is expressed on migrating neurons and binds to growth factors through its CS side chains (34, 59). Several studies also claim that RPTP $\beta$  is associated with CSPG-mediated inhibition in the CNS. For example, Shen et al. (60) have shown that after dorsal column injury, sensory axons grow deeper in RPTP $\beta$  mutant mice than they do in wild-type mice.

Some mechanistic pathways are emerging from our present knowledge on the roles of CS in controlling neuronal outgrowth. For example, blood-brain barrier leakage of blood protein fibrinogen containing transforming growth factor- $\beta$  (TGF- $\beta$ ) is thought to induce CS production in reactive astrocytes by activating the TGF- $\beta$ /Smad signaling pathway (61–64). Fibrinogen, carrying the latent TGF- $\beta$  complex, is then responsible for phosphorylation of Smad2 in astrocytes, leading to inhibitory scar formation

and limiting neurite outgrowth (61). CS has been reported to inhibit axonal growth by interacting with leukocyte common antigen-related phosphatase, Nogo receptors (NgR1 and NgR3), and the EGF receptors (65–67). The converging downstream effector of most CSPG-related inhibitory pathways is the activated Rho, a Ras homologue, which further activates the Rho-associated protein kinase (RhoA/ROCK) pathway. Once activated, ROCK leads to actin depolymerization through Lim kinase and cofilin stimulation. Actin filament degradation leads to immobility or collapse of growth cones present on the axons, leading to termination of axonal outgrowth (Figure 3) (68–70). Sivasankaran et al. (71) have shown that by blocking the RhoA pathway, myelin and CSPG lost their ability to activate Rho and inhibit neurite outgrowth in dorsal column neurons. However, similar growth enhancement was not observed for corticospinal tract neurons in the same animals, suggesting that the effect of CSPG signaling is specific to the neuronal cell type and region of the CNS.

#### (iv) CNS plasticity

HS can alter CNS plasticity by interacting with CNS ligands such as NCAM and EGF. Removal of HSPGs can lead to a

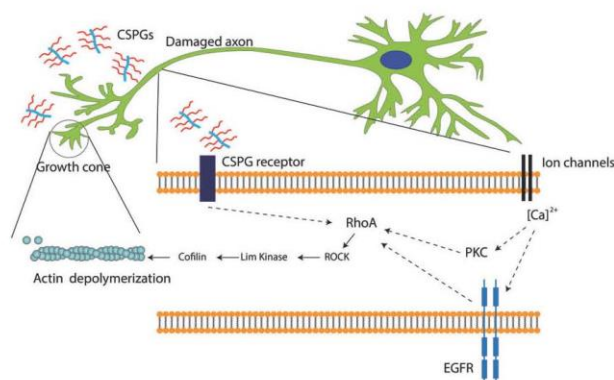


**Figure 3** Intracellular signaling mechanism triggered by CSPG present in the glial scar.

CSPGs are thought to be present in axons, although their molecular identity is not well established. Recent studies have shown that CSPG can interact with leukocyte common antigen-related phosphatase, Nogo, or EGF receptors and lead to growth inhibition (65–67). RhoA activation eventually leads to actin depolymerization and the growth cone retraction. RhoA activation has also been shown to be associated with PKC pathway and epidermal growth factor receptor (EGFR) phosphorylation in a calcium-dependent manner (67, 71). However, the process of calcium influx leading to PKC activation or EGFR activation is not well defined. Dashed arrows suggest that mediators of the represented process are yet to be identified.

loss in synaptogenic activity of postsynaptically expressed PSA-NCAM (72). Conversely, loss of the HB-EGF can affect fear and spatial learning as well as alter long-term potentiation (LTP) in the hippocampus (73). Although these studies have documented the importance of GAG chains in plasticity, it remains unclear which sulfation patterns are required for influencing the plasticity. However, some evidence alludes to their importance. For example, mice that are lacking the endosulfatases Sulf-1 and Sulf-2 show shortcomings in spatial learning. Reduction of Sulf-1 alone leads to deficits in synaptic plasticity in the hippocampus (74). As evidences accumulate for the role of HS-ligand interactions in CNS plasticity, it becomes important to delineate how specific sulfation patterns can regulate CNS plasticity.

At the end of the critical period of development, loss of neuroplasticity is seen in the CNS. The critical period refers to the stage until which neuronal properties and connections can be highly modulated by experience. It has been shown that perineuronal net (PNN) formation coincides with the end of the critical period, and other evidences suggest that CSPGs have a critical role in regulating neuronal plasticity (75–78, and references therein). Aggrecan, brevican, and neurocan are major CSPGs that interact with hyaluronan and tenacins to form the PNN, which are areas of condensed ECM that surround neuronal cell bodies and dendrites (79, 80). (The role of PNN in neuroprotection has been widely studied and is discussed under the neurological disorders section.)

A widely studied model for CNS plasticity is the ocular dominance shift in the visual system, whereby the non-deprived eye becomes more represented in the visual cortex as a result of deprivation of the other eye. It has been reported that increase in the 4S/6S sulfation ratio of the CSPGs present in brain ECM leads to the termination of the critical period of ocular dominance in mouse visual cortex (81). Normally, the capability of plastic shift exists only until the termination of the critical period. However, an ocular dominance shift toward the non-deprived eye can also be seen in the mature CNS following treatment with chondroitinase ABC (ChABC), suggesting that CS-mediated loss of plasticity may be reversible (75). CSPGs are furthermore implicated in regulating memory formation in the CNS. The cellular correlates of memory formation are 'upward' or 'downward' shifts in the synaptic strengths of neurons in response to altered inputs, termed LTP and long-term depression, respectively (82). It was observed that ChABC treatment in the CA1 region of the mice hippocampus led to a reduction in LTP as well as LDP processes at the pyramidal cell synapse (83). Altogether, these findings suggest that, in addition to controlling their

growth/migration, GAGs influence synaptic network stabilization and formation of novel synapses, thereby controlling CNS plasticity and memory formation.

## GAGs in CNS injury

Even though the contribution of HS and CSPGs in the CNS is evident, in the absence of highly sensitive molecular and analytical techniques, it has been difficult to establish their structure-function relation. HSPGs interact with a diverse array of growth factors and often serve as necessary co-factors stabilizing their signaling complex (3). However, little is known about the role of HS in CNS injury. As noted earlier, as HS chains have various functional implications on CNS development, HS-mediated signaling can possibly be associated with axonal regeneration or CNS healing linked to other neurological disorders. However, the majority of research on the role of GAGs in CNS injury has mostly been focused on CSPGs.

After CNS injury such as SCI, axonal regeneration at the affected site is inhibited owing to the formation of glial scars by the reactive astrocytes (52). Glial scars in the CNS restrict the regenerative capability of injured neurons. CSPGs, which are upregulated at the injury site, are among the major components of the inhibitory scar tissues, functioning as a barrier to neuronal pathfinding (4, 84–86, and references therein). Neurocan and phosphacan are the two major CSPGs present in the scar, whereas BEHAB (brain enriched hyaluronan binding)/brevican expression has also been found to be upregulated by reactive astrocytes (87, 88). Enzymatic removal of CSPGs after injury using ChABC has resulted in partial recovery in several *in vivo* studies (89–91). Yick et al. (91) found that enzymatic digestion of CS at the lesion site led to the regeneration of Clarke's nucleus neurons into peripheral nerve grafts implanted at the site. These studies suggest that the upregulation of CS in CNS injuries is the major cause for limited axonal regeneration and therefore is the most thoroughly studied manifestation of CS in the CNS.

In the context of SCI, CS is mostly reported to have an inhibitory effect on neuronal regeneration. However, as described in the sulfation patterns section below, some CS variants were found to promote neurite outgrowth and control polarization (55–57, 92). Therefore, as further discussed in the section on the role of GAGs in sulfation patterns, one cannot draw a simplistic conclusion about the molecular role of CSPGs during CNS injury without a closer examination of their discrete sulfation patterns.

## GAGs in neurological disorders

One of the most well-studied neurological disorders associated with GAGs is Alzheimer's disease (AD), in which patients show signs of cognitive deficits such as memory loss, inability to learn, and confusion (93). PGs appear to play both pathological and neuroprotective roles in AD. The disease is caused by the accumulation of neuritic plaques and neurofibrillary tangles (NFTs) in the cortex. One of the major components of the neuritic plaques is aggregated amyloid- $\beta$  (AB) peptides in the brain. Highly sulfated HS has been found to be co-localized with these deposits. Less sulfated HS mediates uptake and degradation of AB in non-disease states; however, the highly sulfated HS inhibits this cellular uptake of AB (93–95, and references therein). These deposits of highly sulfated HS can be substantially degraded by Sulf-1 and Sulf-2, suggesting the presence of 6-O sulfates in significant amounts (96). It has also been shown that the source of this highly sulfated HS is the nearby neuronal population and that HS is important for the regulation of Alzheimer's  $\beta$ -secretase (BACE1) (97). Studies have reported that HS and heparin, which is similar to HS except that it is more heavily charged, bind to BACE-1 and inhibit cleavage of amyloid precursor protein (APP) (97). Other GAG chains, including CS and DS, are also found within these plaques and may contribute to plaque formation and the overall progression of the disease. Previous research also showed that HS, CS, and KS can all interact with AB peptides and enhance the shift of AB42 peptides to the  $\beta$ -sheet confirmation (95). GAGs have been shown to be involved in aggregation and precipitation of amyloid fibrils, leading to increase in neurotoxicity (98). Low molecular weight heparin can compete with endogenous HS for binding to AB and inhibit the formation of fibrils (95). The sulfation patterns present on the HS thus seem to be important for the formation and progression of these neuritic plaques. Non-sulfated GAGs such as hyaluronic acid have no effect on fibril formation and aggregation (95).

Sulfated GAGs have also been implicated in Alzheimer's-like changes seen in the  $\tau$  protein. Incubation of this protein with heparin results in the formation of Alzheimer's-like filaments and promotes the phosphorylation of  $\tau$ . This phosphorylation prevents the binding of the  $\tau$  protein to stabilized microtubules and results in the rapid disassembly of microtubules assembled from  $\tau$  and tubulin. The effects seen from a variety of GAGs is proportional to the extent of sulfation present on the GAG chain (99).

PGs also play a significant role in gliomas. The neural ECM is naturally resistant to cell and neurite motility.

As discussed in earlier sections, a major component of these inhibitory regions of the ECM is CS. Upregulation of BEHAB/brevican has been reported in gliomas (100, 101, and references therein). The tumor-specific BEHAB/brevican is differentially glycosylated and is cleaved by metalloproteases promoting cell motility and invasion in glioma (102, 103). Neurocan, versican, and tenascin-c are also implicated in the invasiveness of gliomas (104, 105). HSPGs are also upregulated in some gliomas and interact with factors that promote glioma growth and invasion. Specifically, several HSPGs have been found to promote the signaling and mitogenic properties of FGF-2 (106).

Sulfation of GAGs can alter the behavior of glioma cells. Studies have examined how sulfation density affects glioma proliferation and invasion; for example, reduction of sulfation using sodium chlorate treatment on glioma cells resulted in lower levels of cell proliferation (107). Intracerebral inoculation of glioma cells pretreated with sodium chlorate also lead to a decrease in size and instances of glioma, resulting in longer survival of the treated animals (108). Changes were also seen in specific sulfations on HS. Enhanced FGF-2 activity was correlated with higher sulfation levels in the HS present in gliomas with a higher amount of 2-O and 6-O sulfates (106). Sulf-2 expression was reported to regulate tyrosine kinase signaling pathway through PDGFR $\alpha$  activation in glioblastoma cells as well as primary tumors. Knockdown of Sulf2 in human glioblastoma cells or generation of gliomas from *Sulf2*<sup>-/-</sup> resulted in decreased growth *in vivo* in mice (109). These results indicate that endosulfatases expressing gliomas could respond to various external growth factors, and such factors can serve as potential therapeutic targets in such disorders.

Alterations in GAGs are seen in a variety of neurological disorders, including autism, epilepsy, Parkinson's disease, and schizophrenia (Table 2). A mouse model for autistic behavior, the BTBR T+tf/J mice, was recently reported to show alterations in HS associated with fractal structures of the subventricular zone (SVZ), specifically the third and lateral ventricles (110–112). This fractone-associated N-sulfated HS is thought to be involved in growth factor sequestering and in modulating glutamatergic synapses (110–112). Furthermore, eliminating HS in postnatal neurons in mice resulted in autistic symptoms. After conditionally inactivating *Ext 1*, an enzyme involved in HS biosynthesis in the brain after birth, there were no morphological changes; however, these mice showed stereotyped and repetitive behavior and had impaired social interactions (113). In a recent study, Pearson et al. (114) report reduction in N-sulfated HS in the ECM from the SVZ of brain lateral ventricles in postmortem tissue of

Table 2 Association of various PGs and GAGs with neurological disorders.

PG (GAG)	Disorder	Observed effects	References
Neurocan (CS)	Bipolar disorder and schizophrenia	SNP overlap was found in neurocan gene ( <i>NCAM</i> )	(211)
Brevican (CS)	Episodic falling syndrome, related to human paroxysmal exercise-induced dyskinesia episodic ataxias	Deletion reported in brevican gene ( <i>BCAM</i> )	(212)
Nauparin (HS)	AD	Protected neurons against cholinergic lesions; increased arborization and reduced septal caspase 3 and $\tau$ immunoreactivity	(181, 182, 213, 214)
Perlecan (HS)	AD	Disordered processing was associated with amyloidosis	(215)
(HS, DS, CS)	AD	Identified in AD lesions, amyloid deposits, and neurofibrillary tangles	(216–218)
Apican (CS)	AD	APP acted as its core protein, was found in human and rat brain	(219)
(HS)	AD	O-GlcNAc glycosylation was upregulated	(220)
(HS/CS)	AD	Promoted formation of paired helical filaments	(221)
CSPG	HIV-1 infection	Facilitated infective entry of virus; PNN damage was observed in AIDS victims	(222, 223)
Neurocan, phosphacan, brevican (CS)	Epilepsy	Full-length neurocan was deposited after seizures, associated with axonal sprouting; phosphacan-positive PNN decreased; cleaved brevican increased in the temporal lobe and hippocampal regions of the rat brain	(224, 225)
Aggrecan, versican, phosphacan, brevican (CS)	Stroke	Plasticity increased in peri-infarct and remote regions with reduction in aggrecan, versican, and phosphacan, and accumulation of neurocan	(226, 227)
HSPGs	Gerstmann-Straussler syndrome, Creutzfeldt-Jakob disease, and scrapie	Sulfated GAGs were found to be present in amyloid plaques	(228)
HSPGs/CSPGs	Parkinson's disease	Lewy bodies were found to contain PGs	(218, 229)
Brevican, versican (CS)	Glioma	Overexpressed and promoted tumor growth, vascularization, and invasiveness	(100, 101, 230)
CSPGs	Monocular deprivation and amblyopia	ChABC led to complete recovery in rats and moderate recovery in cats	(231, 232)
HSPGs	Pick's disease	Involved in extinction of Pick bodies	(233)
HSPGs	Autism	Reduction in N-sulfated HS in SVZ	(114)

autistic individuals. These studies implicate that decrease in N-sulfated HS in specific regions of the brain could be contributing to the etiology of autism and may serve as a biomarker for the disorder.

CS chains play an etiological role in epilepsy. This is likely due to the ability of CS to stabilize synapses, reduce plasticity, and interact with GABAergic interneurons. A variety of CSPGs are thought to be involved in the onset and progression of epilepsy. Neurocan, which is primarily expressed during development, shows a renewed expression following status epilepticus (SE) in the adult hippocampus (115). Aggrecan has also been examined in relation to PNN remodeling after SE. After SE, the hippocampus showed a decrease in aggrecan expression 1 week post-SE, specifically in the dentate gyrus, followed by a decrease in aggrecan-labeled PNNs. Additionally,

the remaining PNNs show a loss of structural integrity (116).

Both HS and CS appear to play a role in Parkinson's disease (PD). Agrin, an ECM and transmembrane HSPG, has been implicated in fibril formation in AD and PD (117). NG2, a CSPG, has also been implicated in PD. In a study examining two rat models of PD, NG2-positive cells expressed calcium-binding adaptor molecule 1 and GDNF (118). It has also been seen that subcutaneous injection of a cytokine mixture containing granulocyte macrophage colony-stimulating factor and interleukin-3 ameliorated the loss of dopaminergic neurons in one of these rat PD models. One possible mechanism for this reduction of degradation is thought to be the increase in NG2-positive glia found in treated animals (118, 119). Hence, NG2-positive glia seems important for the survival of dopaminergic

neurons and presents NG2 as a possible therapeutic target for PD.

PGs have also been implicated in schizophrenia. Upon examining postmortem brains, researchers found an increase in CSPG-positive glial cells in specific brain nuclei of the schizophrenic patients. The increase was primarily seen in the deep amygdala and entorhinal cortex. A decrease in PNNs was observed in different areas of the amygdala and entorhinal cortex as well (120). However, there was no change in the presence of parvalbumin-positive GABA neurons that are most commonly associated with PNNs in the entorhinal cortex or the amygdala (121). Changes have been seen in fear learning and extinction in schizophrenia patients. This may be directly influenced by alterations in the PNN present in the amygdala, as previous studies have shown that enzymatic degradation of this structure disrupted fear learning (122, 123). This presents evidence that CS could play a key role in development of schizophrenia and its overproduction in certain areas while disruption in others may lead to improper neural functionality.

GAGs are altered in many neurological disease states; however, it remains unclear what is the exact mechanism of their involvement. Although GAGs have been implicated in several CNS pathological processes, there are ample evidences to suggest their neuroprotective role as well. Brain samples from patients with sporadic Creutzfeldt-Jakob disease revealed that PNN surrounding parvalbumin-IR neurons of the cerebral cortex disappear before these cells die. Following their death, this zone becomes occupied with protease-resistant prion protein (PrP), which then spreads into the space and interacts with other GAGs to form protease-resistant aggregates (124, 125). Likewise, cortical neurons associated with PNN were found to be resistant to neurofibrillary changes and  $\tau$  pathology in AD (126, 127). *In vitro* experiments suggest that CSPGs protect PNN-associated neurons against glutamate toxicity, which also plays a role in AD (128). CS chains were also found to elicit neuroprotective effects in an *in vitro* model of calcium-dependent excitotoxicity in a sulfation-dependent manner. Treatment of rat cortical neurons with CS-E reduced cell death by *N*-methyl-D-aspartate (NMDA), (*S*)- $\alpha$ -amino-3-hydroxy-5-methyl-4-isoxazolepropionic acid, or kainate, whereas other sulfation variants of CS or HS had no such protective effect (129). Dopaminergic neurons are associated with the pathophysiology of PD and undergo significant reorganization in their aggrecan-based ECM, leading to degeneration (130). It has been suggested that polyanionic GAGs associated with PNN contribute to the reduction in local oxidative stress by scavenging redox-active ions (131). Taken

together, these studies suggest a paradoxical role of PGs in neurodegenerative diseases. For example, while several evidences suggest strong interaction between GAGs and amyloid deposits and NFTs (132, 133), CSPGs containing PNNs are known to protect cells from degeneration. Therefore, it is evident that GAG structures must play different roles in various states of damaged CNS. Our understanding about the specific roles of PGs in CNS disorders is still growing, and we have summarized observations on their associations with various CNS pathologies in Table 2 and Figure 4.

### The role of GAG sulfation patterns in the CNS

The elaborate molecular interactions of the HSPGs/CSPGs are tightly controlled by their sulfation patterns, which provide their ligands unique selectivity for binding (Table 3). Diverse sulfations are found in both HS and CS (134). Wang et al. (43) reported that highly sulfated HS-like polymers, in comparison with unsulfated HS, increased error in median fiber tract axonal pathfinding of pioneer axons in cockroach embryo. Furthermore, genetic studies done by deleting various sulfotransferase enzymes have shown the importance of sulfation. For example, mutation in the *N*-deacetylase-*N*-sulfotransferase gene in *Drosophila* inhibited activation of the MAPK pathway and led to defects in cell migration during embryogenesis (135). Different sulfotransferase isoforms of CS have been associated with specific regions of the brain (136). With the alternating sulfotransferase activity, the sulfation patterns of HS and CS keep changing during embryonic brain development (137, 138). Therefore, it is understood that sulfated domains of HS and CS are highly regulated by the spatiotemporal expression of various sulfotransferase and endosulfatase enzymes.

HS sulfotransferase enzymes are expressed differentially in the cerebrum during neural development. During mouse embryonic development, significant 3OST and NDST expression was observed in the ventricular zone and the cortical plate (139). NDST was also expressed in other brain areas such as the marginal zone and subplate (139). In juveniles, 3OST and 6OST expression was found to be more widespread, being found in the ventricular zone, layers V/VI, intermediate zone, and cortical plate. 3OST expression in adults was found in layers II/III and V of the cortex, and 3OST-2 and 3OST-4 were found abundantly in trigeminal ganglion neurons. 6OST showed expression in layers I and II/III. NDST expression in juveniles was



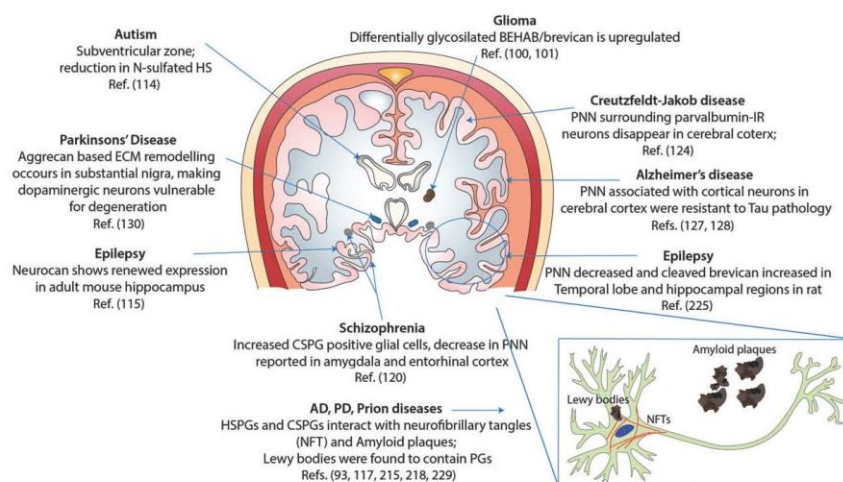


**Figure 4** Observed and potential associations of PGs and GAGs with neurological diseases in various regions of the human brain. This diagram represents a coronal section of the human brain and highlights evidence reported about the involvement of GAGs in various CNS disorders. Observations made in non-human brain samples may suggest that such effects persist in the human brain as well.

**Table 3** Different GAG sulfation patterns and their effects related to the CNS.

GAG	Sulfation	Observed effects	References
HS	2S	Binding of FGF1 and FGF8 to several FGFRs. These interactions were associated with neural plate patterning, neurogenesis, gliogenesis, cell migration, axonal pathfinding, and neuronal regeneration	(145, 234, 235)
HS	6S	Binding of FGF1 and FGF8 to several FGFRs, associated with effects stated in the row above	(145, 235)
HS	2S/3S/6S	Associated with Slit protein binding	(236)
HS	IdoA(2S)-Glc(NS)	Associated with bFGF binding	(237)
HS	NS2S6S	Netrin 1 and semaphorin 5B binding; NS6S was preferred by Slit 2; NS2S was preferred by ephrin A1 and ephrin A2	(238)
HS	Totally desulfated/NS	Failed to bind basic FGF	(239)
CS-A	GlcA-GalNAc(4S)	Provided negative guidance cues to cerebellar granule neurons	(163)
CS-C	GlcA-GalNAc(6S)	Expressed in tissues acting as barrier to axonal advancement in chick embryo; upregulated after CNS injury; upregulation led to axonal regeneration; associated with Schwann cell motility	(159, 160, 167, 240)
CS-E	GlcA-GalNAc(4S,6S)	Stimulated outgrowth in dopaminergic, hippocampal, and DRG neurons; associated with FGF-2, FGF-10, FGF-16, FGF-18, MK, PTN, TNF- $\alpha$ , BDNF, HB-EGF binding; inhibited rat cortical cell binding; inhibited DRG neurite outgrowth through PTP $\alpha$ pathway; assembled neurotrophin-Trk complex	(148, 150, 151, 154, 156, 162, 166, 241)
CS-D/CS-E	GlcA(2S)-GalNAc(4S)/GlcA-GalNAc(4S,6S)	Promoted growth in rat hippocampal neurons	(242, 243)
CS-B/CS-E	IdoA-GalNAc(4S)/GlcA-GalNAc(4S,6S)	Interacted with PTN; promoted neurite outgrowth in hippocampal neurons by interacting with PTN	(1, 244)
CS-A/CS-D/CS-E		Stimulated neurosphere formation through an EGF-dependent pathway	(29)
CS-B/CS-D/CS-E		Promoted FGF-2-mediated proliferation of rat embryonic neuronal stem cells	(30)

seen in layers II/III and V, whereas expression was seen in a manner similar to that of 3OST in adults (139, 140). In adults, 3OST expression can also be induced by environmental cues. Dramatic changes in the expression of various 3OST and 6OST isoforms were observed in a spatiotemporal manner in developing zebrafish (141, 142). The HS fine structure in the pineal gland showed differences when assessed in light versus dark conditions (143). The differential expression in development as well as changes in sulfotransferase expression due to environmental cues such as light implies that control of specific HS sulfation is important to normal development and neural function.

GAG functions are controlled by their sulfation pattern as well as density. The specificity of HS sulfation in determining their binding affinity for different isoforms of FGF has been investigated extensively. IdoA2S-GlcNS was found to increase the binding affinity of HS with basic FGF, and the affinity increased with increasing sulfation density (144). Sulfates seem to impart a defined structure to the HS microdomains, thus controlling their selectivity for binding to various ligands. Many such ligand receptor interactions, such as FGF-FGFR, play crucial roles in various CNS processes, such as neural plate patterning, neurogenesis, gliogenesis, axonal pathfinding, and regeneration during injury. Further details on the role of FGFs in CNS can be found in the review by Guillemot and Zimmer (145 and references cited therein).

Although several distinct roles have been proposed for HS- and CS-mediated signaling, the existence of overlap in their CNS interactions cannot be excluded completely. In fact, crystallographic analysis of RPTP $\sigma$  revealed a shared binding site for HS and CS (146). In fact, Coles et al. (146) proposed that both HS and CS can bind to RPTP $\sigma$  and still mediate their differential response on neurons. The computational model suggested that due to the difference in their sulfation densities, HS and CS are able to differently affect RPTP $\sigma$  signaling. The discretely sulfated domains of HS may promote RPTP $\sigma$  clustering, resulting in compromised phosphatase activity and hence enhanced life of neurite-promoting phosphorylated proteins. In contrast, the uniformly sulfated domain of CS results in higher phosphatase activity mediated by RPTP $\sigma$ , leading to neuronal inhibition (146). Others have also observed the contrasting roles of HS and CS mediated by RPTP $\sigma$ . The role of RPTP $\sigma$  as a CSPG receptor is well known (60). RPTP $\sigma$  have also been reported to promote growth in chick retinal ganglion cell axons in response to basal lamina, which contains HSPG ligands (147). Although the presence of IdoA imparts very distinct structural features to HS, the presence of IdoA in certain other CS variants (CS-B and CS-D) can likely enhance their binding with

HS binding proteins. This suggests that the HS and CS structure may regulate their CNS interactions in two ways. Owing to the gross structural similarity between HS and CS, they may interact with common receptors. However, owing to the distinct, fine differences in their sulfation, the outcomes of such interactions can vary widely.

Distinct sulfated motifs of CS have been shown to control neuronal outgrowth differently. Tully et al. (148) have shown that surface-immobilized CS-E tetrasaccharide can promote outgrowth of hippocampal neurons. Highly sulfated CS structures such as CS-D and CS-E are known to bind many proteins, including FGFs, MK, PTN, EGF, brain-derived neurotrophic factor (BDNF), and chemokines (see Table 3) (149–151). The CS-E motif is enriched in a developing rat brain (136); interacts with several PGs; and acts in association with appican, syndecan-1, syndecan-4, neuroglycan C, and phosphacan (136, 152, 153). In the study by Gama et al. (151), it was shown that BDNF selectively binds to the CS-E motif with a 20-fold preference over those of CS-A and CS-C at physiologically relevant concentrations. Moreover, surface plasmon resonance experiments show that CS-E bound to MK as strongly as heparin, which was followed by other GAGs (154). Similarly, exogenously added CS-E and CS-D were seen to block pleiotrophin-RPTP $\beta$  interaction, resulting in abnormal morphogenesis of Purkinje cell dendrites (155). The observations made on binding of highly sulfated CS with HS-binding growth factors such as MK further strengthens the hypothesis that a combination of gross and fine structural features mediates the interactions of HS and CS with common receptors. Furthermore, the high sulfation density of CS-D and CS-E might structurally be more similar to HS in terms of charge distribution and the presence of 2S-containing IdoA (in CS-D). Hence, these subtle features may enhance the binding of CS motifs to HS-binding growth factors, leading to similarity in their growth-promoting outcomes.

In spite of evidences demonstrating the influence of distinct CS motifs on neurons, the underlying mechanistic pathways are not yet fully understood. Rogers et al. (156) demonstrated another aspect of CS-E signaling by modulating the neutrophin (NT)-tyrosine receptor kinase (Trk) interactions. CS-E, but neither CS-A nor CS-C, was shown to assemble the NT-Trk complex, which led to the formation of CS-E-nerve growth factor (NGF)-TrkA and CS-E-BDNF-TrkB complexes (156). NT-Trk binding mediates neurite outgrowth, differentiation, and survival through the extracellular signal-regulated kinase, phosphatidylinositol 3-kinase, and phospholipase C $\gamma$  pathways (157, 158). Multiple signaling pathways may regulate CS-mediated neuronal growth or inhibition; thus, CS-E-dependent NT-Trk binding presents another way in which CS-E plays

a role in neuronal growth and proliferation. Although NT signaling is mediated by Trk receptor dimerization, the possibility of CS-E in dimerizing Trk itself cannot be excluded completely.

In contrast to highly sulfated units, the monosulfated CS-A and CS-C were shown to have inhibitory influences on neuronal growth. The composition of three barrier tissues between the spinal cord and hind limb of the chick embryo illustrates the expression of peanut agglutinin and CS-C at the time when they are avoided by growing axons (159). In a more recent study, it was shown that CS-C synthesis is upregulated in CNS after injury (160). The study also analyzed mRNA levels of the enzyme chondroitin 6-O-sulfotransferase 1 (CS-6OST1) and showed its upregulation in most glial cells around cortical injuries. Although these results indicate that CS-C acts as an inhibitor for axonal regeneration, others have suggested CS-E or CS-A to be the inhibitory component of the glial scar (161–163).

The role of GAGs in enhancing amyloid aggregation revealed the following order: heparin>HS>CS=DS, suggesting that highly sulfated GAGs such as heparin were most effective in forming plaques. Furthermore, in the case of heparin, the order was found to be heparin>N-desulfated N-acetylated heparin>completely desulfated N-sulfated heparin>completely desulfated N-acetylated heparin. These results clearly show that the sulfate moiety of GAGs plays a critical role in the amyloid- $\beta$  fibril formation (164, 165). Table 3 summarizes various evidences on the influence of CS and HS sulfation patterns in relation to the CNS.

Although there are a growing number of evidences that suggest distinct roles of different sulfation patterns of CS on neurons, a consensus is still lacking. For example, there is overwhelming evidence on the neurite-promoting activity of CS-E; however, Brown et al. (166) have recently shown that CS-E inhibits neurite outgrowth of dorsal root ganglion (DRG) neurons. Likewise, Karumbaiah et al. (161) reported that CS-E is upregulated in rats after SCI and is inhibitory for the growth of cortical neurons. Similarly, some studies point out the growth-promoting effects of 6-O-sulfation. Lin et al. (167) reported that highly 6-O-sulfated CS (CS-C motifs) in glial scar formed after CNS injury promoted axonal regeneration in nigrostriatal axons. Overall, contradictory evidence on the role of distinct CS motifs have been shown in the recent literature, and it seems plausible that the influence of such motifs depends on the neuronal cell type, site, and developmental stage of the CNS. Therefore, a systematic characterization of a library of CS variants is required to examine the relative influence of various sulfation patterns on neuronal growth and plasticity.

Owing to the variations in the chain length and the sulfation pattern of the CS chains used in different studies that also involved different neuronal models/sources, an understanding on the role of specific sulfation patterns is currently lacking. Although many studies utilize CS structural variants isolated from natural sources, these chains do not contain uniform sulfation patterns. Most of the commercially available CS chains are classified on the basis of the dominant sulfation motif present on them. We therefore characterized the sulfation profiles of five major CS variants found in the mammalian brain: CS-A, dermatan sulfate (CS-B), CS-C, CS-D, and CS-E, and assessed their influence on embryonic day 18 rat hippocampal neurons. Structural analysis of CS chains revealed a vast diversity in their sulfation content. Surface-immobilized CSs were used in the neurite growth assay by conjugating CS chains to the poly-L-lysine-coated surfaces. Single CS plain-field patterns revealed differential inhibitory potential of the CS variants. Interestingly, over the three time points of 24, 48, and 72 h, we observed that the neurite length and the number of neurites per cell were maximum in neurons growing over CS-D surfaces, whereas CS-C surfaces were the most inhibitory (unpublished data). These findings support previous reports on the inhibitory role of CS-C toward neuronal growth (160, 168). As already mentioned, disulfated CS chains have been reported to promote neuronal adhesion, migration, and neurogenesis. Likewise, we observed relatively better neuronal growth for both CS-D and CS-E among the CS chains tested. Interestingly, the neurite length and the number on CS-D-coated surfaces were significantly higher than in the other CS variants used (unpublished data). Most importantly, the study demonstrated that sulfation pattern variation could lead to diverse cell response to the GAGs, which might be the basis of the opposing roles of CSPGs in the CNS.

## Expert opinion

It is clear that GAGs play a major role in CNS development and maintenance. The goal for the future will be to exploit these GAGs as therapeutic agents in CNS disorders. From the reported evidence, we understand that bimolecular interactions mediated by GAGs are influenced by the fine sulfation patterns present on HS and CS chains. Multiple approaches are being explored to utilize these molecules for developing solutions for the neurological injuries and disorders discussed earlier. Presently, the efforts on developing therapies for CNS injury/disorders are headed in three directions: (i) removing inhibitory CSPGs from the

injury site (85); (ii) delivering neurotrophic factors for stimulating regeneration (169); and (iii) using stem cells to support neuronal regeneration (170). However, as none of these approaches have shown complete functional restoration independently, there is a need to design combinatorial therapies that modulate the complex neuroinhibitory environment present at the scar/disease site to facilitate neuronal regeneration.

Digestion of CSPGs at the scar site after injury is one of the most widely investigated therapeutic approaches for CNS injuries. Several studies have demonstrated the therapeutic efficacy of combining the digestion of CSPGs with infusions of neurotropic factors (171–174). However, ChABC treatment results in complete degradation of CS chains and may lead to loss of growth-promoting or guiding motifs. Therefore, digestion of specific CS chains using enzymes such as ChAC or ChB should be explored to selectively remove inhibitory motifs and lead to better therapeutic outcomes than ChABC. Such an approach may also be beneficial in AD and schizophrenia, where upregulation of HS or CS leads to disease progression. Partial or complete digestion of such GAG structures with combinations of chondroitinases, heparitinases, or endo-sulfatases could be explored for functional effective restorations recovery in such disorders.

In spite of promising results of ChABC, delivery of the active enzyme for prolonged periods has practical limitations. ChABC has been reported to be thermally unstable, decreasing its activity significantly at body temperature (175). Therefore, Lee et al. (90) have reported the use of trehalose to thermostabilize ChABC for prolonging its activity. The stabilized enzyme could digest CS chains *in vivo* up to 2 weeks after injury. Another potential approach to circumvent the limitations of ChABC could be to modulate GAG biosynthesis using xylosides. As xylosides are small molecules, they can be efficiently targeted and delivered at the scar site to alter the production of inhibitory CS chains. Previously, click-xylosides, containing various aglycone residues, were shown to prime a variety of different GAGs in Chinese hamster ovary (CHO) cells (176). Additionally,  $\beta$ -D-xylosides have been used on astrocytes to enhance neuronal growth (177). Moreover, 4-deoxy-4-fluoro xylosides (fluoro-xylosides) could be exploited to inhibit GAG production at the affected region. A number of fluoro-xylosides have been found to inhibit GAG biosynthesis in CHO and endothelial cells (178, 179). Small molecular inhibitors of GAG sulfotransferases are yet another option that can be used to modulate the HS or CS sulfation pattern at the damage site. By selectively targeting one or more sulfotransferase enzymes, highly specific HS or CS motifs can be generated to stimulate

neuronal regeneration. As GAGs may enhance formation of protease-resistant plaques, inhibiting this binding may increase the turnover of these pathological aggregates by prolonged exposure to proteases. Polysulfonated GAG mimetics have been used for this purpose and were found to be protective against amyloid fibril-induced effects (180–182). Furthermore, 4-deoxy-*N*-acetyl glucosamine was shown to attenuate plaque formation and improve effects of AD (183). Therefore, several permutations and combinations of small molecular inhibitors of GAG biosynthesis could be utilized to create clinically applicable solutions for degrading or modifying pathological PGs in the CNS.

GAG-based approaches may pose some limitations as GAGs have multifunctional roles in CNS injury and pathology. First, even though PGs bind to amyloid fibrils through GAGs, an additional role of the protein core of PGs cannot be excluded. Next, although the use of ChABC or fluoro-xylosides may promote short-term neuronal recovery or plasticity by PNN degradation, it is uncertain whether such non-specific degradation or inhibition of CSPGs will be beneficial for the CNS in the long term. It has been shown that scar formation may have a beneficial role of limiting the injury and restricting the infiltration of inflammatory cells (184). Therefore, limited or transient degradation of CSPGs may be required for optimal recovery, thus making the time window of therapeutic intervention an equally important factor.

Various growth-stimulating factors such as neurotrophin-3, cyclic adenosine-mono-phosphate, and sonic hedgehog have been used to stimulate axonal regeneration at scar sites (169, 185). Many such factors target endogenous progenitor cells that can be stimulated to produce neurons and associated cell members at the injury site. In addition, spinal cord-derived neuronal stem/NPC cells can be transplanted to improve the regenerative capacity of the spinal cord, and to facilitate the functional recovery of experimental models (170, 186). To provide a stimulus for these stem cells to differentiate, they are generally seeded in polymeric scaffolds that mimic the architecture of the healthy spinal cord (170). However, instead of using synthetic polymers, GAG-based natural polymers can be developed to enhance the functionality of the scaffolds and to reproduce the molecular signals found in the developing CNS. HA is an excellent candidate for such applications because of its biocompatibility and its ability to maintain tissue organization, facilitate ion transport, and promote cell proliferation and differentiation (187). HS and CS have numerous effects on neurogenesis and neurodifferentiation, which can be exploited in conjunction with growth factor delivery. Heparin-PEG hybrid hydrogel has

been used to explore its applicability toward neuronal cell replacement strategies (188). Although the functions of KS are largely unknown, KS chains are shown to be associated with some critical aspects of the CNS (189). KS is downregulated in AD (190), is the predominant GAG in the cornea of eye (191), and is involved in glial scar formation (192). The coming years will reveal more about the biology of KS and it is likely that all GAG types will become indispensable in therapies for many neurological disorders including AD. As discussed earlier, the influence of sulfation patterns of GAG in the CNS is highly dependent on the neuron type and the state of the CNS. Therefore, different sulfation motifs or GAG combinations may lead to enhanced neuronal regeneration or recovery for different sets of disorders and injury conditions.

Besides enhancing growth and regenerating neurons, it is imperative to guide axons across the scar site to reform severed neuronal wiring. One proposed treatment involves creating a neuronal bridging device that can facilitate connections of the spinal cord regions separated by the wound site. For this approach to succeed, a growth-supporting biomaterial must act as a conduit for the directional growth of neurons. To provide guidance cues for neuronal pathfinding, the bridging scaffold can be 'sugar coated' with HS and CS chains to create a directional gradient of the growth-promoting ligands. Previously, protein micropatterning techniques have been utilized to create patterns for directing neuronal outgrowth (193, 194). By utilizing an array of differentially sulfated GAG structures, one can create unique signaling combinations

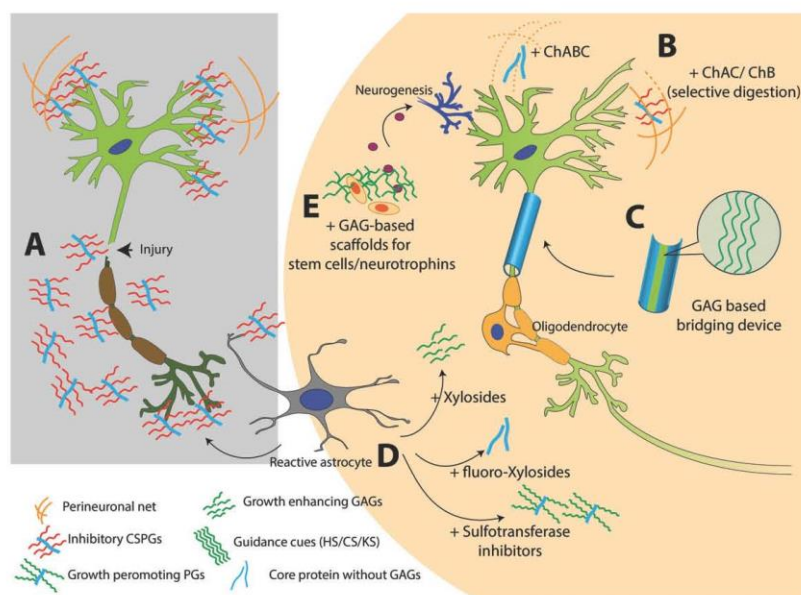


**Figure 5** Use of sugar glues for broken neurons and GAG-based therapies for injured CNS.

(A) Neuronal injury results in overexpression of inhibitory CSPGs from reactive astrocytes. (B) Degrading CS chains to stimulate neuronal growth. ChABC is widely studied for this application; however, unspecific digestion of GAGs can damage growth-promoting motifs and other important structures such as PNN. Selective digestion can be done using ChAC and ChB enzymes. (C) Designing GAG-based bridging device to guide regenerating axons. Surface presented HS, CS, DS, KS, or HA domains can be used to direct axonal pathfinding. (D) Using small molecules to modulate GAG production at the scar site. Xylosides would change the composition or sulfation pattern of the GAGs secreted from reactive astrocytes. Addition of fluoro-xylosides would inhibit GAG biosynthesis and result in generation of core protein without inhibitory GAG chains. Sulfotransferase inhibitors can be used to stop production of inhibitory sulfation patterns present in CSPGs released from reactive astrocytes. (E) Bioactive scaffolds can be designed by using GAGs such as HA, HS, CS, DS, or KS. Such scaffolds can be used to deliver stem cells or neurotrophic factors at the scar site. A combination of two or more such approaches can be utilized to create effective therapies for neurological disorders.

that enhance regeneration, functionality, and directed growth of neurons.

It is clear that GAGs can influence neuronal development through their structural heterogeneity; however, obtaining structurally uniform GAG chains has been a challenging task. As we present the concept of exploiting sulfation patterns to modulate the outcome of GAG-neuron interactions, obtaining uniform structures with defined sulfation motifs is a prerequisite. Significant advances have been made recently in this direction with the development of various chemoenzymatic processes to obtain defined oligosaccharide and polysaccharide structures of HS chains (195–197). Tully et al. (148) have utilized chemically synthesized CS structures in various neuronal assays. These processes can further be extended to create several uniform GAG structures of HS, CS, DS, or KS backbones for use in various CNS applications. Figure 5 summarizes various GAG-based therapies that can be utilized to develop clinical solutions for CNS disorders. It is hence clear that the biology of sulfation patterns in HS and CS chains has finally begun to take shape. The structure-function relations of GAG-mediated interactions can now be utilized to understand CNS signaling mechanisms and to design novel therapies for several neurological disorders.

## Highlights

- GAGs play pivotal roles in CNS development, injury, and diseases.

## References

1. Bao X, Mikami T, Yamada S, Faissner A, Muramatsu T, Sugahara K. Heparin-binding growth factor, pleiotrophin, mediates neurotogenic activity of embryonic pig brain-derived chondroitin sulfate/dermatan sulfate hybrid chains. *J Biol Chem* 2005; 280: 9180–91.
2. Bülow HE, Hobert O. Differential sulfations and epimerization define heparan sulfate specificity in nervous system development. *Neuron* 2004; 41: 723–36.
3. Lee J, Chien C. When sugars guide axons: insights from heparan sulphate proteoglycan mutants. *Nat Rev Genet* 2004; 5: 923–35.
4. Asher RA, Morgenstern DA, Moon LDF, Fawcett JW. Chondroitin sulphate proteoglycans: inhibitory components of the glial scar. *Prog Brain Res* 2001; 132: 611–9.
5. Snow DM, Lemmon V, Carrino DA, Caplan AI, Silver J. Sulfated proteoglycans in astroglial barriers inhibit neurite outgrowth in vitro. *Exp Neurol* 1990; 109: 111–30.
6. Sugahara K, Kitagawa H. Recent advances in the study of the biosynthesis and functions of sulfated glycosaminoglycans. *Curr Opin Struct Biol* 2000; 10: 518–27.
7. Herndon ME, Lander AD. A diverse set of developmentally regulated proteoglycans is expressed in the rat central nervous system. *Neuron* 1990; 4: 949–61.
8. Weigel PH, Hascall VC, Tammi M. Hyaluronan synthases. *J Biol Chem* 1997; 272: 13997–4000.
9. Rapraeger A, Jalkanen M, Endo E, Koda J, Bernfield M. The cell surface proteoglycan from mouse mammary epithelial cells bears chondroitin sulfate and heparan sulfate glycosaminoglycans. *J Biol Chem* 1985; 260: 11046–52.
10. David G, Van den Berghe H. Heparan sulfate-chondroitin sulfate hybrid proteoglycan of the cell surface and basement membrane of mouse mammary epithelial cells. *J Biol Chem* 1985; 260: 11067–74.
11. Bandtlow C, Zimmermann D. Proteoglycans in the developing brain: new conceptual insights for old proteins. *Physiol Rev* 2000; 80: 1267–90.
12. Zimmermann D, Ruoslahti E. Multiple domains of the large fibroblast proteoglycan, versican. *EMBO J* 1989; 8: 2975–81.

- Sulfation patterns of GAG chains have a major influence on the regulation of GAG-protein interactions in the CNS.
- There are ample evidences that suggest the sulfation pattern of HS and CS chains affect the development and maintenance of CNS.
- The presence of remarkable heterogeneity in sulfation patterns of naturally occurring GAG chains is a major impediment in deciphering the role of GAG sulfation patterns in the CNS.
- Recent advances in GAG synthesis and analysis have set the stage for defining and exploiting the sulfation pattern of GAG chains to enhance CNS regeneration.
- We propose various promising therapeutic approaches to tackle CNS disorders, including the use of GAG-degrading enzymes in combination with molecular scaffolds that modulate GAG biosynthetic pathways to facilitate functional regeneration.
- The coming decade is expected to witness novel GAG-based therapeutic approaches for treating several debilitating neurological conditions.

**Acknowledgements:** Research in B.K.'s and V.H.'s laboratories are supported by NIH grants (P01-HL107152, R01-GM075168 and R01-NS057144). V.S. is supported by a Graduate Research Fellowship from the University of Utah, and C.M. is partially supported by a Neuroscience Training Grant.

Received October 9, 2012; accepted February 15, 2013

13. Doege K, Sasaki M, Kimura T, Yamada Y. Complete coding sequence and deduced primary structure of the human cartilage large aggregating proteoglycan, aggrecan. Human-specific repeats, and additional alternatively spliced forms. *J Biol Chem* 1991; 266: 894.
14. Rauch U, Karthikeyan L, Maurel P, Margolis RU, Margolis RK. Cloning and primary structure of neurocan, a developmentally regulated, aggregating chondroitin sulfate proteoglycan of brain. *J Biol Chem* 1992; 267: 19536–47.
15. Yamada H, Watanabe K, Shimonaka M, Yamaguchi Y. Molecular cloning of brevican, a novel brain proteoglycan of the aggrecan/versican family. *J Biol Chem* 1994; 269: 10119–26.
16. Barry FP, Neame PJ, Sasse J, Pearson D. Length variation in the keratan sulfate domain of mammalian aggrecan. *Matrix Biol* 1994; 14: 323–8.
17. Barnea G, Grumet M, Sap J, Margolis R, Schlessinger J. Close similarity between receptor-linked tyrosine phosphatase and rat brain proteoglycan. *Cell* 1994; 76: 205.
18. Bernfield M, Götte M, Park P, Reizes O, Fitzgerald M, Lincecum J, Zako M. Functions of cell surface heparan sulfate proteoglycans. *Annu Rev Biochem* 1999; 68: 729–77.
19. Litwack E, Ivins J, Kumbasar A, Paine-Saunders S, Stipp C, Lander A. Expression of the heparan sulfate proteoglycan glypican-1 in the developing rodent. *Dev Dyn* 1998; 211: 72–87.
20. Watanabe K, Yamada H, Yamaguchi Y. K-glypican: a novel GPI-anchored heparan sulfate proteoglycan that is highly expressed in developing brain and kidney. *J Cell Biol* 1995; 130: 1207–18.
21. Saunders S, Paine-Saunders S, Lander A. Expression of the cell surface proteoglycan glypican-5 is developmentally regulated in kidney, limb, and brain. *Dev Biol* 1997; 190: 78–93.
22. Nakato H, Futch T, Selleck S. The division abnormally delayed (dally) gene: a putative integral membrane proteoglycan required for cell division patterning during postembryonic development of the nervous system in *Drosophila*. *Development* 1995; 121: 3687–702.
23. Pilia G, Hughes-Benzie RM, MacKenzie A, Baybayan P, Chen EY, Huber R, Neri G, Cao A, Forabosco A, Schlessinger D. Mutations in GPC3, a glypican gene, cause the Simpson-Golabi-Behmel overgrowth syndrome. *Nat Genet* 1996; 12: 241–7.
24. Hsueh Y, Sheng M. Regulated expression and subcellular localization of syndecan heparan sulfate proteoglycans and the syndecan-binding protein CASK/LIN-2 during rat brain development. *J Neurosci* 1999; 19: 7415–25.
25. Mizuguchi S, Uyama T, Kitagawa H, Nomura KH, Dejima K, Gengyo-Ando K, Mitani S, Sugahara K, Nomura K. Chondroitin proteoglycans are involved in cell division of *Caenorhabditis elegans*. *Nature* 2003; 423: 443–8.
26. Hwang HY, Olson SK, Esko JD, Horvitz HR. *Caenorhabditis elegans* early embryogenesis and vulval morphogenesis require chondroitin biosynthesis. *Nature* 2003; 423: 439–43.
27. Sirko S, von Holst A, Wizenmann A, Götz M, Faissner A. Chondroitin sulfate glycosaminoglycans control proliferation, radial glia cell differentiation and neurogenesis in neural stem/progenitor cells. *Development* 2007; 134: 2727–38.
28. von Holst A, Sirko S, Faissner A. The unique 473HD-Chondroitin-sulfate epitope is expressed by radial glia and involved in neural precursor cell proliferation. *J Neurosci* 2006; 26: 4082–94.
29. Tham M, Ramasamy S, Gan HT, Ramachandran A, Poonepalli A, Yu YH, Ahmed S. CSPG is a secreted factor that stimulates neural stem cell survival possibly by enhanced EGFR signaling. *PLoS One* 2010; 5: e15341.
30. Ida M, Shuo T, Hirano K, Tokita Y, Nakanishi K, Matsui F, Aono S, Fujita H, Fujiwara Y, Kaji T. Identification and functions of chondroitin sulfate in the milieu of neural stem cells. *J Biol Chem* 2006; 281: 5982–91.
31. Maeda N, Hamanaka H, Oohira A, Noda M. Purification, characterization and developmental expression of a brain-specific chondroitin sulfate proteoglycan, 6B4 proteoglycan/phosphacan. *Neuroscience* 1995; 67: 23–35.
32. Desai CJ, Sun Q, Zinn K. Tyrosine phosphorylation and axon guidance: of mice and flies. *Curr Opin Neurobiol* 1997; 7: 70–4.
33. Kretschmer PJ, Fairhurst JL, Decker MM, Chan CP, Gluzman Y, Bohlen P, Kovsdi I. Cloning, characterization and developmental regulation of two members of a novel human gene family of neurite outgrowth-promoting proteins. *Growth Factors* 1991; 5: 99–114.
34. Maeda N, Nishiwaki T, Shintani T, Hamanaka H, Noda M. 6B4 proteoglycan/phosphacan, an extracellular variant of receptor-like protein-tyrosine phosphatase  $\zeta$ /RPTP $\beta$ , binds pleiotrophin/heparin-binding growth-associated molecule (HB-GAM). *J Biol Chem* 1996; 271: 21446–52.
35. Matsumoto K, Wanaka A, Mori T, Taguchi A, Ishii N, Muramatsu H, Muramatsu T, Tohyama M. Localization of pleiotrophin and midkine in the postnatal developing cerebellum. *Neurosci Lett* 1994; 178: 216–20.
36. Maeda N, Noda M. Involvement of receptor-like protein tyrosine phosphatase  $\zeta$ /RPTP and its ligand pleiotrophin/heparin-binding growth-associated molecule (HB-GAM) in neuronal migration. *J Cell Biol* 1998; 142: 203–16.
37. Landolt RM, Vaughan L, Winterhalter KH, Zimmermann DR. Versican is selectively expressed in embryonic tissues that act as barriers to neural crest cell migration and axon outgrowth. *Development* 1995; 121: 2303–12.
38. Perris R, Perissinotto D, Pettway Z, Bronner-Fraser M, Morgelin M, Kimata K. Inhibitory effects of PG-H/aggrecan and PG-M/versican on avian neural crest cell migration. *FASEB J* 1996; 10: 293–301.
39. Ishii M, Maeda N. Oversulfated chondroitin sulfate plays critical roles in the neuronal migration in the cerebral cortex. *J Biol Chem* 2008; 283: 32610–20.
40. Saunders S, Paine-Saunders S, Lander AD. Expression of the cell surface proteoglycan glypican-5 is developmentally regulated in kidney, limb, and brain. *Dev Biol* 1997; 190: 78–93.
41. Hsueh YP, Sheng M. Regulated expression and subcellular localization of syndecan heparan sulfate proteoglycans and the syndecan-binding protein CASK/LIN-2 during rat brain development. *J Neurosci* 1999; 19: 7415–25.
42. Ivins J, Litwack E, Kumbasar A, Stipp C, Lander A. Cerebroglycan, a developmentally regulated cell-surface heparan sulfate proteoglycan, is expressed on developing axons and growth cones. *Dev Biol* 1997; 184: 320–32.
43. Wang L, Denburg J. A role for proteoglycans in the guidance of a subset of pioneer axons in cultured embryos of the cockroach. *Neuron* 1992; 8: 701–14.
44. Walz A, McFarlane S, Brickman Y, Nurcombe V, Bartlett P, Holt C. Essential role of heparan sulfates in axon navigation and targeting in the developing visual system. *Development* 1997; 124: 2421.
45. Zhou Y, Besner GE. Heparin-binding epidermal growth factor-like growth factor is a potent neurotrophic factor for PC12 cells. *NeuroSignals* 2010; 18: 141–51.

46. Muramatsu T. Midkine, a heparin-binding cytokine with multiple roles in development, repair and diseases. *Proc Jpn Acad Ser B Phys Biol Sci* 2010; 86: 410–25.
47. Liang Y, Annan R, Carr S, Popp S, Mevissen M, Margolis R, Margolis R. Mammalian homologues of the *Drosophila* slit protein are ligands of the heparan sulfate proteoglycan glypican-1 in brain. *J Biol Chem* 1999; 274: 17885–92.
48. Hu H. Cell-surface heparan sulfate is involved in the repulsive guidance activities of Slit2 protein. *Nat Neurosci* 2001; 4: 695–701.
49. Rauvala H, Vanhala A, Nolo R, Raulo E, Meremies J, Panula P. Expression of HB-GAM (heparin-binding growth-associated molecules) in the pathways of developing axonal processes in vivo and neurite outgrowth in vitro induced by HB-GAM. *Dev Brain Res* 1994; 79: 157–76.
50. Kinnunen T, Kaksonen M, Saarinen J, Kalkkinen N, Peng H, Rauvala H. Cortactin-Src kinase signaling pathway is involved in N-syndecan-dependent neurite outgrowth. *J Biol Chem* 1998; 273: 10702–8.
51. Thon N, Haas CA, Rauch U, Merten T, Fässler R, Frotscher M, Deller T. The chondroitin sulphate proteoglycan brevican is upregulated by astrocytes after entorhinal cortex lesions in adult rats. *Eur J Neurosci* 2000; 12: 2547–58.
52. Fawcett J, Asher R. The glial scar and central nervous system repair. *Brain Res Bull* 1999; 49: 377–91.
53. Oohira A, Matsui F, Katoh-Semba R. Inhibitory effects of brain chondroitin sulfate proteoglycans on neurite outgrowth from PC12D cells. *J Neurosci* 1991; 11: 822–7.
54. Mckeon RJ, Höke A, Silver J. Injury-induced proteoglycans inhibit the potential for laminin-mediated axon growth on astrocytic scars. *Exp Neurol* 1995; 136: 32–43.
55. Bicknese A, Sheppard A, O'Leary D, Pearlman A. Thalamic axons extend along a chondroitin sulfate proteoglycan-enriched pathway coincident with the neocortical subplate and distinct from the efferent path. *J Neurosci* 1994; 14: 3500–10.
56. McAdams B, McLoon S. Expression of chondroitin sulfate and keratan sulfate proteoglycans in the path of growing retinal axons in the developing chick. *J Comp Neurol* 1995; 352: 594–606.
57. Sheppard A, Hamilton S, Pearlman A. Changes in the distribution of extracellular matrix components accompany early morphogenetic events of mammalian cortical development. *J Neurosci* 1991; 11: 3928–42.
58. Friedlander D, Milev P, Karthikeyan L, Margolis R, Margolis R, Grumet M. The neuronal chondroitin sulfate proteoglycan neurocan binds to the neural cell adhesion molecules Ng-CAM/L1/NILE and N-CAM, and inhibits neuronal adhesion and neurite outgrowth. *J Cell Biol* 1994; 125: 669–80.
59. Maeda N, Ichihara-Tanaka K, Kimura T, Kadomatsu K, Muramatsu T, Noda M. Receptor-like protein-tyrosine phosphatase PTP $\zeta$ /RPTP $\beta$  binds a heparin-binding growth factor midkine involvement of arginine 78 of midkine in the high affinity binding to PTP $\zeta$ . *J Biol Chem* 1999; 274: 12474–9.
60. Shen Y, Tenney AP, Busch SA, Horn KP, Cuascat FX, Liu K, He Z, Silver J, Flanagan JG. PTP  $\{\sigma\}$  is a receptor for chondroitin sulfate proteoglycan, an inhibitor of neural regeneration. *Sci Signal* 2009; 326: 592.
61. Schachtrup C, Ryu JK, Helmrick MJ, Vagena E, Galanakis DK, Degen JL, Margolis RU, Akassoglou K. Fibrinogen triggers astrocyte scar formation by promoting the availability of active TGF- $\beta$  after vascular damage. *J Neurosci* 2010; 30: 5843–54.
62. Logan A, Berry M, Gonzalez AM, Frautschy SA, Sporn MB, Baird A. Effects of transforming growth factor  $\beta$ 1, on scar production in the injured central nervous system of the rat. *Eur J Neurosci* 2006; 6: 355–63.
63. Rimaniol AC, Lekiéffre D, Serrano A, Masson A, Benavides J, Zavala F. Biphasic transforming growth factor- $\beta$ 1 production flanking the pro-inflammatory cytokine response in cerebral trauma. *Neuroreport* 1995; 7: 133–6.
64. Lagord C, Berry M, Logan A. Expression of TGF $\beta$ 2 but not TGF $\beta$ 1 correlates with the deposition of scar tissue in the lesioned spinal cord. *Mol Cell Neurosci* 2002; 20: 69–92.
65. Fisher D, Xing B, Dill J, Li H, Hoang HH, Zhao Z, Yang XL, Bachoo R, Cannon S, Longo FM, Sheng M, Silver J, Li S. Leukocyte common antigen-related phosphatase is a functional receptor for chondroitin sulfate proteoglycan axon growth inhibitors. *J Neurosci* 2011; 31: 14051–66.
66. Dickendesher TL, Baldwin KT, Mironova YA, Koriyama Y, Raiker SJ, Askew KL, Wood A, Geoffroy CG, Zheng B, Liepmann CD. NgR1 and NgR3 are receptors for chondroitin sulfate proteoglycans. *Nat Neurosci* 2012; 15: 703–12.
67. Koprivica V, Cho KS, Park JB, Yiu G, Atwal J, Gore B, Kim JA, Lin E, Tessier-Lavigne M, Chen DF. EGFR activation mediates inhibition of axon regeneration by myelin and chondroitin sulfate proteoglycans. *Sci STKE* 2005; 310: 106–10.
68. Wong ST, Henley JR, Kanning KC, Huang K, Bothwell M, Poo M. A p75NTR and Nogo receptor complex mediates repulsive signaling by myelin-associated glycoprotein. *Nat Neurosci* 2002; 5: 1302–8.
69. Hsieh SHK, Ferraro GB, Fournier AE. Myelin-associated inhibitors regulate cofilin phosphorylation and neuronal inhibition through LIM kinase and Slingshot phosphatase. *J Neurosci* 2006; 26: 1006–15.
70. Lingor P, Koeberle P, Kügler S, Bähr M. Down-regulation of apoptosis mediators by RNAi inhibits axotomy-induced retinal ganglion cell death in vivo. *Brain* 2005; 128: 550–8.
71. Sivasankaran R, Pei J, Wang KC, Zhang YP, Shields CB, Xu XM, He Z. PKC mediates inhibitory effects of myelin and chondroitin sulfate proteoglycans on axonal regeneration. *Nat Neurosci* 2004; 7: 261–8.
72. Dityatev A, Dityateva G, Sytnyk V, Delling M, Toni N, Nikonenko I, Müller D, Schachner M. Polysialylated neural cell adhesion molecule promotes remodeling and formation of hippocampal synapses. *J Neurosci* 2004; 24: 9372–82.
73. Oyagi A, Moriguchi S, Nitta A, Murata K, Oida Y, Tsuruma K, Shimazawa M, Fukunaga K, Hara H. Heparin-binding EGF-like growth factor is required for synaptic plasticity and memory formation. *Brain Res* 2011; 1419: 97–104.
74. Kalus I, Salmen B, Viebahn C, von Figura K, Schmitz D, D'Hooge R, Dierks T. Differential involvement of the extracellular 6-O-endosulfatases Sulf1 and Sulf2 in brain development and neuronal and behavioural plasticity. *J Cell Mol Med* 2009; 13: 4505–21.
75. Pizzorusso T, Medini P, Berardi N, Chierzi S, Fawcett JW, Maffei L. Reactivation of ocular dominance plasticity in the adult visual cortex. *Science* 2002; 298: 1248–51.
76. Hockfield S, Kalb R, Zaremba S, Fryer H, editors. Expression of neural proteoglycans correlates with the acquisition of mature neuronal properties in the mammalian brain. Cold Spring Harbor Symposia on Quantitative Biology. Cold Spring Harbor, NY: Cold Spring Harbor Laboratory Press, 1990.



77. Galtrey CM, Fawcett JW. The role of chondroitin sulfate proteoglycans in regeneration and plasticity in the central nervous system. *Brain Res Rev* 2007; 54: 1–18.
78. Kwok JCF, Dick G, Wang D, Fawcett JW. Extracellular matrix and perineuronal nets in CNS repair. *Dev Neurobiol* 2011; 71: 1073–89.
79. Aspberg A, Miura R, Bourdoulous S, Shimonaka M, Heinegård D, Schachner M, Ruoslahti E, Yamaguchi Y. The C-type lectin domains of lecticans, a family of aggregating chondroitin sulfate proteoglycans, bind tenascin-R by protein-protein interactions independent of carbohydrate moiety. *Proc Natl Acad Sci USA* 1997; 94: 10116–21.
80. Matthews RT, Kelly GM, Zerillo CA, Gray G, Tiemeyer M, Hockfield S. Aggrecan glycoforms contribute to the molecular heterogeneity of perineuronal nets. *J Neurosci* 2002; 22: 7536–47.
81. Miyata S, Komatsu Y, Yoshimura Y, Taya C, Kitagawa H. Persistent cortical plasticity by upregulation of chondroitin 6-sulfation. *Nat Neurosci* 2012; 15: 414–22.
82. Bliss TVP, Collingridge GL. A synaptic model of memory: long-term potentiation in the hippocampus. *Nature* 1993; 361: 31–9.
83. Bukalo O, Schachner M, Dityatev A. Modification of extracellular matrix by enzymatic removal of chondroitin sulfate and by lack of tenascin-R differentially affects several forms of synaptic plasticity in the hippocampus. *Neuroscience* 2001; 104: 359–69.
84. Moreau-Fauvarque C, Kumanogoh A, Camand E, Jaillard C, Barbin G, Boquet I, Love C, Jones EY, Kikutani H, Lubetzki C. The transmembrane semaphorin Sema4D/CD100, an inhibitor of axonal growth, is expressed on oligodendrocytes and upregulated after CNS lesion. *J Neurosci* 2003; 23: 9229–39.
85. Bradbury E, Moon L, Popat R, King V, Bennett G, Patel P, Fawcett J, McMahon S. Chondroitinase ABC promotes functional recovery after spinal cord injury. *Nature* 2002; 416: 636–40.
86. Silver J, Miller JH. Regeneration beyond the glial scar. *Nat Rev Neurosci* 2004; 5: 146–56.
87. McKeon RJ, Juryneć MJ, Buck CR. The chondroitin sulfate proteoglycans neurocan and phosphacan are expressed by reactive astrocytes in the chronic CNS glial scar. *J Neurosci* 1999; 19: 10778–88.
88. Jaworski DM, Kelly GM, Hockfield S. Intracranial injury acutely induces the expression of the secreted isoform of the CNS-specific hyaluronan-binding protein BEHAB/brevican. *Exp Neurol* 1999; 157: 327–37.
89. Bradbury EJ, Moon LDF, Popat RJ, King VR, Bennett GS, Patel PN, Fawcett JW, McMahon SB. Chondroitinase ABC promotes functional recovery after spinal cord injury. *Nature* 2002; 416: 636–40.
90. Lee H, McKeon RJ, Bellamkonda RV. Sustained delivery of thermostabilized chABC enhances axonal sprouting and functional recovery after spinal cord injury. *Proc Natl Acad Sci USA* 2010; 107: 3340–5.
91. Yick L, Wu W, So K, Yip H, Shum D. Chondroitinase ABC promotes axonal regeneration of Clarke's neurons after spinal cord injury. *Neuroreport* 2000; 11: 1063–7.
92. Nishimura K, Ishii M, Kuraoka M, Kamimura K, Maeda N. Opposing functions of chondroitin sulfate and heparan sulfate during early neuronal polarization. *Neuroscience* 2010; 169: 1535–47.
93. van Horsen J, Wesseling P, van den Heuvel LPWJ, de Waal RMW, Verbeek MM. Heparan sulphate proteoglycans in Alzheimer's disease and amyloid-related disorders. *Lancet Neurol* 2003; 2: 482–92.
94. Kanekiyo T, Zhang J, Liu Q, Liu C-C, Zhang L, Bu G. Heparan sulphate proteoglycan and the low-density lipoprotein receptor-related protein 1 constitute major pathways for neuronal amyloid- $\beta$  uptake. *J Neurosci* 2011; 31: 1644–51.
95. Ariga T, Miyatake T, Yu RK. Role of proteoglycans and glycosaminoglycans in the pathogenesis of Alzheimer's disease and related disorders: amyloidogenesis and therapeutic strategies – a review. *J Neurosci Res* 2010; 88: 2303–15.
96. Hosono-Fukao T, Ohtake-Niimi S, Hoshino H, Britschgi M, Akatsu H, Hossain MM, Nishitsuji K, van Kuppevelt TH, Kimata K, Michikawa M. Heparan sulfate subdomains that are degraded by Sulf accumulate in cerebral amyloid  $\beta$  plaques of Alzheimer's disease: evidence from mouse models and patients. *Am J Pathol* 2012; 180: 2056–67.
97. Scholefield Z, Yates EA, Wayne G, Amour A, McDowell W, Turnbull J. Heparan sulfate regulates precursor protein processing by BACE1 the Alzheimer's B-secretase. *J Cell Biol* 2003; 163: 97–107.
98. Fraser PE, Nguyen JT, Chin DT, Kirschner DA. Effects of sulfate ions on Alzheimer  $\beta$ /A4 peptide assemblies: implications for amyloid fibril-proteoglycan interactions. *J Neurochem* 1992; 59: 1531–40.
99. Hasegawa M, Crowther RA, Jakes R, Goedert M. Alzheimer-like changes in microtubule-associated protein  $\tau$  induced by sulfated glycosaminoglycans. Inhibition of microtubule binding, stimulation of phosphorylation, and filament assembly depend on the degree of sulfation. *J Biol Chem* 1997; 272: 33118–24.
100. Viapiano MS, Matthews RT, Hockfield S. A novel membrane-associated glycovariant of BEHAB/brevican is up-regulated during rat brain development and in a rat model of invasive glioma. *J Biol Chem* 2003; 278: 33239–47.
101. Nutt CL, Matthews RT, Hockfield S. Glial tumor invasion: a role for the upregulation and cleavage of BEHAB/brevican. *Neuroscientist* 2001; 7: 113–22.
102. Viapiano MS, Bi WL, Piepmeier J, Hockfield S, Matthews RT. Novel tumor-specific isoforms of BEHAB/brevican identified in human malignant gliomas. *Cancer Res* 2005; 65: 6726–33.
103. Viapiano MS, Hockfield S, Matthews RT. BEHAB/brevican requires ADAMTS-mediated proteolytic cleavage to promote glioma invasion. *J Neurooncol* 2008; 88: 261–72.
104. Varga I, Hutóczki G, Szemcsák CD, Zahuczky G, Tóth J, Adamecz Z, Kenyeres A, Bognár L, Hanzély Z, Klekner A. Brevican, neurocan, tenascin-c and versican are mainly responsible for the invasiveness of low-grade astrocytoma. *Pathol Oncol Res* 2012; 18: 413–320.
105. Hu B, Kong LL, Matthews RT, Viapiano MS. The proteoglycan brevican binds to fibronectin after proteolytic cleavage and promotes glioma cell motility. *J Biol Chem* 2008; 283: 24848–59.
106. Su G, Meyer K, Nandini CD, Qiao D, Salamat S, Friedl A. Glypican-1 is frequently overexpressed in human gliomas and enhances FGF-2 signaling in glioma cells. *Am J Pathol* 2006; 168: 2014–26.
107. Mendes de Aguiar CBN, Garcez RC, Alvarez-Silva M, Trentin AG. Undersulfation of proteoglycan and proteins alter C6 glioma cells proliferation, adhesion and extracellular matrix organization. *Int J Dev Neurosci* 2002; 20: 563–71.

108. Lobao-Soares B, Alvarez-Silva M, Mendes de Aguiar CBN, Nicolau M, Trentin AG. Undersulfation of glycosaminoglycans induced by sodium chlorate treatment affects the progression of C6 rat glioma, in vivo. *Brain Res* 2007; 1131: 29–36.
109. Phillips JJ, Huillard E, Robinson AE, Ward A, Lum DH, Polley MY, Rosen SD, Rowitch DH, Werb Z. SULF2 regulates PDGFR $\alpha$  signaling and growth in human and mouse malignant glioma. *J Clin Invest* 2012; 122: 911–22.
110. Meyza KZ, Blanchard DC, Pearson BL, Pobbe RLH, Blanchard RJ. Fractone-associated N-sulfated heparan sulfate shows reduced quantity in BTBR T+tf/J mice: a strong model of autism. *Behav Brain Res* 2012; 228: 247–53.
111. Blanchard DC, Defensor EB, Meyza KZ, Pobbe RL, Pearson BL, Bolivar VJ, Blanchard RJ. BTBR T+tf/J mice: autism-relevant behaviors and reduced fractone-associated heparan sulfate. *Neurosci Biobehav Rev* 2012; 36: 285–96.
112. Mercier F, Kwon YC, Douet V. Hippocampus/amygdala alterations, loss of heparan sulfates, fractones and ventricle wall reduction in adult BTBR T+tf/J mice, animal model for autism. *Neurosci Lett* 2012; 506: 208–13.
113. Irie F, Badie-Mahdavi H, Yamaguchi Y. Autism-like socio-communicative deficits and stereotypies in mice lacking heparan sulfate. *Proc Natl Acad Sci USA* 2012; 109: 5052–6.
114. Pearson B, Corley M, Vasconcellos A, Blanchard D, Blanchard R. Heparan sulfate deficiency in autistic postmortem brain tissue from the subventricular zone of the lateral ventricles. *Behav Brain Res* 2013; 243: 138–45.
115. Heck N, Garwood J, Loeffler JP, Larmet Y, Faissner A. Differential upregulation of extracellular matrix molecules associated with the appearance of granule cell dispersion and mossy fiber sprouting during epileptogenesis in a murine model of temporal lobe epilepsy. *Neuroscience* 2004; 129: 309–24.
116. McRae PA, Baranov E, Rogers SL, Porter BE. Persistent decrease in multiple components of the perineuronal net following status epilepticus. *Eur J Neurosci* 2012; 36: 3471–82.
117. Liu IH, Uversky VN, Munishkina LA, Fink AL, Halfter W, Cole GJ. Agrin binds  $\alpha$ -synuclein and modulates  $\alpha$ -synuclein fibrillation. *Glycobiology* 2005; 15: 1320–31.
118. Kitamura Y, Iden M, Minamino H, Abe M, Takata K, Taniguchi T. The 6-hydroxydopamine-induced nigrostriatal neurodegeneration produces microglia-like NG2 glial cells in the rat substantia nigra. *Glia* 2010; 58: 1686–700.
119. Choudhury ME, Sugimoto K, Kubo M, Nagai M, Nomoto M, Takahashi H, Yano H, Tanaka J. A cytokine mixture of GM-CSF and IL-3 that induces a neuroprotective phenotype of microglia leading to amelioration of (6-OHDA)-induced Parkinsonism of rats. *Brain Behav* 2011; 1: 26–43.
120. Pantazopoulos H, Woo TU, Lim MP, Lange N, Berretta S. Extracellular matrix-glia abnormalities in the amygdala and entorhinal cortex of subjects diagnosed with schizophrenia. *Arch Gen Psychiatry* 2010; 67: 155–66.
121. Pantazopoulos H, Lange N, Baldessarini RJ, Berretta S. Parvalbumin neurons in the entorhinal cortex of subjects diagnosed with bipolar disorder or schizophrenia. *Biol Psychiatry* 2007; 61: 640–52.
122. Gogolla N, Caroni P, Lüthi A, Herry C. Perineuronal nets protect fear memories from erasure. *Science* 2009; 325: 1258–61.
123. Holt DJ, Lebron-Milad K, Milad MR, Rauch SL, Pitman RK, Orr SP, Cassidy BS, Walsh JP, Goff DC. Extinction memory is impaired in schizophrenia. *Biol Psychiatry* 2009; 65: 455–63.
124. Belichenko PV, Miklossy J, Belser B, Budka H, Celio MR. Early destruction of the extracellular matrix around parvalbumin-immunoreactive interneurons in Creutzfeldt-Jakob disease. *Neurobiol Dis* 1999; 6: 269–79.
125. Caughey B, Brown K, Raymond G, Katzenstein G, Thresher W. Binding of the protease-sensitive form of PrP (prion protein) to sulfated glycosaminoglycan and congo red [corrected]. *J Virol* 1994; 68: 2135–41.
126. Brückner G, Hausen D, Härtig W, Drlicek M, Arendt T, Brauer K. Cortical areas abundant in extracellular matrix chondroitin sulphate proteoglycans are less affected by cytoskeletal changes in Alzheimer's disease. *Neuroscience* 1999; 92: 791–805.
127. Morawski M, Brückner G, Jäger C, Seeger G, Arendt T. Neurons associated with aggrecan-based perineuronal nets are protected against  $\tau$  pathology in subcortical regions in Alzheimer's disease. *Neuroscience* 2010; 169: 1347–63.
128. Mattson MP. Degenerative and protective signaling mechanisms in the neurofibrillary pathology of AD. *Neurobiol Aging* 1995; 16: 447–57.
129. Sato Y, Nakanishi K, Tokita Y, Kakizawa H, Ida M, Maeda H, Matsui F, Aono S, Saito A, Kuroda Y. A highly sulfated chondroitin sulfate preparation, CS-E, prevents excitatory amino acid-induced neuronal cell death. *J Neurochem* 2008; 104: 1565–76.
130. Brückner G, Morawski M, Arendt T. Aggrecan-based extracellular matrix is an integral part of the human basal ganglia circuit. *Neuroscience* 2008; 151: 489–504.
131. Morawski M, Brückner MK, Riederer P, Brückner G, Arendt T. Perineuronal nets potentially protect against oxidative stress. *Exp Neurol* 2004; 188: 309–15.
132. Goedert M, Jakes R, Spillantini M, Hasegawa M, Smith M, Crowther R. Assembly of microtubule-associated protein  $\tau$  into Alzheimer-like filaments induced by sulphated glycosaminoglycans. *Nature* 1996; 383: 550–3.
133. Pérez M, Valpuesta JM, Medina M, Montejó de Garcini E, Avila J. Polymerization of  $\tau$  into filaments in the presence of heparin: the minimal sequence required for  $\tau$ - $\tau$  interaction. *J Neurochem* 1996; 67: 1183–90.
134. Gama C, Hsieh-Wilson L. Chemical approaches to deciphering the glycosaminoglycan code. *Curr Opin Chem Biol* 2005; 9: 609–19.
135. Lin X, Buff EM, Perrimon N, Michelson AM. Heparan sulfate proteoglycans are essential for FGF receptor signaling during Drosophila embryonic development. *Development* 1999; 126: 3715–23.
136. Shuo T, Aono S, Matsui F, Tokita Y, Maeda H, Shimada K, Oohira A. Developmental changes in the biochemical and immunological characters of the carbohydrate moiety of neuroglycan C, a brain-specific chondroitin sulfate proteoglycan. *Glycoconj J* 2003; 20: 267–78.
137. Brickman Y, Ford M, Gallagher J, Nurcombe V, Bartlett P, Turnbull J. Structural modification of fibroblast growth factor-binding heparan sulfate at a determinative stage of neural development. *J Biol Chem* 1998; 273: 4350–9.
138. Kitagawa H, Tsutsumi K, Tone Y, Sugahara K. Developmental regulation of the sulfation profile of chondroitin sulfate chains in the chicken embryo brain. *J Biol Chem* 1997; 272: 31377–81.
139. Yabe T, Hata T, He J, Maeda N. Developmental and regional expression of heparan sulfate sulfotransferase genes in the mouse brain. *Glycobiology* 2005; 15: 982–93.

140. Lawrence R, Yabe T, HajMohammadi S, Rhodes J, McNeely M, Liu J, Lamperti ED, Toselli PA, Lech M, Spear PG. The principal neuronal gD-type 3-O-sulfotransferases and their products in central and peripheral nervous system tissues. *Matrix Biol* 2007; 26: 442–55.
141. Cadwallader AB, Yost HJ. Combinatorial expression patterns of heparan sulfate sulfotransferases in zebrafish: I. The 3-O-sulfotransferase family. *Dev Dyn* 2006; 235: 3423–31.
142. Cadwallader AB, Yost HJ. Combinatorial expression patterns of heparan sulfate sulfotransferases in zebrafish: II. The 6-O-sulfotransferase family. *Dev Dyn* 2006; 235: 3432–7.
143. Kuberan B, Lech M, Borjigin J, Rosenberg RD. Light-induced 3-O-sulfotransferase expression alters pineal heparan sulfate fine structure. *J Biol Chem* 2004; 279: 5053–4.
144. Habuchi H, Suzuki S, Saito T, Tamura T, Harada T, Yoshida K, Kimata K. Structure of a heparan sulphate oligosaccharide that binds to basic fibroblast growth factor. *Biochem J* 1992; 285: 805–13.
145. Guillemot F, Zimmer C. From cradle to grave: the multiple roles of fibroblast growth factors in neural development. *Neuron* 2011; 71: 574–88.
146. Coles CH, Shen Y, Tenney AP, Siebold C, Sutton GC, Lu W, Gallagher JT, Jones EY, Flanagan JG, Aricescu AR. Proteoglycan-specific molecular switch for RTPP  $\alpha$  clustering and neuronal extension. *Sci STKE* 2011; 332: 484–8.
147. Aricescu AR, McKinnell IW, Halfter W, Stoker AW. Heparan sulfate proteoglycans are ligands for receptor protein tyrosine phosphatase  $\alpha$ . *Mol Cell Biol* 2002; 22: 1881–92.
148. Tully S, Mabon R, Gama C, Tsai S, Liu X, Hsieh-Wilson L. A chondroitin sulfate small molecule that stimulates neuronal growth. *J Am Chem Soc* 2004; 126: 7736–7.
149. Kawashima H, Atarashi K, Hirose M, Hirose J, Yamada S, Sugahara K, Miyasaka M. Oversulfated chondroitin/dermatan sulfates containing GlcA $\beta$ 1/IdoA $\alpha$ 1-3GalNAc (4, 6-O-disulfate) interact with L- and P-selectin and chemokines. *J Biol Chem* 2002; 277: 12921–30.
150. Deepa S, Umehara Y, Higashiyama S, Itoh N, Sugahara K. Specific molecular interactions of oversulfated chondroitin sulfate E with various heparin-binding growth factors. *J Biol Chem* 2002; 277: 43707–16.
151. Gama CI, Tully SE, Sotogaku N, Clark PM, Rawat M, Vaidehi N, Goddard WA, Nishi A, Hsieh-Wilson LC. Sulfation patterns of glycosaminoglycans encode molecular recognition and activity. *Nat Chem Biol* 2006; 2: 467–73.
152. Tsuchida K, Shioi J, Yamada S, Boghosian G, Wu A, Cai H, Sugahara K, Robakis NK. Appican, the proteoglycan form of the amyloid precursor protein, contains chondroitin sulfate E in the repeating disaccharide region and 4-O-sulfated galactose in the linkage region. *J Biol Chem* 2001; 276: 37155–60.
153. Deepa SS, Yamada S, Zako M, Goldberger O, Sugahara K. Chondroitin sulfate chains on syndecan-1 and syndecan-4 from normal murine mammary gland epithelial cells are structurally and functionally distinct and cooperate with heparan sulfate chains to bind growth factors. *J Biol Chem* 2004; 279: 37368–76.
154. Ueoka C, Kaneda N, Okazaki I, Nadanaka S, Muramatsu T, Sugahara K. Neuronal cell adhesion, mediated by the heparin-binding neuroregulatory factor midkine, is specifically inhibited by chondroitin sulfate E. *J Biol Chem* 2000; 275: 37407–13.
155. Tanaka M, Maeda N, Noda M, Marunouchi T. A chondroitin sulfate proteoglycan PTPC $\zeta$ /RPTP $\beta$  regulates the morphogenesis of Purkinje cell dendrites in the developing cerebellum. *J Neurosci* 2003; 23: 2804–14.
156. Rogers CJ, Clark PM, Tully SE, Abrol R, Garcia KC, Goddard WA, Hsieh-Wilson LC. Elucidating glycosaminoglycan-protein interactions using carbohydrate microarray and computational approaches. *Proc Natl Acad Sci USA* 2011; 108: 9747–52.
157. Huang EJ, Reichardt LF. Neurotrophins: roles in neuronal development and function. *Annu Rev Neurosci* 2001; 24: 677–736.
158. Kaplan DR, Miller FD. Neurotrophin signal transduction in the nervous system. *Curr Opin Neurobiol* 2000; 10: 381–91.
159. Oakley RA, Tosney KW. Peanut agglutinin and chondroitin-6-sulfate are molecular markers for tissues that act as barriers to axon advance in the avian embryo. *Dev Biol* 1991; 147: 187–206.
160. Properzi F, Carulli D, Asher RA, Muir E, Camargo LM, Van Kuppevelt TH, Ten Dam GB, Furukawa Y, Mikami T, Sugahara K, Toida T, Geller HM, Fawcett JW. Chondroitin 6-sulfate synthesis is up-regulated in injured CNS, induced by injury-related cytokines and enhanced in axon growth-inhibitory glia. *Eur J Neurosci* 2005; 21: 378–90.
161. Karumbaiah L, Anand S, Thazhath R, Zhong Y, Mckeon RJ, Bellamkonda RV. Targeted downregulation of N-acetylgalactosamine 4-sulfate 6-O-sulfotransferase significantly mitigates chondroitin sulfate proteoglycan mediated inhibition. *Glia* 2011; 59: 981–96.
162. Gilbert RJ, McKeon RJ, Darr A, Calabro A, Hascall VC, Bellamkonda RV. CS-4, 6 is differentially upregulated in glial scar and is a potent inhibitor of neurite extension. *Mol Cell Neurosci* 2005; 29: 545–58.
163. Wang H, Katagiri Y, McCann TE, Unsworth E, Goldsmith P, Yu ZX, Tan F, Santiago L, Mills EM, Wang Y. Chondroitin-4-sulfation negatively regulates axonal guidance and growth. *J Cell Sci* 2008; 121: 3083–91.
164. Castillo GM, Cummings JA, Yang W, Judge ME, Sheardown MJ, Rimmvall K, Hansen JB, Snow AD. Sulfate content and specific glycosaminoglycan backbone of perlecan are critical for perlecan's enhancement of islet amyloid polypeptide (amylin) fibril formation. *Diabetes* 1998; 47: 612–20.
165. Castillo GM, Lukito W, Wight TN, Snow AD. The sulfate moieties of glycosaminoglycans are critical for the enhancement of  $\beta$ -amyloid protein fibril formation. *J Neurochem* 1999; 72: 1681–7.
166. Brown JM, Xia J, Zhuang BQ, Cho KS, Rogers CJ, Gama CI, Rawat M, Tully SE, Uetani N, Mason DE, Tremblay ML, Peters EC, Habuchi O, Chen DF, Hsieh-Wilson LC. A sulfated carbohydrate epitope inhibits axon regeneration after injury. *Proc Natl Acad Sci USA* 2012; 109: 4768–73.
167. Lin R, Rosahl TW, Whiting PJ, Fawcett JW, Kwok JCF. 6-Sulphated chondroitins have a positive influence on axonal regeneration. *PLoS One* 2011; 6: e21499.
168. Shum DKY, Chau CH. Changes in glycosaminoglycans during regeneration of post crush sciatic nerves of adult guinea pigs. *J Neurosci Res* 1996; 46: 465–76.
169. Lu P, Yang H, Jones LL, Filbin MT, Tuszynski MH. Combinatorial therapy with neurotrophins and cAMP promotes axonal regeneration beyond sites of spinal cord injury. *J Neurosci* 2004; 24: 6402–9.

170. Teng YD, Lavik EB, Qu X, Park KI, Ourednik J, Zurakowski D, Langer R, Snyder EY. Functional recovery following traumatic spinal cord injury mediated by a unique polymer scaffold seeded with neural stem cells. *Proc Natl Acad Sci USA* 2002; 99: 3024–9.
171. Massey JM, Amps J, Viapiano MS, Matthews RT, Wagoner MR, Whitaker CM, Alilain W, Yonkof AL, Khalyfa A, Cooper NGF. Increased chondroitin sulfate proteoglycan expression in denervated brainstem targets following spinal cord injury creates a barrier to axonal regeneration overcome by chondroitinase ABC and neurotrophin-3. *Exp Neurol* 2008; 209: 426–45.
172. Fouad K, Schnell L, Bunge MB, Schwab ME, Liebscher T, Pearse DD. Combining Schwann cell bridges and olfactory-ensheathing glia grafts with chondroitinase promotes locomotor recovery after complete transection of the spinal cord. *J Neurosci* 2005; 25: 1169–78.
173. Houle JD, Tom VJ, Mayes D, Wagoner G, Phillips N, Silver J. Combining an autologous peripheral nervous system “bridge” and matrix modification by chondroitinase allows robust, functional regeneration beyond a hemisection lesion of the adult rat spinal cord. *J Neurosci* 2006; 26: 7405–15.
174. Karimi-Abdolrezaee S, Eftekharpour E, Wang J, Schut D, Fehlings MG. Synergistic effects of transplanted adult neural stem/progenitor cells, chondroitinase, and growth factors promote functional repair and plasticity of the chronically injured spinal cord. *J Neurosci* 2010; 30: 1657–76.
175. Tester NJ, Plaas AH, Howland DR. Effect of body temperature on chondroitinase ABC's ability to cleave chondroitin sulfate glycosaminoglycans. *J Neurosci Res* 2007; 85: 1110–8.
176. Victor XV, Nguyen TKN, Ethirajan M, Tran VM, Nguyen KV, Kuberan B. Investigating the elusive mechanism of glycosaminoglycan biosynthesis. *J Biol Chem* 2009; 284: 25842–53.
177. Smith-Thomas LC, Stevens J, Fok-Seang J, Faissner A, Rogers JH, Fawcett JW. Increased axon regeneration in astrocytes grown in the presence of proteoglycan synthesis inhibitors. *J Cell Sci* 1995; 108: 1307–15.
178. Garud D, Tran V, Victor X, Koketsu M, Kuberan B. Inhibition of heparan sulfate and chondroitin sulfate proteoglycan biosynthesis. *J Biol Chem* 2008; 283: 28881–7.
179. Raman K, Ninomiya M, Nguyen TKN, Tsuzuki Y, Koketsu M, Kuberan B. Novel glycosaminoglycan biosynthetic inhibitors affect tumor-associated angiogenesis. *Biochem Biophys Res Commun* 2011; 404: 86–9.
180. Kisilevsky R, Szarek WA. Novel glycosaminoglycan precursors as anti-amyloid agents part II. *J Mol Neurosci* 2002; 19: 45–50.
181. Rose M, Dudas B, Cornelli U, Hanin I. Protective effect of the heparin-derived oligosaccharide C3, on AF64A-induced cholinergic lesion in rats. *Neurobiol Aging* 2003; 24: 481–90.
182. Rose M, Dudas B, Cornelli U, Hanin I. Glycosaminoglycan C3 protects against AF64A-induced cholinotoxicity in a dose-dependent and time-dependent manner. *Brain Res* 2004; 1015: 96–102.
183. Kisilevsky R, Szarek WA, Ancsin JB, Elimova E, Marone S, Bhat S, Berkin A. Inhibition of amyloid A amyloidogenesis in vivo and in tissue culture by 4-deoxy analogues of peracetylated 2-acetamido-2-deoxy- $\alpha$ - and  $\beta$ -D-glucose: implications for the treatment of various amyloidoses. *Am J Pathol* 2004; 164: 2127–37.
184. Okada S, Nakamura M, Katoh H, Miyao T, Shimazaki T, Ishii K, Yamane J, Yoshimura A, Iwamoto Y, Toyama Y. Conditional ablation of Stat3 or Socs3 discloses a dual role for reactive astrocytes after spinal cord injury. *Nat Med* 2006; 12: 829–34.
185. Lowry N, Goderie SK, Lederman P, Charniga C, Gooch MR, Gracey KD, Banerjee A, Punyani S, Silver J, Kane RS. The effect of long-term release of Shh from implanted biodegradable microspheres on recovery from spinal cord injury in mice. *Biomaterials* 2012; 33: 2892–901.
186. Parr A, Kulbatski I, Zahir T, Wang X, Yue C, Keating A, Tator C. Transplanted adult spinal cord-derived neural stem/progenitor cells promote early functional recovery after rat spinal cord injury. *Neuroscience* 2008; 155: 760–70.
187. Hou S, Xu Q, Tian W, Cui F, Cai Q, Ma J, Lee IS. The repair of brain lesion by implantation of hyaluronic acid hydrogels modified with laminin. *J Neurosci Methods* 2005; 148: 60–70.
188. Freudenberg U, Hermann A, Welzel PB, Stirl K, Schwarz SC, Grimmer M, Zieris A, Panyanuwat W, Zschoche S, Meinhold D. A star-PEG-heparin hydrogel platform to aid cell replacement therapies for neurodegenerative diseases. *Biomaterials* 2009; 30: 5049–60.
189. Funderburgh JL. Mini Review. Keratan sulfate: structure, biosynthesis, and function. *Glycobiology* 2000; 10: 951–8.
190. Lindahl B, Eriksson L, Spillmann D, Catterson B, Lindahl U. Selective loss of cerebral keratan sulfate in Alzheimer's disease. *J Biol Chem* 1996; 271: 16991–4.
191. Quantock AJ, Young RD, Akama TO. Structural and biochemical aspects of keratan sulphate in the cornea. *Cell Mol Life Sci* 2010; 67: 891–906.
192. Zhang H, Uchimura K, Kadomatsu K. Brain keratan sulfate and glial scar formation. *Ann NY Acad Sci* 2006; 1086: 81–90.
193. Hlady V, Hodgkinson G. The effects of proteoglycan surface patterning on neuronal pathfinding. *Materwiss Werksttech* 2007; 38: 975–82.
194. Hodgkinson GN, Tresco PA, Hlady V. The role of well-defined patterned substrata on the regeneration of DRG neuron pathfinding and integrin expression dynamics using chondroitin sulfate proteoglycans. *Biomaterials* 2012; 33: 4288–97.
195. Lindahl U, Li J, Kusche-Gullberg M, Salmivirta M, Alaranta S, Veromaa T, Emeis J, Roberts I, Taylor C, Oreste P. Generation of “neoheparin” from E. coli K5 capsular polysaccharide. *J Med Chem* 2005; 48: 349–52.
196. Kuberan B, Beeler DL, Lech M, Wu ZL, Rosenberg RD. Chemoenzymatic synthesis of classical and non-classical anticoagulant heparan sulfate polysaccharides. *J Biol Chem* 2003; 278: 52613–21.
197. Liu R, Xu Y, Chen M, Welwer M, Zhou X, Bridges AS, DeAngelis PL, Zhang Q, Linhardt RJ, Liu J. Chemoenzymatic design of heparan sulfate oligosaccharides. *J Biol Chem* 2010; 285: 34240–9.
198. Maeda N, Ishii M, Nishimura K, Kamimura K. Functions of chondroitin sulfate and heparan sulfate in the developing brain. *Neurochem Res* 2011; 36: 1228–40.
199. Lanner F, Lee KL, Sohl M, Holmborn K, Yang H, Wilbertz J, Poellinger L, Rossant J, Farnebo F. Heparan sulfation-dependent fibroblast growth factor signaling maintains embryonic stem cells primed for differentiation in a heterogeneous state. *Stem Cells* 2009; 28: 191–200.

200. Morimoto-Tomita M, Uchimura K, Werb Z, Hemmerich S, Rosen S. Cloning and characterization of two extracellular heparin-degrading endosulfatases in mice and humans. *J Biol Chem* 2002; 277: 49175–85.
201. Dhoot GK, Gustafsson MK, Ai X, Sun W, Standiford DM, Emerson Jr CP. Regulation of Wnt signaling and embryo patterning by an extracellular sulfatase. *Sci STKE* 2001; 293: 1663–6.
202. Ai X, Do AT, Lozynska O, Kusche-Gullberg M, Lindahl U, Emerson Jr CP. QSulf1 remodels the 6-O sulfation states of cell surface heparan sulfate proteoglycans to promote Wnt signaling. *J Cell Biol* 2003; 162: 341–51.
203. Rhiner C, Gysi S, Fröhli E, Hengartner MO, Hajnal A. Syndecan regulates cell migration and axon guidance in *C. elegans*. *Development* 2005; 132: 4621–33.
204. Kitagawa H, Fujita M, Ito N, Sugahara K. Molecular cloning and expression of a novel chondroitin 6-O-sulfotransferase. *J Biol Chem* 2000; 275: 21075–80.
205. Yamauchi S, Kurosu A, Hitosugi M, Nagai T, Oohira A, Tokudome S. Differential gene expression of multiple chondroitin sulfate modification enzymes among neural stem cells, neurons and astrocytes. *Neurosci Lett* 2011; 493: 107–11.
206. Kobayashi M, Sugumaran G, Liu J, Shworak N, Silbert J, Rosenberg R. Molecular cloning and characterization of a human uronyl 2-sulfotransferase that sulfates iduronyl and glucuronyl residues in dermatan/chondroitin sulfate. *J Biol Chem* 1999; 274: 10474–80.
207. Fukuta M, Uchimura K, Nakashima K, Kato M, Kimata K, Shinomura T, Habuchi O. Molecular cloning and expression of chick chondrocyte chondroitin 6-sulfotransferase. *J Biol Chem* 1995; 270: 18575.
208. Pacheco B, Malmström A, MacCaran M. Two dermatan sulfate epimerases form iduronic acid domains in dermatan sulfate. *J Biol Chem* 2009; 284: 9788.
209. Dündar M, Müller T, Zhang Q, Pan J, Steinmann B, Vodopietz J, Gruber R, Sonoda T, Krabichler B, Utermann G. Loss of dermatan-4-sulfotransferase 1 function results in aducted thumb-clubfoot syndrome. *Am J Hum Genet* 2009; 85: 873–82.
210. Bian S, Akyüz N, Bernreuther C, Loers G, Laczynska E, Jakovcevski I, Schachner M. Dermatan sulfotransferase Chst14/D4st1, but not chondroitin sulfotransferase Chst11/C4st1, regulates proliferation and neurogenesis of neural progenitor cells. *J Cell Sci* 2011; 124: 4051–63.
211. Mühleisen TW, Mattheisen M, Strohmaier J, Degenhardt F, Priebe L, Schultz CC, Breuer R, Meier S, Hoffmann P, Rivandeneira F. Association between schizophrenia and common variation in neurocan (NCAN), a genetic risk factor for bipolar disorder. *Schizophr Res* 2012; 138: 69–73.
212. Gill JL, Tsai KL, Krey C, Noorai RE, Vanbellighen JF, Garosi LS, Shelton GD, Clark LA, Harvey RJ. A canine BCAN microdeletion associated with episodic falling syndrome. *Neurobiol Dis* 2012; 45: 130–6.
213. Dudas B, Cornelli U, Lee J, Hejna M, Walzer M, Lorenz S, Mervis R, Fareed J, Hanin I. Oral and subcutaneous administration of the glycosaminoglycan C3 attenuates A $\beta$  (25–35)-induced abnormal  $\tau$  protein immunoreactivity in rat brain. *Neurobiol Aging* 2002; 23: 97–104.
214. Dudas B, Lemes A, Cornelli U, Hanin I. Prospective role of glycosaminoglycans in apoptosis associated with neurodegenerative disorders. *Adv Alzheimers Parkinsons Dis* 2008; 57: 247–54.
215. Snow AD, Sekiguchi R, Nochlin D, Fraser P, Kimata K, Mizutani A, Arai M, Schreier WA, Morgan DG. An important role of heparan sulfate proteoglycan (perlecan) in a model system for the deposition and persistence of fibrillar A $\beta$ -amyloid in rat brain. *Neuron* 1994; 12: 219–34.
216. Snow A, Mar H, Nochlin D, Sekiguchi R, Kimata K, Koike Y, Wight T. Early accumulation of heparan sulfate in neurons and in the  $\beta$ -amyloid protein-containing lesions of Alzheimer's disease and Down's syndrome. *Am J Pathol* 1990; 137: 1253–70.
217. Snow A, Mar H, Nochlin D, Kresse H, Wight T. Peripheral distribution of dermatan sulfate proteoglycans (decorin) in amyloid-containing plaques and their presence in neurofibrillary tangles of Alzheimer's disease. *J Histochem Cytochem* 1992; 40: 105–13.
218. Dewitt DA, Richey P, Praprotnik D, Silver J, Perry G. Chondroitin sulfate proteoglycans are a common component of neuronal inclusions and astrocytic reaction in neurodegenerative diseases. *Brain Res* 1994; 656: 205–9.
219. Shioi J, Pangalos MN, Ripellino JA, Vassilacopoulou D, Mytilineou C, Margolis RU, Robakis NK. The Alzheimer amyloid precursor proteoglycan (appican) is present in brain and is produced by astrocytes but not by neurons in primary neural cultures. *J Biol Chem* 1995; 270: 11839–44.
220. Griffith LS, Schmitz B. O-linked N-acetylglucosamine is upregulated in Alzheimer brains. *Biochem Biophys Res Commun* 1995; 213: 424–31.
221. Arrasate M, Perez M, Valpuesta JM, Avila J. Role of glycosaminoglycans in determining the helicity of paired helical filaments. *Am J Pathol* 1997; 151: 1115.
222. Argyris EG, Acheampong E, Nunnari G, Mukhtar M, Williams KJ, Pomerantz RJ. Human immunodeficiency virus type 1 enters primary human brain microvascular endothelial cells by a mechanism involving cell surface proteoglycans independent of lipid rafts. *J Virol* 2003; 77: 12140–51.
223. Belichenko PV, Miklossy J, Celio MR. HIV-1 induced destruction of neocortical extracellular matrix components in AIDS victims. *Neurobiol Dis* 1997; 4: 301–10.
224. Okamoto M, Sakiyama J, Mori S, Kurazono S, Usui S, Hasegawa M, Oohira A. Kainic acid-induced convulsions cause prolonged changes in the chondroitin sulfate proteoglycans neurocan and phosphacan in the limbic structures. *Exp Neurol* 2003; 184: 179–95.
225. Yuan W, Matthews R, Sandy J, Gottschall P. Association between protease-specific proteolytic cleavage of brevican and synaptic loss in the dentate gyrus of kainate-treated rats. *Neuroscience* 2002; 114: 1091–101.
226. Carmichael ST, Archibeque I, Luke L, Nolan T, Momiy J, Li S. Growth-associated gene expression after stroke: evidence for a growth-promoting region in peri-infarct cortex. *Exp Neurol* 2005; 193: 291–311.
227. Deguchi K, Takaishi M, Hayashi T, Oohira A, Nagotani S, Li F, Jin G, Nagano I, Shoji M, Miyazaki M. Expression of neurocan after transient middle cerebral artery occlusion in adult rat brain. *Brain Res* 2005; 1037: 194–9.
228. Snow A, Wight T, Nochlin D, Koike Y, Kimata K, DeArmond S, Prusiner S. Immunolocalization of heparan sulfate proteoglycans to the prion protein amyloid plaques of Gerstmann-Straussler syndrome, Creutzfeldt-Jakob disease and scrapie. *Lab Invest* 1990; 63: 601.

229. Perry G, Richey P, Siedlak SL, Galloway P, Kawai M, Cras P. Basic fibroblast growth factor binds to filamentous inclusions of neurodegenerative diseases. *Brain Res* 1992; 579: 350.
230. Paulus W, Baur I, Dours-Zimmermann MT, Zimmermann DR. Differential expression of versican isoforms in brain tumors. *J Neuropathol Exp Neurol* 1996; 55: 528.
231. Pizzorusso T, Medini P, Landi S, Baldini S, Berardi N, Maffei L. Structural and functional recovery from early monocular deprivation in adult rats. *Proc Natl Acad Sci USA* 2006; 103: 8517–22.
232. Vorobyov V, Kwok JCF, Fawcett JW, Sengpiel F. Effects of digesting chondroitin sulfate proteoglycans on plasticity in cat primary visual cortex. *J Neurosci* 2013; 33: 234–43.
233. Odawara T, Iseki E, Li F, Kosaka K, Ikeda K. Heparan sulfate proteoglycans recognize ghost Pick bodies. *Neurosci Lett* 1998; 242: 120–2.
234. Merry CLR, Bullock SL, Swan DC, Backen AC, Lyon M, Beddington RSP, Wilson VA, Gallagher JT. The molecular phenotype of heparan sulfate in the Hs2st<sup>-/-</sup> mutant mouse. *J Biol Chem* 2001; 276: 35429–34.
235. Allen B, Rapraeger A. Spatial and temporal expression of heparan sulfate in mouse development regulates FGF and FGF receptor assembly. *J Cell Biol* 2003; 163: 637–48.
236. Ronca F, Andersen J, Paech V, Margolis R. Characterization of Slit protein interactions with glypican-1. *J Biol Chem* 2001; 276: 29141–7.
237. Turnbull J, Fernig D, Ke Y, Wilkinson M, Gallagher J. Identification of the basic fibroblast growth factor binding sequence in fibroblast heparan sulfate. *J Biol Chem* 1992; 267: 10337–41.
238. Shipp EL, Hsieh-Wilson LC. Profiling the sulfation specificities of glycosaminoglycan interactions with growth factors and chemotactic proteins using microarrays. *Chem Biol* 2007; 14: 195–208.
239. Ishai-Michaeli R, Svahn C, Weber M, Chajek-Shaul T, Korner G, Ekre H, Wlodavsky I. Importance of size and sulfation of heparin in release of basic fibroblast growth factor from the vascular endothelium and extracellular matrix. *Biochemistry* 1992; 31: 2080–8.
240. Liu J, Chau CH, Liu H, Jang BR, Li X, Chan YS, Shum DKY. Upregulation of chondroitin 6-sulphotransferase-1 facilitates Schwann cell migration during axonal growth. *J Cell Sci* 2006; 119: 933–42.
241. Tully S, Rawat M, Hsieh-Wilson L. Discovery of a TNF-antagonist using chondroitin sulfate microarrays. *J Am Chem Soc* 2006; 128: 7740–1.
242. Sugahara K, Yamada S. Structure and function of oversulfated chondroitin sulfate variants: unique sulfation patterns and neuroregulatory activities. *Trends Glycosci Glycotechnol* 2000; 12: 321–50.
243. Nadanaka S, Clement A, Masayama K, Faissner A, Sugahara K. Characteristic hexasaccharide sequences in octasaccharides derived from shark cartilage chondroitin sulfate D with a neurite outgrowth promoting activity. *J Biol Chem* 1998; 273: 3296–307.
244. Bao X, Muramatsu T, Sugahara K. Demonstration of the pleiotrophin-binding oligosaccharide sequences isolated from chondroitin sulfate/dermatan sulfate hybrid chains of embryonic pig brains. *J Biol Chem* 2005; 280: 35318–28.



Vimal P. Swarup is a graduate student in the Department of Bioengineering at the University of Utah. Vimal received his BE from Birla Institute of Technology, India, and his MS from Illinois Institute of Technology, Chicago. Vimal's current research interest lies in studying the role of glycosaminoglycans in spinal cord injuries and engineering approaches to modify their sulfation pattern at the injury site.



Caitlin P. Mencio is a graduate student in the Neuroscience Program at the University of Utah. Caitlin received her BS in Neuroscience from Texas Christian University in Fort Worth, TX. Caitlin is currently studying the role proteoglycans play in neural development, synapse formation, and plasticity.

**DE GRUYTER**

Vladimir Hlady is a Professor of Bioengineering at University of Utah. He received BS, MS, and DSc degrees in Chemistry from the University of Zagreb, Croatia. His current research focus is on the role of glycocalyx in axonal pathfinding and platelet activation. He has two patents and published more than 120 scientific papers, reviews, and book chapters.



Kuberan (Kuby) Balagurunathan, PhD, is an Associate Professor of Medicinal Chemistry at the University of Utah. Kuby received his BSc from St. Joseph's College, Trichy, India, and his MSc from the Indian Institute of Technology, Madras, India, under the guidance of Prof. Duraikkannu Loganathan, and his PhD from the University of Iowa under the guidance of Prof. Robert Linhardt. He did his postdoctoral training at MIT in Prof. Robert Rosenberg's laboratory where he developed various chemoenzymatic approaches for creating defined structures of heparin and heparan sulfate. Kuby's laboratory works on exploring the chemical biology of carbohydrates such as heparan, chondroitin, dermatan, and keratan sulfates and to determine their pathological and physiological roles at the molecular level.

APPENDIX B

USE OF ENZYMES AND POLYMERS IN  
COLLABORATIVE RESEARCH



## B1.1. Polymer internalization into normal and cancer cells



NIH Public Access

Author Manuscript

*Mol Pharm*. Author manuscript; available in PMC 2014 April 01.

Published in final edited form as:

*Mol Pharm*. 2013 April 1; 10(4): 1442–1449. doi:10.1021/mp300679a.

### Sulfation patterns determine cellular internalization of heparin-like polysaccharides

Karthik Raman<sup>a</sup>, Caitlin Mencio<sup>b</sup>, Umesh R. Desai<sup>c</sup>, and Balagurunathan Kuberan<sup>a,b,d,\*</sup>

<sup>a</sup>Department of Bioengineering, University of Utah, Salt Lake City, UT, USA

<sup>b</sup>Interdepartmental Program in Neuroscience, University of Utah, Salt Lake City, UT, USA

<sup>c</sup>Department of Medicinal Chemistry, Virginia Commonwealth University, Richmond, VA 23284, USA

<sup>d</sup>Department of Medicinal Chemistry, University of Utah, Salt Lake City, UT, USA

#### Abstract

Heparin is a highly sulfated polysaccharide which serves biologically relevant roles as an anticoagulant and anti-cancer agent. While it is well known that modification of heparin's sulfation pattern can drastically influence its ability to bind growth factors and other extracellular molecules, very little is known about the cellular uptake of heparin and the role sulfation patterns serve in affecting its internalization. In this study, we chemically synthesized several fluorescently-labeled heparins consisting of a variety of sulfation patterns. These polysaccharides were thoroughly characterized using anion exchange chromatography and size exclusion chromatography. Subsequently, we utilized flow cytometry and confocal imaging to show that sulfation patterns differentially affect the amount of heparin uptake in multiple cell types. This study provides the first comprehensive analysis of the effect of sulfation pattern on the cellular internalization of heparin or heparan sulfate like polysaccharides. The results of this study expand current knowledge regarding heparin internalization and provide insights into developing more effective heparin-based drug conjugates for applications in intracellular drug delivery.

#### Keywords

Heparin; Cellular Uptake; Internalization; Nucleus localization; Heparan Sulfate; Heparosan

#### Introduction

Heparin is a complex, biocompatible, biodegradable, and water-soluble glycosaminoglycan that is commonly found within mast cell granules. While its biological role is unclear, heparin is utilized clinically for its anti-coagulant properties. As an agonist of anti-thrombin, heparin is an effective treatment against deep-vein thrombosis and pulmonary emboli.[1] Recent studies have also shown that heparin has potent anti-cancer properties including an ability to hinder cancer invasion, metastasis, and tumor-derived angiogenesis.[2–4]

\*Address correspondence to this author at 30 S 2000 E, Skaggs Hall Rm. 307, University of Utah, Salt Lake City, UT 84112, USA; Tel: (1) 801-587-9474; Fax: (1) 801-585-9119; KUBBY@pharm.utah.edu.

**Supporting Information.** Charge and Size of M. Heps. Effect of treatment with multiple uptake inhibitors. This material is available free of charge via the Internet at <http://pubs.aes.org>.

#### Author Contributions

The manuscript was written through contributions of all authors. All authors have given approval to the final version of the manuscript.

NIH-PA Author Manuscript

NIH-PA Author Manuscript

NIH-PA Author Manuscript

It is well known that altering heparin's sulfation pattern can affect its biochemical properties. *N*-desulfation of heparin, removal of 2-*O* sulfate groups from iduronic acid residues, and removal of 6-*O* sulfate groups from glucosamine residues within heparin can inhibit heparin-FGF interactions [5–7]. Additionally, *N*-sulfate and 3-*O* sulfate groups are critical to heparin's anti-coagulant activity [8, 9].

Several recent publications have utilized covalently conjugated heparin-based drug delivery vehicles (DDV) to deliver anti-cancer molecules such as paclitaxel and lithocholate [10, 11]. Conjugation to heparin provides additional therapeutic value because both the DDV as well as the drug prevent cancer progression. However, it is still unclear how altering heparin's sulfation patterns can affect its cellular internalization, localization, and efficacy as a DDV. Previously, researchers have identified heparin scavenger receptors, however these receptors have not yet been isolated and their substrate specificities remain unknown. [12–14]

In this article, we chemically modify heparin and heparosan, a heparin precursor isolated from *E. Coli* K5, to show that modification of heparin's sulfation pattern leads to increased cellular uptake – providing hints to define the ligand specificities of heparin receptors in cells. These exciting results provide new insight into heparin/heparosan sulfate biology and the design of more effective heparin-conjugates for drug delivery.

## Materials and Methods

### Materials

HT-29 colon cancer cells and BXP-3 pancreatic cancer cells were provided by Dr. Scott Kuwada (University of Hawaii). U87-Mg glioma cells were obtained from Dr. Randy Jensen (University of Utah). Hog mucosal heparin was obtained from Ming Han Chemicals (Oakland, CA). K1 CHO cells were obtained from the ATCC. DEAE-Sepharose gel was purchased from Amersham Biosciences. The analytical grade strong anion exchange column, size exclusion column, and weak anion exchange columns were obtained from Dionex, and Tosoh Biosciences, respectively. Disaccharide standards for strong anion exchange were obtained from Iduron Inc (Manchester, UK). Heparitinase I, II and III from *Flavobacterium heparinum* were expressed as previously described [15]. Cell culture reagents were from Invitrogen Inc. Internalization inhibitors Chlorpromazine (CPZ), Filipin (FIL), Dynasore (DYN), 5-(*N*-Ethyl-*N*-isopropyl) amiloride (EIPA), and all other reagents and solvents were from Sigma-Aldrich.

**Synthesis of Modified Heparins (M. Heps)**—Briefly, Heparosan (NA), *N*-sulfo heparosan (NS), completely desulfated heparin (CDSHep), completely desulfated *N*-resulfated heparin (CDSNS), and 2-*O* desulfated heparin (2ODS) were synthesized as described in literature [16–19]. After extensive dialysis, each substrate was digested with a cocktail of heparitinase I, II, and III and subjected to disaccharide analysis by strong anion exchange chromatography [20]. More specifically, the substrates were prepared as described in the following sections.

**Heparosan (NA)**—Heparosan capsular polysaccharide was first isolated and purified from *E. Coli* K5 as previously described in literature [16]. The resulting polysaccharide was then further purified by dialysis against running water through a 3000 MWCO membrane for 3 days. After complete lyophilization, the product was weighed and characterized through anion exchange chromatography as described in the supplementary material.

***N*-Sulfated Heparosan (NS)**—As described in literature, *N*-sulfated heparosan was prepared by *N*-deacetylation of heparosan followed by *N*-sulfation [17]. *N*-deacetylation was carried out by treating 1 g of heparosan with 2.5 M NaOH in water at 55 °C overnight. Next,

N-deacetylated heparosan was neutralized to pH 7.0 and treated with 2.5 g each of NaCO<sub>3</sub> and triethylamine-sulfur trioxide complex and stirred for 24 h at 48 °C. The pH of this reaction was maintained below pH 10 by addition of HCl. Subsequently, an additional 2.5 g each of NaCO<sub>3</sub> and triethylamine-sulfur trioxide complex was added and the reaction was stirred for an additional 24 h. The resulting polysaccharide was dialyzed, lyophilized, and chemically characterized in a similar manner to NA.

**Completely desulfated Heparin (CDSHep)**—CDSHep was prepared by utilizing published protocols.[18] The pyridinium salt of heparin was first synthesized by passing a solution of 1 g of heparin in water through a column packed with Amberlite cation exchange resin. The resulting eluant was collected on ice, adjusted to pH 9 with pyridine, stirred for 30 minutes, and then concentrated in a rotary evaporator. 100 mg of the pyridinium salt of heparin was then completely desulfated by stirring overnight at 100 °C in a 10 ml mixture of 9:1 DMSO:Methanol. The resulting polysaccharide was dialyzed, lyophilized, and characterized as stated before.

**Completely desulfated N-resulfated Heparin (CDSNS)**—To synthesize CDSNS, CDSHep was subjected to *N*-sulfation as previously described for NS preparation.

**2-O Desulfated Heparin (2ODS)**—According to a previously published protocol, 10 mg of heparin was mixed with 1 mg of NaBH<sub>4</sub> in 10 ml of 0.4 N NaOH.[19] This mixture was then frozen in a -80 refrigerator and lyophilized to dryness. The resulting crusty yellow solid was subsequently redissolved in water and neutralized to pH 7 with acetic acid. This polymer was then dialyzed for 3 days, lyophilized, and characterized as stated before.

**Fluoresceinamine conjugation to M. Heps**—First, a stock of 100 mg of fluoresceinamine (FA) was dissolved in a 1 ml mixture of 3:2:1 DMSO:Acetonitrile:Acetone. Additionally, a stock containing 22 mg of 1-Ethyl-3-(3-dimethylaminopropyl)carbodiimide (EDC) in 1 ml of water was created. Next, 100 mg of each M. Hep substrate was dissolved in 1 ml of water. 300 µl of the FA stock was added to the M. Hep along with 300 µl of the EDC stock. This mixture was stirred overnight at room temperature and subsequently dialyzed and lyophilized. Utilizing FA modified heparins, the molecular weight of FA-M. Heps was analyzed by size exclusion HPLC as described previously.[20] The charge density of each substrate was analyzed by weak anion-exchange HPLC as described previously.[20]

**Cell Treatment with FA-M. Heps**—Approximately 50,000 cells were trypsinized and added into wells of a 96 well plate with DMEM containing 10% FBS and 1% Penicillin/Streptomycin (P/S). After approximately 16 hrs cells had been adherent and the media was replaced with HAMS F-12 containing 10% FBS and 1% P/S. To these wells, 200 µg of each FA-M. Hep was added and cells were incubated for 6 hrs in a humidified cell culture incubator.

**Fluorescence assisted cell sorting**—After treatment with FA-M. Heps, cells were resuspended in trypsin without phenol red. Trypsin was neutralized with HAMS F-12 media containing 10% FBS, and cell suspensions were analyzed on a FACScan instrument (Becton Dickinson Immunocytometry Systems, Mountain View, CA) with computer-aid from CellQuant software. A minimum of 5000 gated events were captured for each sample and used for comparison purposes.

**Confocal Imaging**—For confocal imaging, approximately 50,000 cells were grown on glass coverslips within 35 mm cell culture dishes with 1 ml media. Subsequently, 200 µg of

FA-M. Hep conjugates were added and cells were allowed to internalize M. Heps for 16 hrs in a humidified incubator. Subsequently, the media was removed and cells were washed twice with PBS. 500  $\mu$ l of 4% paraformaldehyde solution was then added to the cells and cells were maintained for 10 mins at room temperature. Next, cells were washed twice with PBS and stained with DAPI and Rhodamine Phalloidin for 10 mins each. After incubation with cellular stains, cells were mounted onto microscope slides and imaged with an FV1000-XY Confocal Olympus IX81 microscope with a 60X oil immersion lens.

## Results

The central goal of this study is to determine whether modulation of sulfation pattern affects the cellular internalization of heparin. To achieve this goal, a library of fluoresceinamine-conjugated M. Heps was synthesized (Fig. 1) and extensively characterized via analysis of sulfation pattern, charge density, and size (Table S1 and Fig. S1). A variety of cells were incubated with each M. Hep and FACS was utilized to analyze the total amount of conjugate that was internalized after 6 hours (Fig. 2). Next, the cellular localization of each conjugate was assessed using confocal microscopy in two different cell lines – HT-29 colon cancer cells and U87Mg glioma cells (Figs. 3 and 4). The rate and mechanism of uptake of each conjugate was also assessed using FACS (Figs. 5 and 6).

### Sulfation pattern affects the internalization of M. Heps into multiple cell types

To determine the effects of sulfation pattern on internalization, experiments were conducted to test the relative internalization of several M. Heps in the following cell lines (Fig. 2): bovine lung microvascular endothelial cells (BLMVEC), chinese hamster ovary K1 cells (CHO K1), BXPC-3 human pancreatic cancer cells, HT-29 human colorectal cancer cells, and U87Mg human glioma cells.

All cells were incubated with fluoresceinamine-conjugated M. Heps for 6 hours and subsequently subjected to analysis by FACS (Fig. 2). Relative to heparin, M. Hep substrates showed drastically altered internalization into different cell types. NA, NS, and CDSNS fluoresceinamine conjugates were internalized into all cell types significantly more than heparin. However, a partially positively charged polymer, CDSHep, was not internalized to the same extent as NA, NS, or CDSNS in all the cell lines tested. Furthermore, NS, not NA, was internalized to the greatest extent in all cell types tested; thus, these results indicate that uptake may be receptor-mediated and that the receptor recognizes and internalizes NS more than other M. Heps tested.

### M. Heps are found throughout cellular bodies

To examine the effect of sulfation patterns on cellular localization, U87 Mg and HT-29 cells were incubated with M. Hep-FA conjugates overnight and localization was analyzed by confocal microscopy (Figs. 3 and 4). Rhodamine Phalloidin was utilized as a red dye to identify cellular actin and DAPI was utilized to label the cellular nuclei. Z-Slices were chosen so as to minimize colocalization of the actin stain with the nuclear stain.

Confocal images indicate that NS, CDSNS, 2ODS, CDSHep, and heparin all co-localize with cellular actin in U87 MG cells, and are found throughout cell bodies. Interestingly, NA co-localizes with DAPI, showing that this substrate may enter the nuclei of U87 MG cells. However, in HT-29 cells, all the M. Heps are found in cell bodies – thus indicating that nuclear localization may be both sulfation pattern-dependent and cell-specific.

### Sulfation patterns affect the rate of internalization of M.Heps into cells

In addition to the extent of internalization, the effects of sulfation pattern on the rate of substrate internalization into HT-29 cells was analyzed by incubating equal amounts of each substrate with cells for various time points (Fig. 5). Compared to the amount of each substrate internalized after 30 hours, NA and CDSHep saturated the fastest. NS, CDSNS, and 2ODS saturated at an intermediate rate while heparin saturated at a slower rate. Cellular recognition of GAG sulfation patterns probably determines the rate of saturation.

In contrast, sulfation patterns do not determine the concentration dependence of internalization (Fig. 6). Only CDSHep showed a significant departure from Heparin by saturating at lower concentrations than all other polymers tested. This is most likely due to its amine functionality, as NA and other substrates did not show similar concentration dependence.

### Discussion

In recent years, heparin-based conjugates have shown promise in preclinical studies as drug delivery vehicles. One of the reasons for their efficacy is because heparin-drug conjugates are able to attack cancer cells using multiple pathways – both the drug and the DDV are able to mitigate tumor progression.[21–24] However, the role of sulfation patterns in the cellular uptake of heparin is largely unknown. In this article, chemically modified heparosan from *E. Coli*K5 as well as chemically modified heparin are utilized to show that sulfation patterns determine heparin cellular uptake into several cell types. This knowledge inspires new designs of chemically modified heparin-drug conjugates that are favorable for drug delivery but lack heparin's inherent drawbacks such as bleeding complications and heparin induced thrombocytopenia. Additionally, the results of this study further provide hints to illuminate the ligand specificities of elusive heparin scavenger receptors.

Previous studies have found that modification of sulfation pattern can alter the biological properties of heparin. Controlling the amount of 2-*O*, 3-*O*, and 6-*O* sulfation can drastically affect heparin's ability to bind ligands. [5, 8, 9, 25] To test our hypothesis that sulfation patterns affect cellular internalization and the effectiveness of heparin as a DDV, we designed a library of heparins to represent a diverse group of polymers with different sulfation patterns and densities (Fig. 1). CDSHep, was the only substrate determined to have free amine groups and hence it had the least negative charge density. Unaltered heparin had the highest negative charge while other substrates had intermediate charge density. We also specifically designed molecules derived from heparosan that were non-epimerized and those derived from heparin which contained high iduronic acid content. Analysis by size exclusion chromatography revealed that only minor differences in size and polydispersity exist among the different substrates (Table S1 and Fig. S1).

After structural characterization, a variety of cell types were treated with M. Heps and analyzed via FACS to determine the uptake of each M. Hep (Fig. 2). The experiment was designed to include both tumorigenic as well as non-tumorigenic cell types. As hypothesized, modifying the sulfation patterns of heparin and heparosan significantly altered cellular internalization. One would expect that CDSHep, the most positively charged polymer, would be internalized by cells to the greatest extent. However, NA, NS, and CDSNS accumulated inside the cell to a much larger extent than CDSHep, 2ODS, and heparin in all cell types tested. This indicates that sulfation pattern, not charge density, determines cellular internalization of M. Heps. These results also give a glimpse into the substrate specificities of elusive heparin uptake receptors.[12–14] While researchers have not yet isolated these receptors, it is clear that sulfation pattern greatly affects cellular uptake of heparin and that these receptors prefer *N*-sulfo heparosan to any of the other M. Heps

tested. Further evidence that heparin uptake may be receptor driven is determined by the concentration- dependence of the internalization of M.Heps (Fig 6). If internalization was a purely diffusion-driven process then the concentration dependence of internalization would be linear with concentration. However, it is evident that incubating cells with five times and ten times more substrate does not lead to a linear dose dependent increase in internalization.

Next, the cellular localization of M. Heps was sought after to determine the effects of sulfation pattern on sub-cellular targeting. Previously, it was found that GAGs and proteoglycans such as Syndecan-1 and Glypican-1 can enter the nucleus.[26–30] Additionally, anti-proliferative GAGs primed by xylosides can enter cellular nuclei and modulate histone 3 acetylation and cellular growth.[31] Heparin-poly- $\beta$ -amino ester complexes have also been found to modulate nuclear transcription factors.[32] However, researchers have not yet identified if sulfation patterns affect the nuclear entry of these PGs and GAGs. Therefore, we examined the cellular localization of M. Heps tagged with fluoresceinamine by utilizing confocal microscopy (Figs. 3 and 4). The majority of M. Heps were found throughout cell bodies and excluded from the nucleus in both HT-29 and U87Mg cells. However, in U87Mg, NA was found to co-localize with DAPI. Based on these results, it may be possible to deduce that sulfation patterns can affect nuclear entry of GAGs. It is unlikely that charge density was responsible for nuclear entry as CDSHep did not enter the nuclei. Additionally, none of the epimerized substrates were visible in the nucleus suggesting that chain flexibility may affect nuclear entry as well. However, additional biochemical proof will be necessary to further understand the differential localization of heparin and heparin-like polymers.

In conclusion, this research presents the first comprehensive evidence that sulfation pattern, not charge density, determines heparin/heparan sulfate cellular uptake into several cell types. While the M. Heps are found throughout cells, nuclear localization of these glycosaminoglycans may be both sulfation pattern and cell-type dependent. The results of this study have broad implications in cell biology, heparan sulfate biochemistry, and drug delivery vehicle design. However, several new questions now surface: Why do NS and NA polymers enter cells to a greater extent than heparin? Do NA or NA/NS domains of heparan sulfate promote cellular uptake and nuclear localization of Syndecans and Glypicans? Additionally, would developing NA-, NS-, or CDSNS- based DDV yield better tumor-targeting capability than heparin-based DDV? In-depth analysis of nuclear localization and *in vivo* drug targeting is necessary to answer these intriguing questions.

## Supplementary Material

Refer to Web version on PubMed Central for supplementary material.

## Acknowledgments

This work was supported by NIH grants P01HL107152 and R01GM075168 to B.K and by the NIH fellowship F31CA168198 to K.R.

## ABBREVIATIONS

<b>M. Hep</b>	Modified heparin
<b>FGF</b>	fibroblast growth factor
<b>DDV</b>	drug delivery vehicle
<b>CPZ</b>	Chlorpromazine

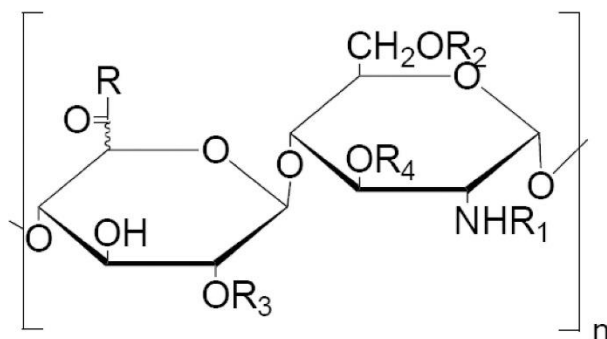
<b>FIL</b>	Filipin
<b>DYN</b>	dynasore
<b>EIPA</b>	5-(N-Ethyl-N-isopropyl) amiloride
<b>FA</b>	fluoresceinamine
<b>NA</b>	Heparosan
<b>NS</b>	<i>N</i> -Sulfo heparosan
<b>CDSHep</b>	Completely desulfated heparin
<b>CDSNS</b>	Completely desulfated <i>N</i> -resulfated heparin
<b>2ODS</b>	2- <i>O</i> desulfated heparin
<b>HS</b>	heparan sulfate

## REFERENCES

- Hull R, Delmore T, Genton E, Hirsh J, Gent M, Sackett D, McLoughlin D, Armstrong P. Warfarin sodium versus low-dose heparin in the long-term treatment of venous thrombosis. *N Engl J Med*. 1979; 301(16):855–858. [PubMed: 384248]
- Borsig L. Antimetastatic activities of modified heparins: selectin inhibition by heparin attenuates metastasis. *Semin Thromb Hemost*. 2007; 33(5):540–546. [PubMed: 17629852]
- Vlodavsky I, Mohsen M, Lider O, Svahn CM, Ekre HP, Vigoda M, Ishai-Michaeli R, Peretz T. Inhibition of tumor metastasis by heparanase inhibiting species of heparin. *Invasion Metastasis*. 1994; 14(1–6):290–302. [PubMed: 7657522]
- Folkman J, Langer R, Linhardt RJ, Haudenschild C, Taylor S. Angiogenesis inhibition and tumor regression caused by heparin or a heparin fragment in the presence of cortisone. *Science*. 1983; 221(4612):719–725. [PubMed: 6192498]
- Guimond S, Maccarana M, Olwin BB, Lindahl U, Rapraeger AC. Activating and inhibitory heparin sequences for FGF-2 (basic FGF). Distinct requirements for FGF-1, FGF-2, and FGF-4. *J Biol Chem*. 1993; 268(32):23906–23914. [PubMed: 7693696]
- Lundin L, Larsson H, Kreuger J, Kanda S, Lindahl U, Salmivirta M, Claesson-Welsh L. Selectively desulfated heparin inhibits fibroblast growth factor-induced mitogenicity and angiogenesis. *J Biol Chem*. 2000; 275(32):24653–24660. [PubMed: 10816596]
- Sugaya N, Habuchi H, Nagai N, Ashikari-Hada S, Kimata K. 6-*O*-sulfation of heparan sulfate differentially regulates various fibroblast growth factor-dependent signalings in culture. *J Biol Chem*. 2008; 283(16):10366–10376. [PubMed: 18281280]
- Atha DH, Lormeau JC, Petitou M, Rosenberg RD, Choay J. Contribution of 3-*O*- and 6-*O*-sulfated glucosamine residues in the heparin-induced conformational change in antithrombin III. *Biochemistry*. 1987; 26(20):6454–6461. [PubMed: 3427019]
- Danishefsky I, Ahrens M, Klein S. Effect of heparin modification on its activity in enhancing the inhibition of thrombin by antithrombin III. *Biochim Biophys Acta*. 1977; 498(1):215–222. [PubMed: 560216]
- Wang Y, Wang Y, Xiang J, Yao K. Target-specific cellular uptake of taxol-loaded heparin-PEG-folate nanoparticles. *Biomacromolecules*. 2010; 11(12):3531–3538. [PubMed: 21086982]
- Yu MK, Lee DY, Kim YS, Park K, Park SA, Son DH, Lee GY, Nam JH, Kim SY, Kim IS, Park RW, Byun Y. Antiangiogenic and apoptotic properties of a novel amphiphilic folate-heparin-lithocholate derivative having cellular internality for cancer therapy. *Pharm Res*. 2007; 24(4):705–714. [PubMed: 17318418]
- Falcone DJ. Heparin stimulation of plasminogen activator secretion by macrophage-like cell line RAW264.7: role of the scavenger receptor. *J Cell Physiol*. 1989; 140(2):219–226. [PubMed: 2501315]

13. Watanabe J, Haba M, Urano K, Yuasa H. Uptake mechanism of fractioned [(3)H]heparin in isolated rat kupffer cells: involvement of scavenger receptors. *Biol Pharm Bull.* 1996; 19(4):581–586. [PubMed: 8860963]
14. Watanabe J, Muranishi H, Haba M, Yuasa H. Uptake of fluorescein isothiocyanate (FITC)-fractionated heparin by rat parenchymal hepatocytes in primary culture. *Biol Pharm Bull.* 1993; 16(9):939–941. [PubMed: 8268865]
15. Babu P, Kuberan B. Fluorescent-tagged heparan sulfate precursor oligosaccharides to probe the enzymatic action of heparitinase I. *Anal Biochem.* 2009; 396(1):124–132. [PubMed: 19732739]
16. Kuberan B, Lech M, Zhang L, Wu ZL, Beeler DL, Rosenberg RD. Analysis of heparan sulfate oligosaccharides with ion pair-reverse phase capillary high performance liquid chromatography-microelectrospray ionization time-of-flight mass spectrometry. *J Am Chem Soc.* 2002; 124(29):8707–8718. [PubMed: 12121115]
17. Lloyd AG, Embery G, Fowler LJ. Studies on heparin degradation. I. Preparation of (35 S) sulphamate derivatives for studies on heparin degrading enzymes of mammalian origin. *Biochem Pharmacol.* 1971; 20(3):637–648. [PubMed: 5170128]
18. Nagasawa K, Inoue Y, Kamata T. Solvolytic desulfation of glycosaminoglycuronan sulfates with dimethyl sulfoxide containing water or methanol. *Carbohydr Res.* 1977; 58(1):47–55. [PubMed: 144018]
19. Ishihara M, Kariya Y, Kikuchi H, Minamisawa T, Yoshida K. Importance of 2-O-sulfate groups of uronate residues in heparin for activation of FGF-1 and FGF-2. *J Biochem.* 1997; 121(2):345–349. [PubMed: 9089410]
20. Victor XV, Nguyen TK, Ethirajan M, Tran VM, Nguyen KV, Kuberan B. Investigating the elusive mechanism of glycosaminoglycan biosynthesis. *J Biol Chem.* 2009; 284(38):25842–25853. [PubMed: 19628873]
21. Vannucchi S, Pasquali F, Chiarugi VP, Ruggiero M. Heparin inhibits A431 cell growth independently of serum and EGF mitogenic signalling. *FEBS Lett.* 1991; 281(1–2):141–144. [PubMed: 2015884]
22. Norrby K. Heparin and angiogenesis: a low-molecular-weight fraction inhibits and a high-molecular-weight fraction stimulates angiogenesis systemically. *Haemostasis.* 1993; 23(Suppl 1):141–149. [PubMed: 7684350]
23. Folkman J, Weisz PB, Joullie MM, Li WW, Ewing WR. Control of angiogenesis with synthetic heparin substitutes. *Science.* 1989; 243(4897):1490–1493. [PubMed: 2467380]
24. Engelberg H. Actions of heparin that may affect the malignant process. *Cancer.* 1999; 85(2):257–272. [PubMed: 10023691]
25. Krauel K, Hackbarth C, Furl B, Greinacher A. Heparin-induced thrombocytopenia: in vitro studies on the interaction of dabigatran, rivaroxaban, and low-sulfated heparin, with platelet factor 4 and anti-PF4/heparin antibodies. *Blood.* 2012; 119(5):1248–1255. [PubMed: 22049520]
26. Ishihara M, Fedarko NS, Conrad HE. Transport of heparan sulfate into the nuclei of hepatocytes. *J Biol Chem.* 1986; 261(29):13575–13580. [PubMed: 2944884]
27. Richardson TP, Trinkaus-Randall V, Nugent MA. Regulation of heparan sulfate proteoglycan nuclear localization by fibronectin. *J Cell Sci.* 2001; 114(Pt 9):1613–1623. [PubMed: 11309193]
28. Hsia E, Richardson TP, Nugent MA. Nuclear localization of basic fibroblast growth factor is mediated by heparan sulfate proteoglycans through protein kinase C signaling. *J Cell Biochem.* 2003; 88(6):1214–1225. [PubMed: 12647303]
29. Chen L, Sanderson RD. Heparanase regulates levels of syndecan-1 in the nucleus. *PLoS One.* 2009; 4(3):e4947. [PubMed: 19305494]
30. Liang Y, Haring M, Roughley PJ, Margolis RK, Margolis RU. Glypican and biglycan in the nuclei of neurons and glioma cells: presence of functional nuclear localization signals and dynamic changes in glypican during the cell cycle. *J Cell Biol.* 1997; 139(4):851–864. [PubMed: 9362504]
31. Nilsson U, Johnsson R, Fransson LA, Ellervik U, Mani K. Attenuation of tumor growth by formation of antiproliferative glycosaminoglycans correlates with low acetylation of histone H3. *Cancer Res.* 2010; 70(9):3771–3779. [PubMed: 20406966]
32. Berry D, Lynn DM, Sasisekharan R, Langer R. Poly(beta-amino ester)s promote cellular uptake of heparin and cancer cell death. *Chem Biol.* 2004; 11(4):487–498. [PubMed: 15123243]





R: OH or Fluorescein

**NA\*:**  $R_1$ : Ac       $R_2, R_3, R_4$ : H

**NS\*:**  $R_1$ :  $\text{OSO}_3^-$        $R_2, R_3, R_4$ : H

**CDSNS:**  $R_1$ :  $\text{OSO}_3^-$        $R_2, R_3, R_4$ : H

**2ODS:**  $R_1$ :  $\text{OSO}_3^-$        $R_2$ :  $\text{OSO}_3^-$        $R_3, R_4$ : H

**CDSHep:**  $R_1, R_2, R_3, R_4$ : H

**Heparin:**  $R_1, R_2, R_3, R_4$ :  $\text{OSO}_3^-$

\* Non-epimerized substrates containing only glucuronic acid

**Figure 1.**  
Structures of modified heparins prepared in this study.

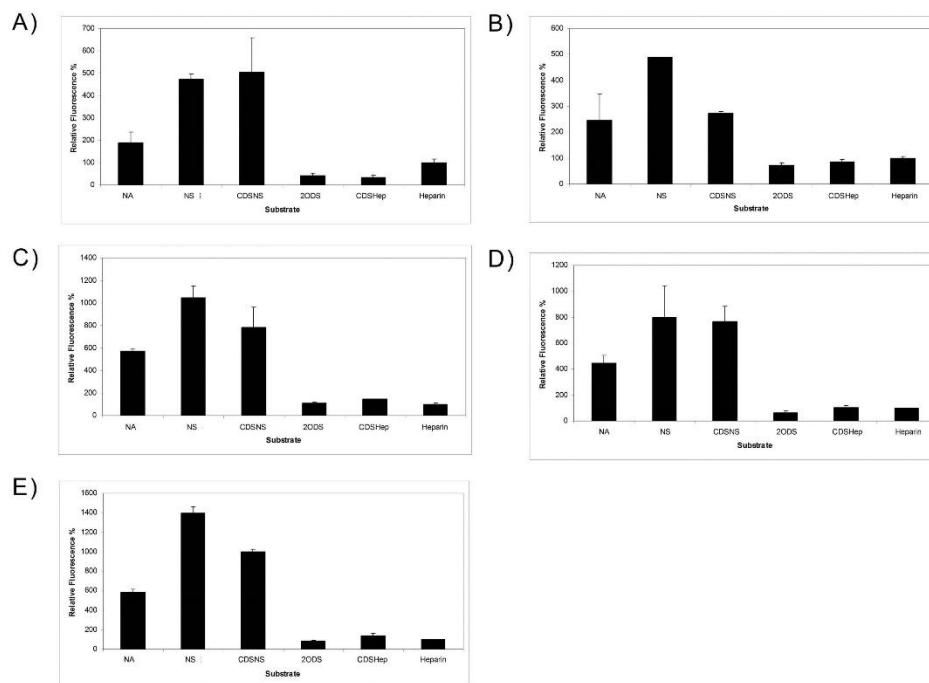


**Figure 2.**

Sulfation patterns determine the total amount of cellular uptake of M. Heps at 6 hours. The different panels indicate M. Hep uptake in a) BLMVEC, b) K1 CHO, c) BXP-3, d) HT-29, and e) U87 Mg cells. Values are normalized against heparin and show that M. Heps such as NA, NS, and CDSNS show enhanced cell uptake relative to heparin. Internalization of M. Heps was determined by fluorescence assisted cell sorting analysis as described in the experimental section. Cellular auto fluorescence at the settings used was minimal.

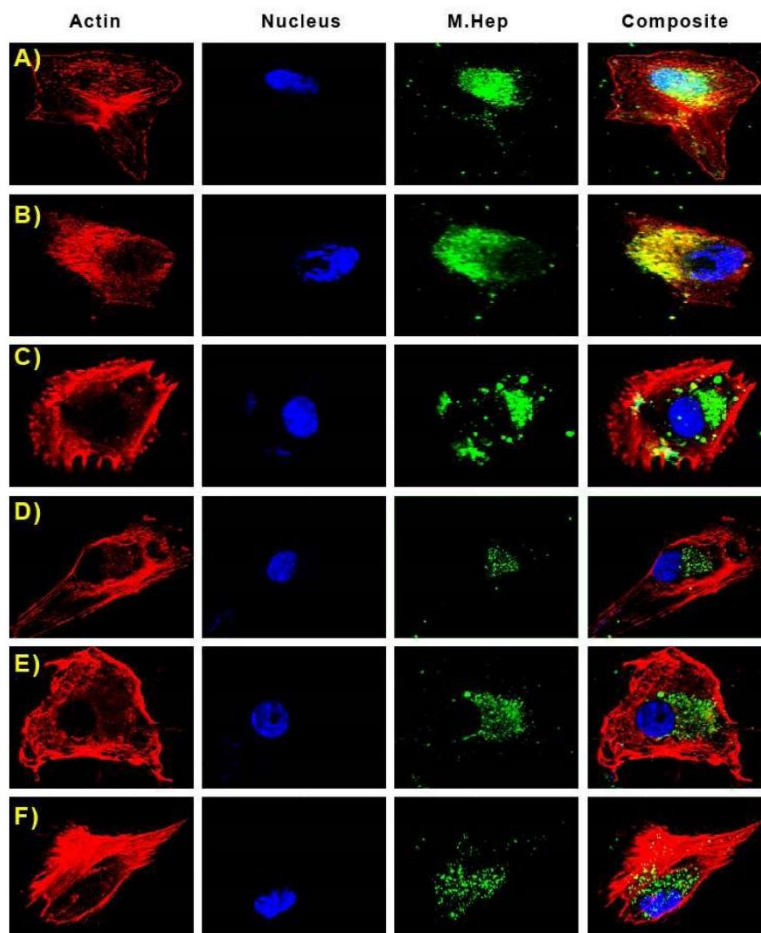


**Figure 3.** Sulfation patterns determine the cellular localization of M. Heps in U87 Mg cells. Panels in this image are fluorescence from Rhodamine Phalloidin (actin), DAPI (nucleus), Fluoresceinamine (M. Heps), and an overlay of all fluorophores. Representative substrates are: **A)** NA, **B)** NS, **C)** CDSNS, **D)** 2ODS, **E)** CDSHep, **F)** Heparin. It is evident that NA polymers colocalize with DAPI in the nucleus of U87 Mg cells.

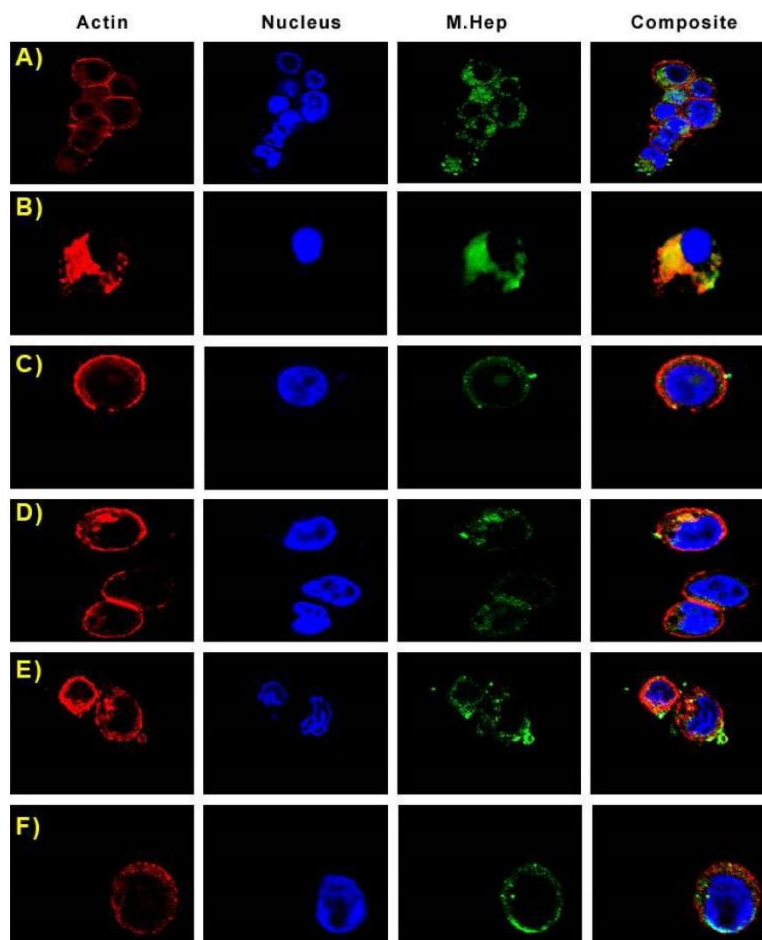


**Figure 4.**

Sulfation patterns determine the cellular localization of M. Heps, however no nuclear localization is visible for any substrate in HT-29 cells. Panels in this image are fluorescence from Rhodamine Phalloidin (actin), DAPI (nucleus), Fluoresceinamine (M. Heps), and an overlay of all fluorophores. Representative substrates are: **A)** NA, **B)** NS, **C)** CDSNS, **D)** 2ODS, **E)** CDSHep, **F)** Heparin.

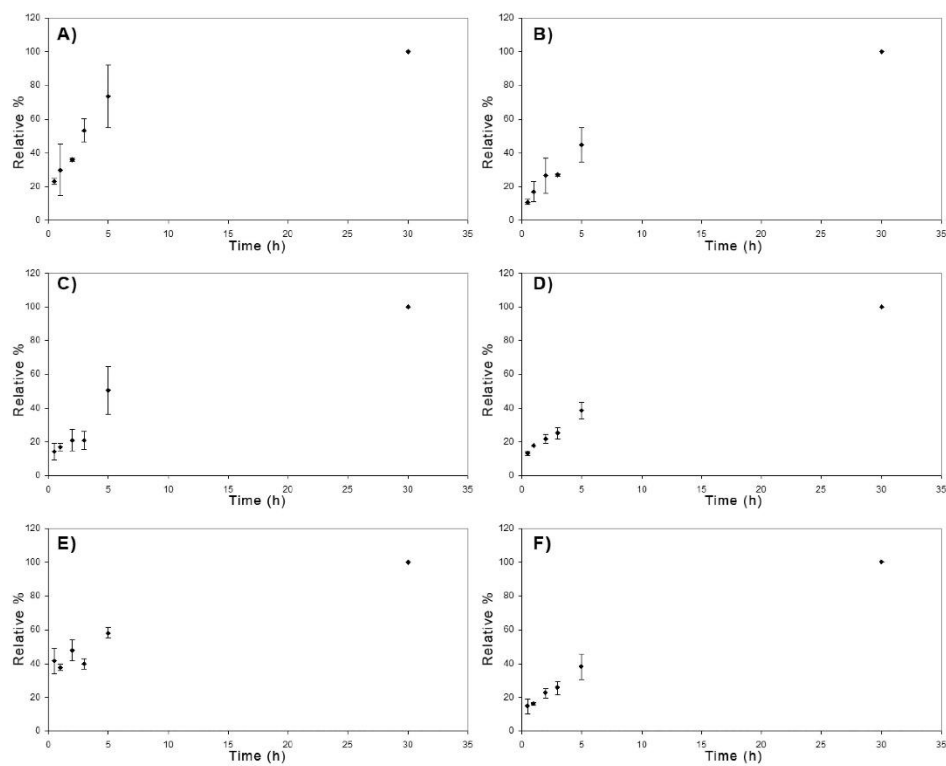


**Figure 5.**

Sulfation patterns determine rate of entry of M. Hepc into HT-29 colon cancer cells. Values are normalized to the 30 hour time points for each substrate. Representative panels indicate the time-dependent internalization of: **A)** NA, **B)** NS, **C)** CDSNS, **D)** 2ODS, **E)** CDSHep, and **F)** Heparin

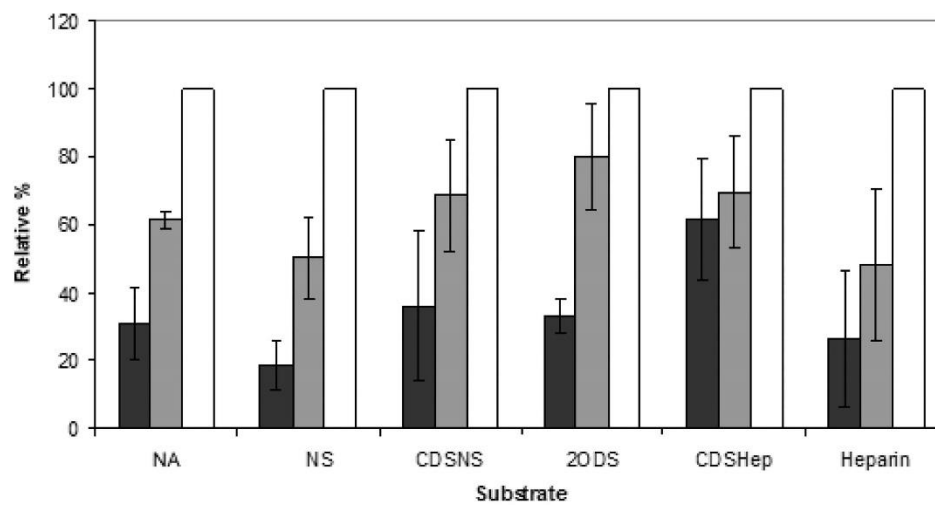


**Figure 6.** Sulfation pattern has little effect on the concentration dependence of internalization. Representative bars indicate the relative fluorescence measured by FACS when 20 µg (■), 100 µg (▒), or 200 µg (□) of M.Heps were incubated with cells for 24 hours. Values are normalized to the total substrate internalized after 24 hours when 200 µg of the respective substrate are added.

## B1.2 Use of heparitinase enzymes in the detection of oversulfated chondroitin sulfate

## A Nanosensor for Ultrasensitive Detection of Oversulfated Chondroitin Sulfate Contaminant in Heparin

Mausam Kalita,<sup>†</sup> Sivasai Balivada,<sup>‡</sup> Vimal Paritosh Swarup,<sup>†</sup> Caitlin Mencio,<sup>†</sup> Karthik Raman,<sup>†</sup> Umesh R. Desai,<sup>§</sup> Deryl Troyer,<sup>‡</sup> and Balagurunathan Kuberan<sup>\*†</sup>

<sup>†</sup>Departments of Medicinal Chemistry and Bioengineering, University of Utah, Salt Lake City, Utah 84112, United States

<sup>‡</sup>Department of Anatomy & Physiology, Kansas State University, Manhattan, Kansas 66506, United States

<sup>§</sup>Department of Medicinal Chemistry and Institute for Structural Biology and Drug Discovery, Virginia Commonwealth University, Richmond, Virginia 23219, United States

Supporting Information

**ABSTRACT:** Heparin has been extensively used as an anticoagulant for the last eight decades. Recently, the administration of a contaminated batch of heparin caused 149 deaths in several countries including USA, Germany, and Japan. The contaminant responsible for the adverse effects was identified as oversulfated chondroitin sulfate (OSCS). Here, we report a rapid, ultrasensitive method of detecting OSCS in heparin using a nanometal surface energy transfer (NSET) based gold-heparin-dye nanosensor. The sensor is an excellent substrate for heparitinase enzyme, as evidenced by ~70% recovery of fluorescence from the dye upon heparitinase treatment. However, the presence of OSCS results in diminished fluorescence recovery from the nanosensor upon heparitinase treatment, as the enzyme is inhibited by the contaminant. The newly designed nanosensor can detect as low as  $1 \times 10^{-9}$  % (w/w) OSCS making it the most sensitive tool to date for the detection of trace amounts of OSCS in pharmaceutical heparins.

Heparin has been used as a clinical anticoagulant for several decades in nearly every major surgery and in the treatment of several clotting disorders such as deep vein thrombosis and acute coronary syndrome.<sup>1–3</sup> Structurally, heparin is a highly sulfated glycosaminoglycan (GAG) consisting of sulfated disaccharide repeating units of predominantly iduronic acid/minor glucuronic acid and glucosamine. However, due to its animal origin, heparin lots have been found to contain other naturally occurring sulfated GAGs too. Over 600 million pigs are used in producing more than 100 t of heparin every year. In 2007–2008, adulteration of hog mucosal heparin led to the contamination of the global heparin supply chain and resulted in severe adverse reactions such as angioedema, hypotension, swelling of the larynx, and anaphylactic reactions.<sup>4–6</sup> Worldwide there were 574 reports of adverse effects and at least 149 deaths in the U.S. and Europe alone due to oversulfated chondroitin sulfate (OSCS), a non-natural highly sulfated GAG identified as the principal contaminant in heparins.<sup>4,5,7,8</sup>

To detect OSCS in heparin, several analytical methods have been developed. These analytical techniques include <sup>1</sup>HNMR,<sup>9</sup>

strong anion exchange (SAX)-HPLC,<sup>10</sup> capillary electrophoresis (CE),<sup>11</sup> polyacrylamide gel electrophoresis (PAGE),<sup>12</sup> near-infrared (NIR)<sup>13</sup> and electrochemical method.<sup>14</sup> The limit of detection (LOD) of these techniques varies from 1% (NIR) to 0.03% (SAX-HPLC) (w/w) OSCS in heparin.<sup>9–14</sup> However, these analytical methods have other drawbacks along with moderate detection limits. To overcome these challenges, several research groups have also developed 96-well microplate assays to detect OSCS contamination. Colorimetric method is routinely used to determine the concentration of heparin.<sup>15,16</sup> Likewise, colorimetric methods are also developed to detect OSCS in heparin; the most sensitive assay to date has an LOD of 0.003% (w/w) OSCS.<sup>17</sup> This method employs water-soluble cationic Leclerc Poly Thiophene Polymer (LPTP), a yellow colored probe that interacts with polyanionic heparin and results in a color change from yellow to red.<sup>18</sup> However, this color change is nonlinear with respect to % (w/w) of OSCS in heparin, and thus, this is less reliable.<sup>17</sup> Therefore, there is an urgent need for the development of a novel sensor that is ultrasensitive, linear and highly reliable in detecting OSCS in heparins.

Here, we report the development of the most sensitive nanosensor to rapidly determine the OSCS contaminant in heparin lots. Compared to the present LOD of 0.003% (w/w) OSCS in heparin reported in the literature, our nanosensor, Au-heparin-dye, can detect  $10^{-9}$  % (w/w) OSCS in heparin in 0.5 h. It is noteworthy that various nanoparticle–GAG conjugates have been employed as imaging agents,<sup>19,20</sup> therapeutics,<sup>21–23</sup> and biochemical tools.<sup>24</sup>

Gold nanoparticles (Au NPs) exert both FRET and NSET on fluorophores that are present on their surfaces. FRET dictates the quenching property of Au NPs at a separation distance of 100 Å between the dye and the Au NP. NSET takes over beyond 100 Å and maintains the quenching character of Au NP to a separation distance of 220 Å.<sup>25,26</sup> We hypothesize that an Au-NP-Hep-dye conjugate would demonstrate strong fluorescence quenching when the dye is conjugated. However, upon enzyme treatment of the heparin linker, the fluorescence should be recovered as dye-heparin fragments are released from the nanoparticle. To test this hypothesis, we first synthesized

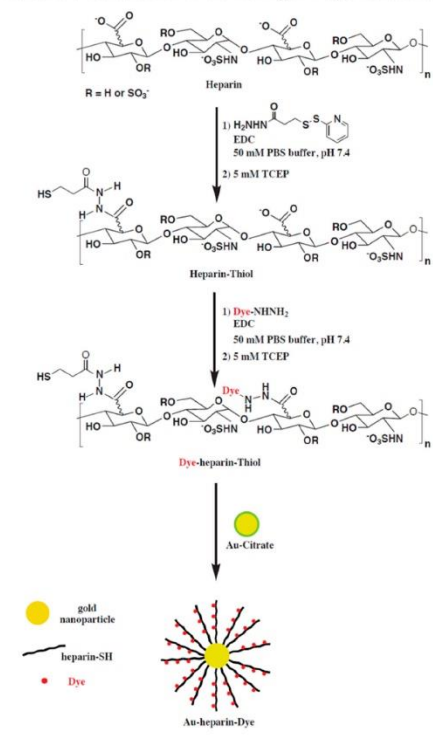
Received: September 4, 2013

Published: October 15, 2013

thiolated heparin-dye stabilized Au NP. The fluorescence quenching property of this conjugate was then analyzed and the fluorescence recovery upon enzyme treatment was observed.

To synthesize Au-Hep-dye nanosensors, a ligand exchange protocol was followed (Scheme 1). The structural morphology

Scheme 1. Construction of the Au-Heparin-Dye Nanosensor



of the nanosensor before and after heparitinase treatment was observed through transmission electron microscopy (Figure 1A,B). The average particle sizes were 18 nm in both cases. Next, the quenching capability of the nanoparticle conjugates was determined using a fluorescence spectrophotometer. We observed an 88% reduction in fluorescence intensity of the dye after conjugation with the Au NPs suggesting an efficient energy transfer from the dye to Au NP (Figure 2A). The Au-heparin-dye nanosensor was then incubated with heparitinase I, II, and III at 37 °C in order to study the efficacy of the enzyme action on the probe. Indeed, a fluorescence recovery of 70% was observed over a period of 4 h (Figure 2B). A heat map of the 96-well microplate imaged using an IVIS imager complemented this observation (Figure 2C).

Once we established that enzyme action causes the fluorescence probe to recover from being quenched, a heparitinase enzyme inhibition study was carried out in the presence of OSCS-contaminated heparin to determine whether

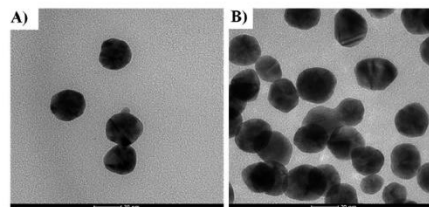


Figure 1. TEM images of (A) Au-Heparin-dye nanosensor and (B) heparitinase-treated Au-heparin-dye nanoparticle after 4 h of incubation. The average size of the particles is  $\sim 18$  nm in both cases. The scale bar is 20 nm.

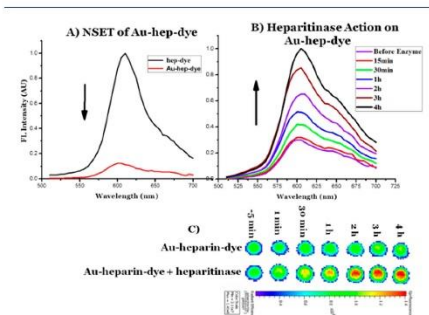
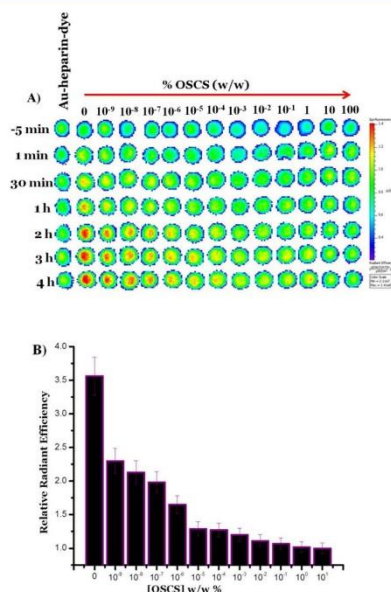


Figure 2. (A) Au-heparin-dye nanosensor shows  $\sim 88\%$  reduction in fluorescence due to NSET. (B) Incubation of the nanosensor with heparitinase enzyme at different time points (before addition of enzyme, 30 min, 1 h, 2 h, 3 h, and 4 h) shows a gradual increase in fluorescence intensity. A recovery of  $\sim 70\%$  fluorescence intensity is recorded over a period of 4 h. (C) A heat map of fluorescence increase is captured through the IVIS's CCD camera using a Ds red filter (575–656 nm). The epifluorescence scale bar represents the increasing order of radiant efficiency [(photons/s/cm<sup>2</sup>/str)/( $\mu$ W/cm<sup>2</sup>)] from blue to red.

OSCS inhibits heparitinase activity. For this study, the following samples were incubated with heparitinases: (a) heparin alone; (b) heparin with 10% (w/w) chondroitin sulfate A and C (CS A and C); and (c) heparin with 10% (w/w) OSCS. The resulting fragments were then analyzed on an analytical HPLC. The results show that 10% (w/w) OSCS is a powerful inhibitor of heparitinase enzyme activity (Figure S1, see Supporting Information). Thus, in the presence of 10% (w/w) OSCS, the heparitinases should not act upon the Au-heparin-dye nanosensor. On the basis of these results, the enzyme activity on the nanosensor should be maximal at low OSCS concentration and minimal at high OSCS concentration. We next tested the quenching of the dye present on the Au-Hep-dye nanosensor in the presence of OSCS upon heparitinase treatment. To develop an analytical method for determining levels of this contaminant in heparin, serial dilutions of OSCS were performed at log increment concentrations from 0.1  $\mu$ g/ $\mu$ L to 0.1 fg/ $\mu$ L. Standard heparin solutions (10  $\mu$ g) were spiked serially with OSCS solutions



from 1  $\mu\text{g}$  (10% w/w) to 0.1 fg ( $10^{-9}$  % w/w) contamination resulting in 11 separate tests. Heparin (10  $\mu\text{g}$ ) and OSCS (10  $\mu\text{g}$ ) were utilized as positive and negative controls, respectively. When these OSCS-spiked heparin samples were incubated with heparitinases in the presence of nanosensor, the fluorescence intensity of the dye recovered quickly in samples with limited contamination (Figure 3A, see Supporting Information for



**Figure 3.** (A) The heat map of the 96-well plate is captured after exciting the wells with 535 nm and recording the emission with a Ds red filter (575–656 nm). The images are recorded before addition of heparitinase, and 1 min, 30 min, 1 h, 2 h, 3 h, and 4 h after incubating the nanoprobe with the heparitinase enzyme treated heparin samples that are spiked with OSCS. (B) A plot of relative average radiant efficiencies of the wells (after incubation with the enzyme cocktail for 30 min) versus [OSCS] (w/w)% in heparin shows that the CCD camera effectively detects 1 fg of OSCS contaminant in 10  $\mu\text{g}$  of heparin. This plot strongly reaffirms the ultrasensitive LOD of the nanosensor.

details). Differences in the enzyme activity could be observed within 30 min of incubation owing to the rapid nature of the assay even at femtomole concentrations of OSCS-contamination (Figure S2, see Supporting Information).

It is known that other glycosaminoglycans such as chondroitin sulfates (CS-A and CS-C) and dermatan sulfate are commonly found as minor impurities in pharmaceutical heparin. To determine whether the newly developed nanosensor system is susceptible to interference from these other glycosaminoglycans, we treated heparin samples containing 10% (w/w) CS-A, CS-C, or dermatan sulfate with heparitinases in the presence of nanosensor. The fluorescence intensity of the dye was recovered quickly in heparin samples containing

natural glycosaminoglycan impurities but not in the heparin sample containing OSCS contaminant (Figure S3, see Supporting Information). Therefore, the nanosensor described here is robust and reliable for routine screening of commercial heparin lots to detect trace levels of OSCS contaminant.

Next, an imaging experiment with an IVIS Lumina II system was designed to capture the emitting photons after treating the nanoprobe with heparitinase/OSCS spiked heparin. The images were taken by exciting the samples at 535 nm and recording emission using a Ds red filter (575–650 nm). A comparative heat map confirmed the gradient decrease in photons as OSCS contamination increases (Figure 3A). When the relative radiant efficiency (radiant efficiency after enzyme treatment/radiant efficiency before enzyme treatment) of each sample is plotted versus (w/w) % OSCS contaminant in heparin,  $10^{-9}$ % (w/w) contaminant was detectable within 30 min. The plot also demonstrates the superior sensitivity of the nanosensor reflected in the relative radiant efficiencies when there is no OSCS contamination (3.56) and  $10^{-9}$ % (w/w) OSCS contamination (2.3) (Figure 3B). With the use of the IVIS scanner, the LOD of this assay system is improved even further.

In summary, the Au-Hep-dye nanosensor described herein can be used to rapidly screen heparin stocks and detect femtogram levels of OSCS contaminants within half an hour. This probe also has potential application in forensic science.<sup>27</sup> We envision that the use of this nanosensor will greatly enhance our ability to maintain a high quality global heparin supply chain, thereby saving human lives.

#### ■ ASSOCIATED CONTENT

##### Supporting Information

Additional figures, materials, and method. This material is available free of charge via the Internet at <http://pubs.acs.org>.

#### ■ AUTHOR INFORMATION

##### Corresponding Author

KUBY@pharm.utah.edu

##### Notes

The authors declare no competing financial interest.

#### ■ ACKNOWLEDGMENTS

We acknowledge funding support from NIH grants (HL107152 and GM075168). We would like to acknowledge David Belnap of the Electron Microscopy Core Laboratory, University of Utah for helping us with the TEM images. We also thank Marla Pyle of Kansas State University for her helpful suggestions in the preparation of the manuscript.

#### ■ REFERENCES

- (1) Dolovich, L. R.; Ginsberg, J. S.; Douketis, J. D.; Holbrook, A. M.; Cheah, G. *Arch. Intern. Med.* **2000**, *160*, 181–188.
- (2) Segal, J. B.; Bolger, D. T.; Jenckes, M. W.; Krishnan, J. A.; Streiff, M. B.; Tamariz, L. J.; Bass, E. B. *Am. J. Med.* **2003**, *115*, 298–308.
- (3) Theroux, P.; Ouimet, H.; McCans, J.; Latour, J. G.; Joly, P.; Levy, G.; Pelletier, E.; Juneau, M.; Stasiak, J.; deGuise, P.; Guy, B.; Pelletier, G. B.; Ringler, D.; Waters, D. D. *N. Eng. J. Med.* **1988**, *319*, 1105–1111.
- (4) Guerrini, M.; Beccati, D.; Shriver, Z.; Naggi, A.; Viswanathan, K.; Bisio, A.; Capila, I.; Lansing, J. C.; Guglieri, S.; Fraser, B.; Al-Hakim, A.; Gunay, N. S.; Zhang, Z.; Robinson, L.; Buhse, L.; Nasr, M.; Woodcock, J.; Langer, R.; Venkataraman, G.; Linhardt, R. J.; Casu, B.; Torri, G.; Sasisekharan, R. *Nat. Biotechnol.* **2008**, *26*, 669–675.

- (5) Kishimoto, T. K.; Viswanathan, K.; Ganguly, T.; Elankumaran, S.; Smith, S.; Pelzer, K.; Lansing, J. C.; Sriranganathan, N.; Zhao, G.; Galcheva-Gargova, Z.; Al-Hakim, A.; Bailey, G. S.; Fraser, B.; Roy, S.; Rogers-Cotrone, T.; Buhse, L.; Whary, M.; Fox, J.; Nasr, M.; Dal Pan, G. J.; Shriver, Z.; Langer, R. S.; Venkataraman, G.; Austen, K. F.; Woodcock, J.; Sasisekharan, R. *N. Engl. J. Med.* **2008**, *358*, 2457–2467.
- (6) Centers for Disease Control and Prevention (CDC). *MMWR Morb. Mortal. Wkly Rep.* **2008**, *57*, 124–125.
- (7) FDA page. <http://www.fda.gov/Drugs/DrugSafety/PostmarketDrugSafetyInformationforPatientsandProviders/ucml12669.htm>.
- (8) (a) Pan, J.; Qian, Y.; Zhou, X.; Pazandak, A.; Frazier, S. B.; Weiser, P.; Lu, H.; Zhang, L. *Nat. Biotechnol.* **2010**, *28* (3), 203–207. (b) Guerrini, M.; Shriver, Z.; Naggi, A.; Casu, B.; Linhardt, R. J.; Torri, G.; Sasisekharan, R. *Nat. Biotechnol.* **2010**, *28* (3), 207–211.
- (9) (a) Mcewen, L.; Mulloy, B.; Hellwig, E.; Kozerski, L.; Beyer, T.; Holzgrabe, U.; Wanko, R.; Spieser, J. M.; Rodomonte, A. *Pharmeuropa Bio* **2008**, 31–39. (b) Langeslay, D. J.; Beecher, C. N.; Naggi, A.; Guerrini, M.; Torri, G.; Larive, C. K. *Anal. Chem.* **2013**, *85* (2), 1247–1255.
- (10) Trehy, M. L.; Reepmeyer, J. C.; Kolinsky, R. E.; Westenberger, B. J.; Buhse, L. F. *J. Pharm. Biomed. Anal.* **2010**, *49*, 670–673.
- (11) Volpi, N.; Maccari, F.; Linhardt, R. J. *Anal. Biochem.* **2009**, *388*, 140–145.
- (12) Zhang, Z.; Li, B.; Suwan, J.; Zhang, F.; Wang, Z.; Liu, H.; Mulloy, B.; Linhardt, R. J. *J. Pharm. Sci.* **2009**, *98*, 4017–4026.
- (13) Spencer, J. A.; Kauffman, J. F.; Reepmeyer, J. C.; Gryniewicz, C. M.; Ye, W.; Toler, D. Y.; Buhse, L. F.; Westenberger, B. J. *J. Pharm. Sci.* **2009**, *98*, 3540–3547.
- (14) Wang, L.; Buchanan, S.; Meyerhoff, M. E. *Anal. Chem.* **2008**, *80*, 9845–9847.
- (15) Zhong, Z.; Anslyn, E. V. *J. Am. Chem. Soc.* **2002**, *124* (31), 9014–9015.
- (16) (a) Bromfield, S. M.; Barnard, A.; Posocco, P.; Fermeglia, M.; Prici, S.; Smith, D. K. *J. Am. Chem. Soc.* **2013**, *135* (8), 2911–2914. (b) Shriver, Z.; Sasisekharan, R. *Nat. Chem.* **2013**, *5* (8), 644–646.
- (17) Sommer, C. D.; Mans, D. J.; Mecker, L. C.; Keire, D. A. *Anal. Chem.* **2011**, *83*, 3422–3430.
- (18) Ho, H. A.; Boissinot, M.; Bergernon, M. G.; Corbeil, G.; Dore, K.; Boudreau, D.; Leclerc, M. *Angew. Chem., Int. Ed.* **2002**, *41*, 1548–1551.
- (19) Lee, K.; Hyukjin, L.; Bae, K. H.; Park, T. G. *Biomaterials* **2010**, *31*, 6530–6536.
- (20) Marradi, M.; Alcántara, D.; de la Fuente, J. M.; García-Martín, M. L.; Cerdá, n S.; Penadés, S. *Chem. Commun.* **2009**, 3922–3924.
- (21) Brinās, R. P.; Sundgren, A.; Sahoo, P.; Morey, S.; Rittenhouse-Olson, K.; Wilding, G. E.; Deng, W.; Barchi, J. J., Jr. *Bioconjugate Chem.* **2012**, *23*, 1513–1523.
- (22) Baram-Pinto, D.; Shukla, S.; Aharon Gedanken, A.; Sarid, R. *Small* **2010**, *6* (9), 1044–1050.
- (23) Kemp, M. M.; Kumar, A.; Mousa, S.; Park, T.-J.; Ajayan, P.; Kubotera, N.; Mousa, S. A.; Linhardt, R. J. *Biomacromolecules* **2009**, *10*, 589–565.
- (24) Duchesne, L.; Gentili, D.; Comes-Franchini, M.; Fernig, D. G. *Langmuir* **2008**, *24*, 13572–13580.
- (25) Yun, C. S.; Javier, A.; Jennings, T.; Fisher, M.; Hira, S.; Peterson, S.; Hopkins, B.; Reich, N. O.; Strouse, G. F. *J. Am. Chem. Soc.* **2005**, *127*, 3115–3119.
- (26) Singh, M. P.; Strouse, G. F. *J. Am. Chem. Soc.* **2010**, *132*, 9383–9391.
- (27) Labadie, J. *Int. J. Risk Saf. Med.* **2012**, *24*, 37–39.

# CURRICULUM VITA

**Caitlin Paige Mencio**

## EDUCATION

**Ph.D, Expected Spring/Summer 2014, University of Utah, Salt Lake City UT**  
Interdepartmental program in Neuroscience

**B. S., 2007, Texas Christian University, Ft Worth TX**  
Neuroscience

## RESEARCH TRAINING

August 2009 – Present: **Graduate Research Assistant**, Laboratory of Dr. Kuberan Balagurunathan, Department of Medicinal Chemistry, in collaboration with Dr. Franz Goller, Department of Biology, University of Utah. Project: Understanding the role of proteoglycans in vocal ontogeny and production in zebra finch.

May 2009-August 2009: **Laboratory Rotation**, Laboratory of Dr. Kuberan Balagurunathan, Department of Medicinal Chemistry, University of Utah. Project: Cloning of Chondroitinase ABC for enzyme expression and purification.

March 2009-May 2009: **Laboratory Rotation**, Laboratory of Dr. Shannon Odleburg, Department of Genetics, University of Utah. Project: *In Situ* staining of notochord sections in newt.

January 2009- March 2009: **Laboratory Rotation**, Laboratory of Dr. Karen Wilcox, Department of Pharmacology and Toxicology, University of Utah. Project: Sectioning and antibody staining of rat neural tissue after induction of status epilepticus.

August 2008 – December 2008: **Laboratory Rotation**, Laboratory of Dr. Gary Rose, Department of Biology, University of Utah. Project: Behavioral observation of tropical fish before and during gender transition.

August 2006 – May 2008: **Undergraduate Research**, Laboratory of Dr. Timothy Barth, Department of Psychology, Texas Christian University. Project: Effect of common sugar substitute on rat spatial memory as determined by performance in the radial arm maze.

## AWARDS

**Neuroscience Training Grant- 07/01/08-06/31/09**  
T32 Training Grant, National Research Service Award

**Outstanding Poster Award**  
Gordon conference in Proteoglycans, New Hampshire, July 2012

## PUBLICATIONS

**Mencio, C.** Kuberan, B. & Goller, F. (2014) GAG modulation using xylosides alters vocal ontogeny in developing zebra finch. (Manuscript in preparation).

**Mencio, C.** Kuberan, B. & Goller F. (2014) Degradation of heparan sulfate in the syrinx leads to changes in muscle activity and alters acoustic features of stereotyped song in zebra finch. (Manuscript in preparation).

**Mencio, C.** Garaud, D., Kuberan, B., & Koketsu, M. (2014) Synthesis and comparison of dimeric click xyloside derivatives. (Manuscript in preparation).

**Mencio, C.,** Swarup, V., Soliai, M. & Kuberan, B. "Synthesis of sulfur isotope labeled sulfate donor, 3'-phosphoadenosine-5'-phosphosulfate" in Methods in Molecular Biology. Kuberan, B., Nakato, H., & Desai, U.R. Eds. Accepted by Editors.

**Mencio, C.,** Garud, D., Kuberan, B. & Koketsu, M. "Synthesis of 4-Deoxy-4-fluoro-xylosides for the inhibition of GAG biosynthesis" in Methods in Molecular Biology. Kuberan, B., Nakato, H., & Desai, U.R. Eds. Accepted by Editors.

Joice, AC, Raman, K., **Mencio, C.**, Nguyen, T., & Kuberan, B. "Enzymatic Synthesis of Heparan Sulfate" in Methods in Molecular Biology. Kuberan, B., Nakato, H., & Desai, U.R. Eds. Accepted by Editors

Kalita, M., Balivada, S., Swarup, VP, **Mencio, C.**, Raman, K., Desai, UR., Troyer, D., & Kuberan, B. A nanosensor for ultrasensitive detection of oversulfated chondroitin sulfate contaminant in heparin. (2014) Journal of the American Chemical Society, 136(2): 554-7. Pubmed ID: 24127748

Raman, K, **Mencio, C**, Desai, UR, & Kuberan, B. Sulfation patterns determine cellular internalization of Heparin-like polysaccharides. (2013) Molecular Pharmaceutics, 10(4): 1442-9 Pubmed ID:23398560

Swarup, V., **Mencio, C.**, Hlady, V. & Kuberan, B. Sugar glues for broken neurons. (2013) Biomolecular Concepts, 4(3):233-257. ISSN (online): 1868-503X

## Abstracts

Presenter is underlined.

**Mencio, C.** Goller, F. & Kuberan, B. Xyloside infusion alters vocal ontogeny in juvenile zebra finch. Programs of Excellence in Glycoscience, Bethesda, MD, March 2014.

**Mencio, C.**, Raman, K., Desai, U.R., & Kuberan, B. Sulfation patterns determine internalization of heparin-like polysaccharides. Programs of Excellence in Glycoscience, Cleveland, OH, April 2013.

\*Joice, AC, Raman, K, Mencio, C, Nguyen, T, Painter, C, Tran, V, Kalita, M, Desai, U, Kuberan, B. The Chemistry and Biology of Heparan Sulfate. Inter-Program of Excellence in Glycoscience Meeting. Cleveland OH. April 2013. (Oral Presentation)

Joice, AC, Mencio, C, Raman, K, Painter, C, Tran, V, Kalita, M, Kuberan, B. Enzymatic Production of Heparin Anticoagulants for Human Use. American Society of Biochemistry and Molecular Biology. Boston MA. April 2013.

\*Joice, AC, Mencio, C, Raman, K, Tran, V, Kalita, M, Brown, S, Kuberan, B. Enzymatic Synthesis of Heparin-like Anticoagulants. Intra-Program of Excellence in Glycoscience Meeting. Richmond VA. January 2013. (Oral Presentation)

\***Mencio, C.**, Tran, V., Goller, F., & Kuberan, B. (2012) Manipulation of chondroitin sulfate alters vocal ontogeny in zebra finch. Snowbird Symposium. Snowbird Ski & Summer Resort, UT, Nov 2012. (Oral Presentation)

**Mencio,C.**, Tran, V., Goller, F., & Kuberan, B. (2012) The presence of chondroitin sulfate in RA influences vocal ontogeny in juvenile male zebra finch. Society for Neuroscience, New Orleans, LA, Oct 2012

**Mencio,C.**, Tran, V., Goller, F., & Kuberan, B. (2012) Manipulation of chondroitin sulfate alters the learning critical period in juvenile zebra finch. Gordon Conference in proteoglycans, Andover, NH, July 2012.

**Mencio,C.**, Friend, D, Sigulinsky, C, Frenchek, Z, Yarch, J, Pfeiffer, R, Calhoon, J, Haack, A, Tucker, J & Parker, R. (2011) Utah brain awareness week 2011: Brain=Awareness. Society for Neuroscience, Washington D.C. Nov 2011

## TEACHING EXPERIENCE

### Judge

Intermountain Junior Science and Humanities Symposium, University of Utah, 2012, 2013, 2014

- read and score scientific research papers from HS students (all years)
- evaluate oral and/or poster presentation of research (2013,2014)

### Teaching Assistant

Molecular Biology Lab (NEUSC 6250), University of Utah, August 2013

- instructing and assisting trainees with all laboratory procedures
- preparing slides and a lecture based on a molecular biology technique

### Undergraduate Research Mentor

Scott Willie: Native American Research Internship, Summer 2013

- currently employed at San Juan Regional Medical Center

### Instructor

Programs of Excellence in Glycoscience Training Camp I, University of Utah, May 2012

- involves creating protocols for teaching lab
- instructing and assisting trainees with all laboratory procedures

## SERVICE

### Brain Awareness Week Coordinator

Coordinated the interaction of graduate students with local schools (K through college) and the Salt Lake Public Library to educate the general population about the brain, focusing on how it works and safety, University of Utah, March 2012

- creating and organizing stations that focus on different aspects of brain function (visual illusions, brain dissections, microscopes, etc)
- coordinating between volunteers and venues (schools and the library)

### Brain Awareness Week Volunteer

Volunteered to go to schools to educate the public on brain health and safety as part of the University of Utah's brain awareness week, March 2008,2009, 2010, 2011, 2012, 2013, 2014

## ORGANIZATIONS

Society for Neuroscience, Member, December 2010 – Present